The Petz (lite) recovery map for scrambling channel

Yasuaki Nakayama

Department of Physics, Kyoto University, Kyoto 606-8502, Japan

E-mail: nakayama@gauge.scphys.kyoto-u.ac.jp

ABSTRACT: The island rule provides the consistent method to tackle the black hole information loss problem. Holographic derivation and replica wormhole derivation of the island rule suggest that the quantum information inside a black hole can be extracted from an island region through the Hawking radiation. We are interested in the operational procedure to recover the black hole information from the Hawking radiation. Hayden and Preskill studied the condition to succeed decoding of a quantum state thrown into a black hole by considering the black hole dynamics as a random matrix. Chandrasekaran and Levine studied the Hayden-Preskill decoding protocol in another chaotic system, the SYK model. These two models can be studied by the theoretical framework of quantum error correction, in which the Petz recovery map is constructed as a general recovery map for a quantum noise channel when the Knill-Laflamme condition is satisfied. We study properties of the Petz recovery map in chaotic systems, such as the Hayden-Preskill setup for evaporating black holes and the SYK model. Since these systems exhibit the phenomenon called scrambling, we expect that the expression of the recovery channel $\mathcal{R}$ gets simplified, given by just the adjoint $\mathcal{N}^\dagger$ of the original channel $\mathcal{N}$ which defines the time evolution of the states in the code subspace embedded into the physical Hilbert space. We check this phenomenon in two examples. The first one is the Hayden-Preskill setup described by Haar random unitaries. We compute the relative entropy $S(\mathcal{R}\left[\mathcal{N}[\rho]\right]||\rho)$ and show that it vanishes when the decoupling is archived. We further show that the simplified recovery map is equivalent to the protocol proposed by Yoshida and Kitaev. The second example is the SYK model where the two-dimensional code subspace is defined by an insertion of a fermionic operator, and the system is evolved by the SYK Hamiltonian. We check the recovery phenomenon by relating some matrix elements of an output density matrix $\langle T|\,\mathcal{R}[\mathcal{N}[\rho]]\,|T'\rangle$ to Rényi-two modular flowed correlators, and show that they coincide with the elements for the input density matrix with a small error after twice the scrambling time. In this Ph.D thesis, we add the review of fundamental tools and motivation to understand our paper, which contains the island rule, the Hayden-Preskill decoding protocol, the theory of quantum error correction, the SYK model, the replica trick calculation of modular flowed correlators in the SYK model.

Contents

1   Introduction

The black hole information loss problem is one of the most important problems in theoretical physics. It was proposed by S. W. Hawking in 1975. Hawking showed that a black hole has finite temperature and evaporates emitting thermal radiation called Hawking radiation by applying the perturbative quantum field theory (QFT) to the black hole. Although the black hole is made of some astronomical object written by a pure quantum state, after the black hole evaporates, only thermal radiation remains and it contradicts to quantum mechanics. This is called black hole information loss problem. It means that the entanglement entropy of Hawking radiation $S_R = -\text{tr}[\rho_R \log \rho_R]$ remains finite quantity after the black hole evaporates and disappears. Here, ρ_R is the density matrix of Hawking radiation. Against to this paradox, D. N. Page proposed that since the whole state starts with a pure state $|\psi\rangle$ and time evolves with a unitary operator, the remaining radiation is written by a pure state $\rho_R = U |\psi\rangle \langle\psi| U^\dagger$ and S_R must become zero even if S_R gradually increases in the radiation emitting process since the entanglement between the radiation and the black hole becomes bigger and bigger. This behavior that S_R increases at first but starts to decrease at some time called the Page time and becomes zero eventually is called the Page curve. The reason why the Hawking's calculation does not realize the Page curve is that it cannot deal with non-perturbative effects in quantum gravity. It was not until the island rule[1–5] was discovered in 2019 that the method to consider non-perturbative effects in the black hole physics is developed and we become able to tackle the black hole information loss problem without contradictions. It has been over 40 years since the Hawking's proposal.

The black hole entropy was evaluated as $S_{BH} = \frac{A}{4G_N}$ by J. D. Bekenstein and S. W. Hawking. Here, A is the area of the event horizon of the black hole and G_N is Newton constant. S_{BH} is called the Bekentein-Hawking entropy. It is important that S_{BH} is proportional to not the black hole volume but the area of event horizon. It seems that the black hole microscopic freedom exists on the surface of the black hole. From this interpretation, G. 't Hooft and L. Susskind proposed the holography principle, which suggests that quantum gravity is described by the boundary QFT. A. Strominger and C. Vafa discovered that the black hole entropy corresponds to the number of microstate in string theory. Soon after their proposal, the famous example of the holography principle, the AdS/CFT correspondence was discovered by J. Maldacena in 1997. It states that string theory, the strong candidate of quantum gravity, in $(d+1)$-dimensional anti de-Sitter (AdS) space has correspondence with d-dimensional boundary conformal field theory (CFT). Here, string theory in the AdS space is called the bulk theory comparing to the boundary theory. After Maldacena's paper, it was proppsed by Gubser, Klebanov, Polyakov and E. Witten (GKP-Witten) that the partition function and correlation functions in the bulk string theory and the boundary CFT is the same with an

appropriate boundary condition. It makes non-pertubative calculations of quantum gravity posssible. After the AdS/CFT correspondence was proposed, many important works which solve CFT problems by calculation of the bulk gravity theory were provided, for example the Ryu-Takayanagi formula and the Sakai-Sugimoto model. According to the AdS/CFT correspondence, a black hole in AdS corresponds to the finite temperature boundary CFT, and since CFT is a unitary quantum theory, it was believed that the black hole information loss problem is solved by the AdS/CFT correspondence. However the concrete method to tackle the black hole information loss problem was difficult to discover, so the island rule is amazing and has a great impact in our study field of quantum gravity.

From here, we introduce briefly the story from the Ryu-Takayanagi's holographic entanglement entropy formula to the East Coast model of the island rule. In 2006, S. Ryu and T. Takayanagi showed that on some time slice, the entanglement entropy S_A of subsystem A in boundary CFT is evaluated by the area of a minimal surface in the AdS space as

$$S_A = \min_{\gamma_A} \frac{Area(\gamma_A)}{4G_N} \,. \tag{1.1}$$

Here, γ_A expresses a surface in the AdS bulk which ends on an A's boundary ∂A. This can be interpreted as an extent of the Bekentein-Hawking entropy $S_{BH} = \frac{A}{4G_N}$. When the space-time is dynamical, the RT formula is extended to the Hubeny-Rangamani-Takayanagi (HRT) formula:

$$S_A = \frac{Area(\gamma_A^{\text{ext}})}{4G_N} \,, \quad \left.\frac{\delta Area}{\delta \gamma_A}\right|_{\gamma_A = \gamma_A^{\text{ext}}} = 0 \,. \tag{1.2}$$

By using the Ryu-Takayanagi (RT) formula, we can evaluate the entanglement entropy of CFT by the gravitational calculation. Inversely, it is expected that quantum gravity in the bulk can be studied by the entanglement of the boundary CFT. This motivation to reconstruct the bulk theory by the entanglement of the boundary theory is called bulk reconstruction. Especially, it is suggested that the bulk region reconstructed by the entanglement of region A in CFT should be the entanglement wedge Σ_A, which is surrounded by A and the minimal surface γ_A. This is called entanglement wedge reconstruction. Here, if the whole state in some time slice of CFT is a pure state, the entanglement entropy of A and $\bar{A}$ is the same: $S_A = S_{\bar{A}}$, so the minimal surface is the same: $\gamma_A = \gamma_{\bar{A}}$. In this case the AdS bulk is divided to two entanglement wedges $\Sigma_A, \Sigma_{\bar{A}}$. The RT formula holds when the bulk gravity is classical: $G_N \to 0$. Since we do not know quantum gravity completely, we consider classical gravity and the bulk QFT as the contribution of G_N^0 semi-classically. According to the entanglement wedge reconstruction, the RT formula including quantum corrections is

$$S_A = \min_{\gamma_A} \text{ext} \left[\frac{Area(\gamma_A)}{4G_N} + S_{bulk}(\Sigma_A) \right] \,. \tag{1.3}$$

Here, $S_{bulk}(\Sigma_A)$ is the entanglement entropy of the region Σ_A in the bulk QFT. We extremize the quantity inside the square bracket, and choose the minimal value if we have multiple extreme values. We can obtain the island rule by applying the RT formula including quantum corrections to an evaporating black hole setup as

$$S(\rho_R) = \min_I \operatorname{ext} \left[\frac{Area(\partial I)}{4G_N} + S_{bulk}(I \cup R) \right] \tag{1.4}$$

where $S(\rho_R)$ is the entanglement entropy of Hawking radiation and I is the island region. We can interpret the island rule as the fact that the quantum information inside the black hole escapes out through Hawking radiation, so it can be said that the black hole information loss problem was partially solved because the Page curve of Hawking radiation is realized.

However, it still remains to be understood the precise way to recover a black hole interior region from Hawking radiation. It has been realized that for this purpose, it is convenient to regard the black hole interior as a code subspace embedded in the Hilbert space of Hawking radiation as a quantum error correcting code [6–8]. For instance, the decoupling theorem by Hayden and Preskill [6] implies that the black hole interior region is protected against the erasure of black hole degrees of freedom, which assures the recovery. Once we regard an evaporating black hole as a quantum error correcting (QEC) code, then the general argument of QEC [9] tells us that the recovery is achieved by applying the Petz recovery map [10, 11].

In this paper, we study properties of the Petz recovery map in chaotic systems, such as the Hayden-Preskill (HP) setup for evaporating black holes and the SYK model. Since these systems exhibit the phenomenon called scrambling, we expect that the recovery channel $\mathcal{R}$ gets simplified, given by just the adjoint $\mathcal{N}^\dagger$ of the original channel $\mathcal{N}$ which defines the embedding of the black hole interior into the Hawking radiation. Therefore, schematically, we have

$$\mathcal{R} \sim a \, \mathcal{N}^\dagger, \tag{1.5}$$

where a is some numerical factor depending on the dimensions of the Hilbert spaces of black holes and Hawking radiation.

We will see this phenomenon in two examples. The first one is the Hayden-Preskill setup where the dynamics of an evaporating black hole and Hawking radiation is described by Haar random unitaries. We do this by computing the relative entropy $S(\mathcal{R}\left[\mathcal{N}[\rho]\right] || \rho)$ and show that it is vanishing when the decoupling is archived. We further show that the simplified recovery map is equivalent to the Yoshida-Kitaev protocol[1]. The second example is one of the SYK model versions of the Hayden-Preskill setup, discussed in [14][2]. In this setup, code

---

[1]This equivalence has not been directly shown, but such an equivalence is suggested by B. Yoshida in [12, 13].

[2]In [15], the authors discuss another Hayden-Preskill setup in the SYK model, and their setup is different from ours.

information is expressed as excitations, and a system is evolved by the SYK Hamiltonian. We check the recovery phenomenon by relating some elements of an output density matrix $\langle T | \mathcal{R}[\mathcal{N}[\rho]] | T' \rangle$ to Rényi-two modular flowed correlators, and show that they give an input density matrix $\langle T | \rho | T' \rangle$ with small error after twice the scrambling time. However, there are still remaining matrix elements, which we need to check, but it is difficult to evaluate them directly. In an upcoming paper [16], we will give their direct evaluations. In this paper, we do not evaluate them directly, but indirectly guess their expectations based on the result we obtained.

We use the paper with Akihiro Miyata and Tomonori Ugajin in the abstract, Introduction, section 5, section 8, Conclusion and discussion, and Appendices C, D, E, F. We review fundamental topics on our study in section 2, section 3, section 4, section 6, section 7, Appendices A, B. This Ph.D thesis is organized as follows. In section 2, we introduce Island formula and explain the motivation of our study. In section 3, we review the Hayden-Preskill decoding protocol and the Yoshida-Kitaev decoding protocol. In section 4, we review quantum error correction and the Petz recovery map. In section 5, we start with introducing a quantum channel induced by the Hayden-Preskill setup, and explain how we write down the simplified recovery map in the original Hayden-Preskill setup, which is applicable to the SYK case. We also explain a convenient notation to treat quantum channels induced by the Hayden-Preskill setup, and in the notation, one can imagine gravitational interpretation simply. In section 5.2, by using the convenient notation, we compute some relative entropies to check the sufficiency that we can use the simplified recovery map as a recovery map. Also, we show that the Yoshida-Kitaev protocol can be written as the recovery map. In section 6, we review the fundamental topics of the SYK model. In section 7, we review the replica trick calculation of modular flowed correlator in the SYK model proposed by Chandrasekaran and Levine. In section 8, we explain one of the Hayden-Preskill setups using the SYK model, and introduce a corresponding quantum channel. After that, we give the simplified recovery map, and show that some matrix elements of output results can be written as "Rényi-two modular flowed correlator". By evaluating the "Rényi-two modular flowed correlators" analytically, we show some matrix elements of output results by the simplified recovery map give desired results. In section 8.3, from the previous section result we have computed, we estimate the remaining matrix elements of output results, which we are evaluating. The details of the remaining ones will be reported in the upcoming paper [16]. In section 9, we conclude this paper with the discussion of our results and future directions. In appendix A, we review the Uhlmann's monotonicity theorem. In appendix B, we review JT graivty and Schwarzian action. In appendix C, we give another derivation of the simplified recovery map using a Kraus representation. In appendix D, we show the relation that holds for an EPR state, which is used in section 5.2. In appendix E, conventions used in section 8 are listed. In appendix F,

we show that, in the SYK version of the Hayden-Preskill setup, some recovery results can be written as "Rényi-two modular flowed correlators".

2 Island rule and West Coast Paper

In this section, we introduce the island rule, which gives a motivation of our study. There are two methods to realize the Page curve: the method of the entanglement wedge reconstruction in the context of holography, and the method to average the randomness of microscopic states in quantum gravity without holographic calculation. We call the former method the East Coast model because it was developed by the Princeton team, and the latter method the West Coast model because it was developed by the Stanford team. We introduce the East Coast model in 2.1 and the West Coast model in 2.2. The calculation of the West Coast model is essentially the same as the random matrix calculation, which we explain in 2.3 where we also discuss the meaning of the Page curve. Finally, in 2.4, we explain the motivation of our study.

2.1 Island rule (East Coast model)

We attach two non-gravitational heat baths ($G_N = 0$) to both of two-sided AdS black hole's boundaries in order to collect Hawking radiation like figure 1. We can think of an AdS$_2$ black hole in JT gravity. We review JT gravity briefly in Appendix B. We can discuss a one-sided black hole but here we consider the two-sided black hole. The whole pure state in some time slice is given by

$$|\Psi\rangle = \frac{1}{\sqrt{k}} \sum_{i=1}^{k} |\psi_i\rangle_{\text{AdS BH}} \otimes |i\rangle_R \ . \tag{2.1}$$

Here, total Hilbert space is $\mathcal{H}_{tot} = \mathcal{H}_{\text{AdS BH}} \otimes \mathcal{H}_R$. $|\psi_i\rangle_{\text{AdS BH}} \in \mathcal{H}_{\text{AdS BH}}$ expresses a microstate of the AdS black hole and $|i\rangle_R \in \mathcal{H}_R$ expresses a Hawking radiation state. $\mathcal{H}_{\text{AdS BH}}$ is defined on the boundary CFT holographically. Since the Hawking radiation and the black hole make a pure state, if we write a state of the CFT corresponding to the black hole $\rho_{CFT,BH}$, the entanglement entropy of Hawking radiation is evaluated as

$$
\begin{aligned}
S(\rho_R) &= S(\rho_{CFT,BH}) \\
&= \min_{\gamma_A} \text{ext} \left[\frac{Area(\gamma_A)}{4G_N} + S_{bulk}(\Sigma_A) \right] \\
&= \min_{I} \text{ext} \left[\frac{Area(\partial I)}{4G_N} + S_{bulk}(I \cup R) \right]
\end{aligned}
\tag{2.2}
$$

The third line is the island formula. I in the third line is an island, which is a variable and decided by extremizing and taking minimal value by this formula. In the second line, we used the RT formula including quantum corrections. In the third line, we used the fact that the RT surface of the black hole region in the CFT becomes the surface of the island, and an entanglement wedge of the Hawking radiation and that of the black hole are complement

$$G_N = 0 \qquad \text{AdS BH } (G_N \neq 0) \qquad G_N = 0$$
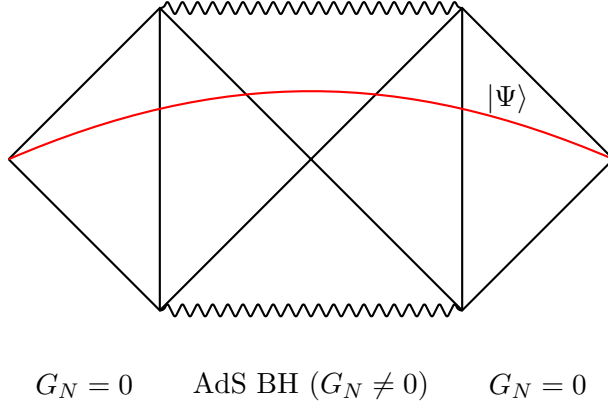
Figure 1: Penrose diagram of the AdS black hole coupled to thermal baths for collecting Hawking radiation. The red line expresses the whole quantum state $|\Psi\rangle$ corresponding to (2.1)
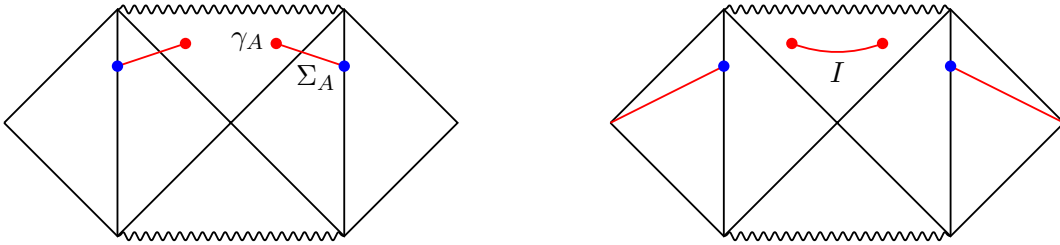
Figure 2: **Left**: Entanglement wedge of black hole. Blue dots express black hole microstates in the boundary CFTs and red dots express the RT surfaces. **Right**: Entanglement wedge of the Hawking radiation. An island region can appear in the AdS bulk.

with each other. See figure 2 for Penrose diagrams. In the East Coast model paper, it is shown that the island region actually appears after the Page time using JT gravity.

2.2 West Coast model

In this section we review the West Coast model [4] of the island rule, in which the entanglement entropy is calculated by considering replica wormholes. The replica wormhole saddle is a key point for realizing the Page curve. First, we consider the setup as a one-sided black hole with an end of the world (EoW) brane. We can realize this situation by inserting an EoW brane behind the horizon of a two-sided black hole. See figure 3 for the Lorentzian geometry and the Euclidean path integral to prepare a Hartle-Hawking state with the EoW brane. We call this Euclidean path integral, a gravitational path integral. In the original paper, this setup
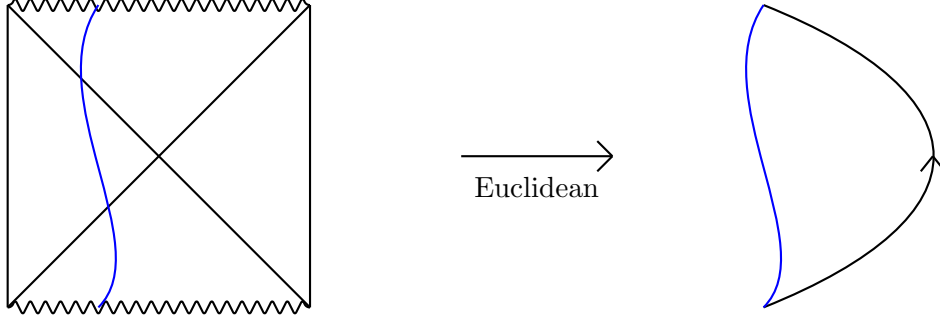
Figure 3: One-sided black hole coupled to an EoW brane. The blue line represents the EoW behind the horizon. The left Penrose diagram is the Lorentzian geometry. The right diagram represents the Euclidean gravitational path integral.

is made by Euclidean JT gravity coupled to the EoW brane. The action is

$$I = I_{JT} + \mu \int_{brane} ds \,. \tag{2.3}$$

The pure JT gravity action is

$$I_{JT} = -\frac{S_0}{2\pi} \left[\frac{1}{2} \int_{\mathcal{M}} \sqrt{g} R + \int_{\partial \mathcal{M}} \sqrt{h} K \right] - \frac{1}{2} \int_{\mathcal{M}} \sqrt{g} \phi (R+2) + \int_{\partial \mathcal{M}} \sqrt{h} \phi K \,. \tag{2.4}$$

On the AdS boundary, we impose an ordinary boundary condition to be asymptotic free:

$$ds^2|_{\partial \mathcal{M}} = \frac{1}{\epsilon^2} d\tau^2, \quad \phi = \frac{1}{\epsilon}, \quad \epsilon \to 0 \,. \tag{2.5}$$

On the EoW brane, we impose the following dynamical boundary condition:

$$\partial_n \phi = \mu, \quad K = 0 \,. \tag{2.6}$$

The whole state is given by

$$|\Psi\rangle = \frac{1}{\sqrt{k}} \sum_{i=1}^{k} |\psi_i\rangle_B \otimes |i\rangle_R \,. \tag{2.7}$$

Here, $\{|\psi_i\rangle_B\}$ is the basis of the black hole system and $\{|i\rangle_R\}$ is the basis of the Hawking radiation system. $\{|i\rangle_R\}$ is the orthogonal basis, but $\{|\psi_i\rangle_B\}$ is not always orthogonal due to gravitational effects. k is the dimension of the Hawking radiation system. The density matrix of the Hawking radiation becomes

$$\begin{aligned} \rho_R &= \text{tr}_B[|\Psi\rangle \langle \Psi|] \\ &= \frac{1}{k} \sum_{i,j=1}^{k} |j\rangle_R \langle i| \langle \psi_i|\psi_j\rangle_B \end{aligned} \tag{2.8}$$
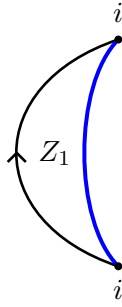
Figure 4: Gravitational path integral to calculate tr[ρ_R]. The EoW brane is the blue line.
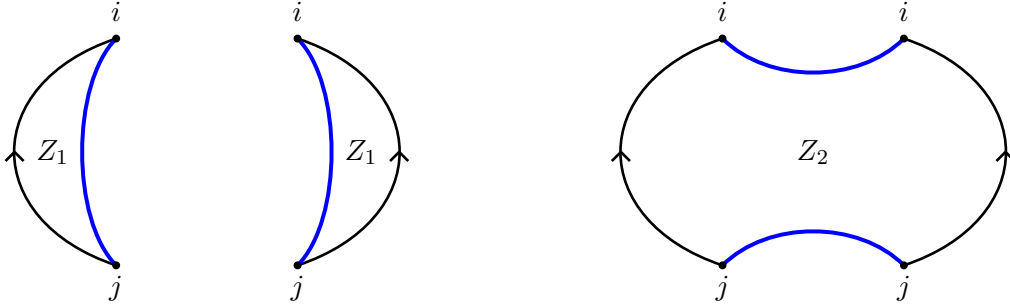
Figure 5: **Left**: Hawking saddle. **Right**: Replica wormhole saddle.

If we take the trace of ρ_R to take average of randomness of gravitational microstates as in figure 4,

$$
\begin{aligned}
\text{tr}[\rho_R] &= \frac{1}{k} \sum_i \langle \psi_i | \psi_i \rangle_B \\
&= \frac{1}{k} Z_1 \sum_i \delta_{ii} \\
&= Z_1 \,.
\end{aligned}
\tag{2.9}
$$

$Z_n \propto e^{S_{BH} \cdot \chi}$ represents a gravitational path integral with the boundary condition which we are considering. It comes from the topological term of JT gravity (2.4) and gives the Euler character χ. See also Appendix B for the fundamental of JT gravity.

The average of ρ_R has only trivial Hawking saddle. On the other hand, the average of ρ_R^n ($n \geq 2$) and S_R have replica wormhole saddles in which the space-time is connected by EoW branes. If we take average of ρ_R^2 with figure 5,

$$
\begin{aligned}
\text{tr}[\rho_R^2] &= \frac{1}{k^2} \sum_{i,j=1}^k \langle \psi_i | \psi_j \rangle_B \langle \psi_j | \psi_i \rangle_B \\
&= \frac{1}{k^2} \left(Z_1^2 \sum_{i,j} \delta_{ij} \delta_{ij} + Z_2 \sum_{i,j} \delta_{ii} \delta_{jj} \right) \\
&= \frac{1}{k^2} (Z_1^2 k + Z_2 k^2)
\end{aligned}
\tag{2.10}
$$

Here, $Z_1, Z_2 = e^{S_{BH}}$. After we normalize (2.10) with $(\text{tr}[\rho_R])^2$, we obtain

$$\text{tr}\big[\rho_R^2\big] = \frac{\frac{1}{k^2}(Z_1^2 k + Z_2 k^2)}{Z_1^2} = \frac{1}{k} + \frac{Z_2}{Z_1^2}$$
$$= \frac{1}{k} + e^{-S_{BH}} = \begin{cases} \frac{1}{k} & k \ll e^{BH} \\ e^{-S_{BH}} & k \gg e^{BH} \end{cases} . \tag{2.11}$$

Similarly, we can get the average of the entanglement entropy of the Hawking radiation $S_R = S(\rho_R)$ with the replica trick:

$$S_R = \begin{cases} \log k & k \ll e^{BH} \\ S_{BH} & k \gg e^{BH} \end{cases} . \tag{2.12}$$

We can realize the Page curve by this result.

2.3 Random matrix calculation

The West Coast model deals with the calculation of averaging randomness of gravitational microstates. It is essentially the same as the quantum informational calculation with the random matrix dynamics, which appears in the Hayden-Preskill decoding protocol. In this subsection, we explain that the purely quantum informational calculation with the random unitary matrix realizes the Page curve like the West Coast model. As we considered in the last subsection, we divide the whole Hilbert space to the black hole and the Hawking radiation: $\mathcal{H}_{tot} = \mathcal{H}_{BH} \otimes \mathcal{H}_R$. We assume that dimension of each system is $\dim \mathcal{H}_{BH} \equiv d_{BH} = e^{S_{BH}}$, $\dim \mathcal{H}_R \equiv d_R$, respectively. Therefore the number of qubits is $\log d_{BH}$, $\log d_R$, respectively. As the black hole evaporates, d_{BH} decreases and d_R increases. d_R also decides a time scale. The microscopic state of quantum gravity is given by

$$|\Psi\rangle = \frac{1}{\sqrt{d_{BH}d_R}} \sum_{\alpha=1}^{d_{BH}} \sum_{i=1}^{d_R} C_{\alpha i} |\psi_\alpha\rangle_{BH} \otimes |i\rangle_R . \tag{2.13}$$

Here, $C_{\alpha i}$ is a $d_{BH} \times d_R$-dimensional random matrix which represents the gravitational dynamics. We use the following Wick contraction-like rule to take average over the Gaussian random matrix $C_{\alpha i}$. Here we write the average of the product of less than four matrices, but the average of the product of more than four matrices is defined similarly as the Wick contraction.

$$\overline{C_{\alpha i} C_{j\beta}^\dagger} = \delta_{\alpha\beta}\delta_{ij} \tag{2.14}$$

$$\overline{C_{\alpha i} C_{j\beta}^\dagger C_{\gamma k} C_{m\delta}^\dagger} = \overline{C_{\alpha i} C_{j\beta}^\dagger} \cdot \overline{C_{\gamma k} C_{m\delta}^\dagger} + \overline{C_{\alpha i} C_{m\delta}^\dagger} \cdot \overline{C_{\gamma k} C_{j\beta}^\dagger} \tag{2.15}$$

In (2.13), we set the normalization factor by imposing $\overline{\text{tr}[\rho_R]} = 1$. We take average over $C_{\alpha i}$ to evaluate physical quantities such as entanglement entropy. Let us calculate the entanglement
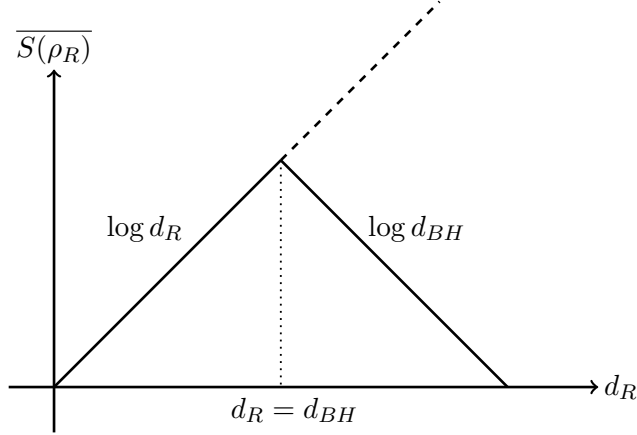
Figure 6: Initial growth of $\overline{S(\rho_R)}$ shows the Hawking's result $\log d_R$. If we consider the non-perturbative fluctuation from the randomness of the gravitational state, we realize the Page curve $\log d_{BH}$. The vertical axis means $\overline{S(\rho_R)}$ in qubit numbers.

entropy $S_R = \overline{S(\rho_R)}$ of the Hawking radiation. The density matrix of the Hawking radiation is

$$\rho_R = \frac{1}{d_R d_{BH}} \sum_{i,j=1}^{d_R} \sum_{\alpha=1}^{d_{BH}} C_{\alpha i} C_{j\alpha}^\dagger |i\rangle_R \langle j| , \tag{2.16}$$

and ρ_R^2 is

$$\rho_R^2 = \frac{1}{d_R^2 d_{BH}^2} \sum_{i,j,k=1}^{d_R} \sum_{\alpha,\beta=1}^{d_{BH}} C_{\alpha i} C_{j\alpha}^\dagger C_{\beta j} C_{k\beta}^\dagger |i\rangle_R \langle k| . \tag{2.17}$$

By taking average of $\mathrm{tr}\big[\rho_R^2\big]$, we obtain

$$\begin{aligned}
\overline{\mathrm{tr}\big[\rho_R^2\big]} &= \frac{1}{d_R^2 d_{BH}^2} \sum_{i,j=1}^{d_R} \sum_{\alpha,\beta=1}^{d_{BH}} \overline{C_{\alpha i} C_{j\alpha}^\dagger C_{\beta j} C_{i\beta}^\dagger} \\
&= \frac{1}{d_R} + \frac{1}{d_{BH}} = \begin{cases} \frac{1}{d_R} & d_R \ll d_{BH} \\ \frac{1}{d_{BH}} & d_R \gg d_{BH} \end{cases} .
\end{aligned} \tag{2.18}$$

We can calculate average of $\overline{S(\rho_R)} = \overline{-\mathrm{tr}[\rho_R \log \rho_R]} = -\lim_{n\to 1} \partial_n \overline{\mathrm{tr}\big[\rho_R^n\big]}$ as

$$\overline{S(\rho_R)} = \begin{cases} \log d_R & d_R \ll d_{BH} \\ \log d_{BH} & d_R \gg d_{BH} \end{cases} . \tag{2.19}$$

See figure 6 for this result. Hawking's calculation tells only $\log d_R$ growth, but we can reproduce the Page curve behavior $\log d_{BH}$. We can see that the second term of (2.15) makes a replica wormhole saddle. If we average ρ_R first, then we can consider only Hawking saddle by (2.14). It is important to understand that if we consider two or more replicas

like the calculation of the entanglement entropy or the Rényi-two entropy, the fluctuation $\delta\rho_R$ in $\rho_R = \overline{\rho_R} + \delta\rho_R$ cannot be ignored. The order of the fluctuation by the gravitational randomness is $\mathcal{O}(e^{-S_{BH}})$, so it is initially small, but becomes large when the black hole becomes small. Finally, we discuss the entanglement structure between the black hole and the radiation. In early time, since there is little radiation, we cannot identify the quantum information with ρ_R, i.e. ρ_R is a maximally mixed state $\frac{I_R}{d_R}$. We find $\overline{S(\rho_R)} = \log d_R$. However, in late time, since the radiation system is larger than the black hole system, the radiation is not maximally mixed. Gradually the quantum information seeps into the radiation system, and eventually the whole information can be identified by the radiation, i.e. ρ_R becomes a pure state. In late time, the black hole system becomes maximally mixed $\rho_{BH} = \frac{I_{BH}}{d_{BH}}$. Therefore, the entanglement entropy behaves as $S_R = S_{BH} = \overline{S_{BH}(\rho_{BH})} = \log d_{BH}$ and S_R decreases as d_{BH} decreases.

2.4 Motivation of our study

The island rule papers elucidated that the quantum information of the black hole seeps out through Hawking radiation, by the holographic calculation in the East Coast model and by more abstract randomness calculation in the West Coast model. After the Page time, an island region appears which is contained in the same entanglement wedge of the Hawking radiation, so the black hole information can be extracted by the island through the Hawking radiation. It provides the method to realize an information recovery scenario. We are strongly interested in the problem whether the quantum information is actually contained in the Hawking radiation and if so, how we can recover the original information with the Hawking radiation operationally. We can solve this problem if we succeed to construct a decoder to recover the original information by collecting the Hawking radiation and acting the decoder to it. Hayden and Preskill discussed the condition to recover the quantum state thrown into the black hole by acting some decoder to the Hawking radiation after the Page time. This discussion provides the starting point of our study. In the next section, we introduce this Hayden-Preskill thought experiment and the Yoshida-Kitaev decoder to realize the recovery.

3 Hayden-Preskill decoding protocol and Yoshida-Kitaev decoding protocol

In this section, we review the Hayden-Preskill decoding protocol and the Yoshida-Kitaev decoding protocol.

3.1 Hayden-Preskill decoding protocol

The Hayden-Preskill decoding protocol [6] is a purely quantum informational experiment that deals with the black hole information loss problem. According to the island rule, quantum information which consists of the black hole will be emitted through the Hawking radiation after the Page time. Hayden-Preskill asked that how long does it take for Bob who sits away from the black hole to catch the information that has been thrown into the black hole by Alice after the Page time. The answer is that if the decoupling condition is satisfied, Bob can catch the information immediately. If we think of a finite temperature black hole, Bob has to wait for the scrambling time. The Hayden-Preskill setup deals with the black hole dynamics as a random unitary gate. The motivation to consider the black hole dynamics as a random matrix comes from the fast scrambling conjecture, which expects that the black hole dynamics realizes the upper bound of the Lyapunov exponent, namely the chaos bound. When the system realize the chaos bound, the chaos is realized in the scrambling time. The random matrix dynamics is also considered to realize the chaos bound, so Hayden and Preskill considered the random matrix dynamics as a toy model of the black hole dynamics. We will review the setup of the thought experiment.

After the Page time, the black hole has emitted the half of the original black hole. We call them the old black hole and the early radiation. They can be thought of making a Einstein Podolsky Rosen brige, namely a EPR state.

$$|\text{EPR}\rangle_{AB} = \frac{1}{\sqrt{d_A}} \sum_{i=1}^{d_A} |i\rangle_A |i\rangle_B \tag{3.1}$$

The old black hole A is maximally entangled with the early radiation B. It is a high temperature limit of a thermo-field-double (TFD) state. It can be thought of as an infinite temperature black hole.

$$|\text{TFD}\rangle_{AB} = \frac{1}{\sqrt{Z_\beta}} \sum_n e^{-\beta E_n/2} |n\rangle_A |n\rangle_B \tag{3.2}$$

Here, Z_β is the partition function, $Z_\beta = \sum_n e^{-\beta E_n}$.

Alice throws the quantum state $|\psi\rangle_T$ into the old black hole. The density matrix is $\rho_T = |\psi\rangle_T \langle\psi|$. This state has the information of complex numbers c_i.
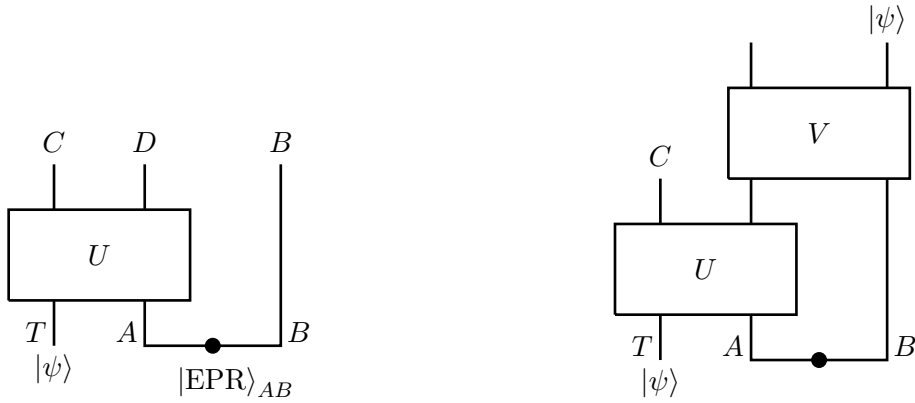
Figure 7: **Left**: $|\Psi_{CDB}\rangle$, corresponding to eq.(3.4). **Right**: The state after the decoder is acted.

$$|\psi\rangle_T = \sum_{i=1}^{d_T} c_i |i\rangle \tag{3.3}$$

After the scrambling with a unitary operator U, we have the remaining black hole C and the late radiation D. The state becomes

$$|\Psi\rangle_{CDB} = (U_{TA\rightarrow CD} \otimes I_B) |\psi\rangle_T \otimes |\text{EPR}\rangle_{AB} \tag{3.4}$$

The density matrix of $|\Psi\rangle_{CDB}$ is $\rho_{CDB} = |\Psi\rangle_{CDB}\langle\Psi|$. Bob can access to the radiation DB, so we trace out the remaining black hole system C. The result state is $\rho_{DB} = \text{tr}_C[\rho_{CDB}]$. The successive process of throwing the state ρ_T to the black hole, scrambling with the random unitary U and tracing out the remaining black hole is called the Hayden-Preskill noise channel, which is stated as $\mathcal{N}_{T\rightarrow DB}$.

$$\mathcal{N}_{T\rightarrow DB}[\rho_T] = \rho_{DB} \tag{3.5}$$

The Hayden-Preskill decoding protocol asks the condition that there exists a recovery map $\mathcal{R}_{DB\rightarrow T}$ which acts on the radiation DB and recovers the original state ρ_T.

$$\mathcal{R}_{DB\rightarrow T}[\rho_{DB}] \equiv V_{DB\rightarrow T}\, \rho_{DB}\, V_{DB\rightarrow T}^\dagger = \rho_T \tag{3.6}$$

$V_{DB\rightarrow T}$ is called a decoder. Hayden-Preskill show that if the decoupling condition $d_T \ll d_D$ is satisfied, there exists a decoder and we succeed a recovery immediately. Figures of $|\Psi_{CDB}\rangle$ and the state after the decoder is acted are shown in figure 7.

Figure 8: Hayden-Preskill state $|\Psi_{HP}\rangle$, corresponding to (3.7)

3.1.1 Decoupling condition

It is useful to introduce an additional system R called a reference system which is entangled with the diary system T. In this setup, we obtain a Hayden-Preskill state $|\psi_{HP}\rangle$. We describe the dynamics as a random unitary in this maxi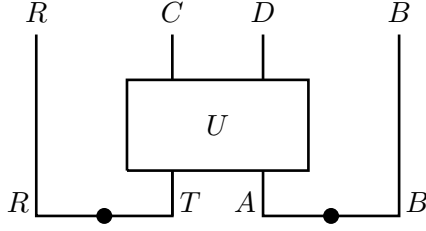mally chaotic situation. When we calculate an entropy, we take average with a Haar measure of the random unitary matrix.

$$|\Psi_{HP}\rangle = (I_R \otimes U_{TA \to CD} \otimes I_B) |\text{EPR}\rangle_{RT} \otimes |\text{EPR}\rangle_{AB} \tag{3.7}$$

$|\Psi_{HP}\rangle$ is shown in figure 8.

If we act $\langle \psi^*|$ to the R system, then we can reproduce $|\Psi\rangle_{CDB}$ with some normalization. Here, if we write $|\psi\rangle = \sum_i c_i |i\rangle$, we define $\langle \psi^*| = \sum_i \langle i| c_i$ as opposed to $\langle \psi| = \sum_i \langle i| c_i^*$. The reference system does not have the information of c_i but is entangled with the diary system T.

$$_R\langle \psi^*|\Psi_{HP}\rangle = \frac{1}{\sqrt{d_T}} (U_{TA \to CD} \otimes I_B) |\psi\rangle_T \otimes |\text{EPR}\rangle_{AB} \tag{3.8}$$

$$\to (U_{TA \to CD} \otimes I_B) |\psi\rangle_T \otimes |\text{EPR}\rangle_{AB} = |\Psi\rangle_{CDB} \tag{3.9}$$

The reference system R is maximally entangled with the diary system T. So, if R is maximally entangled with the radiation system DB, T is maximally entangled with DB and the information of the diary can be extracted by collecting the radiation DB. This situation occurs if R is decoupled with C. This is the decoupling theorem.

The result of the decoupling theorem is stated as follows.

$$\overline{\|\rho_{RC} - \rho_R \otimes \rho_C\|_1} \leq \frac{d_T}{d_D} \tag{3.10}$$

where $\rho_{RC}, \rho_R, \rho_C$ are reduced density matrices:

$$\rho_{RC} = \text{tr}_{DB} \left[|\Psi_{HP}\rangle \langle \Psi_{HP}| \right] \tag{3.11}$$

$$\rho_R = \text{tr}_{CDB} \left[|\Psi_{HP}\rangle \langle \Psi_{HP}| \right] \tag{3.12}$$

$$\rho_C = \text{tr}_{RDB} \left[|\Psi_{HP}\rangle \langle \Psi_{HP}| \right] \tag{3.13}$$

The overline in (3.10) means average with the Haar measure.

$$\overline{\|\rho_{RC} - \rho_R \otimes \rho_C\|_1} = \int dU \|\rho_{RC} - \rho_R \otimes \rho_C\|_1 \tag{3.14}$$

We use two norms $\|\cdot\|_1$ and $\|\cdot\|_2$, which are called the trace norm and the Hilbert-Schmidt norm, respectively. They are examples of the Schatten p-norm.

$$\|M\|_1 = \operatorname{tr} \sqrt{M^\dagger M} \tag{3.15}$$

$$\|M\|_2 = \sqrt{\operatorname{tr}(M^\dagger M)} \tag{3.16}$$

where M is an arbitrary matrix. The two norms satisfy the following relation.

$$\|M\|_2 \le \|M\|_1 \le \sqrt{d}\,\|M\|_2 \tag{3.17}$$

where d is the dimension of the Hilbert space that M acts.

By using this relation, $(\overline{\|\rho_{RC} - \rho_R \otimes \rho_C\|_1})^2$ is bounded from above by the average of a second Rényi entropy of ρ_{RC}.

$$\begin{aligned}
\left(\overline{\|\rho_{RC} - \rho_R \otimes \rho_C\|_1}\right)^2 &\le \overline{\|\rho_{RC} - \rho_R \otimes \rho_C\|_1^2} \\
&\le d_R d_C \overline{\|\rho_{RC} - \rho_R \otimes \rho_C\|_2^2} \\
&= d_R d_C \overline{\operatorname{tr}\left[\rho_{RC}^2\right]} - 1
\end{aligned} \tag{3.18}$$

In the last line, we use the facts $\rho_R \approx \frac{I_R}{d_R}$ and $\rho_C \approx \frac{I_C}{d_C}$. R and C are sufficiently smaller systems than the whole system, so they are maximally mixed. This can be proved by evaluating the distance between the reduced density matrix and the maximally mixed state.

We can calculate the second Rényi entropy of ρ_{RC}

$$\operatorname{tr}\left[\rho_{RC}^2\right] = \frac{1}{d_T^2 d_A^2} \sum U_{CD,TA} U_{T'A,C'D}^\dagger U_{C'D',T'A'} U_{TA',CD'}^\dagger \tag{3.19}$$

where the summation is taken over the indices of unitary matrices.

We use the Weingarten calculus to integrate over the Haar random unitary matrix $U(d)$.

$$\overline{1} = 1 \tag{3.20}$$

$$\overline{U_{i_1 j_1} U_{i_2 j_2}^\dagger} = \frac{1}{d} \delta_{i_1 j_2} \delta_{j_1 i_2} \tag{3.21}$$

$$\begin{aligned}
\overline{U_{i_1 j_1} U_{i_2 j_2}^\dagger U_{i_3 j_3} U_{i_4 j_4}^\dagger} &= \frac{1}{d^2 - 1} \left(\delta_{i_1 j_2} \delta_{j_1 i_2} \cdot \delta_{i_3 j_4} \delta_{j_3 i_4} + \delta_{i_1 j_4} \delta_{j_1 i_4} \cdot \delta_{i_3 j_2} \delta_{j_3 i_2} \right) \\
&\quad - \frac{1}{d(d^2 - 1)} \left(\delta_{i_1 j_2} \delta_{j_1 i_4} \cdot \delta_{i_3 j_4} \delta_{j_3 i_2} + \delta_{i_1 j_4} \delta_{j_1 i_2} \cdot \delta_{i_3 j_2} \delta_{j_3 i_4} \right)
\end{aligned} \tag{3.22}$$

The last line in (3.22) is an $\mathcal{O}(\frac{1}{d^3})$ subleading term, so in the large d limit we can ignore this term.

$$\overline{U_{i_1 j_1} U_{i_2 j_2}^\dagger U_{i_3 j_3} U_{i_4 j_4}^\dagger} \approx \frac{1}{d}\delta_{i_1 j_2}\delta_{j_1 i_2} \cdot \frac{1}{d}\delta_{i_3 j_4}\delta_{j_3 i_4} + \frac{1}{d}\delta_{i_1 j_4}\delta_{j_1 i_4} \cdot \frac{1}{d}\delta_{i_3 j_2}\delta_{j_3 i_2}$$
$$= \overline{U_{i_1 j_1} U_{i_2 j_2}^\dagger} \cdot \overline{U_{i_3 j_3} U_{i_4 j_4}^\dagger} + \overline{U_{i_1 j_1} U_{i_4 j_4}^\dagger} \cdot \overline{U_{i_3 j_3} U_{i_2 j_2}^\dagger} \qquad (3.23)$$

Then the Haar random average of the second Rényi entropy is

$$\overline{\mathrm{tr}\left[\rho_{RC}^2\right]} = \frac{1}{d_T^2 d_A^2}\sum \overline{U_{CD,TA} U_{T'A,C'D}^\dagger U_{C'D',T'A'} U_{TA',CD'}^\dagger}$$
$$\approx \frac{1}{d_T^2 d_A^2}\sum \left(\overline{U_{CD,TA} U_{T'A,C'D}^\dagger} \cdot \overline{U_{C'D',T'A'} U_{TA',CD'}^\dagger} + \overline{U_{CD,TA} U_{TA',CD'}^\dagger} \cdot \overline{U_{C'D',T'A'} U_{T'A,C'D}^\dagger} \right)$$
$$= \frac{1}{d_T^2 d_A^2}\left(d_A d_D + d_T d_C \right)$$
$$\qquad (3.24)$$

Using (3.18), we can evaluate the distance between ρ_{RC} and $\rho_R \otimes \rho_C$ as

$$\left(\overline{\|\rho_{RC} - \rho_R \otimes \rho_C\|_1} \right)^2 \le d_R d_C \overline{\mathrm{tr}\left[\rho_{RC}^2\right]} - 1$$
$$= \frac{d_C d_D}{d_T d_A} + \frac{d_C^2}{d_A^2} - 1$$
$$= \frac{d_C^2}{d_A^2}$$
$$= \left(\frac{d_T}{d_D}\right)^2 . \qquad (3.25)$$

In the third line, we used that dimensions of both sides of unitary matrix U is the same, i.e. $d_T d_A = d_C d_D$.

If the decoupling condition $d_T \ll d_D$ is satisfied, R and C decouple with each other and there exists a recovery map. In the finite temperature case, d_D has to be a bit more larger because the entanglement between the black hole system and the radiation system is weak and a bit more time is needed to send information with the weak entanglement. The scrambling time $t_{\mathrm{scr}} \sim \beta \log S_A$ is needed in the finite temperature black hole. In the infinite temperature limit, t_{scr} becomes zero thanks to the strongest entanglement of the EPR pair. There are several kinds of decoder that realize the recovery for the Hayden-Preskill noise channel. Famous decoders are the Gao-Jafferis-Wall decoder[17] and the Yoshida-Kitaev decoder[18]. Gao-Jafferis-Wall uses unitary gates for the decoder and is known as a quantum teleportation protocol by a traversable wormhole. Yoshida-Kitaev uses a projection measurement for its decoder. It can also be thought of as a quantum teleportation using the projection. We explain this Yoshida-Kitaev decodeing protocol in the following subsection.
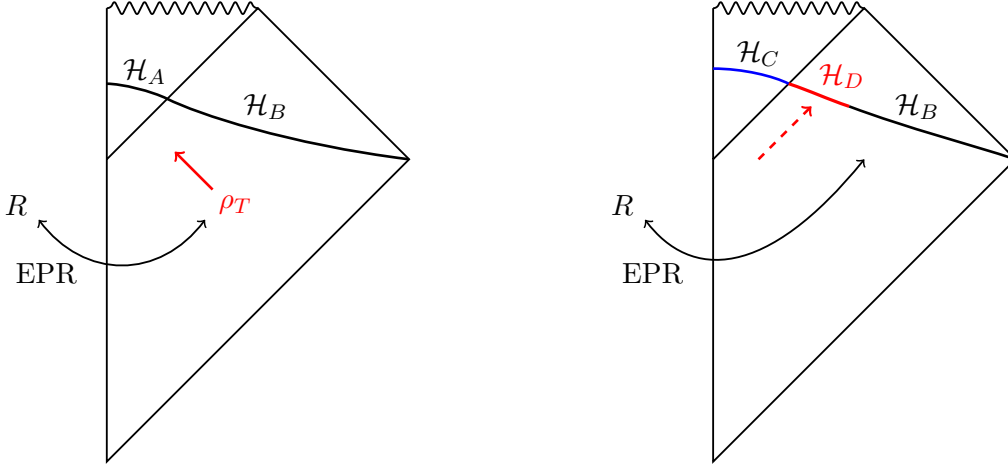
Figure 9: **Left**: Penrose diagram for showing a gravitational image of the HP protocol. We throw the quantum state ρ_T into the black hole. **Right**: After the late radiation is emitted sufficiently, R becomes maximally entangled with the radiation systems.

3.1.2 Gravitational image of Hayden-Preskill decoupling discussion

We show a gravitational image of the HP protocol by illustrating the Penrose diagram (figure 9). After the gravitational collapse, a black hole space-time and a Minkowski flat space-time emerge. First, the whole quantum state Ψ is divided to an old black hole state $|\psi\rangle_{BH} \in \mathcal{H}_A$ and an early Hawking radiation state $|i\rangle_R \in \mathcal{H}_B$. We consider the situation of the infinite temperature after the Page time, so they make an EPR state. We throw the diary state ρ_T which makes an EPR pair with the reference system R into the black hole. After time evolution with the black hole's random dynamics, which we consider the random unitary dynamics in this section, if the late radiation is emitted sufficiently, the reference system R becomes maximally entangled with the radiation systems DB and we can collect the quantum information of the original diary state ρ_T. More realistically, the old black hole and the early radiation should make a TFD state in finite temperature and there should be a more concrete bulk picture. We can overcome these requests by considering the SYK model, which we study in the latter part of this Ph.D. thesis.

3.2 Yoshida-Kitaev decoding protocol

In this subsection, we introduce the Yoshida-Kitaev decoding protocol[18], which is well known as the concrete decoder for the Haydne-Preskill noise channel. First, we explain the property of a decoder using the reference system. We act a decoder $V_{DB \to \bar{C}\bar{R}}$ to the Hayden-Preskill state $|\Psi_{HP}\rangle$ (See eq. (3.7)) in order to make the state $V_{DB \to \bar{C}\bar{R}}|\Psi_{HP}\rangle$. See figure 10. As we comment in the previous section, the reference system R contains the information of the
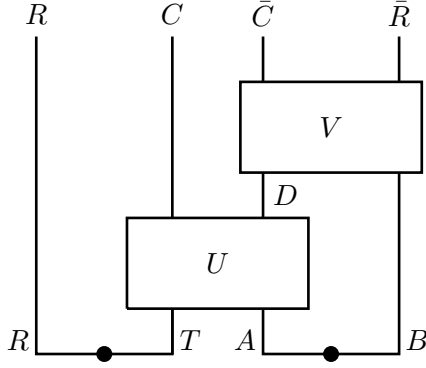
Figure 10: The state $V_{DB} |\Psi_{HP}\rangle$ after some decoder acted on the Hayden-Preskill state $|\Psi_{HP}\rangle$

system T in the way that R is maximally entangled with T. In other words, R is the system before the diary state acts: $_R\langle\psi^*|\text{EPR}\rangle_{RT} = \frac{1}{\sqrt{d_T}} |\psi\rangle_T \sim |\psi\rangle_T$.

After acting a decoder to the radiation systems D, B, if R and $\bar{R}$ are maximally entangled, i.e.

$$V_{DB} |\Psi_{HP}\rangle = |\text{EPR}\rangle_{R\bar{R}} \otimes |\varphi\rangle_{C\bar{C}} , \tag{3.26}$$

then it can be said that the information of T is successfully teleported to $\bar{R}$. Here, $|\varphi\rangle_{C\bar{C}}$ is an arbitrary state on $C\bar{C}$. The teleportation succeeds if R and $\bar{R}$ make an EPR state and then the original state can be recovered on $\bar{R}$:

$$_R\langle\psi^*|\text{EPR}\rangle_{R\bar{R}} = \frac{1}{\sqrt{d_R}} |\psi\rangle_{\bar{R}} \sim |\psi\rangle_{\bar{R}} . \tag{3.27}$$

Yoshida and Kitaev said that the decoder in the figure 11 satisfies the property (3.26) and can be used as the decoder for the Hayden-Preskill noise channel. We call this decoder the Yoshida-Kitaev decoder.

The Yoshida-Kitaev decoder can be constructed by the following process:

1. Bob, who tries to decode the original state which Alice threw into the black hole knows that the black hole dynamics is random unitary and can prepare the EPR pair $|\text{EPR}\rangle_{\bar{T}\bar{R}}$ of variable number of qubits. Bob acts the state $(I_D \otimes U^*_{\bar{D}\bar{C}\to B\bar{T}} \otimes I_{\bar{R}}) |\text{EPR}\rangle_{\bar{T}\bar{R}}$ to $|\Psi_{HP}\rangle$ and makes

$$|\Psi_{in}\rangle = (I_{RC} \otimes I_D \otimes U^*_{\bar{D}\bar{C}\to B\bar{T}} \otimes I_{\bar{R}}) |\Psi_{HP}\rangle \otimes |\text{EPR}\rangle_{\bar{T}\bar{R}} . \tag{3.28}$$

   Here, U^*, the complex conjugate of U, physically means the reverse time evolution.

2. Bob carries out the projection measurement on $D, \bar{D}$. The projection measurement is realized by the projection operator $P_D = |\text{EPR}\rangle_{D\bar{D}} \langle\text{EPR}| \otimes I_{\bar{C}\bar{R}}$. The outcome state is

$$\left|\Psi'_{out}\right\rangle = \frac{1}{\sqrt{P_{out}}} (I_{RC} \otimes P_D) |\Psi_{in}\rangle \tag{3.29}$$
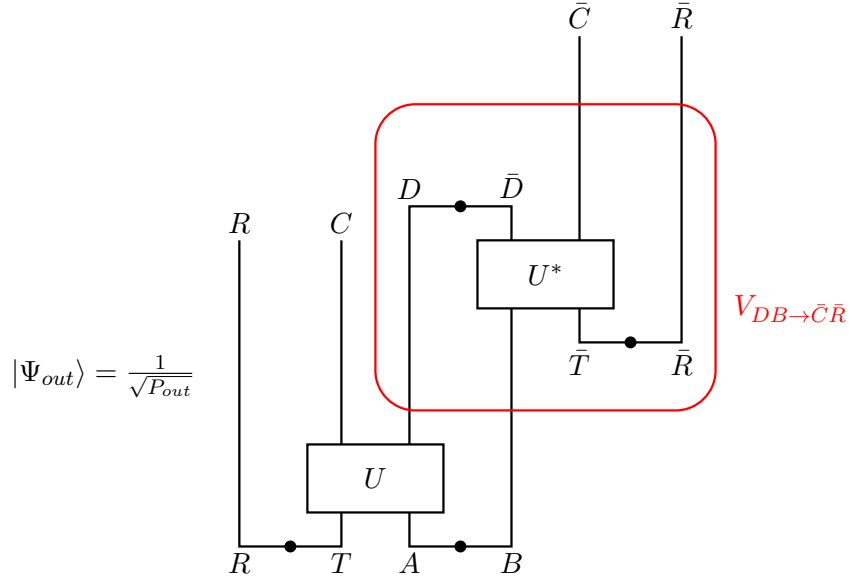
Figure 11: The Yoshida-Kitaev decoder $V_{DB \to \bar{C}\bar{R}}$
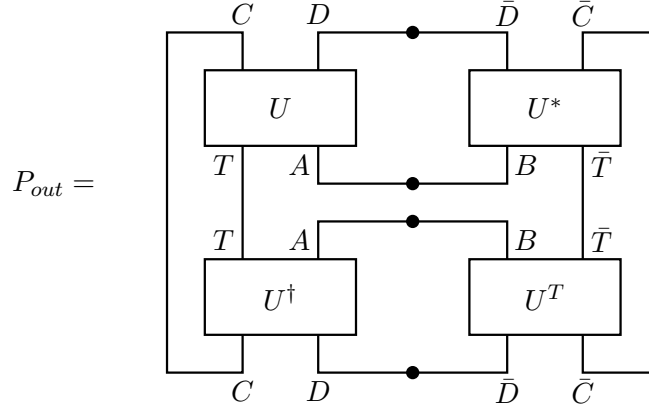
Figure 12: The probability P_{out} of getting $|\Psi'_{out}\rangle$ by the projection measurement $P_D = |\text{EPR}\rangle_{D\bar{D}} \langle \text{EPR}| \otimes I_{\bar{C}\bar{R}}$

Here, P_{out} is the probability of getting $|\Psi'_{out}\rangle$ and represented in the figure 12. $|\Psi'_{out}\rangle$ differs from $|\Psi_{out}\rangle$ by just $|\text{EPR}\rangle_{D\bar{D}}$. However, since $_{D\bar{D}}\langle \text{EPR}|\text{EPR}\rangle_{D\bar{D}} = 1$, we need not mind this in the following calculation.

We show that the Yoshida-Kitaev decoder can be used as a decoder, which realizes a recovery map by showing that we can express

$$|\Psi_{out}\rangle = |\text{EPR}\rangle_{R\bar{R}} \otimes |\varphi\rangle_{C\bar{C}} \ . \tag{3.30}$$

We can show this by guaranteeing that the fidelity between $|\Psi_{out}\rangle$ and $|\text{EPR}\rangle_{R\bar{R}}$ becomes 1. $C, \bar{C}$ can be contracted naturally. We define the projection measurement on $R, \bar{R}$ as $P_R = |\text{EPR}\rangle_{R\bar{R}} \langle \text{EPR}|$. The fidelity is calculated as follows:

$$
\begin{aligned}
F(|\Psi_{out}\rangle, |\text{EPR}\rangle_{R\bar{R}}) &= \langle \Psi_{out}| P_R |\Psi_{out}\rangle \\
&= \langle \Psi'_{out}| P_R |\Psi'_{out}\rangle \\
&= \frac{\langle \Psi_{in}| P_R(I_{RC} \otimes P_D) |\Psi_{in}\rangle}{P_{out}} \\
&\geq \frac{\langle \Psi_{in}|\text{EPR}\rangle_{RCD} \langle \text{EPR}|\Psi_{in}\rangle}{P_{out}} \\
&= \frac{1}{d_R d_A P_{out}} \\
&= \frac{1}{d_R d_C \operatorname{tr}\left[\rho_{RC}^2\right]} \\
&\rightarrow \frac{1}{1 + \left(\frac{d_T}{d_D}\right)^2}
\end{aligned}
\tag{3.31}
$$

In the fourth line, we used $P_R(I_{RC} \otimes P_D) = P_R \otimes (P_C + P_C^\perp) \otimes P_D$. Here, $P_C^\perp$ is the projection measurement orthogonal to $P_C = |\text{EPR}\rangle_{C\bar{C}} \langle \text{EPR}|$. Note that the projection measurements $P_C, P_C^\perp$ are both positive operators. The arrow in the last line expresses carrying out the Haar random average. If the decoupling condition $d_T \ll d_D$ is satisfied, the fidelity becomes close to 1, successfully.

We discuss the meaning of the Yoshida-Kitaev decoding protocol here. Why the EPR pair appears on $R, \bar{R}$ by the projection measurement on $D, \bar{D}$? Let us think of the entanglement structure in the state before the projection measurement on $D, \bar{D}$. Since the decoupling condition is satisfied if sufficient late Hawking radiation has been emitted, R is decoupled by C, so R is entangled with $D, \bar{D}, \bar{C}, \bar{R}$. In the same manner, since the dynamics of U^* also satisfies the decoupling condition, which means the time-scale around the Page time, $\bar{R}$ is decoupled by $\bar{C}$ and is entangled with $R, C, D, \bar{D}$. Since C and $\bar{C}$ are the systems which are decoupled by the whole system, so C and $\bar{C}$ make a maximal entanglement structure with each other. Therefore, $R, D, \bar{D}, \bar{R}$ make a maximal entanglement structure in themselves. In this situation, the maximal entanglement structure is imposed to $D, \bar{D}$ by the projection measurement on $D, \bar{D}$. Thus R and R must make a maximal entanglement structure with each other, so an EPR pair on $R, \bar{R}$ is realized. Thinking of the Yoshida-Kitaev protocol as a two-sided black hole, the EPR pair means infinite temperature of Hartle-Hawking like TFD state. We can interpret that if the entanglement between two-sided black hole is too strong like the EPR, then the black hole realizes a traversable wormhole and a quantum teleportation from one side to the other realizes. We discuss the relation between the Yoshida-Kitaev protocol and the quantum teleportation in the next subsection.

3.2.1 Relation with quantum teleportation

Finally, we introduce quantum teleportation and explain that the Yoshida-Kitaev protocol can be interpreted as quantum teleportation. Quantum teleportation is the protocol to send a quantum state $|\psi\rangle_T$ which Alice possesses to Bob using the quantum entanglement of a EPR state which is shared by Alice and Bob. The algorithm is as follows:

1. In its setup, Alice has a quantum state $|\psi\rangle_T = \psi(0)|0\rangle_T + \psi(1)|1\rangle_T$ to send to Bob.

2. Alice (A) and Bob (B) share an EPR state $|\text{EPR}\rangle_{AB}$ so they are maximally entangled. The whole state can be expressed as

$$
\begin{aligned}
|\psi\rangle_T |\text{EPR}\rangle_{AB} = \frac{1}{2}\bigg[&|1\rangle_{TA} \otimes (\psi(0)|0\rangle_B + \psi(1)|1\rangle_B) \\
&+ |x\rangle_{TA} \otimes (\psi(0)|1\rangle_B + \psi(1)|0\rangle_B) \\
&+ |y\rangle_{TA} \otimes (\psi(0)|1\rangle_B - \psi(1)|0\rangle_B) \\
&+ |z\rangle_{TA} \otimes (\psi(0)|0\rangle_B - \psi(1)|1\rangle_B) \bigg] \\
= \frac{1}{2\sqrt{2}} &\sum_{i=1,x,y,z} |i\rangle_{TA} \otimes \sigma_i^{-1} |\psi\rangle_B \ .
\end{aligned}
\tag{3.32}
$$

$|1\rangle_{TA}, |x\rangle_{TA}, |y\rangle_{TA}, |z\rangle_{TA}$ are Bell states on TA:

$$
\begin{aligned}
|1\rangle_{TA} &= \frac{1}{\sqrt{2}}(|0\rangle_T |0\rangle_A + |1\rangle_T |1\rangle_A) \\
|x\rangle_{TA} &= \frac{1}{\sqrt{2}}(|0\rangle_T |1\rangle_A + |1\rangle_T |0\rangle_A) \\
|y\rangle_{TA} &= \frac{1}{\sqrt{2}}(|0\rangle_T |1\rangle_A - |1\rangle_T |0\rangle_A) \\
|z\rangle_{TA} &= \frac{1}{\sqrt{2}}(|0\rangle_T |0\rangle_A - |1\rangle_T |1\rangle_A) ,
\end{aligned}
\tag{3.33}
$$

and they are made by $|\psi\rangle_B = \psi(0)|0\rangle_B + \psi(1)|1\rangle_B$ by unitary operators $I, \sigma_x, i\sigma_y = \sigma_z\sigma_x, \sigma_z$, respectively. We write these $\{\sigma_i\}$. These four operations make the Klein four group which is isomorphic to discrete components of the Lorentz group I, T, P, TP.

3. Alice carries out a Bell state measurement on TA. It measures which of the Bell states $\{|1\rangle_{TA}, |x\rangle_{TA}, |y\rangle_{TA}, |z\rangle_{TA}\}$ the state on TA is. After this measurement, Bob's state is decided to some $|\psi_i\rangle_B \equiv \sigma_i^{-1}|\psi\rangle_B$.

4. Alice sends the result of the measurement classically to Bob.

5. Bob acts σ_i to $|\psi_i\rangle_B$ depending on the measurement result received from Alice in order to recover $|\psi\rangle$ on B.

This algorithm is made of local quantum operation (LO) and non-local classical communication (CC), which is called LOCC. Next, we try the same algorithm when T makes an EPR pair with the reference system R. Since the whole state can be written as

$$|\text{EPR}\rangle_{RT} \otimes |\text{EPR}\rangle_{AB} = \frac{1}{\sqrt{2}} \sum_i |i\rangle_R \otimes (|i\rangle_T |\text{EPR}\rangle_{AB})$$

$$= \frac{1}{\sqrt{2}} \sum_i |i\rangle_R \otimes \left(\frac{1}{2} \sum_j |j\rangle_{TA} \otimes \sigma_j^{-1} |i\rangle_B \right) , \tag{3.34}$$

by carrying out the projection measurement on TA, the whole state becomes

$$\frac{1}{\sqrt{2}} \sum_i |i\rangle_R \otimes \left(\frac{1}{2} |j\rangle_{TA} \otimes \sigma_j^{-1} |i\rangle \right) . \tag{3.35}$$

After receiving the information of j from Alice, Bob acts unitary σ_j to make the state

$$\left(\frac{1}{\sqrt{2}} \sum_i |i\rangle_R \otimes |i\rangle_B \right) \otimes \frac{1}{2} |j\rangle_{TA} . \tag{3.36}$$

By the projection measurement on TA, we realize an EPR state on RB. This is the similar situation as the YK protocol.

In the ordinary quantum teleportation algorithm above, Alice checks the result of the measurement and send it to Bob classically. This can be expressed with only quantum operations. We introduce the algorithm below:

1. Alice has $|\psi\rangle_T$, one side of $|\text{EPR}\rangle_{AB}$ and two ancilla qubits $|0\rangle_{M_A} = |00\rangle$. The initial state can be written as

$$|\Psi_0\rangle = |\psi\rangle_T \otimes |\text{EPR}\rangle_{AB} \otimes |0\rangle_{M_A}$$

$$= \frac{1}{2\sqrt{2}} \sum_i |i\rangle_{TA} \otimes |0\rangle_{M_A} \otimes \sigma_i^{-1} |\psi\rangle_B . \tag{3.37}$$

2. Alice makes an interaction between TA and M_A to make the state

$$|\Psi_1\rangle = \mathcal{M}_A |\Psi_0\rangle = \frac{1}{2\sqrt{2}} \sum_i |i\rangle_{TA} \otimes |i\rangle_{M_A} \otimes \sigma_i^{-1} |\psi\rangle_B . \tag{3.38}$$

3. Bob also prepares two ancilla qubits $|0\rangle_{M_B} = |00\rangle$. If Bob has the state $|\Phi_0\rangle_B$, the initial state of Bob becomes

$$|\Phi\rangle_B = |\Phi_0\rangle_B \otimes |0\rangle_{M_B} . \tag{3.39}$$

Bob makes the rule to act a decoder to $|\Phi\rangle_B$ as

$$\Sigma_B |\Phi\rangle_B = \sum_j Z_B^j |\Phi_0\rangle_B \otimes |j\rangle_{M_B} , \tag{3.40}$$

where Z_B^j is set to be $Z_B^j = \sigma_j$.

4. Bob acts the decoder to $|\Psi_1\rangle$. The whole state becomes

$$
\begin{aligned}
|\Psi_2\rangle &= (I_{TAM_A} \otimes \Sigma_B) |\Psi_1\rangle \\
&= \frac{1}{2\sqrt{2}} \sum_i |i\rangle_{TA} |i\rangle_{M_A} \otimes \left(\sum_j Z_B^j \sigma_i^{-1} |\psi\rangle_B \otimes |j\rangle_{M_B} \right) \\
&= \frac{1}{2\sqrt{2}} \sum_{ij} |i\rangle_{M_A} |j\rangle_{M_B} \otimes \left(\sigma_j \sigma_i^{-1} |\psi\rangle_B \right) \otimes |i\rangle_{TA} .
\end{aligned}
\tag{3.41}
$$

5. Finally, we post select to the EPR on $M_A M_B$, which means acting the projection operator $|\text{EPR}\rangle_{M_A M_B} \langle \text{EPR}|$. Since $|\text{EPR}\rangle_{M_A M_B} = \frac{1}{2} \sum_{k=1,x,y,z} |k\rangle_{M_A} |k\rangle_{M_B}$, the final state is obtained as

$$
\begin{aligned}
|\Psi_3\rangle &= |\text{EPR}\rangle_{M_A M_B} \langle \text{EPR}|\Psi_2\rangle \\
&= \frac{1}{8\sqrt{2}} \sum_k |k\rangle_{M_A} |k\rangle_{M_B} \otimes \sigma_k \sigma_k^{-1} |\psi\rangle_B |k\rangle_{TA} \\
&= \frac{1}{8\sqrt{2}} \sum_k |k\rangle_{M_A} |k\rangle_{M_B} |k\rangle_{TA} \otimes |\psi\rangle_B .
\end{aligned}
\tag{3.42}
$$

Bob succeeds to get $|\psi\rangle_B$.

The situation that the original state can be sent to distant place by a post-selection of the projection measurement is the same as the Yoshida-Kitaev decoding protocol. That is why the YK protocol is explained as a quantum teleportation.

4 Quantum Error Correction and Petz recovery map

The Hayden-Preskill decoding protocol can be reconsidered by the theory of quantum error correction(QEC). The Hayden-Preskill noise channel $\mathcal{N}_{T \to DB}$ is one kind of the quantum noise channel which attaches an EPR pair to the original state, then time evolves with a random unitary gate and traces out the remaining black hole system. The decoupling condition can be interpreted as a special form of the quantum error correction condition. If the QEC conditon is satisfied, there exists a recovery map which is realized as a decoder. In the theory of QEC, if the QEC condition is satisfied, we can constitute the Petz recovery map in general. We show that the Yoshida-Kitaev decoder is one kind of Petz recovery map in the next section. In this section, we introduce the basic idea of the QEC theory, quantum noise channel and quantum error correction. Then we explain the QEC condition and the Petz recovery map in detail.

4.1 Quantum noise channel

First, we introduce a quantum noise channel $\mathcal{N}$.

Definition 1 (Quantum noise channel). Let $\mathcal{H}$ and $\mathcal{K}$ are finite dimensional Hilbert spaces. Let $B(\mathcal{H})$ is a set of operators which act to the Hilbert space $\mathcal{H}$. A quantum noise channel $\mathcal{N} : B(\mathcal{H}) \to B(\mathcal{K}) \quad (\rho \mapsto \mathcal{N}[\rho])$ is defined as a linear map which satisfies complete positive(CP) and trace preserving(TP). (CP): If ρ is a positive operator($\rho \in B(\mathcal{H})$, $\forall |\psi\rangle \in \mathcal{H}$, $\langle\psi| \rho |\psi\rangle \geq 0$), $\mathcal{N}[\rho]$ is also a positive operator. (TP): $\mathrm{tr}[\rho] = \mathrm{tr}[\mathcal{N}[\rho]]$. We call that kind of the linear map as a CPTP map.

The CPTP map contains operations such as unitary operators, a measument, attaching to some environment, tracing out a environment and so on. Then we introduce the adjoint channel of $\mathcal{N}$ as follows.

Definition 2 (Adjoint channel). Let $\mathcal{N}$ a quantum noise channel. Let $\mathcal{O} \in B(\mathcal{K})$. The adjoint channel $\mathcal{N}^\dagger : B(\mathcal{K}) \to B(\mathcal{H})$ is defined as a linear map which satisfies the following.

$$\mathrm{tr}_\mathcal{K}[\mathcal{N}[\rho]\,\mathcal{O}] = \mathrm{tr}_\mathcal{H}[\rho\,\mathcal{N}^\dagger[\mathcal{O}]].$$

It is easy to show that $\mathcal{N}^\dagger$ is also a CPTP map.

There are two equivalent representations for a quantum noise channel. They are called the Stinespring dilation theorem and the Kraus representation.

4.1.1　Stinespring dilation and Kraus representation

Theorem 1 (Stinespring dilation theorem). *For any quantum channel $\mathcal{N} : B(\mathcal{H}) \to B(\mathcal{K})$, if we prepare environment $\mathcal{H}_{env}$ of appropriate dimensions and some operator $\rho_{env} \in B(\mathcal{H}_{env})$, there exists some unitary $U \in B(\mathcal{H} \otimes \mathcal{H}_{env})$ and $\mathcal{N}$ can be expressed as follows:*

$$\mathcal{N}[\rho] = \mathrm{tr}_{env'}[U(\rho \otimes \rho_{env})U^{\dagger}] \tag{4.1}$$

This theorem tells that the CPTP map can be interpreted as a unitary evolution if we attach an appropriate environment to the state which we consider. The quantum noise channel is also expressed as the Kraus representation as follows and this expression is usually more convenient in the theory of QEC.

Theorem 2 (Kraus representation). *For any quantum channel $\mathcal{N} : B(\mathcal{H}) \to B(\mathcal{K})$, there exists the Kraus operators $\{E_i\}_{1 \leq i \leq dim\mathcal{H}} \in B(\mathcal{H})$ and $\mathcal{N}$ can be expressed as follows:*

$$\mathcal{N}[\rho] = \sum_i E_i \rho E_i^{\dagger} \tag{4.2}$$

When $\mathcal{N}$ is TP, the Kraus operators satisfy the following relation

$$\sum_i E_i^{\dagger} E_i = I \tag{4.3}$$

The last relation is satisfied because

$$\mathrm{tr}[\mathcal{N}[\rho]] = \mathrm{tr}\left[\sum_i E_i \rho E_i^{\dagger}\right] = \mathrm{tr}\left[\sum_i E_i^{\dagger} E_i \rho\right]. \tag{4.4}$$

Here we check that the Kraus representation is satisfied if we assume the Stinespring dilation theorem. We set the state in the environment $\rho_{env} = |e_0\rangle_{env} \langle e_0|$. We can assume this without loss of generality because any mixed state can be purified by considering an appropriate dimensional environment. Then we can construct the Kraus operators in the following way. See also figure 13.

$$\mathcal{N}[\rho] = \mathrm{tr}_{env'}[U(\rho \otimes \rho_{env})U^{\dagger}] \tag{4.5}$$

$$= \sum_{i=1}^{d_{env'}} {}_{env'}\langle e_i| U |e_0\rangle_{env}\, \rho\, {}_{env}\langle e_0| U^{\dagger} |e_i\rangle_{env'} \tag{4.6}$$

$$= \sum_{i=1}^{d_{env'}} E_i \rho E_i^{\dagger} \tag{4.7}$$
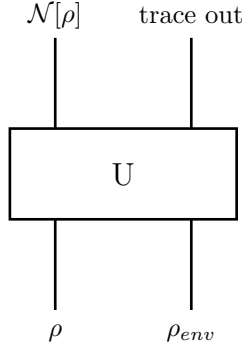
Figure 13: Stinespring dilation theorem can be represented as the form of Kraus representation.

Let (u_{ij}) a unitary matrix. If we act u_{ij} to the Kraus operator E_i, then the result $F_j \equiv \sum_i E_i u_{ij}$ is also the Kraus operator. There is a unitary arbitrariness in the Kraus operators.

$$\begin{aligned}
\sum_j F_j \rho F_j^\dagger &= \sum_{ijk} E_i u_{ij} \rho u_{jk}^\dagger E_k^\dagger \\
&= \sum_i E_i \rho E_i^\dagger \\
&= \mathcal{N}[\rho]
\end{aligned} \tag{4.8}$$

We review the adjoint of Kraus operator here.

$$\begin{aligned}
\text{tr}_\mathcal{K} \left[\mathcal{N}[\rho]\mathcal{O} \right] &= \text{tr}_\mathcal{K} \left[\sum_i E_i \rho E_i^\dagger \mathcal{O} \right] \\
&= \sum_i \text{tr}_\mathcal{H} \left[\rho E_i^\dagger \mathcal{O} E_i \right] \\
&= \text{tr}_\mathcal{H} \left[\rho \sum_i E_i^\dagger \mathcal{O} E_i \right] \\
&= \text{tr}_\mathcal{H} \left[\rho \mathcal{N}^\dagger[\mathcal{O}] \right]
\end{aligned} \tag{4.9}$$

So we conclude that the adjoint channel is represented by the Kraus operator as follows.

$$\mathcal{N}^\dagger[\mathcal{O}] = \sum_i E_i^\dagger \mathcal{O} E_i \tag{4.10}$$

4.2 Quantum error correction

In this subsection, we explain the motivation of the theory of quauntum error correction(QEC) and the simplest example of QEC[19]. When we consider a quantum computation process

or a quantum communication, quantum states are exposed to quantum errors such as bit flip error and erasure error and so on. We should construct the theory where the method to correct the state and recover the original state. That is the main motivation of the theory of QEC. We reviewed the quantum noise in the previous subsection. In this subsection we consider the condition where there exists a recovery map $\mathcal{R} : B(\mathcal{K}) \to B(\mathcal{H})$ which satisifies $\mathcal{R}[\mathcal{N}[\rho]] = \rho$ after some quantum noise $\mathcal{N}$ acts on the initial state ρ. That condition is called the quantum error correction condition(QEC condition). We also study the method to construct the recovery map which recovers the origianal state ρ. The Hayden-Preskill's decoupling condition is interpreted as a QEC condition where the noise channel is the Hayden-Preskill noise channel. First we review the quantum error correcting code(QEC code). If we add redundancy to the original state by some encoding method like adding redundant logical qubits, it becomes easy to recover the original state. We explain the simplest example here. The original state is $|\psi\rangle = a|0\rangle + b|1\rangle$ and we assume a bit flip error which causes a bit flip with a probability $p > 0$. Without adding any redundancy by the QEC coding, the expectation that the result state is $a|0\rangle + b|1\rangle$ is wrong with the probability p. Then we embed the code subspace $\mathcal{H}_{code}$ in which the original state $|\psi\rangle = a|0\rangle + b|1\rangle$ lives to a three qubit Hilbert space $\mathcal{H}_{physical}$ and identify $a|0\rangle + b|1\rangle$ with $a|0_L\rangle + b|1_L\rangle$. Here we identify $|0\rangle$ and $|1\rangle$ to $|0_L\rangle = |000\rangle$ and $|1_L\rangle = |111\rangle$. We write the embedding map $V = V_{code \to physical}$. Let us consider whether we succeed to recover $a|0_L\rangle + b|1_L\rangle = a|000\rangle + b|111\rangle$ with a recovery map $\mathcal{R}$ after the bit flip error to one qubit. The answer is that we can recover the original state by a error detection and a recovery. The error detection is succeeded with the following projection operators:

$$P_0 \equiv |000\rangle\langle000| + |111\rangle\langle111| \tag{4.11}$$

$$P_1 \equiv |100\rangle\langle100| + |011\rangle\langle011| \tag{4.12}$$

$$P_2 \equiv |010\rangle\langle010| + |101\rangle\langle101| \tag{4.13}$$

$$P_3 \equiv |001\rangle\langle001| + |110\rangle\langle110| \tag{4.14}$$

Suppose for example that a bit flip occurs on the second qubit. Then the result becomes $\mathcal{N}[V[\rho]] = a|010\rangle + b|101\rangle \equiv |\psi_{error}\rangle$. In this case, $\langle\psi_{error}|P_2|\psi_{error}\rangle = 1$ and the other measurements lead to 0. We can successfully detect the error with the four projection measurements. Then we can recover the original physical state $a|0_L\rangle + b|1_L\rangle$ with the recovery map of the bit flip operation to the second qubit and finally recover $|\psi\rangle = a|0\rangle + b|1\rangle$ with a decoding map $V^\dagger$. Here we point out that we can recover $|\psi\rangle$ without any information of a and b. The above method can recover one or fewer bit flip error but we cannot recover two or more bit flip error. The probability of two or more bit flip is $p_e = (1-p)^3 + 3p(1-p)^2$ and if $p < \frac{1}{2}$ then $p_e < p$, so the probability of making wrong expectation becomes smaller with the QEC code. The process from the encoding to the decoding is summarized as the following
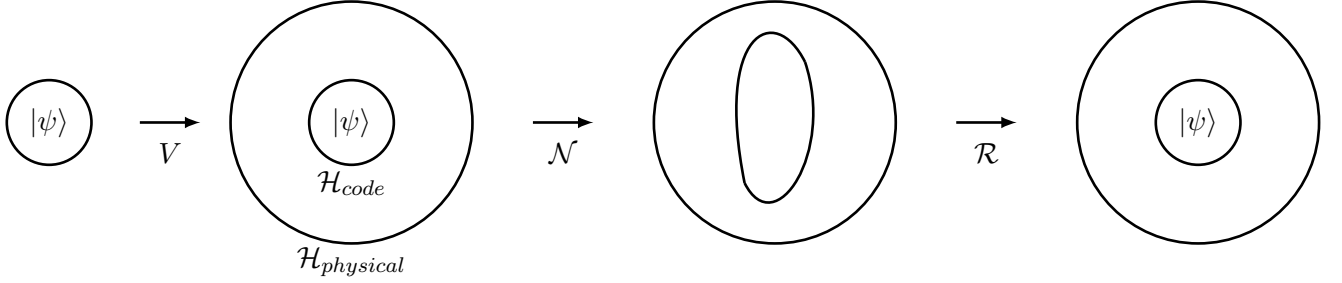
Figure 14: The process of the encoding map V to the physical Hilbert space, a noise channel $\mathcal{N}$ and a recovery map $\mathcal{R}$. We recover $|\psi\rangle$ with the decoding map $V^\dagger$.

equation:

$$V^\dagger \left[\mathcal{R}\left[\mathcal{N}\left[V[\rho]\right]\right]\right] = \rho \quad , \quad \mathcal{R} \circ \mathcal{N} = I \tag{4.15}$$

Here, V is an isometry, satisfying $V^\dagger V = I$. See also the following picture (figure14).

In the above example, we consider the method made of the projection measurement and the recovery. However we can construct a recovery map without checking the result of the projection measurement. Suppose that U_i is a recovery unitary operator corresponding to a projection P_i and $|i\rangle$ is an ancilla state. Then in the following equation, W becomes a recovery map.

$$W|\psi_{error}\rangle \equiv U|\psi_{error}\rangle|0\rangle \equiv \sum_i \left(U_i P_i |\psi_{error}\rangle\right)|i\rangle \tag{4.16}$$

Here, U is unitary and W is an isometry($W^\dagger W = I$).

$$\begin{aligned}
\langle\psi_1|W^\dagger W|\psi_2\rangle &= \sum_{ij} \langle\psi_1|\langle i| P_i^\dagger U_i^\dagger U_j P_j |\psi_2\rangle|j\rangle \\
&= \sum_i \langle\psi_1| P_i^\dagger P_i |\psi_2\rangle \\
&= \sum_i \langle\psi_1| P_i |\psi_2\rangle \\
&= \langle\psi_1|\psi_2\rangle
\end{aligned} \tag{4.17}$$

See also figure 15 for the diagram corresponding to (4.17).

The encoding map V and the noise channel $\mathcal{N}$ must satisfy the QEC condition for the existence of a recovery map $\mathcal{R}$. There are several forms of QEC conditions. We introduce two famous equivalent forms, the Knill-Laflamme conditon and the sufficiency condition. (We call the sufficiency condition just like sufficiency in later discussion.)
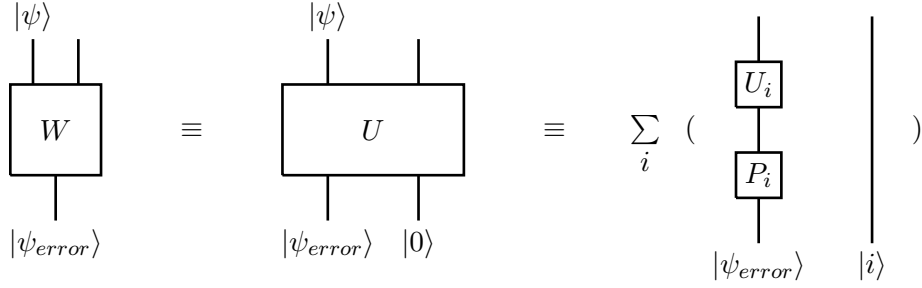
Figure 15: diagram of equation (4.17)

4.2.1 QEC conditon(Knill-Laflamme condition)

Theorem 3 (Knill-Laflamme condition[20]). *For all quantum state $\rho \in B(\mathcal{H}_{code})$, when a quantum channel $\mathcal{N} : B(\mathcal{H}_{code}) \to B(\mathcal{K})$ is expressed with Kraus operators $\{E_i\}$*

$$\mathcal{N}[\rho] = \sum_i E_i \rho E_i^\dagger \,,$$

then the necessary and sufficient condition that there exists a recovery map $\mathcal{R} : B(\mathcal{K}) \to B(\mathcal{H}_{code})$ such that $\mathcal{R}[\mathcal{N}[\rho]] = \rho$ is that the Kraus operators satisfy the following Knill-Laflamme condition:

$$P_{code} E_i^\dagger E_j P_{code} = \alpha_{ij} P_{code} \tag{4.18}$$

Here, P_{code} is a projection operator to a code subspace. (α_{ij}) is some Hermitian matrix. When the Knill-Laflamme condition is satisfied, we call errors $\{E_i\}$ correctable errors.

Proof. $\leftarrow$) First, we show that if we assume the Knill-Laflamme condition, we can construct a recovery map $\mathcal{R}$. α is a Hermitian matrix, so it can be diagonalized to $d = u^\dagger \alpha u$ where u is some unitary matrix. If we use this unitary u and make operators $F_k \equiv \sum_i E_i u_{ik}$, the adjoint operators satisfy $F_k^\dagger = \sum_i u_{ki}^\dagger E_i^\dagger$. We showed that $\{F_i\}$ can also be used as Kraus operators, which are equivalent to $\{E_i\}$. We get a simpler diagonalized form of the Knill-Laflamme condition by using $\{F_i\}$.

$$
\begin{aligned}
P_{code} F_k^\dagger F_l P_{code} &= \sum_{ij} u_{ki}^\dagger u_{jl} P_{code} E_i^\dagger E_j P_{code} \\
&= \sum_{ij} u_{ki}^\dagger \alpha_{ij} u_{jl} P_{code} \\
&= d_{kl} P_{code}
\end{aligned}
\tag{4.19}
$$

Then we consider the operational meaning of F_k. From a polar decomposition[3], $F_k P_{code}$ is decomposed as the following.

$$\begin{aligned}
F_k P_{code} &= U_k \sqrt{P_{code} F_k^\dagger F_k P_{code}} \\
&= \sqrt{d_{kk}} U_k P_{code} \\
&= \sqrt{d_{kk}} U_k P_{code} U_k^\dagger U_k \\
&= \sqrt{d_{kk}} P_k U_k
\end{aligned} \tag{4.21}$$

Here, we difine P_k as

$$P_k \equiv U_k P_{code} U_k^\dagger = \frac{1}{\sqrt{d_{kk}}} F_k P_{code} U_k^\dagger \tag{4.22}$$

P_k is a projection operator because $P_k^\dagger = P_k$ and $P_k^2 = P_k$ are satisfied, so $\{P_k\}$ satisfy $\sum_k P_k = I$. From calculation 4.21, we can interpret F_k as an operator which rotates a state $|\psi\rangle = \sqrt{\rho} \in \mathcal{H}_{code}$ to $U_k |\psi\rangle \in \mathcal{H}_{physical}$ and projects to the subspace $\mathcal{H}_k$ corresponding to each noise F_k by using the projection operator P_k.

$$F_k |\psi\rangle = \sqrt{d_{kk}} P_k U_k |\psi\rangle \in \mathcal{H}_k \tag{4.23}$$

We see that subspaces $\{\mathcal{H}_k\}$ do not have overlap with each other.

$$P_k P_l = P_k^\dagger P_l = \frac{U_k P_{code} F_k^\dagger F_l P_{code} U_l}{\sqrt{d_{kk} d_{ll}}} = 0 \tag{4.24}$$

We see that if $\mathcal{N}$ acts to ρ, the state will go to some subspace $\mathcal{H}_k$ corresponding to the label k which has no overlap with the other subspaces.

Rather, we can recover the original state ρ by constructing a recovery map in the following way. The essence is returning by $U_k^\dagger$ to the original code subspace $\mathcal{H}_{code}$. For $\mathcal{O} \in B(\mathcal{K})$, suppose a recovery map $\mathcal{R} : B(\mathcal{K}) \to B(\mathcal{H})$:

$$\mathcal{R}[\mathcal{O}] \equiv \sum_k U_k^\dagger P_k \mathcal{O} P_k U_k \tag{4.25}$$

---

[3]From the polar decomposition, any linear operator A is decomposed by using a unitary operator U and positive operators J, K as follows:

$$A = UJ = KU \tag{4.20}$$

Here, J and K are defined as $J = \sqrt{A^\dagger A}$, $K = \sqrt{AA^\dagger}$. We call UJ and KU, left polar decomposition and right polar decomposition, respectively.

Then we can show that we recover ρ by this recovery map.

$$
\begin{aligned}
\mathcal{R}[\mathcal{N}[\rho]] &= \sum_{kl} U_k^\dagger P_k F_l \rho F_l^\dagger P_k U_k \\
&= \sum_{kl} U_k^\dagger P_k^\dagger F_l P_{code} \rho P_{code} F_l^\dagger P_k U_k \\
&= \frac{1}{d_{kk}} \sum_{kl} U_k^\dagger U_k P_{code} F_k^\dagger F_l P_{code} \rho P_{code} F_l^\dagger F_k P_{code} U_k^\dagger U_k \\
&= \frac{1}{d_{kk}} \sum_{kl} d_{kk} \delta_{kl} \rho d_{kk} \delta_{kl} \\
&= \sum_l d_{ll} \rho \\
&= \rho
\end{aligned}
\tag{4.26}
$$

In the third line, we used $P_k^\dagger = \frac{1}{\sqrt{d_{kk}}} U_k P_{code} F_k^\dagger$. In the fourth line, we use the Knill-Laflamme condition. In the final line, we use the fact[4] that $\sum_l d_{ll} = \sum_l p_l = 1$. Here we define p_l as the diagonal element of d.

$\rightarrow$) Next, we show that if a recovery map exists, the noise channel $\mathcal{N}$ and its Kraus operators satisfy the Knill-Laflamme condition. Suppose $\rho \in B(\mathcal{H}_{code})$, then

$$
\mathcal{N}[\rho] = \mathcal{N}[P_{code} \rho P_{code}]
\tag{4.28}
$$

Since a recovery map exists,

$$
\mathcal{R}[\mathcal{N}[\rho]] = P_{code} \rho P_{code}
\tag{4.29}
$$

Since $\mathcal{R}$ is a CPTP map, it can be expressed with the Kraus operators and satisfies the TP relation.

$$
\mathcal{R}[\mathcal{O}] = \sum_i R_i \mathcal{O} R_i^\dagger, \quad \sum_i R_i^\dagger R_i = I
\tag{4.30}
$$

In the Kraus representation, equation (4.29) becomes

$$
\sum_{ij} R_j E_i P_{code} \rho P_{code} E_i^\dagger R_j^\dagger = P_{code} \rho P_{code}
\tag{4.31}
$$

Then we get the equations as follows:

$$
R_j E_i P_{code} = c_{ji} P_{code}, \quad P_{code} E_i^\dagger R_k^\dagger = c_{ik}^\dagger P_{code}
\tag{4.32}
$$

---

[4]Since $\mathcal{N}$ satisfies TP, by using (4.21),

$$
P_{code} = \sum_i P_{code} F_i^\dagger F_i P_{code} = \sum_i p_i P_{code}
\tag{4.27}
$$

is satisfied and so we conclude $\sum_i p_i = 1$.

From these equations,

$$\sum_k P_{code} E_i^\dagger R_k^\dagger R_k E_j P_{code} = \sum_k c_{ik}^\dagger c_{kj} P_{code} \tag{4.33}$$

By using the TP relation of the recovery map $\sum_k R_k^\dagger R_k = I$ in the left hand side of the last equation, we get

$$\begin{aligned} P_{code} E_i^\dagger E_j P_{code} &= (c^\dagger c)_{ij} P_{code} \\ &= \alpha_{ij} P_{code} \end{aligned} \tag{4.34}$$

We write $\alpha = c^\dagger c$ and this matrix is an Hermitian matrix. In the end, we derived the Knill-Laflamme condition(eq.(4.34)).

$\square$

4.2.2 Sufficiency

Another form of the QEC condition is sufficiency[21], which is equivalent to the Knill-Laflamme condition. We give the statement of the theorem without proof. See also appendixA for more detailed discussion on the relative entropy and sufficiency.

Theorem 4 (Sufficiency[21]). *For all quantum state ρ, $\sigma \in B(\mathcal{H}_{code})$, the necessary and sufficient condition that there exists a recovery map $\mathcal{R} : B(\mathcal{K}) \to B(\mathcal{H}_{code})$ such that $\mathcal{R}[\mathcal{N}[\rho]] = \rho$ is that the relative entropy between ρ and σ satisfies the following equation(sufficiency):*

$$S(\rho||\sigma) = S(\mathcal{N}[\rho]\,||\,\mathcal{N}[\sigma]) \tag{4.35}$$

Here, the relative entropy between ρ and σ is defined as

$$S(\rho||\sigma) = \mathrm{tr}[\rho(\log\rho - \log\sigma)] \tag{4.36}$$

When the above equation is satisfied, $\mathcal{N}$ constructs so-called "sufficient algebra".

$S(\rho||\sigma) \geq 0$ defines the distance between the quantum information ρ and σ. It is a quantum extension of the classical relative entropy:

$$S(p,q) = \sum_i p_i(\log p_i - \log q_i) \tag{4.37}$$

Here, $p = (p_1, p_2, \cdots, p_n)$ and $q = (q_1, q_2, \cdots, q_n)$ are probability distributions. H. Umegagi made great progress in applying operator algebra to the relative entropy and construct the theory of quantum relative entropy[11], which is the fundamental of quantum information theory especially in continuous, infinite dimensional quantum information theory. When ρ and σ are close to each other, the relative entropy comes down to the Fisher information.

According to the Uhlmann's monotonicity theorem [21](See also appendix A), for the CPTP map $\mathcal{N}$, the relative entropy $S(\rho||\sigma)$ monotonically decreases in general:

$$S(\rho||\sigma) \geq S(\mathcal{N}[\rho]||\mathcal{N}[\sigma]) \tag{4.38}$$

We can interpret that the noise channel acts as a coarse graining and the quantum information becomes blurry due to the noise because the relative entropy measures the uncertainty between two kinds of information. The derivation from the success of QEC to the conditon of sufficiency is easy to check. If there exists a recovery map $\mathcal{R} : B(\mathcal{K}) \to B(\mathcal{H})$ such that $\mathcal{R}[\mathcal{N}[\rho]] = \rho$, since $\mathcal{R}$ is a CPTP map,

$$S(\rho||\sigma) \geq S(\mathcal{N}[\rho]||\mathcal{N}[\sigma]) \geq S(\mathcal{R}[\mathcal{N}[\rho]]||\mathcal{R}[\mathcal{N}[\sigma]]) \tag{4.39}$$

is satisfied. Since the first term and the third term are the same, sifficiency

$$S(\rho||\sigma) = S(\mathcal{N}[\rho]||\mathcal{N}[\sigma]) \tag{4.40}$$

is satisfied for the noise channel $\mathcal{N}$.

4.2.3   Relations between QEC conditions

Here, we check the relations between QEC conditions. First, we show that sufficiency is satisfied in an assumption of the Knill-Laflamme condition. We use a replica trick

$$\mathrm{tr}[\rho \log \rho] = \lim_{n \to 1} \mathrm{tr}[\rho^n \log \rho] = \lim_{n \to 1} \partial_n \mathrm{tr}[\rho^n] \tag{4.41}$$

in calculating the relative entropy.

$$
\begin{aligned}
S(\mathcal{N}[\rho]||\mathcal{N}[\sigma]) &= \mathrm{tr}[\mathcal{N}[\rho](\log \mathcal{N}[\rho] - \log \mathcal{N}[\sigma])] \\
&= \lim_{n \to 1} \partial_n [\mathrm{tr}[(\mathcal{N}[\rho])^n] - \mathrm{tr}\big[\mathcal{N}[\rho](\mathcal{N}[\sigma])^{n-1}\big]]
\end{aligned} \tag{4.42}
$$

By using the Knill-Laflamme condition, the first term becomes

$$
\begin{aligned}
\mathrm{tr}[(\mathcal{N}[\rho])^n] &= \mathrm{tr}\left[\left(\sum_i E_i \rho E_i^\dagger\right)^n\right] \\
&= \mathrm{tr}\left[\sum_{i_1, i_2, \cdots, i_n} E_{i_1} \rho E_{i_1}^\dagger E_{i_2} \rho E_{i_2}^\dagger \cdots E_{i_n} \rho E_{i_n}^\dagger\right] \\
&= \mathrm{tr}\left[\sum_{i_1, i_2, \cdots, i_n} \rho E_{i_1}^\dagger E_{i_2} \rho E_{i_2}^\dagger \cdots E_{i_n} \rho E_{i_n}^\dagger E_{i_1}\right] \\
&= \sum_{i_1, i_2, \cdots, i_n} \alpha_{i_1 i_2} \alpha_{i_2 i_3} \cdots \alpha_{i_n i_1} \mathrm{tr}[\rho^n] \\
&= \mathrm{tr}[\alpha^n] \, \mathrm{tr}[\rho^n]
\end{aligned} \tag{4.43}
$$

In the third line, we use the cyclic property of the trace. By similarly calculating the second term of (4.42),

$$
\begin{aligned}
S(\mathcal{N}[\rho]||\mathcal{N}[\sigma]) &= \lim_{n \to 1} \partial_n [\text{tr}[\alpha^n](\text{tr}[\rho^n] - \text{tr}[\rho\sigma^{n-1}])] \\
&= \lim_{n \to 1} [\partial_n \text{tr}[\alpha^n] \cdot (\text{tr}[\rho^n] - \text{tr}[\rho\sigma^{n-1}]) + \text{tr}[\alpha^n] \cdot \partial_n (\text{tr}[\rho^n] - \text{tr}[\rho\sigma^{n-1}])] \\
&= \text{tr}[\alpha] \cdot S(\rho||\sigma)
\end{aligned}
$$

$$(4.44)$$

From the Knill-Laflamme condition,

$$
\sum_i P_{code} E_i^\dagger E_i P_{code} = \sum_i \alpha_{ii} P_{code} \tag{4.45}
$$

The trace preserving property of $\mathcal{N}$ leads to $\sum_i E_i^\dagger E_i = I$, so we get

$$
\text{tr}[\alpha] = \sum_i \alpha_{ii} = 1 \tag{4.46}
$$

Thus we get the sufficiency $S(\mathcal{N}[\rho]||\mathcal{N}[\sigma]) = S(\rho||\sigma)$.

Next, we show the relation between the Knill-Laflamme condition and the decoupling principle, which we introduced in the Hayden-Preskill protocol. The Knill-Laflamme condition leads to the decoupling between reference system which is isomorphic with the code subspace and the environment system. In the Hayden-Preskill setup, the situation that the quantum information thrown into the code subspace T completely flows into the radiation systems D, B is equivalent to the decoupling between the reference system R which has the same information as the code subspace with an EPR pair and the remaining black hole system C. Here, before a time evolution with a random unitary, $\mathcal{H}_{phisical}$ is TAB ($\mathcal{H}_{code}$ is T) and the environment $\mathcal{H}_{env}$ does not exist. After a time evolution, $\mathcal{H}_{physical}$ is DB and $\mathcal{H}_{env}$ is C. (See diagram of figure 7.) However the environment is contained in the physical Hilbert space, we distinguish the subspace to be traced out from $\mathcal{H}_{physical}$ and tell "environment" $\mathcal{H}_{env}$. By preparing $\mathcal{H}_{ref}$ isomorphic to $\mathcal{H}_{code}$, the whole system after the noise channel becomes

$$
\begin{aligned}
|\Psi\rangle &= \frac{1}{\sqrt{d_{code}}} \sum_{i=1}^{d_{code}} \sum_m |i\rangle_{ref} \, E_m \, |\psi_i\rangle_{physical} \, |e_m\rangle_{env} \\
&= (I_{ref} \otimes U_\mathcal{N}) \left[\frac{1}{\sqrt{d_{code}}} \left(\sum_{i=1}^{d_{code}} |i\rangle_{ref} \, |\psi_i\rangle_{physical} \right) |e_0\rangle_{env} \right]
\end{aligned}
$$

$$(4.47)$$

By defining $\rho_{ref,env}, \rho_{ref}, \rho_{env}$ as

$$
\rho_{ref,env} = \text{tr}_{physical}[|\Psi\rangle \langle\Psi|] \tag{4.48}
$$

$$
\rho_{ref} = \text{tr}_{env}[\rho_{ref,env}], \quad \rho_{env} = \text{tr}_{ref}[\rho_{ref,env}] \tag{4.49}
$$

and using the Knill-Laflamme condition, we get the decoupling between the reference and the environment:

$$
\begin{aligned}
\rho_{ref,env} &= \frac{1}{d_{code}} \sum_{ij} \sum_{mn} |i\rangle_{ref} \langle j| \otimes |e_m\rangle_{env} \langle e_n| \cdot {}_{physical}\langle \psi_j| E_n^\dagger E_m |\psi_i\rangle_{physical} \\
&= \left(\frac{1}{d_{code}} \sum_i |i\rangle_{ref} \langle i| \right) \otimes \left(\sum_{mn} \alpha_{mn} |e_m\rangle_{env} \langle e_n| \right) \\
&= \rho_{ref} \otimes \rho_{env}
\end{aligned}
\tag{4.50}
$$

We can show the opposite in the similar manner. In conclusion, the Knill-Laflamme condition is equivalent to the decoupling principle.

4.3 Petz recovery map

From both the Knill-Laflamme condition and the sufficiency, it is derived that the Petz recovery map

$$
\mathcal{R}_{\sigma,\mathcal{N}}^{Petz}[\mathcal{O}] = \sigma^{\frac{1}{2}} \mathcal{N}^\dagger \left[\mathcal{N}[\sigma]^{-\frac{1}{2}} \mathcal{O} \mathcal{N}[\sigma]^{-\frac{1}{2}} \right] \sigma^{\frac{1}{2}}
\tag{4.51}
$$

can be used as a recovery map for the quantum noise channel $\mathcal{N}$. Here, $\mathcal{O} \in B(\mathcal{K})$ and $\mathcal{R}_{\sigma,\mathcal{N}}^{Petz} : B(\mathcal{K}) \to B(\mathcal{H})$. σ is an arbitrary state in the code subspace: $\forall \sigma \in B(\mathcal{H}_{code})$.

4.3.1 Construction of Petz map

We derive the Petz recovery map from the quantum information discussion used in the proof of the Knill-Laflamme condition. This is the method developed by Barnum and Knill[22]. In eq.(4.21), if we define $w_k \equiv P_k U_k$ then

$$
F_k P_{code} = \sqrt{p_k} P_k U_k = \sqrt{p_k} w_k
\tag{4.52}
$$

Here, $d_{kl} = p_k \delta_{kl}$. By using the expression of w_k and $w_k^\dagger$:

$$
w_k = P_k U_k = \frac{1}{\sqrt{p_k}} F_k P_{code} = U_k P_{code}
\tag{4.53}
$$

$$
w_k^\dagger = U_k^\dagger P_k^\dagger = U_k^\dagger P_k = \frac{1}{\sqrt{p_k}} P_{code} F_k^\dagger = P_{code} U_k^\dagger
\tag{4.54}
$$

and eq.(4.24), we find that $\{w_k\}$ are isometries.

$$
w_k^\dagger w_l = \delta_{kl} P_{code}
\tag{4.55}
$$

From the calculation of (4.26), we found that $\mathcal{R}$ in eq.(4.25) realizes the recovery map. Eq.(4.25) can be written as

$$
\mathcal{R}[\mathcal{O}] = \sum_j w_j^\dagger \mathcal{O} w_j
\tag{4.56}
$$

We repeat the recoverability check here. Since $\mathcal{N}$ can be expressed as

$$
\begin{aligned}
\mathcal{N}[\rho] &= \mathcal{N}[P_{code}\rho P_{code}] \\
&= \sum_i F_i P_{code}\rho P_{code} F_i^\dagger \\
&= \sum_i p_i w_i \rho w_i^\dagger \quad,
\end{aligned}
\tag{4.57}
$$

we calculate

$$
\begin{aligned}
\mathcal{R}[\mathcal{N}[\rho]] &= \sum_{ij} p_i w_j^\dagger w_i \rho w_i^\dagger w_j \\
&= \sum_j p_j P_{code}\rho P_{code} \\
&= \rho
\end{aligned}
\tag{4.58}
$$

In the last line, we used $\sum_i p_i = 1$ from the TP property of $\mathcal{N}$:

$$
P_{code} = \sum_i P_{code} F_i^\dagger F_i P_{code} = \sum_i p_i w_i^\dagger w_i = \sum_i p_i P_{code}
\tag{4.59}
$$

Suppose σ is an arbitrary state in the code subspace $\sigma \in B(\mathcal{H}_{code})$. Then $P_{code}\sigma P_{code} = \sigma$ is satisfied. In fact, $w_j^\dagger$ is expressed as follows.

$$
w_j^\dagger = \sigma^{\frac{1}{2}} F_j^\dagger \mathcal{N}[\sigma]^{-\frac{1}{2}}
\tag{4.60}
$$

We give a proof:

$$
\begin{aligned}
(rhs) &= \sigma^{\frac{1}{2}} P_{code} F_j^\dagger \left(\sum_i p_i w_i \sigma w_i^\dagger \right)^{-\frac{1}{2}} \\
&= \sigma^{\frac{1}{2}} w_j^\dagger \sqrt{p_j} \left(\sum_i \frac{1}{\sqrt{p_i}} w_i \sigma^{-\frac{1}{2}} w_i^\dagger \right) \\
&= \sigma^{\frac{1}{2}} P_{code} \sigma^{-\frac{1}{2}} w_j^\dagger \\
&= w_j^\dagger
\end{aligned}
\tag{4.61}
$$

To derive the second line, we squared the second line, acted to the first line and used $\sum_i P_i = I$. From eq.(4.60), we get

$$
w_j = \mathcal{N}[\sigma]^{-\frac{1}{2}} F_j \sigma^{\frac{1}{2}}
\tag{4.62}
$$

Substituting $w_j^\dagger, w_j$ to eq.(4.56), we get the form of the Petz recovery map.

$$
\begin{aligned}
\mathcal{R}[\mathcal{O}] &= \sum_j w_j^\dagger \mathcal{O} w_j \\
&= \sum_j \sigma^{\frac{1}{2}} F_j^\dagger \mathcal{N}[\sigma]^{-\frac{1}{2}} \mathcal{O} \mathcal{N}[\sigma]^{-\frac{1}{2}} F_j \sigma^{\frac{1}{2}} \\
&= \sigma^{\frac{1}{2}} \mathcal{N}^\dagger \left[\mathcal{N}[\sigma]^{-\frac{1}{2}} \mathcal{O} \mathcal{N}[\sigma]^{-\frac{1}{2}} \right] \sigma^{\frac{1}{2}} \\
&= \mathcal{R}_{\sigma,\mathcal{N}}^{Petz}[\mathcal{O}]
\end{aligned}
\tag{4.63}
$$

4.3.2 Derivation of Petz map with operator algebra

In this section, we rederive the Petz recovery map with operator algebra. This is the derivation by Petz[10, 21, 23], which we discuss in more detail in Appendix A. Sufficiency $S(\rho||\sigma) = S(\mathcal{N}[\rho]||\mathcal{N}[\sigma])$ is satisfied if and only if

$$\rho^{it}\sigma^{-it} = \mathcal{N}^\dagger \left[\mathcal{N}[\rho]^{it} \mathcal{N}[\sigma]^{-it} \right] , \ \forall t \in \mathbb{R} \tag{4.64}$$

We get the sufficiency by acting $-i\frac{d}{dt}$ and $t \to 0$ on both sides of this equation. For some unitary U,

$$S(U\rho U^\dagger || U\sigma U^\dagger) = S(\rho||\sigma) \tag{4.65}$$

is satisfied, so we can change the sufficiency relation for a little bit:

$$S(\sigma||\sigma^{is_1}\rho\sigma^{-is_1}) = S(\mathcal{N}[\sigma]||\mathcal{N}[\sigma]^{is_2}\mathcal{N}[\rho]\mathcal{N}[\sigma]^{-is_2}) \quad , \forall s_1, s_2 \in \mathbb{R} \tag{4.66}$$

By the similar manner as deriving eq.(4.64) from the sufficiency, we can derive

$$\sigma^{is_1}\rho^{it}\sigma^{-i(t+s_1)} = \mathcal{N}^\dagger \left[\mathcal{N}[\sigma]^{is_2}\rho^{it}\mathcal{N}[\sigma]^{-i(t+s_2)} \right] \tag{4.67}$$

By analytic continuation $t \to -i$, $s_1 = s_2 \to s + \frac{i}{2}$, we get

$$\sigma^{is-\frac{1}{2}}\rho\sigma^{-is-\frac{1}{2}} = \mathcal{N}^\dagger \left[\mathcal{N}[\sigma]^{is-\frac{1}{2}}\mathcal{N}[\rho]\mathcal{N}[\sigma]^{-is-\frac{1}{2}} \right] \tag{4.68}$$

By continuing the calculation,

$$
\begin{aligned}
\rho &= \sigma^{-is}\sigma^{\frac{1}{2}}\mathcal{N}^\dagger \left[\mathcal{N}[\sigma]^{is-\frac{1}{2}}\mathcal{N}[\rho]\mathcal{N}[\sigma]^{-is-\frac{1}{2}} \right] \sigma^{\frac{1}{2}}\sigma^{is} \\
&= \sigma^{-is}\mathcal{R}_{\sigma,\mathcal{N}}^{Petz} \left[\mathcal{N}[\sigma]^{is}\mathcal{N}[\rho]\mathcal{N}[\sigma]^{-is} \right] \sigma^{is} \\
&= \mathcal{R}_{\sigma,\mathcal{N}}^{Rotated\,Petz}[\mathcal{N}[\rho]]
\end{aligned}
\tag{4.69}
$$

We defined the rotated Petz map:

$$\mathcal{R}_{\sigma,\mathcal{N}}^{Rotated\,Petz}[\mathcal{O}] \equiv \sigma^{-is}\mathcal{R}_{\sigma,\mathcal{N}}^{Petz} \left[\mathcal{N}[\sigma]^{is}\,\mathcal{O}\,\mathcal{N}[\sigma]^{-is} \right] \sigma^{is} \tag{4.70}$$

It reduces to the Petz map by taking $s = 0$. From here, we derived the Petz recovery map from the sufficiency as the QEC condition.

4.4 Petz lite – chaotic case

The Petz recovery map is too complicated to understand the operational meaning directly. However in some chaotic systems such as the Hayden-Preskill setup and the SYK model, the Petz recovery map is known to reduce to a simpler form "the Petz lite":

$$\mathcal{R}^{\text{Lite}}[\mathcal{O}] = c\mathcal{N}^\dagger[\mathcal{O}] \tag{4.71}$$

c is some normalization constant. In next section, we study the recovery map for the Hayden-Preskill noise channel. We expect that the Petz lite realizes a recovery. In this section, we explain why the Petz map reduces to the simpler Petz lite in scrambling channel[4]. When scrambling is realized, Kraus operators are expected to realize a flat spectrum and the diagonal element of the diagonalized Knill-Laflamme condition is the same with each other. If we repeat eq.(4.19) for convenience,

$$P_{code}F_i^\dagger F_j P_{code} = d_{ij}P_{code} = p_i\delta_{ij}P_{code} \tag{4.72}$$

$\{p_i\}$ realize a flat spectrum:

$$p_1 = p_2 = \cdots = p_n = \frac{1}{d_{env}} \tag{4.73}$$

In this case, the noise channel and the recovery map satisfy

$$\mathcal{N}[P_{code}\rho P_{code}] = \sum_i p_i w_i \rho w_i^\dagger = \frac{1}{d_{env}}\sum_i w_i \rho w_i^\dagger \tag{4.74}$$

$$\begin{aligned} \mathcal{R}[\mathcal{O}] &= \sum_i w_i^\dagger \mathcal{O} w_i \\ &= d_{env}\sum_i P_{code}F_i^\dagger \mathcal{O} F_i P_{code} \\ &= d_{env}P_{code}\mathcal{N}^\dagger[\mathcal{O}]P_{code} \end{aligned} \tag{4.75}$$

This is the Petz lite.

We can derive the Petz lite from the operator algebra method. If in eq.(4.64), we take the analytic continuation $t = -i$ and take $\sigma \to I_{code} = P_{code}$, we get

$$\rho = P_{code}\mathcal{N}^\dagger \left[\mathcal{N}[\rho]\mathcal{N}[I_{code}]^{-1} \right] P_{code} \tag{4.76}$$

If we take $\mathcal{N}[I_{code}]$ to a flat spectrum: $\mathcal{N}[I_{code}] = \frac{1}{d_{env}}I_{supp\,\mathcal{N}[\rho]}$, we get the Petz lite

$$\rho = d_{env}P_{code}\mathcal{N}^\dagger[\mathcal{N}[\rho]]P_{code} \tag{4.77}$$

5 Recovery map for the Hayden-Preskill channel

The Hayden-Preskill setup is a tractable toy model for studying information flow in evaporating black holes. The setup consists of a black hole A that has been emitting Hawking radiation B. We are particularly interested in the system after the Page time where the black hole has emitted more than half of its original entropy [5], therefore approximately forming a maximally entangled state $|\text{EPR}\rangle_{AB}$. Suppose Alice throws a quantum state ρ_T (often called a diary) into this old black hole. Then, as the black hole further evaporates $A \to C + D$ by emitting late Hawking radiation D, information thrown into the black hole will eventually appear in total Hawking radiation DB. Here, we denoted by C the remaining black hole after emitting the late radiation D, see the left panel of figure 16. The analysis of Hayden and Preskill [6] showed that the diary appears in Hawking radiation almost immediately, namely after the scrambling time.

To see this, it is useful to introduce an additional system called reference R and form a maximally entangled state $|\text{EPR}\rangle_{RT}$ with the diary T. Then, in this setup, the initial condition of the process is $|\text{EPR}\rangle_{RT} \otimes |\text{EPR}\rangle_{AB}$.

Owing to its chaotic dynamics, information of the diary thrown into the black hole gets scrambled and spreads over the entire degrees of freedom. The resulting state is given by

$$|\Psi_{HP}\rangle = (I_R \otimes U_{T,A\to C,D} \otimes I_B) |\text{EPR}\rangle_{R,T} \otimes |\text{EPR}\rangle_{A,B}, \tag{5.1}$$

where I_R and I_B are identities in R and B respectively, and $U_{T,A\to C,D}$ is a random unitary matrix from A, T to C, D, which models the chaotic dynamics of the black hole. By finding the Hilbert space with which R is mostly entangled, one can find where information of the original diary is in the final time slice. See again the left panel of figure 16.

The surprising result of HP is summarized in the following inequality,

$$\overline{\|\rho_{RC} - \rho_R \otimes \rho_C\|_1^2} \leq \left(\frac{d_T}{d_D}\right)^2, \tag{5.2}$$

where $\|A\|_1 = \text{tr}\sqrt{A^\dagger A}$, $\rho_{RC}, \rho_R, \rho_C$ are the reduced density matrices of (5.1) on the indicated subsystems, d_D, d_T are the Hilbert space dimensions of subsystems D and T respectively, and in the left hand side we take average over random unitaries. This inequality (5.2) implies that if one collects a sufficient number of late Hawking quanta so that $d_D \gg d_T$ the system of the remaining black hole and the reference becomes no longer correlated $\rho_{RC} = \rho_R \otimes \rho_C$, and therefore the information of the diary has to be encoded in Hawking radiation DB.

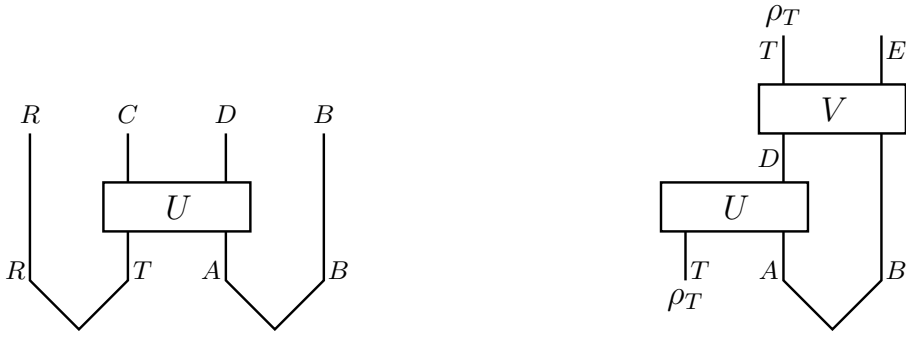[5] We follow the notation of Yoshida-Kitaev [18].

Figure 16: **Left**: Hayden-Preskill setup, corresponding to state (5.1). **Right**: Its decoder.

This result is also natural from the viewpoint of the framework of quantum error correction[6]. A quantum error correcting code is a scheme to protect quantum states (logical states) in code subspace H_{code} against various errors. Such an error is mathematically modeled by a CPTP map called quantum channel $\mathcal{N}$. The basic idea of quantum error correction is protecting these quantum states in code subspace H_{code} by embedding it to the larger Hilbert space, often called physical Hilbert space H_{phys}. In the HP protocol, the Hilbert space of the diary H_T corresponds to H_{code} in QEC, and H_{phys} is H_{DB}. The quantum channel $\mathcal{N} : T \to DB$, is obtained by tracing out the remaining black hole and the reference system degrees of freedom C and R from $|\Psi_{HP}\rangle$ in (5.1) with replacing the reference state $|\text{EPR}\rangle_{R,T}$ by $\sqrt{d_T \rho_T} \, |\text{EPR}\rangle_{R,T}$ (ρ_T is an input state),

$$\mathcal{N}_{T \to D,B}[\rho_T] = \text{tr}_C \left[(U_{T,A \to C,D} \otimes I_B)(\rho_T \otimes |\text{EPR}\rangle_{A,B}\langle\text{EPR}|)(U^\dagger_{T,A \to C,D} \otimes I_B) \right]$$

$$= \frac{1}{d_B} \sum_{\tilde{D},\tilde{D}'=1}^{d_D} \sum_{\tilde{B},\tilde{B}'=1}^{d_B} \left|\tilde{D}\right\rangle_D \left\langle\tilde{D}'\right| \otimes \left|\tilde{B}\right\rangle_B \left\langle\tilde{B}'\right| \sum_{C=1}^{d_C} \sum_{\tilde{T},\tilde{T}'=1}^{d_T} U_{C,\tilde{D};\tilde{T},\tilde{B}} \, (\rho_T)_{\tilde{T}\tilde{T}'} \, U^\dagger_{C,\tilde{D}';\tilde{T}',\tilde{B}'}.$$

(5.3)

We call this quantum channel the HP channel.

Then, a general theorem of QEC[7] tells us that the decoupling condition is equivalent to the existence of a recovery map $\mathcal{R} : DB \to T$ which satisfies

$$\mathcal{R}[\mathcal{N}[\rho_T]] = \rho_T \quad \forall \rho_T \in H_T. \tag{5.4}$$

This again implies that the information of the diary is recoverable from Hawking radiation DB. See the right panel of figure 16. Moreover, the concrete expression of the recovery map is known [9], and is called the Petz recovery map

$$\mathcal{R}^{\text{Petz}}_{\sigma,\mathcal{N}}[\tau] = \sigma^{\frac{1}{2}} \mathcal{N}^\dagger [(\mathcal{N}[\sigma])^{-\frac{1}{2}} \tau (\mathcal{N}[\sigma])^{-\frac{1}{2}}] \sigma^{\frac{1}{2}}. \tag{5.5}$$

---

[6]We note that the possible maximum number of late Hawking radiation d_D is given by the input for the Haar random unitary, implying $d_D \leq d_T d_B$. Due to this bound, the combination d_T/d_D can not be 0, but at most $1/d_B$. Thus, the exact equality does not hold $\rho_{RC} = \rho_R \otimes \rho_C$, as long as d_B is finite. This means that strictly speaking, the recovery of the diary from Hawking radiation is, at best, approximate. However, for a sufficiently large dimension of the early radiation, $d_B \gg 1$, we can almost ignore the deviation from the exact factorization of ρ_{RC} for late times.

[7]See, e.g., [24, 25] for the theorem.

where σ is a full rank arbitrary density matrix on the code subspace H_{code}. $\mathcal{N}^{-1/2}$ factor of the Petz recovery map is difficult to compute in general. One way for doing this is, as in [4] first making the replacement $\mathcal{N}^{-1/2} \to \mathcal{N}^n$, where n is a positive integer, computing it for all n, then taking analytic continuation $n \to -\frac{1}{2}$. Also, the $\mathcal{N}^{-1/2}$ part is preventing us from having an operational meaning of the map.

However, in systems exhibiting quantum chaos, we expect that the recovery map gets simplified, because $\mathcal{N}[\sigma]$ has a flat spectrum, therefore the approximation $\mathcal{R} \sim \mathcal{N}^\dagger$ appears to be possible[8]. If this is the case, since $\rho \sim \mathcal{N}^\dagger[\mathcal{N}[\rho]]$ for arbitrary density matrix ρ in the code subspace, therefore the relative entropy between them $S(\rho||\mathcal{N}^\dagger[\mathcal{N}[\rho]])$ vanishes.

For the HP channel, the adjoint HP channel $\mathcal{N}^\dagger$ is given by

$$
\begin{aligned}
\mathcal{N}^\dagger_{D,B \to T}[\mathcal{O}_{DB}] &= \text{tr}_{A,B} \left[|\text{EPR}\rangle_{A,B} \langle \text{EPR}| \, (U^\dagger_{T,A \to C,D} \, \mathcal{O}_{DB} \, U_{T,A \to C,D}) \right] \\
&=_{A,B} \langle \text{TFD}| \, (U^\dagger_{T,A \to C,D} \otimes I_B) \, (\mathcal{O}_{DB} \otimes I_C) \, (U_{T,A \to C,D} \otimes I_B) \, |\text{TFD}\rangle_{A,B} \, .
\end{aligned}
\tag{5.6}
$$

Here, the adjoint channel is defined by the relation[9]

$$
\text{tr}_{D,B} \left[\mathcal{N}_{T \to D,B}[\rho_T] \, O_{DB} \right] = \text{tr}_T \left[\rho_T \, \mathcal{N}^\dagger_{D,B \to T}[\mathcal{O}_{DB}] \right] . \tag{5.8}
$$

For later convenience, we introduce a correctly normalized recovery map

$$
\mathcal{R}^{\text{Lite}}_{D,B \to T}[\mathcal{O}_{DB}] := \frac{1}{N} \cdot \frac{d_B d_D}{d_T} \mathcal{N}^\dagger_{D,B \to T}[\mathcal{O}_{DB}] , \tag{5.9}
$$

and define it as the *Petz-lite*[10]. Here, N is the normalization constant

$$
N = \left(\frac{d_D}{d_T} \right)^2 + 1, \tag{5.10}
$$

determined by the condition $\overline{\text{tr}_T \left[\mathcal{R}^{\text{Lite}}_{D,B \to T}[\mathcal{N}_{T \to D,B}[\sigma_T]] \right]} = 1$, where σ_T is some reference state in T. In the Haar random case, the choice of the reference state σ_T is not important as long as it is normalized.

---

[8]In appendix C, we give another equivalent argument supporting our expectation of this simplification in terms of the Kraus representation of the HP channel.

[9]More generally, for a quantum channel $\mathcal{N}$, its adjoint channel is defined by the similar relation,

$$
\text{tr}[\mathcal{N}[\rho] \, O] = \text{tr} \left[\rho \mathcal{N}^\dagger[O] \right] . \tag{5.7}
$$

[10]The terminology "Petz-lite" is introduced in [4], and we also use this terminology in this paper.

With this N, the Petz-lite can be expressed as

$$\mathcal{R}_{D,B\to T}^{\text{Lite}}[\mathcal{O}_{DB}] = \frac{1}{\left(\dfrac{d_D}{d_T}\right)^2 + 1} \cdot \frac{d_B d_D}{d_T} \mathcal{N}_{D,B\to T}^{\dagger}[\mathcal{O}_{DB}]$$

$$= \frac{1}{1 + \left(\dfrac{d_T}{d_D}\right)^2} \cdot d_C \, \mathcal{N}_{D,B\to T}^{\dagger}[\mathcal{O}_{DB}],$$

(5.11)

where in the second line, we used the relation $d_B d_T = d_C d_D$ due to the unitarity of the Haar random unitary. For the parameter region $d_T/d_D \ll 1$, the normalization is just given by d_C, which coincides with an expression obtained from another discussion. In appendix C, we give the discussion.

5.1 West-coast notation and replica-wormhole-like objects

In the following, we are interested in the typical properties of the recovery map $\mathcal{R}$ for the HP channel $\mathcal{N}$. To investigate these properties, we will consider replicated quantities, such as $\text{tr}(\mathcal{N}[\rho_T])^n$ involving a product of Haar random unitaries and its average. Since such averaging involves Wick type contractions between various pairs of Haar random unitaries in the product, it is convenient to introduce a graphical notation that manifests which pair of unitaries are contracted. Therefore, here we introduce a notation similar to the one employed in [4] for modeling the black hole microstates and their statistical properties, and call this West-coast notation.

To begin with, let us define the following black hole microstate on C, involving a Haar random unitary

$$\left|\psi_i^T\right\rangle_C := \sqrt{d_C \, d_D} \sum_{C=1}^{d_C} |C\rangle \, U_{C,T;i} \quad .$$

(5.12)

Here, $\{|C\rangle\}$ is the set of basis states on the Hilbert space H_C and the index i collectively denote the indices for both late radiation D and early radiation B, $i : (D, B)$ or more concretely $|i\rangle = |D\rangle \otimes |B\rangle$, thus the label i rums from 1 to $d_D d_B \equiv k$.

In the following, we use this type of states $\left|\psi_i^T\right\rangle_C$ to write quantities of our interest, instead of random unitary matrices $U_{C,D;T,B}$. Under this notation, we can write

$$\left\langle \psi_i^T \middle| \psi_j^{T'} \right\rangle = d_C \, d_D \sum_{C=1}^{d_C} U_{i;C,T}^{\dagger} \, U_{C,T';j}$$

(5.13)

and therefore the HP channel (5.3) is given by

$$\mathcal{N}_{T\to D,B}[\rho_T] = \frac{1}{k d_C} \sum_{i,j=1}^{k} |i\rangle\langle j| \cdot \sum_{\tilde{T},\tilde{T}'=1}^{d_T} \left\langle \psi_j^{\tilde{T}'} \middle| \psi_i^{\tilde{T}} \right\rangle (\rho_T)_{\tilde{T}\tilde{T}'} \quad .$$

(5.14)

In this notation, we call the subscript index i Hawking radiation index, and the superscript T code index.

The West-coast model treats each of these microstate $|\psi_i\rangle$ by a single-sided AdS black hole with insertion of "end of the world brane" (or EoW brane in short) labeled by the index i behind the horizon. This state has a Hartle-Hawking type preparation, in terms of a Euclidean path integral with the EoW brane which starts from the Euclidean conformal boundary. In this model, the overlap between two such states $\langle\psi_i|\psi_j\rangle$ is computed by a Euclidean gravitational path integral on a region of Euclidean disc enclosed by the part of the asymptotic boundary (an interval) and the EoW brane in the bulk.

With this gravitational path integral picture in mind, here we explain the fact that there is a simple diagrammatic prescription to compute a product of such overlaps $\overline{\prod_{m=1}^{n}\langle\psi_{i_m}^{a_m}|\psi_{j_m}^{b_m}\rangle}$[11] without directly applying the formulae for the Haar random averages, which becomes quite involved when the number of unitary matrices appearing increases.

Then the prescription is the following:

1. For each overlap in the product $\langle\psi_{i_m}^{a_m}|\psi_{j_m}^{b_m}\rangle$ draw an interval with two endpoints, and associate the labels (i_m, a_m) to one end and (j_m, b_m) to the other. (In the West-coast model, this interval with indices at the endpoints provides the boundary condition to the gravitational path integral for the product of the overlaps.)

2. The n intervals prepared in this way have $2n$ endpoints in total. We pick up two of these endpoints and connect them by a line, which we call the EoW brane. We repeat this until all the endpoints are connected to the other by EoW branes. There are many different ways to do this. One possibility is that the endpoint of the m-th interval is always connected to the other endpoint of the same interval. Or the other possibility is that the endpoint of the m-th interval is always connected to the point on the next $(m+1)$-th interval.

3. Each diagram D constructed in this way contains n EoW branes. We then associate each EoW brane in the diagram with a Kronecker delta factor. If the EoW brane is connecting two endpoints with the labels (i_l, a_l) and (j_m, b_m), then this factor is given by $\delta_{i_l j_m}\delta_{a_l b_m}$. We compute this for all EoW branes in the diagram and then multiply these factors. Let us denote this factor for the diagram by I_D.

4. Since each diagram can be regarded as (disjoint union of) two-dimensional surfaces, we can associate an Euler number χ_D to the diagram. We then pick up the factor $(d_C)^{\chi_D}$

---

[11]In the West-coast paper, this quantity is just called the product of overlap and denoted without the bar, i.e., $\overline{\prod_{m=1}^{n}\langle\psi_{i_m}^{a_m}|\psi_{j_m}^{b_m}\rangle}\big|_{ours} = \prod_{m=1}^{n}\langle\psi_{i_m}^{a_m}|\psi_{j_m}^{b_m}\rangle_{WC}$. We will use the convention with the bar to keep in mind that we do average over random unitaries in the computation.

Figure 17: Diagrams for computing the average of overlaps (5.19). A black line connects two points that appear in the same overlap, and the blue lines correspond to the EoW branes in Haar random averaging. **Left**: The disconnected diagram. **Right**: The connected diagram.

which corresponds to the gravitational path integral part in the West-coast model. We then sum the total factor $I_D(d_C)^{\chi_D}$ for all possible diagram D.

5. The average of the overlaps is equal to the sum of these factors over all possible diagrams;

$$\overline{\prod_{m=1}^{n} \langle \psi_{i_m}^{a_m} | \psi_{j_m}^{b_m} \rangle} = \sum_{D \in \text{All diagrams}} I_D \, (d_C)^{\chi_D}. \tag{5.15}$$

Let us provide a few examples. First, for the single overlap $\overline{\langle \psi_i^T | \psi_j^{T'} \rangle}$. We can easily evaluate it

$$
\begin{aligned}
\overline{\langle \psi_i^T | \psi_j^{T'} \rangle} &= d_C \, d_D \sum_{C=1}^{d_C} \overline{U_{i;C,T}^{\dagger} \, U_{C,T';j}} \\
&= d_C \underbrace{\delta_{D_i D_j} \, \delta_{B_i B_j}}_{\delta_{ij}} \, \delta_{TT'} \\
&= d_C \, \delta_{ij} \, \delta_{TT'},
\end{aligned} \tag{5.16}
$$

where in the second line, we used the general result for two Haar random unitaries

$$\overline{U_{a,b} U_{c,d}^{\dagger}} = \frac{1}{d} \delta_{ad} \delta_{bc} \qquad (a, b, c, d = 1, \cdots, d). \tag{5.17}$$

This result can be easily reproduced from the West-coast prescription.

Next, let us evaluate the Haar average of the combination of the overlaps for later convenience,

$$\left\langle \psi_i^{T_1} \middle| \psi_j^{T_1'} \right\rangle \cdot \left\langle \psi_j^{T_2'} \middle| \psi_i^{T_2} \right\rangle. \tag{5.18}$$

Clearly, by setting $T_1 = T_2 = T$ and $T_1' = T_2' = T'$, the above combination reduces to the variance of the overlap $\left| \left\langle \psi_i^T \middle| \psi_j^{T'} \right\rangle \right|^2$. We can evaluate the above quantity by the diagrammatic prescription mentioned above (see figure 17),

$$\overline{\left\langle \psi_i^{T_1} \middle| \psi_j^{T_1'} \right\rangle \cdot \left\langle \psi_j^{T_2'} \middle| \psi_i^{T_2} \right\rangle} \approx (d_C)^2 \, \delta_{ij} \delta_{T_1 T_1'} \cdot \delta_{ji} \delta_{T_2' T_2} + d_C \, \delta_{ii} \delta_{T_1 T_2} \cdot \delta_{jj} \delta_{T_2' T_1'}. \tag{5.19}$$

This coincides with the result obtained by using the Weingarten formula,

$$\overline{U_{a_1,b_1} U^\dagger_{c_1,d_1} \cdot U_{a_2,b_2} U^\dagger_{c_2,d_2}} = \frac{1}{d^2-1} \left(\delta_{a_1 d_1} \delta_{b_1 c_1} \cdot \delta_{a_2 d_2} \delta_{b_2 c_2} + \delta_{a_1 d_2} \delta_{b_1 c_2} \cdot \delta_{a_2 d_1} \delta_{b_2 c_1} \right)$$

$$+ \frac{1}{d(d^2-1)} \left(\delta_{a_1 d_1} \delta_{a_2 d_2} \delta_{b_1 c_2} \delta_{b_2 c_1} + \delta_{a_1 d_2} \delta_{a_2 d_1} \delta_{b_1 c_1} \delta_{b_2 c_2} \right)$$

$$(a, b, c, d = 1, \cdots, d). \tag{5.20}$$

In general, the prescription introduced here correctly computes the average over Haar random unitaries in the product of overlaps, as long as the rank of the random unitaries $d = d_C \, d_D = d_T \, d_A$ is large.

Furthermore, the adjoint channel (5.6), in terms of the West-coast notation, is given by

$$\mathcal{N}^\dagger_{D,B\to T}[\mathcal{O}_{DB}] = \frac{1}{k d_C} \sum_{T,T'=1}^{d_T} |T'\rangle\langle T| \cdot \sum_{i,j=1}^{k} \left\langle \psi_j^{T'} \middle| \psi_i^T \right\rangle \langle j| \, \mathcal{O}_{DB} \, |i\rangle \quad . \tag{5.21}$$

Below, using this graphical expression, we evaluate several relative entropies to check the validity of the approximation $\mathcal{R} \sim \mathcal{N}^\dagger$.

5.2 Relative entropy: Sufficiency

As we have mentioned, the decoupling condition (5.2) implies that there is a recovery map for the Hayden-Preskill channel (5.3). Another characterization of the existence of the recovery map $\mathcal{R}$ for given $\mathcal{N}$ is the notion of sufficiency [10, 11, 21]. To state this, let us first recall the fact that relative entropy satisfies the monotonicity property

$$S(\rho||\sigma) \geq S(\mathcal{N}[\rho]||\mathcal{N}[\sigma]) \tag{5.22}$$

for any CPTP map $\mathcal{N}$. By repeating this, we have

$$S(\rho||\sigma) \geq S(\mathcal{N}[\rho]||\mathcal{N}[\sigma]) \geq S(\mathcal{R}\,[\mathcal{N}[\rho]]\,||\mathcal{R}\,[\mathcal{N}[\sigma]]), \tag{5.23}$$

therefore if the recovery map exists $\mathcal{R} \circ \mathcal{N} = 1_{\text{code}}$, then $S(\rho||\sigma) = S(\mathcal{N}[\rho]||\mathcal{N}[\sigma])$, for any density matrices on the code subspace. This condition is known as sufficiency, and it was shown that if $\mathcal{N}$ satisfies this condition, the recovery map is given by (5.5). Here we would like to check the HP channel (5.3) does satisfy sufficiency, by directly computing the relative entropy $S(\mathcal{N}[\rho]||\mathcal{N}[\sigma])$ in the presence of the quantum channel $\mathcal{N}$ [12].

Since our interest is a typical result under the Haar random average, we consider the Haar averaged relative entropy, $\overline{S(\mathcal{N}[\rho]||\mathcal{N}[\sigma])}$. To evaluate the relative entropy, we use the replica trick [28]

$$\overline{S(\mathcal{N}[\rho]||\mathcal{N}[\sigma])} = \lim_{n\to 1} \frac{1}{n-1} \left(\overline{\log \text{tr}\,[\mathcal{N}[\rho]^n]} - \overline{\log \text{tr}\,[\mathcal{N}[\rho]\mathcal{N}[\sigma]^{n-1}]} \right). \tag{5.24}$$

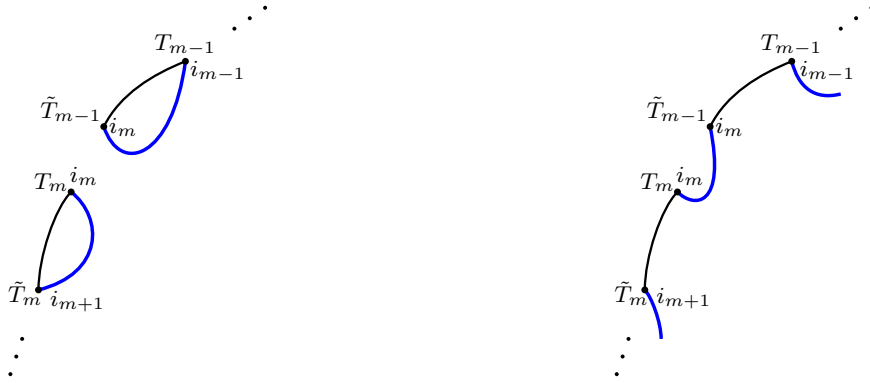[12]See [26, 27] for related discussions on original Petz map cases.

Figure 18: **Left**: The dominant diagram for (5.26) when $d_D \ll d_T$ (disconnected diagram). **Right**: The connected diagram dominating the sum at $d_T \ll d_D$.

Generally, since it is difficult to evaluate the Haar average of logarithmic functional, instead of the expression, we consider

$$\overline{S(\mathcal{N}[\rho]||\mathcal{N}[\sigma])} \approx \lim_{n \to 1} \frac{1}{n-1} \left(\log \overline{\mathrm{tr}\,[\mathcal{N}[\rho]^n]} - \log \overline{\mathrm{tr}\,[\mathcal{N}[\rho]\mathcal{N}[\sigma]^{n-1}]} \right). \qquad (5.25)$$

It is known that in the large Hilbert dimension limit, this quantity is almost equal to the original one [29, 30]. For a moment, let us focus on the first term of (5.25). Using the West-coast notation (5.14), the trace $\mathrm{tr}\,[\mathcal{N}[\rho]^n]$ can be written in terms of overlaps,

$$\mathrm{tr}\,[\mathcal{N}[\rho]^n] = \frac{1}{(k\,d_C)^n} \sum_{\boldsymbol{i}=1}^{k} \sum_{\boldsymbol{T},\tilde{\boldsymbol{T}}=1}^{d_T} \prod_{m=0}^{n-1} \left(\langle \psi_{i_m}^{\tilde{T}_m} | \psi_{i_{m+1}}^{T_m} \rangle \, \rho_{T_m \tilde{T}_m} \right), \qquad (5.26)$$

where $i_0 = i_n$, and the bold fonts $\boldsymbol{i}, \boldsymbol{T}$ in the summation symbol mean the sum with respect to the set of indices; $\sum_{\boldsymbol{i}=1}^{k} = \sum_{i_0=1}^{k} \cdots \sum_{i_{n-1}=1}^{k}$.

In computing the Rényi entropy (5.26) we need to evaluate the product of overlaps $\prod_{m=0}^{n-1} \langle \psi_{i_m}^{\tilde{T}_m} | \psi_{i_{m+1}}^{T_m} \rangle$ with $| \psi_{i_n}^T \rangle \equiv | \psi_{i_0}^T \rangle$ and its Haar random average. We do this using the diagrammatic technique introduced in the previous section.

Among all possible diagrams, we are particularly interested in the ones dominating the sum, both in early times ($d_D \ll d_T$) and late times ($d_D \gg d_T$). We now argue that the fully-disconnected diagram (the left panel of figure 18) where, for all EoW branes, the starting point and endpoint are on the same interval dominates in early times, and the fully connected diagram (the right panel of figure 18) where the indices form a single loop, dominates in late times by explicit calculations. The calculation here is very similar to the ones in [4, 30].

First, let us evaluate the contribution of the fully disconnected diagram. Since the contribution of this diagram is evaluated as

$$\overline{\left(\prod_{m=0}^{n-1} \langle \psi_{i_m}^{\tilde{T}_m} | \psi_{i_{m+1}}^{T_m} \rangle \right)}_{\mathrm{discon}} = d_C^n \prod_{m=0}^{n-1} \left(\delta_{i_m i_{m+1}} \delta_{\tilde{T}_m T_m} \right). \qquad (5.27)$$

The contribution of this diagram to the Rényi entropy is

$$\overline{\text{tr}\,[\mathcal{N}[\rho]^n]}\Big|_{\text{fully discon}} = \frac{1}{(k\,d_C)^n} \cdot k\,(d_C)^n \sum_{\bm{T}=1}^{d_T} \rho_{T_1 T_1}\,\rho_{T_2 T_2} \cdots \rho_{T_n T_n} = \frac{1}{(k)^{n-1}}\,(\text{tr}\,[\rho])^n\,. \quad (5.28)$$

Similarly, the value of the fully connected diagram is given by

$$\overline{\left(\prod_{m=0}^{n-1} \langle \psi_{i_m}^{\tilde{T}_m} | \psi_{i_{m+1}}^{T_m} \rangle\right)}\Bigg|_{\text{fully conn}} = d_C \prod_{m=0}^{n-1} \left(\delta_{\tilde{T}_{m+1} T_m}\right) \;\Rightarrow\; \overline{\text{tr}\,[\mathcal{N}[\rho]^n]}\Big|_{\text{fully conn}} = \frac{1}{(d_C)^{n-1}}\,\text{tr}\,[\rho^n]\,.$$

$$(5.29)$$

Combining these two results, $\overline{\text{tr}\,[\mathcal{N}[\rho]^n]}$ is given by

$$\overline{\text{tr}\,[\mathcal{N}[\rho]^n]} = \frac{1}{(k)^{n-1}}\,(\text{tr}\,[\rho])^n + \frac{1}{(d_C)^{n-1}}\,\text{tr}\,[\rho^n] + \cdots\,, \quad (5.30)$$

where $\cdots$ means contributions coming from partially connected saddles.

Since there are upper and lower bounds on $\text{tr}\,[\rho^n]$, that is, $1/(d_T)^{n-1} \le \text{tr}\,[\rho^n] \le 1$, we can see that

$$\overline{\text{tr}\,[\mathcal{N}[\rho]^n]} = \frac{1}{(k)^{n-1}}\,(\text{tr}\,[\rho])^n + \frac{1}{(d_C)^{n-1}}\,\text{tr}\,[\rho^n] + \cdots\,,$$

$$\approx \begin{cases} \dfrac{1}{(k)^{n-1}} & k \ll d_C \Leftrightarrow d_T \ll \left(\dfrac{d_T}{d_D}\right)^2 \\[3mm] \dfrac{1}{(d_C)^{n-1}}\,\text{tr}\,[\rho^n] & d_C\,d_T \ll k \Leftrightarrow \left(\dfrac{d_T}{d_D}\right)^2 \ll 1 \end{cases}. \quad (5.31)$$

Thus, when the necessary condition for the decoupling condition, $d_T/d_D \ll 1$, holds, the dominant contribution is given by the fully connected saddle.

We have to carefully evaluate the precise range of m where the value of the connected saddle gets larger than that of the disconnected saddle. This value of m depends on the density matrix ρ on the code subspace, and gets maximized when it is the maximally mixed state $\rho = I_T/d_T$. Therefore, after $k > d_C d_T$, the connected saddle becomes the dominant one for all density matrices in H_{code}.

Next, let us evaluate the second term of (5.25). This computation is completely parallel to the above computation. In terms of the overlaps, it is given by

$$\text{tr}\,[\mathcal{N}[\rho]\mathcal{N}[\sigma]^{n-1}] = \frac{1}{(k\,d_C)^n} \sum_{i=1}^{k} \sum_{\bm{T},\tilde{\bm{T}}=1}^{d_T} \left(\prod_{m=0}^{n-1} \langle \psi_{i_m}^{\tilde{T}_m} | \psi_{i_{m+1}}^{T_m} \rangle\right) \rho_{T_0 \tilde{T}_0} \left(\prod_{m=1}^{n-1} \sigma_{T_m \tilde{T}_m}\right). \quad (5.32)$$

The contribution of the fully disconnected diagram and the connected diagram to the second term of (5.25) can be evaluated, again by substituting the result (5.27) and (5.29)

$$\text{tr}\,[\mathcal{N}[\rho]\mathcal{N}[\sigma]^{n-1}]\big|_{\text{discon}} = \frac{1}{(k)^{n-1}}\,\text{tr}\,[\rho]\,(\text{tr}\,[\sigma])^{n-1}\,, \quad \overline{\text{tr}\,[\mathcal{N}[\rho]\mathcal{N}[\sigma]^{n-1}]}\big|_{\text{conn}} = \frac{1}{(d_C)^{n-1}}\,\text{tr}\,[\rho\,\sigma^{n-1}]\,.$$

$$(5.33)$$

Thus, using these results, we obtain

$$\overline{\mathrm{tr}\left[\mathcal{N}[\rho]\mathcal{N}[\sigma]^{n-1}\right]} = \frac{1}{(k)^{n-1}}\,\mathrm{tr}\left[\rho\right]\left(\mathrm{tr}\left[\sigma\right]\right)^{n-1} + \frac{1}{(d_C)^{n-1}}\,\mathrm{tr}\left[\rho\sigma^{n-1}\right] + \cdots,$$

$$\approx \begin{cases} \dfrac{1}{(k)^{n-1}} & k \ll d_C \Leftrightarrow d_T \ll \left(\dfrac{d_T}{d_D}\right)^2 \\[4mm] \dfrac{1}{(d_C)^{n-1}}\,\mathrm{tr}\left[\rho\sigma^{n-1}\right] & k \gg d_C d_T \Leftrightarrow \left(\dfrac{d_T}{d_D}\right)^2 \ll 1 \end{cases}, \tag{5.34}$$

where $\cdots$ again means contributions coming from partially connected saddles, and also in the second approximate equality, we assumed that $1/(d_T)^{n-1} \lesssim \mathrm{tr}\left[\rho\sigma^{n-1}\right] \leq 1$ in order to obtain the conditions[13].

Now that we have evaluated the two terms that appeared in the relative entropy, we can obtain the resulting relative entropy

$$\overline{S(\mathcal{N}[\rho]||\mathcal{N}[\sigma])} \approx \lim_{n\to 1}\frac{1}{n-1}\left(\log\overline{\mathrm{tr}\left[\mathcal{N}[\rho]^n\right]} - \log\overline{\mathrm{tr}\left[\mathcal{N}[\rho]\mathcal{N}[\sigma]^{n-1}\right]}\right),$$

$$\approx \begin{cases} 0 & k \ll d_C \Leftrightarrow d_T \ll \left(\dfrac{d_T}{d_D}\right)^2 \\[4mm] \displaystyle\lim_{n\to 1}\frac{1}{n-1}\left(\log\mathrm{tr}\left[\rho^n\right] - \log\mathrm{tr}\left[\rho\sigma^{n-1}\right]\right) & k \gg d_C d_T \Leftrightarrow \left(\dfrac{d_T}{d_D}\right)^2 \ll 1 \end{cases}$$

$$= \begin{cases} 0 & k \ll d_C \Leftrightarrow d_T \ll \left(\dfrac{d_T}{d_D}\right)^2 \\[4mm] S(\rho||\sigma) & k \gg d_C d_T \Leftrightarrow \left(\dfrac{d_T}{d_D}\right)^2 \ll 1. \end{cases} \tag{5.35}$$

Thus we can conclude that, when the condition $d_T/d_D \ll 1$ is satisfied, the relative entropies obeys the relation

$$\overline{S(\mathcal{N}[\rho]||\mathcal{N}[\sigma])} \approx S(\rho||\sigma). \tag{5.36}$$

This result implies that the condition of sufficiency holds for the Hayden-Preskill channel when $\left(\frac{d_T}{d_D}\right)^2 \ll 1$.

5.3 Check the recovery map

We argued that in chaotic systems, the Petz recovery map (5.5) gets simplified and is reduced to so-called Petz-lite map $\mathcal{R}^{\mathrm{Lite}}$ defined in (5.11). In this section, we show this by checking

$$\overline{S(\mathcal{R}^{\mathrm{Lite}}\left[\mathcal{N}[\rho_T]\right]||\rho_T)} = 0, \quad \text{when} \quad \left(\frac{d_T}{d_D}\right)^2 \ll 1. \tag{5.37}$$

---

[13]If the support of the density matrix ρ is not contained in that of σ, then $\mathrm{tr}\left[\rho\sigma^{n-1}\right] = 0$, implying the divergent relative entropy $S(\rho||\sigma) = \infty$. In that case, we would need another treatment, thus we do not consider such a case in this paper.

for any density matrix ρ_T on the code subspace. This means that at sufficiently late times, one can recover ρ_T from the state of the Hawking radiation $\mathcal{N}[\rho_T]$ by applying the recovery map $\mathcal{R}^{\mathrm{Lite}}$.

One can show this by computing the relative entropy by the replica trick similar to (5.24),

$$\overline{S(\mathcal{R}^{\mathrm{Lite}}\left[\mathcal{N}[\rho_T]\right]||\rho_T)} = \lim_{n\to 1}\frac{1}{n-1}\left(\log\overline{\mathrm{tr}(\mathcal{R}^{\mathrm{Lite}}\left[\mathcal{N}[\rho]\right])^n} - \log\overline{\mathrm{tr}(\mathcal{R}^{\mathrm{Lite}}\left[\mathcal{N}[\rho]\right]\rho^{n-1})}\right). \quad (5.38)$$

In terms of Haar random unitaries, $\mathcal{R}^{\mathrm{Lite}}\left[\mathcal{N}[\rho_T]\right]$ is given by

$$\mathcal{R}^{\mathrm{Lite}}\left[\mathcal{N}[\rho_T]\right] = \frac{1}{N}\cdot\frac{d_B d_D}{d_T}\cdot\mathcal{N}^\dagger_{D,B\to T}\left[\mathcal{N}_{T\to D,B}[\rho]\right]$$

$$= \frac{1}{N}\sum_{\tilde{T},\tilde{T}'=1}^{d_T}\left|\tilde{T}\right\rangle_T\left\langle\tilde{T}'\right|\cdot\frac{1}{k(d_C)^2 d_T}\sum_{T,T'=1}^{d_T}\sum_{i,j=1}^k\left\langle\psi_i^{\tilde{T}}\Big|\psi_j^{\tilde{T}'}\right\rangle\left\langle\psi_j^{T'}\Big|\psi_i^T\right\rangle(\rho)_{TT'}. \quad (5.39)$$

Therefore the first term in (5.38) is given by

$$\mathrm{tr}(\mathcal{R}^{\mathrm{Lite}}\left[\mathcal{N}[\rho]\right])^n = \frac{1}{(Nkd_C^2 d_T)^n}\sum_{\boldsymbol{T},\boldsymbol{T}'=1}^{d_T}\sum_{\tilde{\boldsymbol{T}},\tilde{\boldsymbol{T}}'=1}^{d_T}\sum_{\boldsymbol{i},\boldsymbol{j}=1}^k\prod_{m=1}^n\left(\left\langle\psi_{i_m}^{T_m}\Big|\psi_{j_m}^{T_{m+1}}\right\rangle\left\langle\psi_{j_m}^{\tilde{T}_m}\Big|\psi_{i_m}^{\tilde{T}'_m}\right\rangle\rho_{\tilde{T}_m\tilde{T}'_m}\right). \quad (5.40)$$

We compute this by following the procedure explained in section 5.1, namely by preparing an interval for each overlap, and connecting the endpoints of the intervals by EoW branes, then evaluating each diagram generated in this way. As shown in the figure 19, the m-th replica consists of two intervals with indices for Hawking radiation i_m, j_m. Therefore, it is clear that when $k = d_D d_B$ is sufficiently large, the dominant diagram is the one connecting the endpoint with the index i_m in the first interval to the endpoint of the second replica with the same index in the same replica (the right panel of figure 19). Similarly, we connect the endpoints with j_m in this replica. This is because, if there is an EoW brane connecting endpoints with distinct Hawking indices (say i, j), then the value of the diagram is significantly reduced in the large-k limit because of the Kronecker delta factor δ_{ij} coming from the EoW brane.

This means that in the dominant saddle, two different replicas are not connected by any EoW brane, because they start and end at the same replica. This means that the Rényi entropy is a self-averaging quantity

$$\overline{\mathrm{tr}(\mathcal{R}^{\mathrm{Lite}}\left[\mathcal{N}[\rho]\right])^n} = \mathrm{tr}\left(\overline{\mathcal{R}^{\mathrm{Lite}}\left[\mathcal{N}[\rho]\right]}\right)^n. \quad (5.41)$$

A similar statement holds for the second term of (5.38); therefore, we conclude that the relative entropy of our interest is also self-averaging,

$$\overline{S(\mathcal{R}^{\mathrm{Lite}}\left[\mathcal{N}[\rho_T]\right]\,||\rho_T)} = S(\overline{\mathcal{R}^{\mathrm{Lite}}\left[\mathcal{N}[\rho_T]\right]}\,||\rho_T). \quad (5.42)$$
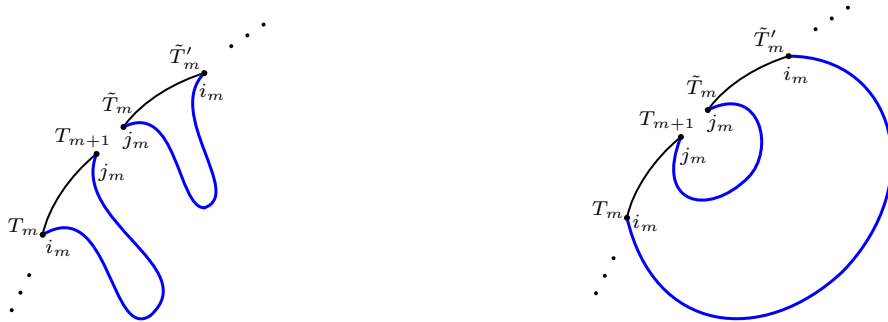
Figure 19: Diagrams for the product of overlaps appearing in the calculation of (5.40). **Left**: disconnected diagram. **Right**: The connected diagram.

when k is sufficiently large. This implies that in the relative entropy, one can replace $\mathcal{R}^{\text{Lite}}[\mathcal{N}[\rho_T]]$ with its average $\overline{\mathcal{R}^{\text{Lite}}[\mathcal{N}[\rho_T]]}$. The average of the density matrix is given by

$$\overline{\mathcal{R}^{\text{Lite}}[\mathcal{N}[\rho_T]]} = \frac{1}{1 + \left(\dfrac{d_T}{d_D}\right)^2}\left(\rho + \left(\frac{d_T}{d_D}\right)^2 \cdot \frac{I_T}{d_T}\right). \tag{5.43}$$

A more precise way to argue this is the following: Let us compute

$$\overline{\text{tr}\left[\left(\mathcal{R}^{\text{Lite}}[\mathcal{N}[\rho_T]] - \overline{\mathcal{R}^{\text{Lite}}[\mathcal{N}[\rho_T]]}\right)^2\right]} = \overline{\text{tr}\left[(\mathcal{R}^{\text{Lite}}[\mathcal{N}[\rho_T]])^2\right]} - \text{tr}\left[\left(\overline{\mathcal{R}^{\text{Lite}}[\mathcal{N}[\rho_T]]}\right)^2\right]. \tag{5.44}$$

Then, the right hand side of the above equation is given by

$$\frac{(k\,d_C)^4}{(Nk(d_C)^2 d_T)^2}\Bigg\{\frac{1}{k\,d_C}\Bigg[\frac{1}{k^2}\left(2 + d_T\,\text{tr}\left[\rho^2\right] + (d_T)^2\right)$$

$$+ \frac{1}{k\,d_C}\left((d_T)^2\,\text{tr}\left[\rho^2\right] + 2d_T + 2\,\text{tr}\left[\rho^2\right]\right) + \frac{1}{(d_C)^2}d_T\,\text{tr}\left[\rho^2\right]\Bigg]\Bigg\}, \tag{5.45}$$

which becomes small when $k \gg d_C d_T$. By plugging this expression, we have

$$\overline{S(\mathcal{R}^{\text{Lite}}[\mathcal{N}[\rho_T]]\,||\rho_T)} \approx S(\overline{\mathcal{R}^{\text{Lite}}[\mathcal{N}[\rho_T]]}\,||\rho_T)$$

$$= \begin{cases} S\left(\rho\,\Big\|\dfrac{I_T}{d_T}\right) & k \ll d_C \Leftrightarrow d_T \ll \left(\dfrac{d_T}{d_D}\right)^2 \\ 0 & k \gg d_C d_T \Leftrightarrow \left(\dfrac{d_T}{d_D}\right)^2 \ll 1. \end{cases} \tag{5.46}$$

Thus, for early times $k \ll d_C$, the relative entropy is non-vanishing unless $\rho = I_T/d_T$, but for late times $d_C\,d_T \ll k$, the relative entropy is vanishing. This result implies that when $k \gg d_C d_T$, $\mathcal{R}^{\text{Lite}}$ indeed works as a recovery map.

5.4 Relation to the Yoshida-Kitaev protocol

So far, we have shown that when $k \gg d_C d_T$, the Petz-lite $\mathcal{R}^{\text{Lite}} \sim \mathcal{N}^\dagger$ indeed works as a recovery map. However, we have not discussed the physical interpretation of the Petz-lite. Thus, in this subsection, we explain the interpretation by showing the equivalence between the Petz-lite and the well-known Yoshida-Kitaev (YK) protocol. The relation between the Yoshida-Kitaev protocol and the Petz map has been suggested by Yoshida [12, 13].

In [18], Yoshida and Kitaev proposed an interesting recovery protocol for the object thrown into the black hole T from late and early radiation DB. A brief summary of their protocol is as follows:

1. In addition to the original Hayden-Preskill setup, introduce a copy of the diary and the reference, denoted by $R'T'$. We choose the state on $R'T'$ to be an EPR state. Bob can manipulate Hawking radiation DB and $R'T'$. Before applying the decoding protocol, the state of the total system is

$$|\Psi_{HP}\rangle \otimes |\text{EPR}\rangle_{R'T'}, \tag{5.47}$$

   where $|\Psi_{HP}\rangle$ is the state on $RCDB$ given by (5.1).

2. We then use the early Hawking radiation B and the copy of the diary T' to simulate the black hole dynamics by applying U^* which is the complex conjugate of U for the time evolution of the original system. After the simulation, the total system consists of $RCDR'C'D'$, and the state is

$$|\Psi_{YK}\rangle_{RCDD'C'R'} = (I_{RC} \otimes I_D \otimes U^*_{D'C'\to BT'} \otimes I_R)\,|\Psi_{HP}\rangle \otimes |\text{EPR}\rangle_{R'T'}. \tag{5.48}$$

3. Post-select to the EPR pair on DD'. If it succeeds, the state on RR' is the EPR state with high fidelity, meaning the success of information recovery.

The quantum circuit for the protocol is shown in the left panel of figure 20. Combining these steps, the quantum channel $\mathcal{R}^{YK}_{D,B\to R'}$ for the Yoshida-Kitaev (YK) recovery map is given by

$$
\begin{aligned}
&\mathcal{R}^{\text{YK}}_{D,B\to R'}[\mathcal{O}_{DB}] \\
&= \frac{1}{N_{\text{YK}}} \text{tr}_{C'}\left[\, {}_{D,D'}\langle\text{EPR}|\, U^*_{B,T'\to C',D'}\left(\mathcal{O}_{DB} \otimes |\text{EPR}\rangle_{T',R'}\langle\text{EPR}|\right) U^T_{B,T'\to C',D'}\,|\text{EPR}\rangle_{D,D'}\right],
\end{aligned} \tag{5.49}
$$

where N_{YK} is a normalization factor given by

$$N_{\text{YK}} = \overline{\left|{}_{D,D'}\langle\text{EPR}|\Psi_{YK}\rangle\right|^2} \approx \frac{1}{(d_T)^2} + \frac{1}{(d_D)^2}. \tag{5.50}$$
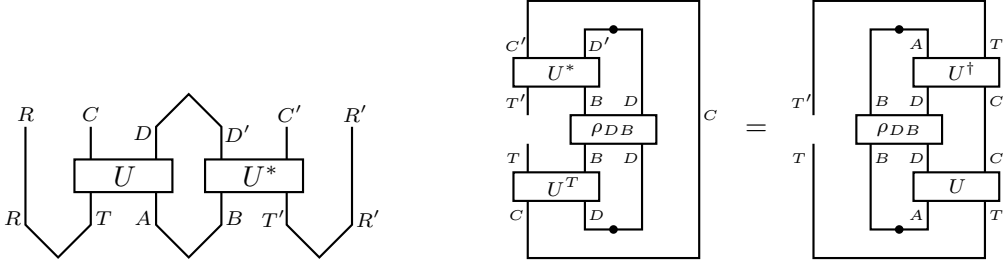
Figure 20: **Left**: Yoshida-Kitaev decoding protocol. **Right**: operator transpose that providing the key equivalence (5.54).

For the above YK recovery map, we show the equivalence between the YK recovery map $\mathcal{R}^{\mathrm{YK}}_{D,B\to R'}$ and the Petz-lite (5.9), $\mathcal{R}^{\mathrm{Lite}}_{D,B\to T}$ up to the isomorphism $V_{T\to R'}$ between systems T and R',

$$\mathcal{R}^{YK}_{D,B\to R'}[\mathcal{O}_{DB}] = V_{T\to R'}\,\mathcal{R}^{\mathrm{Lite}}_{D,B\to T}[\mathcal{O}_{DB}]\,V^{\dagger}_{T\to R'}\quad, \tag{5.51}$$

where $V_{T\to R'}$ is explicitly given by

$$V_{T\to R'} := d_T\,{}_{T,T'}\langle\mathrm{EPR}|\mathrm{EPR}\rangle_{T',R'} = \sum_{\tilde{T}=1}^{d_T}\left|\tilde{T}\right\rangle_{R'\,T}\left\langle\tilde{T}\right|. \tag{5.52}$$

The argument for the equivalence is summarized in the right panel of figure 20. We start with the YK recovery map (5.49). First, we rewrite the trace of subsystem C' in the YK recovery map as

$$\mathrm{tr}_{C'}[\mathcal{O}] = d_C\,{}_{C,C'}\langle\mathrm{EPR}|\,(I_C\otimes\mathcal{O})\,|\mathrm{EPR}\rangle_{C,C'}\,, \tag{5.53}$$

and introduce two EPR states $|\mathrm{EPR}\rangle_{D,D'}$ and $|\mathrm{EPR}\rangle_{C,C'}$.

Next, by using (5.53) and the relation (see appendix D for the derivation)

$$U^{T}_{C',D'\to B,T'}\,|\mathrm{EPR}\rangle_{C,C'}\otimes|\mathrm{EPR}\rangle_{D,D'} = U_{A,T\to C,D}\,|\mathrm{EPR}\rangle_{A,B}\otimes|\mathrm{EPR}\rangle_{T,T'}\,, \tag{5.54}$$

the YK recovery map (5.51) can be rewritten as

$$\mathcal{R}^{YK}_{D,B\to R'}[\mathcal{O}_{DB}]$$
$$= \frac{d_C}{N_{\mathrm{YK}}}\left({}_{A,B}\langle\mathrm{EPR}|\otimes{}_{T,T'}\langle\mathrm{EPR}|\right)\left[U^{\dagger}_{A,T\to C,D}\left(\mathcal{O}_{DB}\otimes|\mathrm{EPR}\rangle_{T',R'}\langle\mathrm{EPR}|\right)U_{A,T\to C,D}\right]$$
$$\times\left(|\mathrm{EPR}\rangle_{A,B}\otimes|\mathrm{EPR}\rangle_{T,T'}\right)$$
$$= \frac{d_C}{N_{\mathrm{YK}}}\left({}_{T,T'}\langle\mathrm{EPR}|\mathrm{EPR}\rangle_{T',R'}\right)$$
$$\times\,{}_{A,B}\langle\mathrm{EPR}|\left[U^{\dagger}_{T,A\to C,D}\,\mathcal{O}_{DB}\,U_{T,A\to C,D}\right]|\mathrm{EPR}\rangle_{A,B}$$
$$\times\left({}_{T',R'}\langle\mathrm{EPR}|\mathrm{EPR}\rangle_{T,T'}\right)$$
$$= \frac{d_C}{(d_T)^2\,N_{\mathrm{YK}}}\,V_{T\to R'}\,\mathcal{N}^{\dagger}_{D,B\to T,A}[\mathcal{O}_{D,B}]\,V^{\dagger}_{T\to R'}, \tag{5.55}$$

where in the final line, we used the definition of the isomorphism (5.52) and the adjoint HP channel (5.6). Additionally, the above overall constant $\frac{d_C}{(d_T)^2 \, N_{\mathrm{YK}}}$ coincides with that of the Petz-lite (5.11), since

$$\frac{d_C}{(d_T)^2 \, N_{\mathrm{YK}}} = \frac{d_C}{1 + \left(\dfrac{d_T}{d_D}\right)^2}, \tag{5.56}$$

where we used the definition of N_{YK}, (5.50). Therefore, the above expression implies the desired relation (5.51).

6 SYK model and OTOC

The Sachdev-Ye-Kitaev (STK) model[31–36] is one-demensional quantum mechanics with all-to-all random coupling made of N Majorana fermions. It gives a great insight of holography, quantum gravity and also condenced matter physics such as strange metal and non Fermi liquid. We review this SYK model here because we use this model as the chaotic system causing scrambling in the latter half of our paper. In the large N limit, the SYK model becomes solvable and in low energy (IR) limit, it has a conformal symmetry. Small deformation from the IR CFT theory is stated with the Schwarzian theory, which is a holographic dual theory of JT gravity, so the SYK model is used in study of traversable wormhole in two dimensional gravity. JT gravity with matter coupled is a fundamental tool of East Coast model of Island rule, which we explain briefly in Appendix B. In this section, we introduce the basics of the SYK model. First, we introduce the definition of the SYK model and show that in the large N limit, the thoery becomes classical and solvable with a Schwinger-Dyson equation of the propagators G and Σ. We explain this by two methods: diagrammatic perturbation theory and an effective action. Then we show that in low energy (IR) limit, G and Σ have conformal symmetry, so G can be decided as a conformal two point function. Next, we derive the Schwarzian theory as a small deformation by CFT. Finally, we briefly explain the calculation of four point functions. There, behaviors of soft mode contributions by the Schwarzian action in out-of-time orderd correlator (OTOC) case and time orderd correlator (TOC) case are different in time dependence. In OTOC case, the correlator grows exponentially in time whereas independent of time in TOC case. This behavior caused by scrambling of the SYK model and has strong relation with quantum chaos. We explain OTOC and Lyapunov growth briefly in the end.

6.1 Definition of SYK model

In this section, we review the fundamental topics of the SYK model, following the paper of Sárosi [33] and the paper of Trunin [34]. The SYK model consists of N Majorana fermions with all-to-all random coupling. The action is

$$I_{SYK} = \int d\tau \left[-\frac{1}{2} \sum_{i=1}^{N} \psi_i(\tau) \partial_\tau \psi_i(\tau) - \frac{1}{4!} \sum_{i,j,k,l=1}^{N} J_{ijkl}\, \psi_i(\tau)\psi_j(\tau)\psi_k(\tau)\psi_l(\tau) \right] \tag{6.1}$$

where τ is a Euclidean time and is obtained by the Wick rotation $\tau = it$. Fermion operators ψ_i is Hermitian ($\psi_i^\dagger = \psi_i$) and satisfy the anti-commutation relations:

$$\{\psi_i, \psi_j\} = \delta_{ij} \qquad i, j = 1, \cdots, N \tag{6.2}$$

Here, N is even ($N = 2K$, $K \in \mathbb{N}$). We set a complex basis

$$c_i = \frac{1}{\sqrt{2}}(\psi_{2i} - i\psi_{2i+1})$$
$$c_i^\dagger = \frac{1}{\sqrt{2}}(\psi_{2i} + i\psi_{2i+1}) \qquad i = 1, \cdots, K, \tag{6.3}$$

then we get canonical commutation relations of fermions:

$$\{c_i, c_j\} = \{c_i^\dagger, c_j^\dagger\} = 0, \quad \{c_i, c_j^\dagger\} = \delta_{ij} \tag{6.4}$$

A vacuum state $|0\rangle$ is defined by $c_i |0\rangle = 0$ and then we get a general state as

$$(c_1^\dagger)^{n_1}(c_2^\dagger)^{n_2} \cdots (c_K^\dagger)^{n_K} |0\rangle \qquad (n_k = 0, 1) \tag{6.5}$$

There are $2^K = 2^{\frac{N}{2}}$ states. These are the irreducible representation of the Clifford algebra.

J_{ijkl} is chosen randomly and independently by the Gaussian distribution with mean $\mu = 0$ and variance $\sigma^2 = \frac{3!J^2}{N^3}$. It means that the probability distribution of J_{ijkl} is

$$P(J_{ijkl}) = \exp\left(-\frac{N^3 J_{ijkl}^2}{12 J^2}\right) \tag{6.6}$$

In the above explanation, we think of a four-body interaction. We can generalize it to q-body interaction (q: even)

$$H = i^{\frac{q}{2}} \sum_{1 \leq i_1 < \cdots < i_q \leq N} J_{i_1 \cdots i_q} \psi_{i_1} \cdots \psi_{i_q} \tag{6.7}$$

Here, $J_{i_1 \cdots i_q}$ is chosen randomly and independently by the Gaussian distribution with mean $\mu = 0$ and variance $\sigma^2 = \frac{(q-1)!J^2}{N^{q-1}}$. By thinking of $\frac{1}{q}$ expansion and taking large q limit of the theory, we can get the deep and important essence of the SYK model.

6.2 large N

In the large N limit, the SYK model becomes solvable and gives a classical equation of motion: the Schwinger-Dyson equation. We derive the Schwinger-Dyson equation by two methods. First we explain a pertubation theory of coupling J

6.2.1 Diagrammatic derivation of Schwinger-Dyson equation

The mass dimension of ψ is 0, so J_{ijkl} and J have the dimension of energy. A time ordered two point function is defined as

$$G_{ij}(\tau - \tau') = \langle \mathcal{T} \psi_i(\tau) \psi_j(\tau') \rangle$$
$$\equiv \Theta(\tau - \tau')\langle \psi_i(\tau)\psi_j(\tau') \rangle - \Theta(\tau' - \tau)\langle \psi_j(\tau')\psi_i(\tau) \rangle \tag{6.8}$$

where $\Theta(\tau)$ is the Heaviside function and $\psi_i(\tau) = e^{\tau H}\psi_i e^{-\tau H}$. We define an averaged two point function as

$$G(\tau - \tau') \equiv \frac{1}{N}\sum_{i=1}^{N} G_{ii}(\tau - \tau') \tag{6.9}$$

We think of a free theory before explicating perturbation theory. In the free theory, $H = 0$ because of zero coupling, so $\psi_i(\tau) = \psi_i$. Then the free propagator becomes

$$\begin{aligned}
G_{ij}^{\text{free}}(\tau - \tau') &= \frac{1}{2}(\Theta(\tau - \tau') - \Theta(\tau' - \tau))\langle\psi_i\psi_j + \psi_j\psi_i\rangle \\
&= \frac{1}{2}\delta_{ij}\,\text{sgn}(\tau - \tau')\,.
\end{aligned} \tag{6.10}$$

Here, we used the symmetry of $i \leftrightarrow j$ in $G_{ij}^{\text{free}}(\tau - \tau')$ and the anticommutation relation (6.2). The signature function is defined as $\text{sgn}\,\tau \equiv \Theta(\tau) - \Theta(-\tau)$. Averaged free propagator becomes

$$\begin{aligned}
G^{\text{free}}(\tau - \tau') &= \frac{1}{N}\sum_{i=1}^{N} G_{ii}^{\text{free}}(\tau - \tau') \\
&= \frac{1}{2}\text{sgn}(\tau - \tau')
\end{aligned} \tag{6.11}$$

In order to consider a thermal system with finite temperature $\beta = \frac{1}{T}$, we move from the Euclidean line $\tau_{line} \in (-\infty, \infty)$ to the Euclidean circle $\tau_{circle} \in [-\frac{\beta}{2}, \frac{\beta}{2})$ with a monotone function such as

$$\tau_{line} = \tan\frac{\pi\tau_{circle}}{\beta} \tag{6.12}$$

τ_{circle} has β periodicity: $\tau_{circle} \sim \tau_{circle} + \beta$. Thermal two point function is defined as

$$G_{ij,\beta}(\tau - \tau') = \langle\mathcal{T}\psi_i(\tau)\psi_j(\tau')\rangle_\beta \tag{6.13}$$

$$G_\beta(\tau - \tau') = \frac{1}{N}\sum_{i=1}^{N} G_{ii,\beta}(\tau - \tau') \tag{6.14}$$

where $\langle\cdots\rangle_\beta$ denotes the average over the canonical ensemble:

$$\langle\cdots\rangle_\beta = \frac{\text{tr}\left[e^{-\beta H}\cdots\right]}{\text{tr}[e^{-\beta H}]} \tag{6.15}$$

In the free theory, the propagator and the averaged propagator become

$$G_{ij,\beta}^{\text{free}}(\tau - \tau') = \frac{1}{2}\delta_{ij}\text{sgn}\left(\sin\frac{\pi(\tau - \tau')}{\beta}\right) \tag{6.16}$$

$$G_\beta^{\text{free}}(\tau - \tau') = \frac{1}{2}\text{sgn}\left(\sin\frac{\pi(\tau - \tau')}{\beta}\right) \tag{6.17}$$

This reflects the fact that the thermal propagator is antiperiodic with $\tau \to \tau + \beta$. Indeed, for $\tau > 0$,

$$
\begin{aligned}
G_{ij,\beta}(\tau + \beta) &= \frac{\text{tr}\left[e^{-\beta H}\psi_i(\tau + \beta)\psi_j(0)\right]}{\text{tr}[e^{-\beta H}]} \\
&= \frac{\text{tr}\left[\psi_i(\tau)e^{-\beta H}\psi_j(0)\right]}{\text{tr}[e^{-\beta H}]} \\
&= \frac{\text{tr}\left[e^{-\beta H}\psi_j(0)\psi_i(\tau)\right]}{\text{tr}[e^{-\beta H}]} \\
&= -\frac{\text{tr}\left[e^{-\beta H}\psi_i(\tau)\psi_j(0)\right]}{\text{tr}[e^{-\beta H}]} = -G_{ij,\beta}(\tau)
\end{aligned}
\tag{6.18}
$$

In the third line, we used the cyclic property. Also $G_{ij,\beta}(\tau - \tau')$ is antisymmetric with τ, i.e. $G_{ij,\beta}(\tau - \tau') = -G_{ij,\beta}(\tau' - \tau)$.
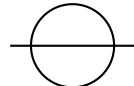
From here, we consider the perturbation theory of a four-body interaction. It can be easily applied to a q-body interaction theory. By an ordinary calculation of the loop correction to the free propagator, a two point function is obtained as the product of J_{ijkl}'s. Then we take average of randomness of J_{ijkl}'s, which is written as $\langle J \cdots J \rangle_J$ where J's express J_{ijkl}'s. Because of the average over the Gaussian distribution, the product of even number of J's can be divided to the product of $\langle J J \rangle_J$ called a "disorder pairing". We divide like $\langle J \cdots J \rangle_J \to \langle J J \rangle_J \cdots \langle J J \rangle_J$. The disorder pairing is calculated as

$$
\langle J_{i_1 j_1 k_1 l_1} J_{i_2 j_2 k_2 l_2} \rangle_J = 3! \frac{J^2}{N^3} \delta_{i_1 i_2} \delta_{j_1 j_2} \delta_{k_1 k_2} \delta_{l_1 l_2}
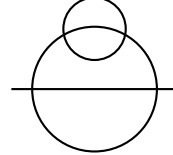\tag{6.19}
$$

There are several ways of the disorder pairing in the Wick contraction calculation. In the Feynman diagram, a four point vertex corresponds to J_{ijkl}. Diagrams which contain odd number of J_{ijkl} become zero. For example,

$$
= \langle J_{ijkl} G_{kl}^{\text{free}} \rangle_J = 0
$$

The diagram with two vertices is the following melon diagram. There is one $\langle J J \rangle_J$ so it is necessary to calculate one disorder pairing.

$$
\begin{aligned}
&= \langle J_{i_1 j_1 k_1 l_1} J_{i_2 j_2 k_2 l_2} \rangle_J \, G_{l_1 l_2}^{\text{free}} G_{k_1 k_2}^{\text{free}} G_{j_1 j_2}^{\text{free}} \\
&= 3! J^2 (G^{\text{free}})^3 \delta_{i_1 i_2} = O(N^0)
\end{aligned}
$$

When we consider a melonic diagram with more than two vertices, we must consider several disorder pairings because there are several ways to divide $\langle J \cdots J \rangle_J$ to $\langle JJ \rangle_J \cdots \langle JJ \rangle_J$. In fact, disorder pairings between different melons cause $O(N^{-1})$ suppression and it is necessary to think of only disorder pairings in the same melon if we take the large N limit. For example, the following melonic diagram with four vertices has three ways of division $\langle JJJJ \rangle_J \to \langle JJ \rangle_J \langle JJ \rangle_J$.

$$
\begin{aligned}
= \ & \langle J_{i_1 j_1 k_1 l_1} J_{i_2 j_2 k_2 l_2} J_{i_3 j_3 k_3 l_3} J_{i_4 j_4 k_4 l_4} \rangle_J \\
& \times G^{\text{free}}_{l_1 i_3} G^{\text{free}}_{l_2 i_4} G^{\text{free}}_{l_3 l_4} G^{\text{free}}_{k_3 k_4} G^{\text{free}}_{j_3 j_4} G^{\text{free}}_{k_1 k_2} G^{\text{free}}_{j_1 j_2} \\[6pt]
= \ & (\langle J_{i_1 j_1 k_1 l_1} J_{i_2 j_2 k_2 l_2} \rangle_J \langle J_{i_3 j_3 k_3 l_3} J_{i_4 j_4 k_4 l_4} \rangle_J \\
& + \langle J_{i_1 j_1 k_1 l_1} J_{i_3 j_3 k_3 l_3} \rangle_J \langle J_{i_2 j_2 k_2 l_2} J_{i_4 j_4 k_4 l_4} \rangle_J \\
& + \langle J_{i_1 j_1 k_1 l_1} J_{i_4 j_4 k_4 l_4} \rangle_J \langle J_{i_2 j_2 k_2 l_2} J_{i_3 j_3 k_3 l_3} \rangle_J) \\
& \times G^{\text{free}}_{l_1 i_3} G^{\text{free}}_{l_2 i_4} G^{\text{free}}_{l_3 l_4} G^{\text{free}}_{k_3 k_4} G^{\text{free}}_{j_3 j_4} G^{\text{free}}_{k_1 k_2} G^{\text{free}}_{j_1 j_2}
\end{aligned}
$$

The first term, which takes disorder pairings in the same melon, becomes

$$
\begin{aligned}
\langle J_{i_1 j_1 k_1 l_1} J_{i_2 j_2 k_2 l_2} \rangle_J \langle J_{i_3 j_3 k_3 l_3} J_{i_4 j_4 k_4 l_4} \rangle_J \, G^{\text{free}}_{l_1 i_3} G^{\text{free}}_{l_2 i_4} G^{\text{free}}_{l_3 l_4} G^{\text{free}}_{k_3 k_4} G^{\text{free}}_{j_3 j_4} G^{\text{free}}_{k_1 k_2} G^{\text{free}}_{j_1 j_2} &= \frac{(3!)^2}{2} J^4 (G^{\text{free}})^6 \delta_{i_1 i_2} \\
&= O(N^0)
\end{aligned}
\tag{6.20}
$$

On the other hand, the second term, which takes disorder pairing between different melons, becomes

$$
\begin{aligned}
\langle J_{i_1 j_1 k_1 l_1} J_{i_3 j_3 k_3 l_3} \rangle_J \langle J_{i_2 j_2 k_2 l_2} J_{i_4 j_4 k_4 l_4} \rangle_J \, G^{\text{free}}_{l_1 i_3} G^{\text{free}}_{l_2 i_4} G^{\text{free}}_{l_3 l_4} G^{\text{free}}_{k_3 k_4} G^{\text{free}}_{j_3 j_4} G^{\text{free}}_{k_1 k_2} G^{\text{free}}_{j_1 j_2} &= \frac{(3!)^2}{4} \frac{1}{N^2} J^4 (G^{\text{free}})^4 \delta_{i_1 i_2} \\
&= O(N^{-2})
\end{aligned}
\tag{6.21}
$$

and is suppressed by $O(N^{-1})$. The third term is similarly suppressed by $O(N^{-1})$. Therefore, we can carry out the ordinary process of loop correction to propagator, in which two point function $G(\tau - \tau')$ is obtained by the expression like figure 21. If we express a self energy Σ and define a bilinear kernel as

$$
(AB)(\tau, \tau') = \int d\tau'' A(\tau, \tau'') B(\tau'', \tau')
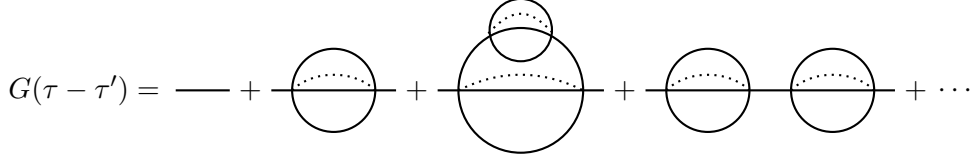\tag{6.22}
$$

Figure 21: Loop correction to the propagator to calculate $G(\tau - \tau')$. Dotted lines express disorder pairing.

Then we get the Schwinger-Dyson equation as follows.

$$
\begin{aligned}
G &= G^{\text{free}} + G^{\text{free}} \Sigma G^{\text{free}} + \cdots \\
&= G^{\text{free}}[1 + \Sigma G^{\text{free}} + \cdots] \\
&= G^{\text{free}}[1 - \Sigma G^{\text{free}}]^{-1} \\
&= [(G^{\text{free}})^{-1} - \Sigma]^{-1}
\end{aligned}
\tag{6.23}
$$

Because of $(G^{\text{free}})^{-1}(\tau, \tau') = \delta(\tau - \tau')\partial_{\tau'}$, we can express the Schwinger-Dyson equation as

$$
G = [\partial_\tau - \Sigma]^{-1}
\tag{6.24}
$$

where Σ is calculated as

$$
\Sigma(\tau, \tau') = J^2 [G(\tau, \tau')]^3
\tag{6.25}
$$

In the q-body interaction theory, the Schwinger-Dyson equation can be obtained similarly as

$$
\begin{aligned}
G &= [\partial_\tau - \Sigma]^{-1} \\
\Sigma &= J^2 G^{q-1}
\end{aligned}
\tag{6.26}
$$

6.2.2 Effective action

In this subsection, we introduce the large N effective action I_{eff} of the SYK model and expalin that the Schwinger-Dyson equation is derived as the classical equation of motion extremizing I_{eff}. We assume $q = 4$ here, but the generalization to the q-body interaction is straightforward. The partition function is expressed as the path integral

$$
Z(J_{ijkl}) = \int \mathcal{D}\psi_i \exp\left[-\int d\tau \left(\frac{1}{2} \sum_i \psi_i \partial_\tau \psi_i + \sum_{1 \le i < j < k < l \le N} J_{ijkl} \psi_i \psi_j \psi_k \psi_l \right) \right].
\tag{6.27}
$$

We evaluate $\langle Z \rangle_J$, the average of the partition function about J_{ijkl} and derive large N effective action. The essence of the calculation is giving up the path integral calculation in N Majorana fermion field ψ_i in eq. (6.27) and changing the variables to the fermion bilinear field $G(\tau, \tau')$ which is constructed by averaging large N Majorana fermions. Let us explain the method.

Since J_{ijkl} is chosen randomly and independently from the Gaussian distribution with mean $\mu = 0$ and variance $\sigma^2 = \frac{3!J^2}{N^3}$,

$$\langle Z \rangle_J = \sqrt{\frac{N^3}{12\pi J^2}} \int dJ_{ijkl} \exp\left[-\sum_{1 \leq i < j < k < l \leq N} \frac{J_{ijkl}^2}{2 \cdot \frac{3!J^2}{N^3}}\right] Z(J_{ijkl}). \qquad (6.28)$$

This integral can be carried out by the formula $\int dx e^{-ax^2 + bx} = \sqrt{\frac{\pi}{a}} e^{\frac{b^2}{4a}}$ and we obtain

$$\langle Z \rangle_J = \int \mathcal{D}\psi_i \exp\left[-\int d\tau \frac{1}{2}\sum_i \psi_i(\tau)\partial_\tau \psi_i(\tau) + \sum_{1 \leq i < j < k < l \leq N} \frac{3J^2}{N^3} \int\int d\tau d\tau' (\psi_i \psi_j \psi_k \psi_l)(\tau)(\psi_i \psi_j \psi_k \psi_l)(\tau')\right].$$
$$(6.29)$$

Using $\psi_i^2(\tau) = 0$, the second term can be rewritten as

$$\sum_{1 \leq i < j < k < l \leq N} (\psi_i \psi_j \psi_k \psi_l)(\tau)(\psi_i \psi_j \psi_k \psi_l)(\tau') = \frac{1}{4!}\left[\sum_i \psi_i(\tau)\psi_i(\tau')\right]^4. \qquad (6.30)$$

Then just like the Faddev-Popov path integral method, inserting 1:

$$1 = \int \mathcal{D}G \delta\left(NG(\tau, \tau') - \sum_i \psi_i(\tau)\psi_i(\tau')\right)$$
$$= \int \mathcal{D}G\mathcal{D}\Sigma \exp\left[-\frac{N}{2}\int\int d\tau d\tau' \Sigma(\tau, \tau')\left(G(\tau, \tau') - \frac{1}{N}\sum_i \psi_i(\tau)\psi_i(\tau')\right)\right] \qquad (6.31)$$

to the path integral. Here, $G(\tau, \tau')$ is the fermion bilinear field defined as $G(\tau, \tau') = \frac{1}{N}\sum_i \psi_i(\tau)\psi_i(\tau')$ and the first line expresses the constraint. $\Sigma(\tau, \tau')$ is the Lagrange multiplier giving the Delta functional. After inserting 1 to the path integral, we obtain

$$\langle Z \rangle_J = \int \mathcal{D}\psi_i \mathcal{D}G\mathcal{D}\Sigma \exp\left[-\int d\tau \frac{1}{2}\sum_i \psi_i(\tau)\partial_\tau \psi_i(\tau)\right.$$
$$-\frac{1}{2}\int\int d\tau d\tau' N\Sigma(\tau, \tau')\left(G(\tau, \tau') - \frac{1}{N}\sum_i \psi_i(\tau)\psi_i(\tau')\right) \quad (6.32)$$
$$\left.+\frac{J^2 N}{8}\int\int d\tau d\tau' (G(\tau, \tau'))^4\right].$$

Carrying out the path integral about ψ_i by using the Gaussian Berezin integral formula $\int d\psi e^{-\frac{1}{2}\psi A \psi} = \sqrt{\det A}$, we obtain

$$\langle Z \rangle_J = \int \mathcal{D}G\mathcal{D}\Sigma \left[\det(\partial_\tau - \Sigma)\right]^{\frac{N}{2}} \exp\left[-\frac{N}{2}\int\int d\tau d\tau'\left(\Sigma G - \frac{J^2}{4}G^4\right)\right]$$
$$= \int \mathcal{D}G\mathcal{D}\Sigma e^{-NI_{eff}[G,\Sigma]}. \qquad (6.33)$$

Here we defined the large N effective action $I_{eff}[G, \Sigma] = -\frac{1}{2}\log(\det(\partial_\tau - \Sigma)) + \frac{1}{2}\int\int d\tau d\tau'(\Sigma G - \frac{J^2}{4}G^4)$. We keep in mind that $\det(\partial_\tau - \Sigma)$ means $\det(\delta(\tau - \tau')\partial_\tau - \Sigma(\tau, \tau'))$. We find out that the reason why N^{-3} factor is contained in the Gaussian distribution is that we can exclude N from the effective action I_{eff}. N behaves like $\hbar^{-1}$, so the large N limit is correspond to the classical limit. Finally, by applying the principle of the least action to I_{eff}, we can obtain the Schwinger-Dyson equation. In q-body interaction theory, the large N effective action becomes

$$I_{eff}[G, \Sigma] = -\frac{1}{2}\log(\det(\partial_\tau - \Sigma)) + \frac{1}{2}\int\int d\tau d\tau'(\Sigma G - \frac{J^2}{q}G^q) \tag{6.34}$$

and the Schwinger-Dyson equation is eq. (6.26).

6.3 Conformal limit

In low energy (IR) limit, the SYK model becomes a one-dimensional CFT. We see the behavior of the SD equation (6.26) in IR limit. The coupling constant J has the dimension of energy, so IR limit means $\omega \ll J$. Using $i\partial_\tau = \omega$, the SD equation in the Fourier space becomes

$$\frac{1}{G(\omega)} = -i\omega - \Sigma(\omega). \tag{6.35}$$

Since $\Sigma \propto J^2 \gg \omega$, we can drop the first term in the right hand side and the IR equation becomes $G(\omega)\Sigma(\omega) = -1$. By inverse Fourier transform, we obtain the IR equation:

$$\int d\tau'' G(\tau, \tau'')\Sigma(\tau'', \tau') = \delta(\tau - \tau'),$$
$$\Sigma(\tau, \tau') = J^2[G(\tau, \tau')]^{q-1}. \tag{6.36}$$

This means that we can drop ∂_τ in IR limit. We can show that G and Σ satisfy a conformal Ward identity with a conformal dimension $\Delta = \frac{1}{q}$:

$$G(\tau, \tau') \longmapsto [\varphi'(\tau)\varphi'(\tau')]^\Delta G(\varphi(\tau), \varphi(\tau'))$$
$$\Sigma(\tau, \tau') \longmapsto [\varphi'(\tau)\varphi'(\tau')]^{\Delta(q-1)}\Sigma(\varphi(\tau), \varphi(\tau')) \tag{6.37}$$

with some reparametrization $\tau \mapsto \varphi(\tau)$. We found that in the IR limit large N SYK model has a conformal symmetry, which is realized as reparametrization symmetry $\tau \mapsto \varphi(\tau)$. $\omega \ll J$ is equivalent to $|\tau - \tau'| \gg J^{-1}$. This reparametrization symmetry is broken away from IR due to ∂_τ term. In the CFT, the form of correlation function is decided without solving equation of motion made by specific Lagrangian. By the conformal Ward identity, the conformal two point function is decided as $\langle\phi(x_1)\phi(x_2)\rangle = \frac{const}{|x_1 - x_2|^\Delta}$ for some quasi primary $\phi(x)$, we can expect that in IR limit, $G(\tau, \tau')$ becomes

$$G_c(\tau, \tau') = \frac{b}{|\tau - \tau'|^{2\Delta}}\text{sgn}(\tau - \tau') \tag{6.38}$$

with some constant b. Here, the subscript c of G_c means "conformal" and Δ is a conformal dimension. We can guarantee this solution and decide b by solving the IR equation. If we consider an ansatz like

$$G_c(\tau, \tau') = b\, d_\Delta(\tau - \tau'), \ \Sigma_c(\tau, \tau') = J^2 b^{q-1} d_{\Delta(q-1)}(\tau - \tau'), \ d_\Delta(\tau - \tau') = \frac{\mathrm{sgn}(\tau - \tau')}{|\tau - \tau'|^{2\Delta}} \quad (6.39)$$

the second equation of the IR equation (6.36) is satisfied. Thus we solve the first equation, which is $G(\omega)\Sigma(\omega) = -1$ in the Fourier space. The Fourier transformation of $d_\Delta(\tau - \tau')$ is

$$d_\Delta(\omega) = 2i \cos(\pi \Delta)\Gamma(1 - 2\Delta)\frac{1}{\omega^{1-2\Delta}} \quad (6.40)$$

in $\omega > 0$, and $\omega < 0$ case is considered by $d_\Delta(-\omega) = -d_\Delta(\omega)$. Plugging this into $G(\omega)\Sigma(\omega) = -1$, we can conclude

$$\begin{aligned}
G_c(\tau, \tau') &= b\, d_\Delta(\tau - \tau') \\
\Sigma_c(\tau, \tau') &= J^2 b^{q-1}\, d_{\Delta(q-1)}(\tau - \tau') \\
d_\Delta(\tau) &= \frac{\mathrm{sgn}(\tau - \tau')}{|\tau - \tau'|^{2\Delta}} \\
\Delta &= \frac{1}{q} \\
b^q &= \frac{1}{\pi J^2}\left(\frac{1}{2} - \frac{1}{q}\right)\tan\frac{\pi}{q}.
\end{aligned} \quad (6.41)$$

We obtain the exact solution in IR limit. In the UV theory, we can also get an exact solution. UV means $\tau \ll J^{-1}$, so $J \to 0, \Sigma \to 0$ leads to $G \sim \partial_\tau^{-1}$. We obtain $G(\tau, \tau') \to \frac{1}{2}\mathrm{sgn}(\tau - \tau')$ in UV limit.

In a finite temperature theory on the circle $\tau \sim \tau + \beta$, the thermal two point function is obtained by the relation (6.12) as

$$\begin{aligned}
G_{\beta,c}(\tau, \tau') &= b\left[\frac{\pi}{\beta\left|\sin\frac{\pi(\tau-\tau')}{\beta}\right|}\right]^{2\Delta} \mathrm{sgn}(\tau - \tau') \\
&\propto \frac{1}{(\beta J)^{\frac{2}{q}}}\frac{1}{\left|\sin\frac{\pi(\tau-\tau')}{\beta}\right|^{2\Delta}}.
\end{aligned} \quad (6.42)$$

We used that for $\tau \in \left[-\frac{\beta}{2}, \frac{\beta}{2}\right)$, $\mathrm{sgn}\left(\tan\frac{\pi\tau}{\beta}\right) = \mathrm{sgn}\left(\sin\frac{\pi\tau}{\beta}\right) = \mathrm{sgn}(\tau)$ is satisfied. By the analytic continuation to the Lorentzian time $t = -i\tau$, we find that

$$G_{\beta,c}(t) \propto \frac{1}{(\beta J)^{\frac{2}{q}}}\frac{1}{\left|\sinh\frac{\pi t}{\beta}\right|^{2\Delta}} \propto e^{-\frac{2\pi\Delta}{\beta}t} \quad (6.43)$$

and this becomes exponentially small as the time scale $t_d = \frac{\beta}{2\pi\Delta} \sim \beta$. We call this as a "dissipation time".

6.4 Schwarzian action

In the previous section, we saw that in IR limit, the large N classical theory has a conformal symmetry and the saddle point of the two point function $\tilde{G}$ is decided to conformal two point function without solving the full SD equation. The appearance of ∂_τ due to leaving away from IR limit breaks the conformal symmetry. In this section, we review this symmetry breaking carefully, following the paper of Trunin [34]. We consider $q = 4$ case. We divide the effective action (6.34) to a conformally invariant part and a non-invariant part: $I_{eff} = I_{CFT} + I_S$. We call I_S the Schwarzian action. I_{CFT} and I_S are written as

$$I_{CFT} = -\frac{1}{2}\log\left(\det\left(-\Sigma(\tau,\tau')\right)\right) + \frac{1}{2}\int\int d\tau d\tau'\left(\Sigma(\tau,\tau')G(\tau,\tau') - \frac{J^4}{4}G(\tau,\tau')^4\right), \quad (6.44)$$

$$I_S = -\frac{1}{2}\int\int d\tau d\tau'\delta(\tau-\tau')\partial_\tau G(\tau,\tau') = -\frac{1}{2}\int\int d\tau d\tau' G_0^{-1}(\tau,\tau')G(\tau,\tau'), \quad (6.45)$$

where we defined $G_0^{-1}(\tau,\tau') \equiv \delta(\tau-\tau')\partial_\tau$. I_{CFT} reproduces the IR equation (6.36). I_S is not effective in IR limit ($\beta J \gg 1$) and is expected to be proportional to $\frac{1}{\beta J}$, representing the physics around $|\tau - \tau'| \ll J^{-1}$. We consider the deformation from the saddle point $(\tilde{G}, \tilde{\Sigma})$ as $G = \tilde{G} + \frac{\delta G}{|\tilde{G}|}$, $\Sigma = \tilde{\Sigma} + |\tilde{G}|\delta\Sigma$. I_{eff} is written as

$$\begin{aligned}
I_{eff} &\approx \frac{1}{4}\int d\tau_1 d\tau_2 d\tau_3 d\tau_4 \delta\Sigma(\tau_1,\tau_2)\left(|\tilde{G}(\tau_1,\tau_2)|\,\tilde{G}(\tau_1,\tau_3)\tilde{G}(\tau_2,\tau_4)\,|\tilde{G}(\tau_3,\tau_4)|\right)\delta\Sigma(\tau_3,\tau_4)\\
&\quad + \frac{1}{2}\int d\tau_1 d\tau_2\left(\delta G(\tau_1,\tau_2)\delta\Sigma(\tau_1,\tau_2) - \frac{3J^2}{2}\delta G(\tau_1,\tau_2)^2\right)\\
&= -\frac{1}{12J^2}\langle\delta\Sigma|\,K\,|\delta\Sigma\rangle + \frac{1}{2}\langle\delta G|\delta\Sigma\rangle - \frac{3J^2}{4}\langle\delta G|\delta G\rangle = I_{eff}[\delta G, \delta\Sigma],
\end{aligned}$$
$$(6.46)$$

where we defined the ladder kernel K as

$$K(\tau_1,\tau_2;\tau_3,\tau_4) \equiv -3J^2|\tilde{G}(\tau_1,\tau_2)|\,\tilde{G}(\tau_1,\tau_3)\tilde{G}(\tau_2,\tau_4)\,|\tilde{G}(\tau_3,\tau_4)| \quad (6.47)$$

and $|A\rangle \equiv A(\tau,\tau')$ is acted by K as

$$K\,|A\rangle \equiv \int d\tau_3 d\tau_4 K(\tau_1,\tau_2;\tau_3,\tau_4)A(\tau_3,\tau_4). \quad (6.48)$$

An identity operator is defined as

$$\begin{aligned}
I(\tau_1,\tau_2;\tau_3,\tau_4) &\equiv \frac{1}{2}\left(\delta(\tau_1-\tau_3)\delta(\tau_2-\tau_4) - \delta(\tau_1-\tau_4)\delta(\tau_2-\tau_3)\right)\\
I\,|A\rangle &= |A\rangle
\end{aligned}$$
$$(6.49)$$

and an inner product of $|A\rangle = A(\tau,\tau')$ and $|B\rangle = B(\tau,\tau')$ is defined as

$$\langle A|B\rangle \equiv \int d\tau_1 d\tau_2 A^*(\tau_1,\tau_2)B(\tau_1,\tau_2). \quad (6.50)$$

The ladder kernel K and the identity operator I are antisymmetric under $\tau_1 \leftrightarrow \tau_2$ and $\tau_3 \leftrightarrow \tau_4$, and symmetric under $(\tau_1, \tau_2) \leftrightarrow (\tau_3, \tau_4)$. After we integrate out the Lagrange multiplier Σ, we obtain

$$I_{eff}[\delta G] = -\log \int \mathcal{D}\delta\Sigma e^{-I_{eff}[\delta G, \delta\Sigma]} = \frac{3J^2}{4} \langle \delta G | (K^{-1} - I) | \delta G \rangle . \tag{6.51}$$

If we take IR limit of this action naively, we may think of as

$$I_{eff}[\delta G] \xrightarrow[\text{IR}]{} I_{CFT}[\delta G] \approx \frac{3J^2}{4} \langle \delta G | (K_c - I) | \delta G \rangle \tag{6.52}$$

where K_c is the ladder kernel (6.47) with $\tilde{G}$ changed by G_c. However, this naive guess cannot fully treat the fluctuation around the saddle point. The conformally invariant action (6.52) becomes zero if we consider the fluctuation δG which conserves the conformal invariance. Using $G = G_c + \frac{\delta G}{|G_c|}$ and $\Sigma = J^2 G_c^3 + 3J^2 |G_c| \delta G$ and solving the IR equation (6.36), we reach $(I - K_c)\delta G = 0$ and (6.52) becomes zero. Thus we must study how I_S changes under the conformal transformation (6.37). After the reparametrization $\tau \mapsto \varphi(\tau)$, $G_c(\tau_1, \tau_2)$ changes as

$$G_c(\varphi(\tau_1), \varphi(\tau_2)) = \frac{\text{sgn}(\tau_1 - \tau_2)}{(4\pi)^{\frac{1}{4}} J^{2\Delta}} \frac{\varphi'(\tau_1)^\Delta \varphi'(\tau_2)^\Delta}{|\varphi(\tau_1) - \varphi(\tau_2)|^{2\Delta}} . \tag{6.53}$$

If we expand this near $\tau = \frac{\tau_1 + \tau_2}{2}$ in the power of $\tau_{12} = \tau_1 - \tau_2$,

$$G(\tau_1, \tau_2) = G_c(\tau_1, \tau_2) \left(1 + \frac{\Delta}{6} \tau_{12}^2 \,\text{Sch}[\varphi(\tau), \tau] + \mathcal{O}(\tau_{12}^3) \right) \tag{6.54}$$

where $\text{Sch}[\varphi(\tau), \tau] \equiv \frac{\varphi'''}{\varphi'} - \frac{3}{2} \left(\frac{\varphi''}{\varphi'} \right)^2$ is the Schwarzian derivative. Using this and dropping $\mathcal{O}(\tau_{12}^3)$ term, we can evaluate the Schwarzian action as

$$
\begin{aligned}
I_S = -\frac{1}{2} \langle G_0^{-1} | \delta G \rangle &= -\frac{1}{2} \int d\tau d\tau_{12} G_0^{-1}(\tau_{12}) \tilde{G}(\tau_{12}) \frac{\Delta}{6} \tau_{12}^2 \,\text{Sch}[\varphi(\tau), \tau] \\
&= -\frac{\Delta}{12} \int d\tau_{12} \delta(\tau_{12}) \partial_{\tau_{12}} \left(\tau_{12}^2 \tilde{G}(\tau_{12}) \right) \int d\tau \,\text{Sch}[\varphi(\tau), \tau] \\
&= -\frac{1}{J} \frac{\Delta}{12} \int d\eta \,\delta(\eta) \partial_\eta \left(\eta^2 \tilde{G}(\eta) \right) \int d\tau \,\text{Sch}[\varphi(\tau), \tau]
\end{aligned}
\tag{6.55}
$$

where $\eta = J\tau_{12}$. We set $\alpha_S = \frac{\Delta}{12} \int d\eta \,\delta(\eta) \partial_\eta \left(\eta^2 \tilde{G}(\eta) \right)$. This can be calculated as $\alpha_S \approx 0.48 \times \frac{\Delta}{12}$ by smearing $\delta(\eta)$ and introducing suitable UV and IR cutoffs. We reached the concrete form of the Schwarzian action:

$$I_S = -\frac{\alpha_S}{J} \int d\tau \,\text{Sch}[\varphi(\tau), \tau] . \tag{6.56}$$

In the finite temperature theory, it becomes as follows.

$$I_S = -\frac{\alpha_S}{J} \int_{-\frac{\beta}{2}}^{\frac{\beta}{2}} d\tau \,\text{Sch}\left[\tan \frac{\pi\varphi(\tau)}{\beta}, \tau \right] \tag{6.57}$$

6.5 Four point function

In this subsection, we explain the calculation of the four point function of the SYK model, following the paper of Trunin [34]. We consider the following averaged four point function, which is averaged over large N Majorana fermions:

$$
\frac{1}{N^2} \sum_{i,j=1}^{N} \langle \mathcal{T} \psi_i(\tau_1) \psi_i(\tau_2) \psi_j(\tau_3) \psi_j(\tau_4) \rangle
$$
$$
= \frac{1}{Z} \int \mathcal{D}G \mathcal{D}\Sigma \left[G(\tau_1, \tau_2) G(\tau_3, \tau_4) + \frac{1}{N} \left(G(\tau_1, \tau_4) G(\tau_2, \tau_3) - G(\tau_1, \tau_3) G(\tau_2, \tau_4) \right) \right] e^{-NI_{eff}[G, \Sigma]} .
$$
(6.58)

Here, I_{eff} is the partition function which the effective action I_{eff} is used for the path integral. We can set $\tau_1 > \tau_2, \tau_3 > \tau_4, \tau_1 > \tau_3$ without loss of generality. We define $\tilde{G}$ as a saddle point (classical solution) of I_{eff} and define the connected four point function as follows.

$$
\mathcal{F}(\tau_1, \tau_2; \tau_3, \tau_4) \equiv \frac{1}{N^2} \sum_{i,j=1}^{N} \langle \mathcal{T} \psi_i(\tau_1) \psi_i(\tau_2) \psi_j(\tau_3) \psi_j(\tau_4) \rangle - \tilde{G}(\tau_1, \tau_2) \tilde{G}(\tau_3, \tau_4)
$$
(6.59)

In the IR limit, $\tilde{G}$ is the conformal two point function G_c^β. We consider a small deformation from the saddle point $\tilde{G} = G_c^\beta$ which conserves the conformal symmetry as $\delta G^\parallel$ and a small deformation which breaks the conformal symmetry as $\delta G^\perp$. If $\varphi(\tau)$ is some reparametrization which conserves the conformal symmetry,

$$
\delta G_\varphi^\parallel(\tau_1, \tau_2) = G_c^\beta(\varphi(\tau_1), \varphi(\tau_2)) - G_c^\beta(\tau_1, \tau_2) .
$$
(6.60)

The connected four point function $\mathcal{F}$ can be expressed in the following expansion:

$$
\mathcal{F} = \mathcal{F}_0 + \frac{1}{Z} \int \mathcal{D}\delta G^\parallel \mathcal{D}\delta G^\perp \mathcal{D}\Sigma \left(\delta G^\parallel(\tau_1, \tau_2) + \delta G^\perp(\tau_1, \tau_2) \right)
$$
$$
\times \left(\delta G^\parallel(\tau_3, \tau_4) + \delta G^\perp(\tau_3, \tau_4) \right) e^{-N(I_{CFT} + I_S)}
$$
(6.61)
$$
= \mathcal{F}_0 + \mathcal{F}_S + \mathcal{F}_{CFT} + \mathcal{O}\left(\frac{1}{N^2} \right)
$$

Here, the bare four point function $\mathcal{F}_0$, the Schwarzian term $\mathcal{F}_S$, the CFT term $\mathcal{F}_{CFT}$ are defined as:

$$
\mathcal{F}_0 \equiv \frac{1}{N} (\tilde{G}(\tau_1, \tau_4) \tilde{G}(\tau_2, \tau_3) - \tilde{G}(\tau_1, \tau_3) \tilde{G}(\tau_2, \tau_4))
$$
(6.62)

$$
\mathcal{F}_S \equiv \langle \delta G^\parallel(\tau_1, \tau_2) \, \delta G^\parallel(\tau_3, \tau_4) \rangle_S = \frac{\int \mathcal{D}\varphi \, \delta G_\varphi^\parallel(\tau_1, \tau_2) \delta G_\varphi^\parallel(\tau_3, \tau_4) \, e^{-NI_S[\varphi]}}{\int \mathcal{D}\varphi \, e^{-NI_S[\varphi]}}
$$
(6.63)

$$
\mathcal{F}_{CFT} \equiv \langle \delta G^\perp(\tau_1, \tau_2) \, \delta G^\perp(\tau_3, \tau_4) \rangle_{CFT} = \frac{\int \mathcal{D}\delta G^\perp \, \delta G^\perp(\tau_1, \tau_2) \delta G^\perp(\tau_3, \tau_4) \, e^{-NI_{eff}[\delta G^\perp]}}{\int \mathcal{D}\delta G^\perp \, e^{-NI_{eff}[\delta G^\perp]}}
$$
(6.64)

respectively. The term which mainly contributes to the exponential growth by OTOC in large βJ is the Schwarzian term $\mathcal{F}_S$, which is calculated by the path integral with the Schwarzian action I_S. Although $\mathcal{F}_{CFT}$ also shows OTOC behavior, $\mathcal{F}_S$ is larger than $\mathcal{F}_{CFT}$ by the factor βJ, so we focus on evaluating $\mathcal{F}_S$. We review the formula to calculate $\mathcal{F}_S$ in the next subsection. See [34] for the detailed derivation.

6.5.1 Soft mode contribution of four point function

The Schwarzian term of the connected four point function can be evaluated by the following equation.

$$
\begin{aligned}
\frac{\mathcal{F}_S(\tau_1, \tau_2; \tau_3, \tau_4)}{G_c^\beta(\tau_1, \tau_2) G_c^\beta(\tau_3, \tau_4)} &= \frac{\langle \delta G_\varphi^\parallel(\tau_1, \tau_2) \delta G_\varphi^\parallel(\tau_3, \tau_4) \rangle_S}{G_c^\beta(\tau_1, \tau_2) G_c^\beta(\tau_3, \tau_4)} \\
&= \frac{\pi^2}{4} \int_{\tau_2}^{\tau_1} \frac{d\tau_5}{2\pi} \int_{\tau_4}^{\tau_3} \frac{d\tau_6}{2\pi} \langle \delta O(\tau_5) \delta O(\tau_6) \rangle_S \cdot \frac{s_{15} s_{52}}{s_{12}} \frac{s_{36} s_{64}}{s_{34}}
\end{aligned}
\tag{6.65}
$$

Here, we defined $s_{ij} \equiv 2\sin\left(\frac{\tau_i - \tau_j}{2}\right)$ and $\delta O(\tau) \equiv \mathrm{Sch}\left(\tan\frac{\varphi(\tau)}{2}, \tau\right) - \frac{1}{2}$. We repeat the definition of the Schwarzian derivative: $\mathrm{Sch}(f(\tau), \tau) \equiv \frac{f'''}{f'} - \frac{3}{2}\left(\frac{f''}{f'}\right)^2$.

By the expansion of the Schwarzian derivative and omitting the boundary term and $\mathcal{O}((\varphi(\tau) - \tau)^3)$ terms, the two point function of δO can be evaluated as follows.

$$
\langle \delta O(\tau_5) \delta O(\tau_6) \rangle_S = \frac{1}{2\pi C} \frac{\beta J}{N} [1 - 2\pi \delta(\tau_{56}) - 2\pi \delta''(\tau_{56})]
\tag{6.66}
$$

Here, $\tau_{56} \equiv \tau_5 - \tau_6$. C is the coefficient which appears in the Schwarzian action. In the case of $\tau_2 < \tau_3$, the integral in (6.65) overlaps whereas in the case of $\tau_2 \geq \tau_3$ there is no overlap. We should divide in cases to an OPE case and an OTO case for the evaluation of (6.65). Here OPE is a time ordering case, so we call this a time ordered correlator (TOC), and OTO stands for an out of time ordering and we call this out of time ordered correlator (OTOC):

$$
\begin{aligned}
&\mathrm{TOC}: 2\pi > \tau_1 > \tau_2 > \tau_3 > \tau_4 > 0, \\
&\mathrm{OTOC}: 2\pi > \tau_1 > \tau_3 > \tau_2 > \tau_4 > 0.
\end{aligned}
\tag{6.67}
$$

In TOC case, the integrals over τ_5 and τ_6 decouples and the Schwarzian term is evaluated as:

$$
\frac{\mathcal{F}_S(\tau_1, \tau_2; \tau_3, \tau_4)}{G_c^\beta(\tau_1, \tau_2) G_c^\beta(\tau_3, \tau_4)} = \frac{1}{8\pi C} \frac{\beta J}{N} \left(\frac{\tau_{12}}{2\tan\frac{\tau_{12}}{2}} - 1\right) \left(\frac{\tau_{34}}{2\tan\frac{\tau_{34}}{2}} - 1\right).
\tag{6.68}
$$

The concrete example of TOC case is $\tau_1 = \frac{\beta}{2} + it, \tau_2 = it, \tau_3 = 0, \tau_4 = -\frac{\beta}{2}$. If we extract the

contribution of the Schwarzian term of the four point function, TOC becomes

$$\mathrm{TOC}(t) = \frac{1}{N^2} \sum_{i,j=1}^{N} \mathrm{tr}\left[\psi_i(t)\rho^{\frac{1}{2}}\psi_i(t)\psi_j(0)\rho^{\frac{1}{2}}\psi_j(0)\right]$$

$$= \tilde{G}\left(\frac{\beta}{2}\right)\tilde{G}\left(\frac{\beta}{2}\right) + \mathcal{F}\left(\frac{\beta}{2}+it, it; 0, -\frac{\beta}{2}\right)$$

$$\approx \tilde{G}\left(\frac{\beta}{2}\right)\tilde{G}\left(\frac{\beta}{2}\right) + \mathcal{F}_S\left(\frac{\beta}{2}+it, it; 0, -\frac{\beta}{2}\right) \qquad (6.69)$$

$$\approx \frac{\sqrt{\pi}}{2\beta J} + \frac{const}{N}$$

In the first line, we regularized the four point function by $\rho = \frac{1}{Z}e^{-\beta H}$ because the product of simultaneous operators appears and it is necessary to smear them with some density matrix. In TOC case, the correlator does not depend on t.

In OTOC case, the Schwarzian term becomes

$$\frac{\mathcal{F}_S(\tau_1, \tau_2; \tau_3, \tau_4)}{G_c^{\beta}(\tau_1, \tau_2) G_c^{\beta}(\tau_3, \tau_4)} = \frac{1}{8\pi C}\frac{\beta J}{N}\left[-\frac{3\pi}{8}\frac{\sin\tau_{12;34}}{\sin\left(\frac{\tau_{12}}{2}\right)\sin\left(\frac{\tau_{34}}{2}\right)} + \frac{\pi}{16}\frac{\sin(\tau_{12;34}-\tau_{12})}{\sin\left(\frac{\tau_{12}}{2}\right)\sin\left(\frac{\tau_{34}}{2}\right)} + \frac{\pi}{16}\frac{\sin(\tau_{12;34}-\tau_{34})}{\sin\left(\frac{\tau_{12}}{2}\right)\sin\left(\frac{\tau_{34}}{2}\right)}\right.$$

$$-\frac{\pi}{8}\frac{2\tau_{12;34}-\tau_{12}-\tau_{34}}{\tan\left(\frac{\tau_{12}}{2}\right)\tan\left(\frac{\tau_{34}}{2}\right)} + \frac{3\pi}{8}\frac{1}{\tan\left(\frac{\tau_{12}}{2}\right)} + \frac{3\pi}{8}\frac{1}{\tan\left(\frac{\tau_{34}}{2}\right)}$$

$$\left.+ \left(\frac{\tau_{12}}{2\tan\frac{\tau_{12}}{2}}-1\right)\left(\frac{\tau_{34}}{2\tan\frac{\tau_{34}}{2}}-1\right)\right]$$

$$(6.70)$$

Here, we defined $\tau_{ij;kl} \equiv \frac{\tau_1+\tau_2}{2}-\frac{\tau_3+\tau_4}{2}$. The concrete example of OTOC case is $\tau_1 = \frac{\beta}{4}+it, \tau_2 = -\frac{\beta}{4}+it, \tau_3 = 0, \tau_4 = -\frac{\beta}{2}$. If we extract the contribution of the Schwarzian term of the four point function, OTOC becomes

$$\mathrm{OTOC}(t) = \frac{1}{N^2}\sum_{i,j=1}^{N}\mathrm{tr}\left[\rho^{\frac{1}{4}}\psi_i(t)\rho^{\frac{1}{4}}\psi_j(0)\rho^{\frac{1}{4}}\psi_i(t)\rho^{\frac{1}{4}}\psi_j(0)\right]$$

$$= \tilde{G}\left(\frac{\beta}{2}\right)\tilde{G}\left(\frac{\beta}{2}\right) + \mathcal{F}\left(\frac{\beta}{4}+it, -\frac{\beta}{4}it; 0, -\frac{\beta}{2}\right)$$

$$\approx \tilde{G}\left(\frac{\beta}{2}\right)\tilde{G}\left(\frac{\beta}{2}\right) + \mathcal{F}_S\left(\frac{\beta}{4}+it, -\frac{\beta}{4}it; 0, -\frac{\beta}{2}\right) \qquad (6.71)$$

$$\approx \frac{\sqrt{\pi}}{2\beta J}\left[1 - \frac{\Delta^2}{2C}\frac{\beta J}{N}e^{\frac{2\pi}{\beta}t}\right]$$

We can see $\mathcal{F}_S$ exponentially grows in $\beta \ll t \ll \beta\log\frac{N}{\beta J}$. We call the time $\beta\log\frac{N}{\beta J} \approx \beta\log N \equiv t_{scr}$ as scrambling time, around which $\mathrm{OTOC}(t)$ becomes small.

The reason why we consider the decline of $\mathrm{OTOC}(t)$ [34] is that the correlator which

measures the quantum chaos

$$C(t) = -\operatorname{tr}\left(\rho^{\frac{1}{2}}[V(t),W(0)]\rho^{\frac{1}{2}}[V(t),W(0)]\right)$$
$$= 2\operatorname{TOC}(t) - \operatorname{OTOC}\left(t - \frac{i\beta}{4}\right) - \operatorname{OTOC}\left(t + \frac{i\beta}{4}\right) \tag{6.72}$$

exponentially grows as $C(t) \sim \frac{1}{N}e^{\kappa t}$ when $\operatorname{OTOC}(t)$ rapidly decays around the scrambling time $t_{\mathrm{scr}} \sim \beta \log N$. Here, $N \gg 1$ counts degrees of freedom of the quantum system. We defined $\operatorname{TOC}(t)$ and $\operatorname{OTOC}(t)$ of general quantum operators $V(t)$ and $W(0) = W$ as

$$\operatorname{TOC}(t) \equiv \operatorname{tr}\left(V(t)\rho^{\frac{1}{2}}V(t)W\rho^{\frac{1}{2}}W\right)$$
$$\operatorname{OTOC}(t) \equiv \operatorname{tr}\left(\rho^{\frac{1}{4}}V(t)\rho^{\frac{1}{4}}W\rho^{\frac{1}{4}}V(t)\rho^{\frac{1}{4}}W\right) , \tag{6.73}$$

which are regularized by the density matrix $\rho = \frac{1}{Z}e^{-\beta H}$. The form of $C(t) = -\langle[V(t),W(0)]^2\rangle_\beta$ before the regularization comes from the generalization of

$$C(t) = \sum_n \sum_{out} \frac{1}{Z}e^{-\beta E_n} \langle n|\, [q^i(t), p^j(0)]^\dagger \,|out\rangle \langle out|\, [q^i(t), p^j(0)] \,|n\rangle = -\langle[q^i(t), p^j(0)]^2\rangle_\beta , \tag{6.74}$$

which is the appropriate average of $A_{in\to out} = \langle out|\, [q^i(t), p^j(0)] \,|in\rangle$. This is quantum extension of the classical chaos. The classical chaos is the phenomenon that phase space trajectories from the original small deviation exponentially grow after a time evolution as

$$\|\delta\mathbf{X}(t)\| \le \|\delta\mathbf{X}_0\|e^{\lambda_{max}t} \tag{6.75}$$

where we consider an equation of motion $\dot{X}(t) = F^i[X^i(t)]$ and defined $\delta X^i = X^i - X_0^i$. Here, $\lambda = \lambda_{max}$ is the biggest eigenvalue of $\left(\frac{\partial F^i}{\partial X^j}\right)_{\delta\mathbf{X}=0}$ and does not depend on the initial point $\mathbf{X}_0$ or the choice of the norm. If we choose $\|\mathbf{X}\| = \sum_i |X^i|$, we get

$$\left|\frac{\delta X^i(t)}{\delta X^j(0)}\right| \approx \left|\frac{\partial q^i(t)}{\partial q^j(0)}\right| = |\{q^i(t), p^j(0)\}_{PB}| \sim e^{\lambda t} \tag{6.76}$$

where $\{\cdot\}_{PB}$ is a Poisson bracket and it can be extended to a commutator in the quantum physics: $\{q^i(t), p^j(0)\}_{PB} \to -\frac{i}{\hbar}[q^i(t), p^j(0)]$. That is why we considered (6.74). We call λ as the Lyapunov exponent. In the theory of the quantum chaos, the fast scrambling conjecture claims that κ in $C(t) \sim \frac{1}{N}e^{\kappa t}$ and $\operatorname{OTOC}(t) \sim \langle VV\rangle_\beta\langle VV\rangle_\beta - \frac{A}{N}e^{\kappa t}$ is bounded from above as $\kappa \le \frac{2\pi}{\beta}$. The upper bound is realized when considering the black hole dynamics. It implies that black hole dynamics is most chaotic and it scrambles quantum information most rapidly in the scrambling time $t_{\mathrm{scr}} \sim \beta \log N$.

6.6 Motivation to consider the SYK model in our study

Here, we explain the motivation to consider the SYK model in our study to find the recovery map for the black hole information loss problem. First, in the former half part of this paper, we considered the black hole dynamics as a random unitary matrix and it is too abstract and idealistic. It is more realistic and worth considering that we consider the spin system made of Majorana fermions with random interaction. Second, in the Hayden-Preskill setup, the black hole and the early radiation make an EPR pair and it is the infinite temperature limit. The black hole and the radiation should make a TFD state which can be prepared by the thermal path integral as the setup of the Hartle-Hawking state. Finally, we would like to study the recovery map in QFT. By the holographic point of view, studying with QFT is important. The SYK model is the holographic dual theory of JT gravity, which makes an AdS_2 black hole in the way similar to the original AdS/CFT correspondence but different in its boundary condition. Both JT and SYK have the Schwarzian action in their perturbation in coupling constants. The SYK exhibits scrambling in OTOC four point function and it is thought of as exhibit fast scrambling in the context of the bound on chaos. Therefore, to study the recovery map in the SYK is important. In the next section, we review the method to evaluate a modular flowed correlator in the SYK, which is used in the study of the Petz lite recovery map in section 8.

7 Replica trick calculation of the SYK model

In this section, we introduce the application of the SYK model to the Hayden-Preskill setup. This was precisely dicsussed in the paper of Chandrasekaran and Levine[14]. In this paper, in the first setup, old black hole R makes a thermo field double (TFD) state with the old radiation L. We repeat the definition of the TFD here: $|\text{TFD}\rangle_{LR} = \frac{1}{\sqrt{Z_\beta}} \sum_n e^{-\beta E_n/2} |n\rangle_L |n\rangle_R \equiv |\beta\rangle$. Z_β is a partition function: $Z_\beta = \sum_n e^{-\beta E_n}$. Then quantum information made of Majorana fermion operator ψ_R is inserted into the right black hole system on the time T_R and the right system is time evolved by the SYK random dynamics $U_R = \exp(-itH_{\text{SYK};R})$. After the time evolution, the right system will be divided into the remaining black hole system r and the new Hawking radiation K. As the Hayden-Preskill protocol, we consider how much new radiation we need in order to recover the original quantum information. In order to identify this quantity, the paper [14] defines the price of ψ_R in terms of $|\beta\rangle$ as the number of qubit of K which is necessary to reconstruct the information of ψ_R from radiation systems L, K after tracing out r. This discussion appeared in the paper of Chandrasekaran, Faulkner and Levine [37], in which gravitational calculation in the bulk side is carried out, and its application to the SYK model is studied in [14]. The price is expressed in form of modular flowed correlator, which is defined as an expectation value of fermion operators and a modular operator appeared in the Tomita-Takesaki theory. Our study uses this modular flowed correlator, so we define this and explain how to evaluate it. We summarize what we discuss in this section. First, in 7.1, we define the price of an operator. Then in 7.2, we explain the relation between the fidelity susceptibility and the price, and see the form of modular flowed correlator. In 7.3, we explain the replica trick calculation of the SYK, whose method is essentially the same as other QFT model. We write down the Schwinger-Dyson equation in 7.3 by the method of the replica trick and then solve the Schwinger-Dyson equation in 7.4 in large βJ limit because we are interested in the Schwarzian theory deformed a little by IR limit. Finally we explain the result of the analytic continuation to the Euclidean time and the integer number of replicas in 7.5.

7.1 Definition of price

First, we define a price of the QEC code. As we study in section 4, a physical Hilbert space contains a code subspace: $\mathcal{H}_{code} \subset \mathcal{H}_{physical} \equiv \mathcal{H}$. $B(\mathcal{H}_{code})$ is the set of operators which act to vectors in $\mathcal{H}_{code}$, and it construct von Neumann algebra $\mathcal{A}$. We assume that $\mathcal{H}$ can be decomposed as $\mathcal{H} = \mathcal{H}_A \otimes \mathcal{H}_{\bar{A}}$. $\mathcal{H}_A$ is the Hilbert space on A. We write $\mathcal{H}_{code;A}$ as the restriction of the code subspace to A.

Definition 3 (reconstruction of von Neumann algebra)**.** For all $\rho \in B(\mathcal{H}_{code})$, if there exists $\rho_A \in B(\mathcal{H}_{code;A})$ such that $\rho |\psi\rangle = \rho_A |\psi\rangle$, $\forall |\psi\rangle \in \mathcal{H}_{code}$, we say that the von Neumann
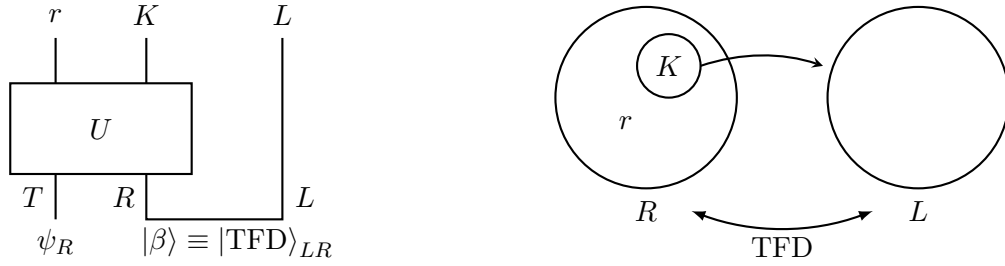
Figure 22: **Left**: Chandrasekaran-Levine's SYK Hayden-Preskill setup. **Right**: The more abstract picure

algebra $\mathcal{A}$ can be reconstructed on subspace A. It is known that when $\mathcal{A}$ can be reconstructed to A, there exists a recovery map for erasure of $\bar{A}$: $\exists \mathcal{R} \, s.t. \, \mathcal{R} \circ \operatorname{tr}_{\bar{A}} = 1$.

Definition 4 (price of von Neumann algebra)**.** Price $p(\mathcal{A})$ of the von Neumann algebra $\mathcal{A}$ is defined as a minimal number of qubits of A such that $\mathcal{A}$ can be reconstruced to A.

In short, the price of QEC code defines how many qubits is necessary to construct a recovery map for the erasure channel of $\bar{A}$. It can be interpreted as a restricted version of the Knill-Laflamme condition to erasure channel. We also define price of a physical operator.

Definition 5 (price of physical operator)**.** For all physical operator O in $B(\mathcal{H})$, consider a reference state $|\phi\rangle \in \mathcal{H}$ such that $\langle \phi | O | \phi \rangle = 0$. Then sub-algebra $\mathcal{A}_O^\phi \subset B(\mathcal{H})$ which is constructed by $O |\phi\rangle \langle\phi| + h.c.$ is isomorphic to the algebra of a single qubit. We define a price of the physical operator O in terms of $|\phi\rangle$ as $p_\phi(O) \equiv p(\mathcal{A}_O^\phi)$.

Chandrasekaran and Levine studied the Hayden-Preskill setup in the SYK model by considering the situation of inserting a Majorana operator ψ_R to the right system, time evolving by the SYK dynamics and tracing out r. They evaluate the price $p_\beta(\psi_R)$, the minimal size of K necessary to reconstruct the sub-algebra $\mathcal{A}_{\psi_R}^\beta$ by radiation systems LK. This is just the Hayden-Preskill analog in the SYK model. See figure 22 for this situation.

7.2 Fidelity susceptibility and modular flowed correlator

In this subsection, we explain the condition to reconstruct the sub-algebra $\mathcal{A}_{\psi_R}^\beta$ by LK from viewpoint of bulk reconstruction. We consider light cone coordinate $x^+ = t + x = e^{T_R}, x^- = t - x$ and make a excitation state with conformal primary ϕ_R of CFT_d.

$$|\phi_\delta\rangle = Z_\delta \phi(x^- = -e^{-i\delta}, x^+ = e^{i\delta}) |\Omega\rangle \tag{7.1}$$

Here, $|\Omega\rangle$ is vacuum state of CFT_d. We regularized with imaginary boost $\Delta_R^{\delta/2\pi} = \sigma_R^{\delta/2\pi} \otimes \sigma_L^{-\delta/2\pi}$ and normalized with $Z_\delta = (2 \sin \delta)^{2\Delta_\phi}$. σ_R, σ_L are vacuum reduced density matrices: $\sigma_R = \operatorname{tr}_L[|\Omega\rangle \langle\Omega|], \sigma_L = \operatorname{tr}_R[|\Omega\rangle \langle\Omega|]$. We assume a light particle $\Delta_\phi \ll 1$ with no backreaction. Then we consider time evolution of $|\phi_\delta\rangle$ and study how long it takes to be contained by

entanglement wedge of LK, which is inside the quantum extremal surface (QES). We consider a time evolution

$$|\phi_\delta\rangle \to \Delta_R^{iT_R/2\pi} |\phi_\delta\rangle \equiv |\phi_\delta(T_R)\rangle \ . \tag{7.2}$$

We consider a code subspace as follows:

$$\begin{aligned}
\mathcal{H}_{code} &= \text{span}\{|\Omega\rangle, |\phi_\delta(T_R)\rangle\} \\
&= \text{span}\{|\Omega\rangle, Z_\delta \Delta_R^\delta \phi_R(T_R) |\Omega\rangle\} \ .
\end{aligned} \tag{7.3}$$

In the Hayden-Preskill setup in the SYK, $|\Omega\rangle$ becomes $|\beta\rangle = Z_\beta^{-1/2} e^{-\frac{\beta}{4}(H_L+H_R)} |0\rangle$ and the code subspace is $\mathcal{H}_{code} = \text{span}\{|\beta\rangle, \phi(T_R) |\beta\rangle\}$. We study the condition that $\mathcal{H}_{code}$ can be reconstructed on LK. We consider the following embedding map.

$$|\Psi_{LKrE}(T_R)\rangle = \frac{1}{\sqrt{2}} \left(|0\rangle_E |\Omega\rangle_{LKr} + |1\rangle_E |\phi_\delta(T_R)\rangle_{LKr}\right) \tag{7.4}$$

Here, E is a reference system used in the Hayden-Preskill setup. If the decoupling condition $I(E:r) \approx 0$[14] is satisfies, there exists a decoder $V_{KL\to KL\tilde{E}\tilde{E}'}$ such that

$$V_{LK\to LK\tilde{E}\tilde{E}'} |\Psi_{LKrE}\rangle = |\text{EPR}\rangle_{E\tilde{E}'} \otimes |\Psi_{\tilde{E}rKL}\rangle \ . \tag{7.6}$$

However, $I(E:r) \approx 0$ is hard to calculate, so we consider the alternative condition that Pauli X and Pauli Y made by $|\Omega\rangle, |\phi_\delta\rangle$ can be reconstructed on LK. We define

$$\begin{aligned}
\sigma_X &= |\phi_\delta\rangle \langle\Omega| + |\Omega\rangle \langle\phi_\delta| \\
\sigma_Y &= i(|\phi_\delta\rangle \langle\Omega| - |\Omega\rangle \langle\phi_\delta|)
\end{aligned} \tag{7.7}$$

and define excited states with $\sigma_{X,Y}$ as $\left|\psi_\lambda^{X,Y}\right\rangle = e^{i\lambda\sigma_{X,Y}} |\Omega\rangle$. When the excitation with $\sigma_{X,Y}$ is reconstructable on LK, the fidelity between the vacuum on r and the excited state $\left|\psi_\lambda^{X,Y}\right\rangle$ becomes 1. By the Uhlmann's theorem, the fidelity is expressed as

$$F\left(\psi_\lambda^{X,Y} |\Omega; r\right) = \sup_{U_{LK}} |\left\langle\psi_\lambda^{X,Y}\right| U_{LK} |\Omega\rangle|^2 \ . \tag{7.8}$$

Here, U_{LK} is unitary on LK. In $\lambda \ll 1$ limit, the fidelity can be expanded as

$$F\left(\psi_\lambda^{X,Y} |\Omega; r\right) = 1 - \lambda^2 \chi\left(\psi^{X,Y}, \Omega; r\right) + \mathcal{O}(\lambda^3) \ . \tag{7.9}$$

---

[14]Mutual information of A and B is defined as

$$I(A:B) = S(A) + S(B) - S(A \cup B) \ . \tag{7.5}$$

We call $\chi\left(\psi^{X,Y}, \Omega; r\right)$ fidelity susceptibility and when $\chi \ll 1$ the information can be reconstructed on LK. χ is evaluated in [37] as

$$\chi\left(\psi^X, \Omega; r\right) = -\frac{Z_\delta^2}{2\pi} \text{Im} \int ds \left(\frac{\langle \phi_R(T_R - i\delta) \Delta_r^{\frac{is}{2\pi}} \phi_R(T_R + i\delta) \rangle}{\sinh \frac{s+i\epsilon}{2}} + i \frac{\langle \phi_R(T_R - i\delta) \Delta_r^{\frac{is}{2\pi}} J_r \phi_R(T_R + i\delta) \rangle}{\cosh \frac{s}{2}} \right) .$$
(7.10)

We call correlators in the form of $\langle \phi_R(T_R - i\delta) \Delta_r^{\frac{is}{2\pi}} \phi_R(T_R + i\delta) \rangle$, "modular flowed correlator[15]". In [14], modular flowed correlator is evaluated concretely in the SYK setup as

$$\langle \psi_L(T_L) \Delta_{LK}^{is} \psi_R(T_R) \rangle_\beta \sim \frac{1}{\left(\cosh(\pi(T_L + T_R + s)) - C_Q \frac{K}{N} \sinh(\pi s) e^{\pi(T_L - T_R)} \right)^{2\Delta}} .$$
(7.13)

Here, C_Q is constant made by SYK parameter and Δ is conformal dimension. We can use this equation to calculate the fidelity susceptibility χ. Price is the number of qubit in K when χ becomes zero. The result is obtained as

$$p_\beta(\psi_R(T_R)) = N(1 - c_Q e^{2\pi T_R}) .$$
(7.14)

7.3   Replica trick and Schwinger-Dyson equation

From here, we introduce the concrete replica trick method to calculate the modular flowed correlator in the SYK model, following the paper of Chandraselaran and Levine [14]. As we explained in the previous subsection, we prepare the systems L, R which are thermally entangled and make a TFD state. L represents the early radiation and R represents the black hole system. After time evolution, R is divided to the late radiation system K and the remaining fermion system r which corresponds to the remaining black hole in the bulk. r consists of $N - K$ fermions. We assume $N \gg 1$ and $K \gg 1$ are even, and K is small compareed with N, i.e. $\frac{K}{N} \ll 1$. The TFD state of LR is given by

$$|\beta\rangle = Z_\beta^{-\frac{1}{2}} e^{-\frac{\beta}{4}(H_L + H_R)} |0\rangle ,$$
(7.15)

---

[15]Modular flowed correlator takes form of the expectation value of particle operators, modular operator Δ and modular conjugation operator J. They are defined in Tomita-Takesaki theory of operator algebra. Let $\mathcal{H}$ Hilbert space on $A \cup \bar{A}$, and let $\mathcal{A}_A$ algebra constructed by operators acting on the subregion A. Tomita operator $S_{\psi,A}$ is defined as

$$S_{\psi,A} \alpha |\psi\rangle = \alpha^\dagger |\psi\rangle , \quad \forall \alpha \in \mathcal{A}_A$$
(7.11)

for $|\psi\rangle \in \mathcal{H}$. When we polar decompose Tomita operator as

$$S_{\psi,A} = J_{\psi,A} \Delta_{\psi,A}^{1/2} ,$$
(7.12)

$\Delta_{\psi,A}$ and $J_{\psi,A}$ are named as modular operator and modular conjugation operator, respectively. When Hilbert space decomposes as $\mathcal{H} = \mathcal{H}_A \otimes \mathcal{H}_{\bar{A}}$, the modular operator also factorize as $\Delta_{\psi,A} = \rho_A \otimes \rho_{\bar{A}}^{-1}$. When $\mathcal{H}$ is finite dimensional, it is always satisfied.

where H_L, H_R are the SYK Hamiltonians of L, R, respectively. Z_β is a partition function. The vacuum state $|0\rangle$ is defined as a maximally entangled state which satisfies

$$(\psi_L^j + i\psi_R^j)\,|0\rangle = 0\,, \quad j = 1, \cdots, N \tag{7.16}$$

We consider that a particle operator ψ_R lives in r. We insert ψ_R to the TFD state and make a regularized state

$$\left|\psi_\delta^j\right\rangle = Z_\delta^{-\frac{1}{2}}\Delta_R^\delta \psi_R^j\,|\beta\rangle \,. \tag{7.17}$$

Here, $\Delta_R = \rho_L^{-1}\otimes\rho_R$ is the modular operator of TFD where $\rho_L = e^{-\beta H_L}$ and $\rho_R = e^{-\beta H_R}$. If we consider time evolution of the operator ψ_R, the operator becomes $\psi_R^j(T_R) = \rho_R^{-iT_R}\psi_R^j\rho_R^{iT_R}$. We should study fidelity susceptibility and modular flowed correlator to identify when entanglement of TFD can be reconstructed on LK, whereas it is reconstructed on r at first. It is hard to evaluate the original modular flowed correlator $\langle\psi_\delta^i|\,\Delta_{LK}^{is}\,|\psi_\delta^i\rangle_\beta$ for some particular $i \in r$. In large N theory, it is sufficient to consider the average of $N - K$ fermions. Therefore, we concentrate on the evaluation of the averaged modular flowed correlator

$$
\begin{aligned}
\langle\Delta_{LK}^{is}\rangle_{\psi_\delta} &= \frac{1}{N-K}\sum_{i=1}^{N-K}\langle\psi_\delta^i|\,\Delta_{LK}^{is}\,|\psi_\delta^i\rangle_\beta \\
&= \frac{Z_\delta^{-1}}{N-K}\sum_{i=1}^{N-K}\langle\psi_L^i(T_L)(\rho_{LK}^p\otimes\rho_r^{n-1-p})\psi_R^i(T_R)\rangle_\beta\,.
\end{aligned}
\tag{7.18}
$$

Here, we should take care that the modular operator to consider is not $\Delta_R = \rho_R\otimes\rho_L^{-1}$ but $\Delta_{LK} = \rho_{LK}\otimes\rho_r^{-1}$ because we consider reconstruction on LK. We make the Scheinger-Dyson (SD) equation and appropriate boundary conditions by replica trick of integer n. Then in 7.4, we solve SD equation in large βJ limit and in 7.5 we consider analytic continuation to $n \to 1$ and $p \to is$.

We consider $p = 2, n = 4$ case in Euclidean signature: $\langle\beta|\,\psi_L(\tau)(\rho_{LK}^2\otimes\rho_r)\psi_R(\tau')\,|\beta\rangle$. We draw diagram for replica trick. See from figure 23 to figure 26. First we prepare $|\beta\rangle$ as figure 23. $|\beta\rangle\langle\beta|$ and $\psi_R(\tau')\,|\beta\rangle$ are prepared as figure 24. We can also prepare reduced density matrices like ρ_{LK} and ρ_r as figure 25. Finally we can use the prepared operators to make $\langle\beta|\,\psi_L(\tau)(\rho_{LK}^2\otimes\rho_r)\psi_R(\tau')\,|\beta\rangle$ as figure 26.

By figure 26, we can identify the boudary condition of the SYK Majorana fermions. Fermions in K live in circles of length β. There are n circles of length β. On the other hand, fermions in r live in circles of length $n\beta$. There is one circle of length $n\beta$. We derive SD equation of n-replica theory using the above boundary condition. The Euclidean action is

$$I = \sum_{k=0}^{n-1}\left(\sum_{i=1}^{N}\psi_i^{(k)}\partial_\tau\psi_i^{(k)} + \sum_{i_1,\cdots,i_q}J_{i_1,\cdots,i_q}\psi_{i_1}^{(k)}\cdots\psi_{i_q}^{(k)}\right) \tag{7.19}$$
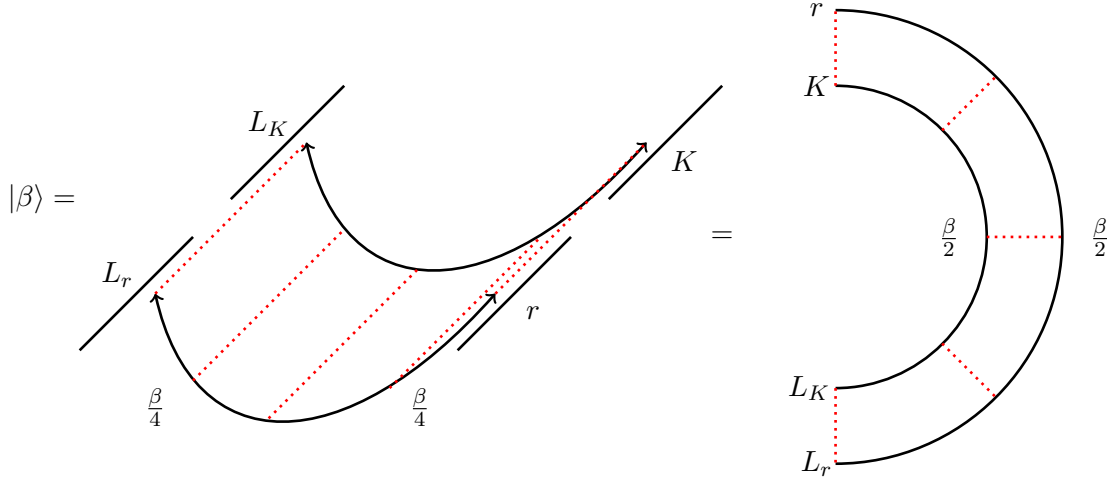
Figure 23: TFD state of $L, R, |\beta\rangle$. Arrows represents Euclidean path integral and red dots represent the same Euclidean time.
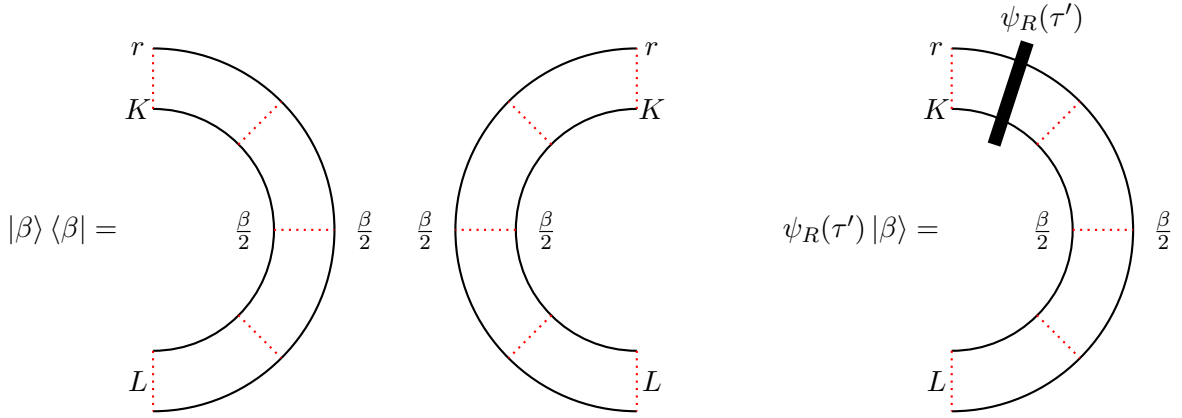

Figure 24: **Left**: The diagram which represents $|\beta\rangle \langle\beta|$. **Right**: $\psi_R(\tau') |\beta\rangle$, where an particle operator is inserted at the Euclidean time τ'.

where superscript (k) is replica index. Then we define the averaged propagator $G(\tau, \tau')$. Since r and K has $N - K$ and K fermions, respectively,

$$G_r^{(j,k)}(\tau, \tau') = \frac{1}{N-K} \sum_{i=1}^{N-K} \psi_i^{(j)}(\tau)\psi_i^{(k)}(\tau') \quad (i \in r)\,, \tag{7.20}$$

$$G_K^{(j,k)}(\tau, \tau') = \frac{1}{K} \sum_{i=1}^{K} \psi_i^{(j)}(\tau)\psi_i^{(k)}(\tau') \quad (i \in K)\,. \tag{7.21}$$
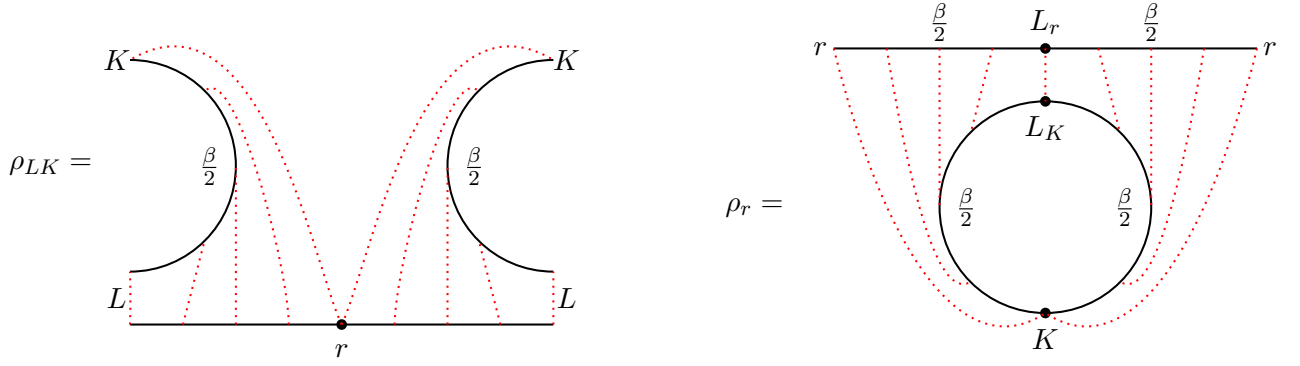
Figure 25: **Left**: The diagram which represents $\rho_{LK} = \text{tr}_r[|\beta\rangle \langle\beta|]$. Red lines represent the same Euclidean time. **Right**: The diagram which represents $\rho_r = \text{tr}_{LK}[|\beta\rangle \langle\beta|]$.
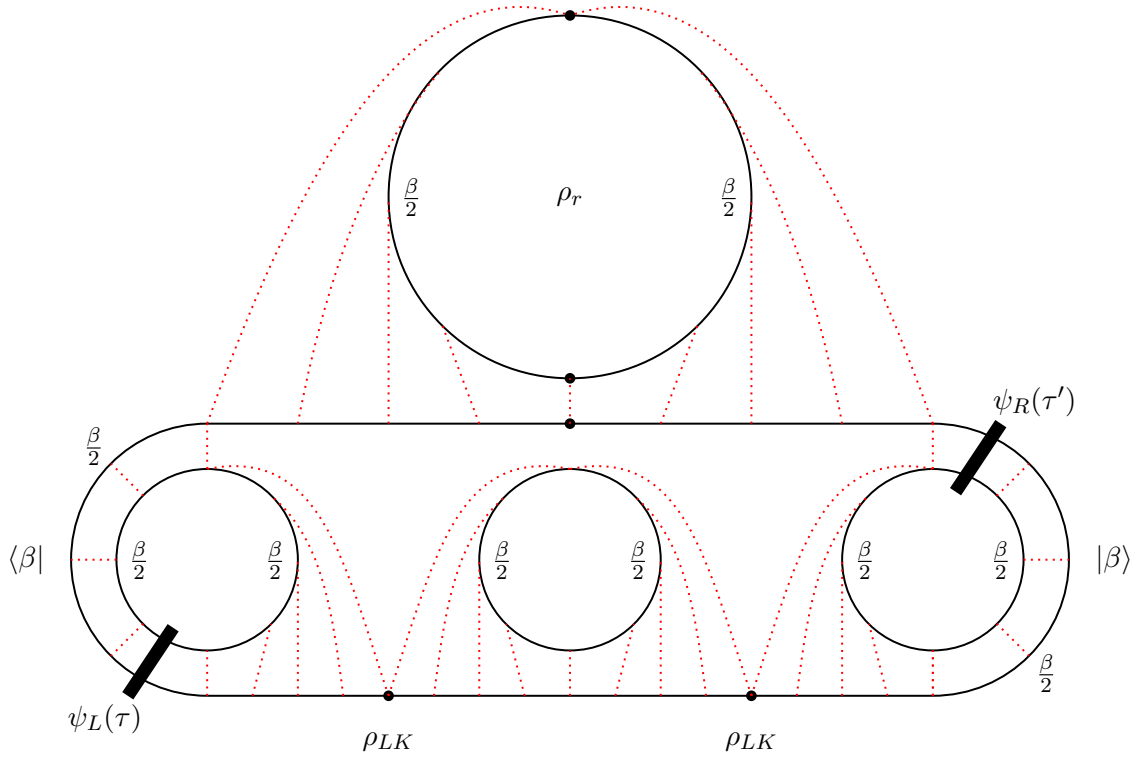

Figure 26: The diagram which represents $\langle\beta| \psi_L(\tau)(\rho_{LK}^2 \otimes \rho_r)\psi_R(\tau') |\beta\rangle$.

Assuming $N, K, N - K \gg 1$, large N effective action becomes

$$I = -\frac{1}{2}\left(\lambda \operatorname{tr}\log(\partial_\tau \mathbf{1} - \boldsymbol{\Sigma_K}) + (1-\lambda)\operatorname{tr}\log(\partial_\tau \mathbf{1} - \boldsymbol{\Sigma_r})\right)$$

$$+ \frac{1}{2}\sum_{j,k=0}^{n-1}\int_0^\beta d\tau d\tau'\left((1-\lambda)\sum_r^{(j,k)}(\tau,\tau')G_r^{(j,k)}(\tau,\tau') + \lambda\Sigma_k^{(j,k)}(\tau,\tau')G_K^{(j,k)}(\tau,\tau')\right) \qquad (7.22)$$

$$-\frac{J^2}{2}\left(\lambda G_K^{(j,k)}(\tau,\tau') + (1-\lambda)G_r^{(j,k)}(\tau,\tau')\right)^q\right)$$

where we defined $\boldsymbol{\Sigma}_{j,k} = \Sigma^{(j,k)}$ and $\lambda \equiv \frac{K}{N} \ll 1$. The number of replicas is n. SD equation becomes

$$\left(\frac{1}{\partial_\tau \mathbf{1} - \boldsymbol{\Sigma_K}}\right)_{j,k} = G_K^{(j,k)}, \qquad \left(\frac{1}{\partial_\tau \mathbf{1} - \boldsymbol{\Sigma_r}}\right)_{j,k} = G_r^{(j,k)} \qquad (7.23)$$

$$\Sigma_K^{(j,k)} = \Sigma_r^{(j,k)} = J^2\left(\lambda G_K^{(j,k)} + (1-\lambda)G_r^{(j,k)}\right)^{q-1}. \qquad (7.24)$$

Fermions in K live in a circle of length β and those in r live in a circle of length $n\beta$, so the boundary condition becomes

$$G_K^{(j,k)}(\beta^-,\tau') = -G_K^{(j,k)}(0^+,\tau')$$
$$G_r^{(j,k)}(\beta^-,\tau') = G_r^{(j+1,k)}(0^+,\tau') \quad (0 \le j \le n-2) \qquad (7.25)$$
$$G_r^{(n-1,k)}(\beta^-,\tau') = -G_r^{(0,k)}(0^+,\tau').$$

See also (6.18). From the anti-commutation of $\psi_i^{(i)}(\tau)$, the conditions

$$G_r^{(j,k)}(\tau,\tau') = -G_r^{(k,j)}(\tau',\tau)$$
$$G_K^{(j,k)}(\tau,\tau') = -G_K^{(k,j)}(\tau',\tau) \qquad (7.26)$$

are satisfied and when fermions exist simultaneously, for $0 \le j \le n-1$,

$$G_r^{(j,j)}(\tau^+,\tau^-) = G_K^{(j,j)}(\tau^+,\tau^-) = \frac{1}{2} \qquad (7.27)$$

is satisfied.

7.4 Solution of SD equation

In this subsection, we solve the SD equation obtained in the last subsection in the large βJ limit. In leading order, SD equation (7.3) becomes

$$\partial_\tau \mathbf{G_K}(\tau,\tau') - (\boldsymbol{\Sigma_K} \star \mathbf{G_K})(\tau,\tau') = \mathbf{1}\delta(\tau-\tau')$$
$$\partial_\tau \mathbf{G_r}(\tau,\tau') - (\boldsymbol{\Sigma_r} \star \mathbf{G_r})(\tau,\tau') = \mathbf{1}\delta(\tau-\tau') \qquad (7.28)$$
$$\Sigma_K^{(j,k)} = \Sigma_r^{(j,k)} = J^2\left(G_r^{(j,k)}\right)^{q-1} + J^2\lambda(q-1)\left(G_K^{(j,k)} - G_r^{(j,k)}\right)\left(G_r^{(j,k)}\right)^{q-2} + \mathcal{O}(\lambda^2)$$

where we defined the star product as the matrix product of continuous time indices and replica number indices:

$$(\mathbf{M} \star \mathbf{N})^{(j,k)}(\tau, \tau') \equiv \sum_{l=0}^{n-1} \int_0^\beta d\tau M^{(j,l)}(\tau, \tau'') N^{(l,k)}(\tau'', \tau') . \tag{7.29}$$

To solve SD equation, we set the ansatz

$$G_r = G_{r,0} + \lambda G_{r,1} + \mathcal{O}(\lambda^2)$$
$$G_K = G_{K,0} + \lambda G_{K,1} + \mathcal{O}(\lambda^2) \tag{7.30}$$

as the perturbative expansion of λ. Later we do not use bold face for matrices of time and replica indices expect for $\mathbf{1}$. λ^0 order of $G_r^{(j,k)}(\tau, \tau')$ becomes

$$G_{r,0}^{(j,k)}(\tau, \tau') = G_{n\beta}(\tau - \tau' + j\beta - k\beta), . \tag{7.31}$$

Here, $G_{n\beta}$ is the thermal two point function of temperature $n\beta$, since fermions in r live in a circle of length $n\beta$. To find $G_{K,0}$, we use reduced SD equation for $G_{K,0}$

$$\partial_\tau G_{K,0} - \Sigma_K^{(0)} \star G_{K,0} = \mathbf{1}\delta(\tau - \tau') \tag{7.32}$$

and the boundary condition that $G_K^{(j,k)}(\tau, \tau')$ lives in a circle of lengh β.

Now we tackle λ order of G_r. The equation for $G_{r,1}$ becomes

$$-\partial_\tau \mathbf{1} \star G_{r,1} + \Sigma \star G_{r,1} + (q-1)J^2 G^{q-2} G_{r,1} \star G = -(q-1)J^2(G_K - G)G^{q-2} \star G \tag{7.33}$$

where we defined $G \equiv G_{n\beta}$. We regard $G_{r,1}$ as the function of two time indices which both live in a circle of length $n\beta$:

$$G_{r,1}^{(j,k)}(\tau, \tau') = G_{r,1}(\tau + j\beta, \tau' + k\beta) . \tag{7.34}$$

Therefore, we consider the star product which carries out integral from 0 to $n\beta$ for $G_{r,1}$. By acting G from the left on both sides of (7.33) and use the equation of motion for G, we get

$$(1 - K_c) \star G_{r,1} = J^2(q-1)G \star (G_K - G)G^{q-2} \star G \tag{7.35}$$

where we defined the ladder kernel

$$K_c(\tau_1, \tau_2; \tau_3, \tau_4) \equiv -J^2(q-1)G(\tau_{13})G(\tau_{24})G^{q-2}(\tau_{34}) . \tag{7.36}$$

We write $\tau_{ij} \equiv \tau_i - \tau_j$. The connected four point function $\mathcal{F}$, which is defined by

$$\frac{1}{N^2} \sum_{i,j=1}^{N} \langle \mathcal{T}\psi_i(\tau_1)\psi_i(\tau_2)\psi_j(\tau_3)\psi_j(\tau_4) \rangle = G(\tau_{12})G(\tau_{34}) + \frac{1}{N}\mathcal{F}(\tau_1, \tau_2; \tau_3, \tau_4) \tag{7.37}$$

can be expressed with the ladder kernel and the bare four point function $\mathcal{F}_0$ as

$$\mathcal{F} = \frac{1}{1 - K_c} \star \mathcal{F}_0$$

$$\mathcal{F}_0(\tau_1, \tau_2; \tau_3, \tau_4) = G(\tau_{13})G(\tau_{24}) - G(\tau_{14})G(\tau_{32}).$$

(7.38)

We act $\frac{1}{1-K_c}$ to (7.35) and obtain

$$G_{r,1} = \frac{J^2}{2}(q-2) \int_0^{n\beta} d\tau \int_0^{n\beta} d\tau' \mathcal{F}(\tau_1, \tau_2; \tau, \tau') \left(G_K(\tau, \tau') - G(\tau, \tau')\right) G^{q-2}(\tau, \tau').$$

(7.39)

We need to solve $G_{K,0}$. Writing the reduced SD equation (7.32) for $G_{K,0}$ more explicitly, it becomes

$$\partial_\tau G_{K,0}^{(j,k)}(\tau, \tau') - J^2 \sum_l \left(G^{(j,l)}\right)^{q-1} \star G_{K,0}^{(l,k)} = \delta^{jk}\delta(\tau - \tau').$$

(7.40)

It is convenient that τ, τ' in $G_K(\tau, \tau')$ are defined from 0 to $n\beta$. However, G_K lives in a circle of length β. Thus we define $G_K(\tau, \tau')$ as

$$G_K(\tau, \tau') \equiv \sum_{j,k} G_K^{(j,k)}(\tau - j, \tau' - k)\mathbf{1}_j(\tau)\mathbf{1}_k(\tau')$$

(7.41)

where we defined $\mathbf{1}_j(\tau)$ as

$$\mathbf{1}_j(\tau) = \begin{cases} 1 \ (j < \tau < j+1) \\ 0 \ (otherwise) \end{cases}.$$

(7.42)

Hereafter, $j < \tau < j+1$ means $j\beta < \tau < (j+1)\beta$. By differentiating $G_{K,0}(\tau, \tau')$ with respect to τ, we obtain

$$\partial_\tau G_{K,0}(\tau, \tau') - J^2 G^{q-1} \star G_{K,0} = \delta(\tau - \tau') + \sum_j \delta(\tau - j)\mathrm{disc}G_{K,0}(j, \tau')$$

(7.43)

where we defined the discontinuity of G_K from $j-1$'th circle to j'th circle as $\mathrm{disc}G_K(j, \tau') \equiv G_K(j^+, \tau') - G_K(j^-, \tau')$. Then we set an ansatz which satisfies (7.43) as

$$G_K(\tau, \tau') = G(\tau - \tau') + \sum_{lm} G(\tau - l)c_{lm}G(m - \tau').$$

(7.44)

We solve c_{lm} later. By the boundary condition that G_K lives in a circle of length β: $G_K(j^+, \tau') = -G_K(j + 1^-, \tau')$, the ansatz becomes

$$\sum_l (G(j^+, l) + G(j + 1^-, l))c_{lm} = -(\delta_{j,m} + \delta_{j+1,m}).$$

(7.45)

By plugging this back into (7.39), we can calculate as follows.

$$
\begin{aligned}
G_{r,1}(\tau_1, \tau_2) &= \frac{J^2}{2}(q-1) \int_0^{n\beta} d\tau \int_0^{n\beta} d\tau' \sum_{lm} c_{lm} \mathcal{F}(\tau_1, \tau_2; \tau, \tau') G(\tau, l) G(m, \tau') G^{q-2}(\tau, \tau') \\
&= \frac{1}{2} \sum_{lm} c_{lm} \int_0^{n\beta} d\tau \int_0^{n\beta} d\tau' K_c(l, m; \tau, \tau') \mathcal{F}(\tau_1, \tau_2; \tau, \tau') \\
&= \frac{1}{2} \sum_{lm} c_{lm} \left(\mathcal{F}(\tau_1, \tau_2; l, m) - \mathcal{F}_0(\tau_1, \tau_2; l, m) \right)
\end{aligned}
$$
(7.46)

In the second line, we used the fact that the ladder kernel is

$$
K_c(l, m; \tau, \tau') = J^2(q-1) G(\tau, l) G(m, \tau') G^{q-2}(\tau, \tau').
$$
(7.47)

In the third line, we used that $K_c \star \mathcal{F}$ can be calculated as

$$
\begin{aligned}
K_c \star \mathcal{F} &= K_c \star \frac{1}{1 - K_c} \star \mathcal{F}_0 \\
&= \mathcal{F}(\tau_1, \tau_2; l, m) - \mathcal{F}_0(\tau_1, \tau_2; l, m)
\end{aligned}
$$
(7.48)

and the symmetry relation $\mathcal{F}(\tau_1, \tau_2; \tau_3, \tau_4) = \mathcal{F}(\tau_3, \tau_4; \tau_1, \tau_2)$.

From here, we assume only large N limit, so we can use the result in any parameter region of βJ and q. Finally we solve c_{lm} for large βJ limit to use in the next section. In large βJ limit, the thermal two point function is effective only when fermions are simultaneous because G is proportional to $\left(\frac{1}{\beta J} \right)^{\frac{2}{q}}$. We assume finite q. We can drop $l \neq j$ or $j+1$ in (7.45), so we get

$$
\frac{1}{2}(c_{j+1,m} - c_{j,m}) = \delta_{j+1,m} + \delta_{j,m}.
$$
(7.49)

By using $c_{jj} = 0$, c_{jm} is solved as

$$
c_{jm} = 2\text{sgn}(j - m) + \mathcal{O}\left(\left(\frac{1}{\beta J} \right)^{\frac{2}{q}} \right).
$$
(7.50)

We can conclude that in large βJ limit, $G_{r,1}$ is given by

$$
G_{r,1}(\tau_1, \tau_2) = 2 \sum_{l>m}^{n-1} (\mathcal{F}(\tau_1, \tau_2; l, m) - \mathcal{F}_0(\tau_1, \tau_2; l, m)).
$$
(7.51)

7.5 Analytic continuation

In this section, we review the calculation result of modular flowed correlator. We consider $K \ll N$ and take leading order in $\lambda = \frac{K}{N}$. In order to evaluate (7.18), we should analytically continue

$$
\frac{1}{N-K} \sum_{i=1}^{N-K} \langle \psi_L^i(\tau) \left(\rho_{LK}^k \otimes \rho_r^{n-1-k} \right) \psi_R^i(\tau') \rangle_\beta
$$
(7.52)

from integer n and $k \leq n$ and take $n \to 1$ and $k \to is$. We must also analytically continue $\tau \to iT_L$ and $\tau' \to -iT_R$ to get (7.18). We can realize this by taking the first fermions on k's replica and the second fermions on the first replica and considering

$$G_r(\tau + k, \tau') = \frac{1}{N-K} \sum_{i=1}^{N-K} \frac{\langle \psi_L^i(\tau)(\rho_{LK}^k \otimes \rho_r^{n-1-k}) \psi_R^i(\tau') \rangle_\beta}{\text{tr}\left[\rho_{LK}^n\right]} . \tag{7.53}$$

Since $\psi_L^i(\tau)$ live in the left side, we should do path integral to carry the operator to the left system and take $0 < \tau' < \frac{1}{2}$ and $\frac{1}{2} < \tau < 1$. We set $\beta = 1$ as the last subsection.

We consider large βJ limit in this subsection. By using (7.51), we obtain

$$G_r(\tau, \tau') = G_n(\tau - \tau') + \frac{2K}{N} \sum_{l>m} (\mathcal{F}(\tau, \tau'; l, m) - \mathcal{F}_0(\tau, \tau'; l, m)) + \mathcal{O}\left(\left(\frac{K}{N}\right)^2\right) . \tag{7.54}$$

Analytical continuation which we consider is $\tau \to \tau + k$ and then $\tau, \tau' \to \frac{1}{2} + iT_L, -iT_R$. The first term is thermal two point function so it becomes

$$G_n\left(\tau + k + \frac{1}{2} - \tau'\right) \to G_1\left(\tau + \frac{1}{2} + is - \tau'\right) = b\left(\frac{\pi}{\cosh(T_L - T_R + s + i\delta)}\right)^{2\Delta} . \tag{7.55}$$

where b is defined with conformal dimension as

$$b^q \pi = \frac{\left(\frac{1}{2} - \Delta\right) \tan \pi \Delta}{(\beta J)^2}, \quad \Delta = \frac{1}{q} . \tag{7.56}$$

Since the bare four point function $\mathcal{F}_0$ is the product of thermal two point function and at most polynomial growth. Exponential growth comes from OTOC paramstor region of connected four point function $\mathcal{F}$. We can write this as the single sum and the double sum as

$$\sum_{l>m} \mathcal{F}(\tau + k, \tau'; l, m)\bigg|_{\text{OTOC}} = \sum_{l=1}^{k} \mathcal{F}(\tau + k, \tau'; l, 0) + \sum_{l=k+1}^{n-1} \sum_{m=1}^{k} \mathcal{F}(\tau + k, \tau'; l, m) . \tag{7.57}$$

The single sum term $\sum_{l=1}^{k} \mathcal{F}(\tau + k, \tau'; l, 0)$ is calculated by contour integral in the paper of Faulkner, whose result is

$$\sum_{l=1}^{k} \mathcal{F}(\tau + k, \tau'; l, 0) \to \frac{i\pi}{2} \int_0^s dt \int_{-\infty}^{\infty} ds' \frac{\mathcal{F}(\tau + is, \tau'; -is' + is + 1/2, 0)}{\cosh^2(\pi(s' - t))} . \tag{7.58}$$

Exponentially growing part comes from OTOC parameter region $\tau_1 > \tau_3 > \tau_2 > \tau_4$ and it is evaluated in [35] as

$$\mathcal{F}(\tau_1, \tau_2; \tau_3, \tau_4) = -\frac{\beta \mathcal{J} F_d}{2\alpha_S q^2 \pi} \frac{\sin\left(\pi(\tau_{12}^+ - \tau_{34}^+)\right)}{\sin\left(\pi \tau_{12}^-\right) \sin\left(\pi \tau_{34}^-\right)} , \tag{7.59}$$

where α_S is coefficient which appears in Schwarzian action and $F_d \equiv G(\tau_{12})G(\tau_{34})$. $\mathcal{J}$ is defined by $\sigma^2 = \frac{(q-1)!J^2}{N^{q-1}} = \frac{2^{q-1}}{q}\frac{(q-1)!\mathcal{J}}{N^{q-1}}$, i.e. $\mathcal{J} \equiv \sqrt{q}\frac{J}{2^{\frac{q-1}{2}}}$. We defined $\tau_{ij}^{\pm} \equiv \tau_i \pm \tau_j$. Eventually, the single sum term is analytically continued to

$$\sum_{l=1}^{k} \mathcal{F}(\tau+k,\tau';l,0) \to C(\beta\mathcal{J},q)\frac{e^{\pi(T_L-T_R)}}{\cosh^{1+2\Delta}(\pi(T_L+T_R+s))}\int_{-\infty}^{\infty} ds' \frac{f_1(s',s)}{\cosh^{1+2\Delta}(\pi s')} \quad (7.60)$$

where $f_0(s',s)$ and $f_1(s',s)$ are defined as

$$f_1(s',s) = e^{\pi(s'+s)}f_0(s',s), \quad f_0(s',s) = \tanh(\pi(s+s')) - \tanh(\pi s'), \quad (7.61)$$

and $C(\beta\mathcal{J},q)$ is defined with SYK parameters as

$$C(\beta\mathcal{J},q) = \frac{b^2\pi^{4\Delta}\beta\mathcal{J}}{8\alpha_S q^2\pi}. \quad (7.62)$$

The double sum term is also evaluated by contour integral and the result becomes

$$\sum_{l=k+1}^{n-1}\sum_{m=1}^{k} \mathcal{F}(\tau+k,\tau';l,m) \to -C(\beta\mathcal{J},q)\frac{e^{\pi(T_L-T_R)}}{\cosh^{1+2\Delta}(\pi(T_L+T_R+s))}\int_{-\infty}^{\infty} \frac{\frac{1}{2}f_2(s_2,s)}{\cosh^{1+2\Delta}(\pi s_2)} \quad (7.63)$$

where $f_2(s_2,s)$ is defined as

$$f_2(s_2-i/2,s) = \pi^2\int_0^s dt_1 \int_0^s dt_2 \int_{-\infty}^{\infty} \frac{e^{\pi(-2s_1-s_2-s)}}{\cosh^2(\pi(s_1+t_1))\cosh^2(\pi(s_1+s_2+t_2+i\epsilon))}. \quad (7.64)$$

Combining the single and double sum parts, we obtain the modular flowed correlator in appropriate index and Lorentzian time as

$$\frac{1}{N-K}\sum_{i=1}^{N-K}\langle\psi_L(T_L)\Delta_{LK}^{is}\Delta_r\psi_R(T_R)\rangle = b\left(\frac{\pi}{\cosh(\pi(T_L+T_R))}\right)^{2\Delta}$$

$$+ \frac{K}{N}\frac{b\pi^{2\Delta}\Delta C_\Delta(\beta\mathcal{J},q)e^{\pi(T_L-T_R)}}{\cosh^{1+2\Delta}(\pi(T_L+T_R))}(e^{2\pi s}-1)$$

$$\approx b\left(\frac{\pi}{\cosh(\pi(T_L+T_R)) - \frac{K}{2N}C_\Delta e^{\pi(T_L-T_R)(e^{2\pi s}-1)}}\right)^{2\Delta}. \quad (7.65)$$

In the second line, we write only leading order in $\frac{K}{N}\cdot C_\Delta$. Here, C_Δ is defined as

$$C_\Delta(\beta\mathcal{J},q) = \frac{\Gamma(\Delta)}{b\pi^{2\Delta+1/2}\Gamma(3/2+\Delta)}C(\beta\mathcal{J},q). \quad (7.66)$$

We see that the modular flowed correlator is written in the form of (7.13).

8 Recovery map for the Hayden-Preskill channel in SYK

So far, we have given the evidence that the Petz-lite works as a recovery map under the Haar random unitary, which is highly chaotic. In this section, we argue that this continues to hold for a more realistic but tractable model of chaotic dynamics: the Sachdev-Ye-Kitaev (SYK) model [31, 32, 38]. In this paper, we briefly explain the relevant calculations, leaving details in the upcoming paper [16].

8.1 Setup of SYK Hayden-Preskill protocol

In this section, we explain the setup to study the Hayden-Preskill-like protocol (what we call SYK HP channel) in the SYK model. This was first introduced in [14, 37].

The SYK model is a theory of N Majorana fermions ψ_i, and its Hamiltonian is given by

$$H = (i)^{q/2} \sum_{1 \leq i_1 < i_2 < \cdots < i_q \leq N} j_{i_1 i_2 \cdots i_q} \psi_{i_1} \psi_{i_2} \cdots \psi_{i_q}, \tag{8.1}$$

where $q \in 2\mathbb{N} \, (q > 2)$, $j_{i_1 i_2 \cdots i_q}$ is a random coefficient drawn from a Gaussian random distribution with zero mean and the variance $\left\langle j_{i_1 i_2 \cdots i_q}^2 \right\rangle = J^2 (q-1)!/N^{q-1}$.

Following [14], we consider two copies of the Hilbert space of the SYK model, say left SYK system L and right one R. Hereafter, we denote the Majorana fermions on the left system by $\psi_{i,L}$ and $\psi_{i,R}$ for the right. For notational simplicity, we use the convention

$$\{\psi_i, \psi_j\} = 2\delta_{i,j}, \tag{8.2}$$

for the anti-commutation relation for the fermions on the same side. In this setup, the right SYK system corresponds to early radiation degrees of freedom of the original Hayden-Preskill setup, and the left SYK system corresponds to the rest; the union of the diary system and the initial black hole before the action of the random unitary, or equivalently the remaining black hole plus late radiation degrees of freedom after the unitary evolution. In particular, the left system L is divided into two subsystems, say $\tilde{L}$ and K; the former corresponds to the remaining black hole, and the latter to the late radiation part of the original HP setup.

On the union of the above SYK systems L and R, we consider the following thermo-field double (TFD) state ;

$$|\text{TFD}\rangle_{L,R} = Z^{-1/2}(\beta) \, e^{-\beta(H_L + H_R)/4} \, |0\rangle_{L,R}, \tag{8.3}$$

where $Z(\beta)$ is a normalization factor of the state, and $|0\rangle_{L,R}$ is given by [39]

$$[\psi_{j,L}(0) + i\psi_{j,R}(0)] \, |0\rangle_{L,R} = 0 \quad \text{for } \forall j. \tag{8.4}$$

Note that the thermo-field double state (8.3) satisfies the relation $(H_L - H_R)\,|\text{TFD}\rangle = 0$. This TFD state corresponds to an entangled state between the initial black hole and the early radiation.

The code subspace (a diary system) of our interest is two-dimensional, and let us denote two basis vectors by $|0\rangle$ and $|1\rangle$. This code subspace is embedded into the physical Hilbert space LR by an isometry. The image of the code subspace is spanned by the TFD state $|\text{TFD}\rangle_{L,R}$ and the excited state $\psi_{i,L}(0)\,|\text{TFD}\rangle_{L,R}$. Here, we assume that the Majorana fermion $\psi_{i,L}(0)$ acting on the TFD state lives in the subsystem $\tilde{L}$, $i \in \tilde{L}$. More explicitly, by the isometry, the states in the code subspace $|T\rangle$ $(T = 0, 1)$ are mapped to

$$
(V_{T,L\to L} \otimes I_R)\left(|T\rangle_T \otimes |\text{TFD}\rangle_{L,R}\right) :=
\begin{cases}
|\text{TFD}\rangle_{L,R} & \text{for } T = 0 \\
\dfrac{1}{(Z_\delta)^{\frac{1}{2}}}\psi_{i,L}(i\delta)\,|\text{TFD}\rangle_{L,R} & \text{for } T = 1,
\end{cases}
\tag{8.5}
$$

where $\psi_{i,L}(i\delta)$ is the regulated Majorana fermion operator

$$
\psi_{i,L}(i\delta) = e^{-\delta H_L}\psi_{i,L}(0)e^{\delta H_L},
\tag{8.6}
$$

and δ is an infinitesimal cutoff parameter to normalize the state with the operator insertion even in the conformal limit, where the SYK model has an effective description in terms of the reparametrization modes [35]. Z_δ is its normalization factor given by the two-point function

$$
\begin{aligned}
Z_\delta &= \frac{1}{N - K}\sum_{i=1}^{N-K}\frac{1}{Z(\beta)}\,\text{tr}\left[e^{-\beta H_L}\psi_{i,L}(-i\delta)\psi_{i,L}(i\delta)\right] \\
&= \frac{1}{N - K}\sum_{i=1}^{N-K}\frac{1}{Z(\beta)}\,\text{tr}\left[e^{-\beta H_L}e^{2\delta H_L}\psi_{i,L}(0)e^{-2\delta H_L}\psi_{i,L}(0)\right] = G_\beta(2\delta).
\end{aligned}
\tag{8.7}
$$

This normalization factor is not for the specific Majorana fermion "i", but averaged over the region $\tilde{L}$ with $N - K$ sites. We expect that the difference between the two only appears in subleading terms with respect to K/N because of typicality. Therefore, we use this normalization factor (8.7) for later convenience.

Using the above embedding, we can holographically prepare an initial entangled state between the early radiation and an initial black hole containing a diary in the SYK model. For this system, we consider a unitary time evolution on the left system L by the SYK Hamiltonian H_L,

$$
U_L(t) = \exp\left(itH_L\right).
\tag{8.8}
$$

By this time evolution, information in the diary gets scrambled and uniformly distributed over the left SYK system after the scrambling time. The resulting state is

$$
|\Psi_{\text{SYK HP}}\rangle = (I_{\text{Ref}} \otimes U_L(t) \otimes I_R)\,(I_{\text{Ref}} \otimes V_{T,L\to L} \otimes I_R)\left(|\text{EPR}\rangle_{\text{Ref},T} \otimes |\text{TFD}\rangle_{L,R}\right),
\tag{8.9}
$$

which corresponds to the state (5.1). In figure 27, we give the circuit diagram corresponding to the state (8.9).

We are interested in recovering the diary information from the early and late radiations R and K by using the Petz-lite for the SYK HP protocol. As in (5.3), the SYK HP channel
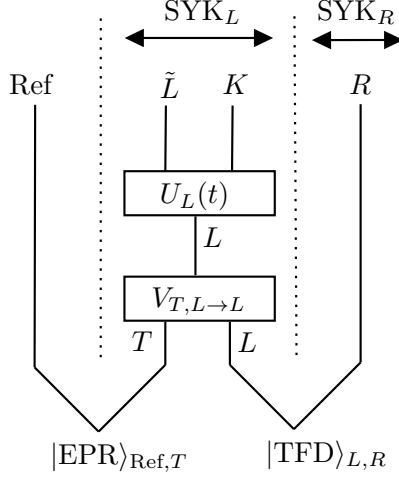

Figure 27: Circuit diagram corresponding to state (8.9).

$\mathcal{N}^{\mathrm{SYK}}_{T \to K,R}$ representing error is obtained by tracing out the remaining black hole part $\tilde{L}$ in the final state (8.9),

$$\mathcal{N}^{\mathrm{SYK}}_{T \to K,R}[\rho_T] := \mathrm{tr}_{\tilde{L}} \left[U_L V_{T,L \to L} \left(\rho_T \otimes |\mathrm{TFD}\rangle_{L,R} \langle \mathrm{TFD}| \right) V^{\dagger}_{T,L \to L} U^{\dagger}_L \right]. \tag{8.10}$$

This channel maps a density matrix on the diary T to the one on the late and early radiation system K, R. Also, the adjoint $\mathcal{N}^{\mathrm{SYK}\dagger}_{K,R \to T}$ of the SYK HP channel is given by

$$\begin{aligned} \mathcal{N}^{\mathrm{SYK}\dagger}_{K,R \to T}[\mathcal{O}_{KR}] &:= \mathrm{tr}_{L,R} \left[|\mathrm{TFD}\rangle_{L,R} \langle \mathrm{TFD}| \left(V^{\dagger}_{L \to T,L} U^{\dagger}_L \, \mathcal{O}_{KR} \, U_L V_{L \to T,L} \right) \right] \\ &= {}_{L,R} \langle \mathrm{TFD}| \left(V^{\dagger}_{L \to T,L} U^{\dagger}_L \, \mathcal{O}_{KR} \, U_L V_{L \to T,L} \right) |\mathrm{TFD}\rangle_{L,R}. \end{aligned} \tag{8.11}$$

The above quantum channels are analogous to the original HP channel and its adjoint for the Haar random unitary. However, we note that there is a difference between them in the sense that the SYK HP channel and its adjoint include the embedding map V, which induces (fermionic) excitations.

8.2 Some matrix elements of the Petz-lite and Rényi-two correlators

Now that we have prepared the SYK HP channel and its adjoint, we can construct the Petz-lite map for this channel. As in the Petz-lite for the Haar random case (5.9), we consider the

Petz-lite for the SYK case,

$$\mathcal{R}^{\text{Lite,SYK}}_{K,R\to T}[\mathcal{O}_{KR}] = \frac{1}{N_{\text{SYK}}}\mathcal{N}^{\text{SYK}\dagger}_{K,R\to T}[\mathcal{O}_{KR}], \qquad (8.12)$$

where N_{SYK} is the normalization factor, which is determined by the condition

$$\text{tr}_T\left[\mathcal{R}^{\text{Lite,SYK}}_{K,R\to T}\left[\mathcal{N}^{\text{SYK}}_{T\to K,R}[\sigma_T]\right]\right] = 1. \qquad (8.13)$$

Here, σ_T is some reference state in T for the normalization. We take it to be $\sigma_T = |0\rangle_T\langle 0|$. For this choice, the normalization factor is given by

$$N_{\text{SYK}} = \sum_{T=0,1} \langle T|\mathcal{N}^{\text{SYK}\dagger}_{K,R\to T}\left[\mathcal{N}^{\text{SYK}}_{T\to K,R}[|0\rangle_T\langle 0|]\right]|T\rangle. \qquad (8.14)$$

We note that due to this normalization, we can see that the Petz-lite (8.12) for the SYK HP protocol has a similar overall constant with the Petz-lite for the original HP protocol (5.11). To see the similarity, we first rewrite the Petz-lite (8.12) with the normalization factor (8.14) as follows,

$$\mathcal{R}^{\text{Lite,SYK}}_{K,R\to T}[\mathcal{O}_{KR}] = \frac{\left\langle\hat{d}_{\tilde{L}}\right\rangle_\beta}{1 + \left\langle\hat{d}_{\tilde{L}}\right\rangle_\beta \langle 1|\mathcal{N}^{\text{SYK}\dagger}_{K,R\to T}\left[\mathcal{N}^{\text{SYK}}_{T\to K,R}[|0\rangle_T\langle 0|]\right]|1\rangle}\mathcal{N}^{\text{SYK}\dagger}_{K,R\to T}[\mathcal{O}_{KR}], \qquad (8.15)$$

where $\left\langle\hat{d}_{\tilde{L}}\right\rangle_\beta$ is an effective dimension of subsystem $\tilde{L}$ defined by the purity $\text{tr}_{\tilde{L}}\left[(\rho_{\tilde{L}})^2\right]$ of the TFD state with respect to the subsystem[16],

$$\langle 0|\mathcal{N}^{\text{SYK}\dagger}_{K,R\to T}\left[\mathcal{N}^{\text{SYK}}_{T\to K,R}[|0\rangle_T\langle 0|]\right]|0\rangle = \text{tr}_{KR}\left[(\rho_{KR})^2\right] = \text{tr}_{\tilde{L}}\left[(\rho_{\tilde{L}})^2\right] =: \frac{1}{\left\langle\hat{d}_{\tilde{L}}\right\rangle_\beta}. \qquad (8.16)$$

The effective dimension is analogous to the dimension of the remaining black hole in the original HP setup. Indeed, in the infinite temperature limit $\beta \to 0$, the effective dimension is almost reduced to the actual dimension of subsystem $\tilde{L}$, $d_{\tilde{L}} = 2^{\frac{N-K}{2}}$[17]. However, in general, the effective dimension is smaller than the actual dimension due to the property of the purity and thermal effects;

$$1 \le \left\langle\hat{d}_{\tilde{L}}\right\rangle_\beta \le d_{\tilde{L}}, \qquad (8.17)$$

---

[16]We note that in our setting, subsystem $\tilde{L}$ is smaller than the complement system KR.

[17]For Majorana fermions, a annihilation operator is constructed from two Majorana fermions, and the corresponding creation operator is given by the Hermitian conjugation. In other words, two Majorana fermions forms a single qubit. Thus, a Hilbert space constructed from m Majorana fermions becomes a $2^{m/2}$-dimensional Hilbert space. See, e.g., [33] for the review.

where this effective dimension becomes closed to 1 in $\beta \to \infty$ and $d_{\tilde{L}}$ in $\beta \to 0$. With this effective dimension, we can compare the Petz-lite (8.15) for the SYK model to that for the original one (5.11) in the HP setup

$$\mathcal{R}^{\text{Lite},HP}_{D,B \to T}[\mathcal{O}_{DB}] = \frac{d_C}{1 + \left(\dfrac{d_T}{d_D}\right)^2} \mathcal{N}^\dagger_{D,B \to T}[\mathcal{O}_{DB}].$$

The similarities between the quantities in the HP and the SYK are summarized in the following identifications;

$$
\begin{aligned}
d_C &\longleftrightarrow \left\langle \hat{d}_{\tilde{L}} \right\rangle_\beta, \\
\left(\frac{d_T}{d_D}\right)^2 &\longleftrightarrow \left\langle \hat{d}_{\tilde{L}} \right\rangle_\beta \cdot \langle 1 | \mathcal{N}^{\text{SYK}\dagger}_{K,R \to T} \left[\mathcal{N}^{\text{SYK}}_{T \to K,R}[|0\rangle_T \langle 0|] \right] | 1 \rangle.
\end{aligned}
\tag{8.18}
$$

Also, we have the unitarity constraint on the dimensions of the Hilbert spaces, $d_T \, d_B = d_C \, d_D$. By using the relation, we can rewrite the dimension as

$$\left(\frac{d_T}{d_D}\right)^2 = \frac{d_C \, d_T}{d_B \, d_D}, \tag{8.19}$$

from which we have the following identification

$$\langle 1 | \mathcal{N}^{\text{SYK}\dagger}_{K,R \to T} \left[\mathcal{N}^{\text{SYK}}_{T \to K,R}[|0\rangle_T \langle 0|] \right] | 1 \rangle \quad \longleftrightarrow \quad \frac{1}{d_C} \cdot \left(\frac{d_T}{d_D}\right)^2 = \frac{d_T}{d_B \, d_D} = \frac{d_T}{k}. \tag{8.20}$$

This might be a good ratio to understand current physics; if we have a sufficiently large amount of Hawking radiation compared with the diary, $d_T \ll d_B \, d_D = k$, the ratio becomes almost 0. As we will soon see, the left quantity also becomes almost 0 around and after a critical time.

With this discussion of the normalization factor in mind, we consider a matrix element of $\mathcal{R}^{\text{Lite},\text{SYK}}_{K,R \to T} \left[\mathcal{N}^{\text{SYK}}_{T \to K,R}[\rho_T] \right]$ for a general density matrix ρ_T in the Hilbert space of the diary,

$$\langle T | \mathcal{R}^{\text{Lite},\text{SYK}}_{K,R \to T} \left[\mathcal{N}^{\text{SYK}}_{T \to K,R}[\rho_T] \right] | T' \rangle. \tag{8.21}$$

To check whether the Petz-lite works as the recovery map, it is sufficient to see whether the following relation holds (approximately) or not,

$$\langle T | \mathcal{R}^{\text{Lite},\text{SYK}}_{K,R \to T} \left[\mathcal{N}^{\text{SYK}}_{T \to K,R}[\rho_T] \right] | T' \rangle \overset{?}{\approx} \langle T | \rho_T | T' \rangle \quad \text{for } \forall \rho_T. \tag{8.22}$$

Checking the above relation is equivalent to focusing on the matrix elements

$$\langle T | \mathcal{R}^{\text{Lite},\text{SYK}}_{K,R \to T} \left[\mathcal{N}^{\text{SYK}}_{T \to K,R} \left[\left| \tilde{T} \right\rangle_T \left\langle \tilde{T'} \right| \right] \right] | T' \rangle \overset{?}{\approx} \left\langle T \middle| \tilde{T} \right\rangle \left\langle \tilde{T'} \middle| T' \right\rangle, \qquad \forall T, T', \tilde{T}, \tilde{T'}. \tag{8.23}$$

Generally, we have 16 components of the above matrix, but half of them, including odd Majorana fermions, are trivially vanishing due to the fermionic parity of the SYK model. In other words, matrix elements which satisfy $(T + T' + \tilde{T} + \tilde{T}') \equiv 1 \mod 2$ are vanishing.

Now, we focus on three non-zero matrix elements, and briefly explain how we can evaluate them[18]. First, we consider the $T, T', \tilde{T}, \tilde{T}' = 0$ case. If (8.23) holds then since its right hand side is 1, and therefore the following identity holds,

$$1 \overset{?}{\approx} \langle 0| \mathcal{R}^{\mathrm{Lite,SYK}}_{K,R \to T} \left[\mathcal{N}^{\mathrm{SYK}}_{T \to K,R} \left[|0\rangle_T \langle 0| \right] \right] |0\rangle = \left(1 + \left\langle \hat{d}_{\tilde{L}} \right\rangle_\beta \cdot \langle 1| \mathcal{N}^{\mathrm{SYK\dagger}}_{K,R \to T} \left[\mathcal{N}^{\mathrm{SYK}}_{T \to K,R} [|0\rangle_T \langle 0|] \right] |1\rangle \right)^{-1}.$$
(8.24)

The second one is for the $T, T' = 1$, $\tilde{T}, \tilde{T}' = 0$ case, where the matrix element is expected to become 0. In this case, we can see that this matrix element has the same ratio as above,

$$0 \overset{?}{\approx} \langle 1| \mathcal{R}^{\mathrm{Lite,SYK}}_{K,R \to T} \left[\mathcal{N}^{\mathrm{SYK}}_{T \to K,R} \left[|0\rangle_T \langle 0| \right] \right] |1\rangle = \frac{\left\langle \hat{d}_{\tilde{L}} \right\rangle_\beta \cdot \langle 1| \mathcal{N}^{\mathrm{SYK\dagger}}_{K,R \to T} \left[\mathcal{N}^{\mathrm{SYK}}_{T \to K,R} [|0\rangle_T \langle 0|] \right] |1\rangle}{1 + \left\langle \hat{d}_{\tilde{L}} \right\rangle_\beta \cdot \langle 1| \mathcal{N}^{\mathrm{SYK\dagger}}_{K,R \to T} \left[\mathcal{N}^{\mathrm{SYK}}_{T \to K,R} [|0\rangle_T \langle 0|] \right] |1\rangle}.$$
(8.25)

The final one is for $T, \tilde{T} = 0$, $T', \tilde{T}' = 1$, the matrix element (8.23), which is expected to be 1, becomes

$$1 \overset{?}{\approx} \langle 0| \mathcal{R}^{\mathrm{Lite,SYK}}_{K,R \to T} \left[\mathcal{N}^{\mathrm{SYK}}_{T \to K,R} \left[|0\rangle_T \langle 1| \right] \right] |1\rangle = \frac{\left\langle \hat{d}_{\tilde{L}} \right\rangle_\beta \cdot \langle 0| \mathcal{N}^{\mathrm{SYK\dagger}}_{K,R \to T} \left[\mathcal{N}^{\mathrm{SYK}}_{T \to K,R} [|0\rangle_T \langle 1|] \right] |1\rangle}{1 + \left\langle \hat{d}_{\tilde{L}} \right\rangle_\beta \cdot \langle 1| \mathcal{N}^{\mathrm{SYK\dagger}}_{K,R \to T} \left[\mathcal{N}^{\mathrm{SYK}}_{T \to K,R} [|0\rangle_T \langle 0|] \right] |1\rangle}.$$
(8.26)

The rest of matrix elements

$$\langle 0| \mathcal{R}^{\mathrm{Lite,SYK}}_{K,R \to T} \left[\mathcal{N}^{\mathrm{SYK}}_{T \to K,R} \left[|1\rangle_T \langle 0| \right] \right] |1\rangle, \quad \langle 1| \mathcal{R}^{\mathrm{Lite,SYK}}_{K,R \to T} \left[\mathcal{N}^{\mathrm{SYK}}_{T \to K,R} \left[|1\rangle_T \langle 1| \right] \right] |1\rangle.$$

are difficult to evaluate directly, as we will mention in footnote 21. In the next section, we evaluate these matrix elements indirectly from the results of this section.

Thus, to see the recovery (8.23), we need to study the behaviors of the matrix elements of $\mathcal{N}^\dagger \mathcal{N}$ which appear in the right hand side of (8.24), (8.25), and (8.26). In order for the recovery to happen, these have to satisfy

$$\left\langle \hat{d}_{\tilde{L}} \right\rangle_\beta \cdot \langle 1| \mathcal{N}^{\mathrm{SYK\dagger}}_{K,R \to T} \left[\mathcal{N}^{\mathrm{SYK}}_{T \to K,R} [|0\rangle_T \langle 0|] \right] |1\rangle \overset{?}{\approx} 0,$$
(8.27)

$$\left\langle \hat{d}_{\tilde{L}} \right\rangle_\beta \cdot \langle 0| \mathcal{N}^{\mathrm{SYK\dagger}}_{K,R \to T} \left[\mathcal{N}^{\mathrm{SYK}}_{T \to K,R} [|0\rangle_T \langle 1|] \right] |1\rangle \overset{?}{\approx} 1.$$
(8.28)

---

[18]The details of the calculation will be discussed in the upcoming paper [16].

We study the behaviors of the left hand sides of (8.27) and (8.28) below. To this end, it is convenient to rewrite the quantities as correlators. From the definitions of the channels (5.3) and (8.11), we obtain the left-left correlators

$$\left\langle \hat{d}_{\tilde{L}} \right\rangle_\beta \cdot \langle 1|\mathcal{N}^{\mathrm{SYK}\dagger}_{K,R\to T} \left[\mathcal{N}^{\mathrm{SYK}}_{T\to K,R}[|0\rangle_T\langle 0|] \right]|1\rangle = \frac{1}{Z_\delta} \cdot \frac{\langle \mathrm{TFD}|\psi_{i,L}(t-i\delta) \left(I_{\tilde{L}} \otimes \rho_{KR} \right) \psi_{i,L}(t+i\delta)|\mathrm{TFD}\rangle}{\mathrm{tr}_{KR}\left[(\rho_{KR})^2 \right]},$$
(8.29)

$$\left\langle \hat{d}_{\tilde{L}} \right\rangle_\beta \cdot \langle 0|\mathcal{N}^{\mathrm{SYK}\dagger}_{K,R\to T} \left[\mathcal{N}^{\mathrm{SYK}}_{T\to K,R}[|0\rangle_T\langle 1|] \right]|1\rangle = \frac{1}{Z_\delta} \cdot \frac{\langle \mathrm{TFD}|\psi_{i,L}(t-i\delta) \left(\rho_{\tilde{L}} \otimes I_{KR} \right) \psi_{i,L}(t+i\delta)|\mathrm{TFD}\rangle}{\mathrm{tr}_{KR}\left[(\rho_{KR})^2 \right]},$$
(8.30)

where the two fermions are put on the left system, and ρ_{KR} and $\rho_{\tilde{L}}$ are defined by

$$\rho_{\tilde{L}} = \mathrm{tr}_{KR}\left[|\mathrm{TFD}\rangle_{LR}\langle \mathrm{TFD}| \right], \qquad \rho_{KR} = \mathrm{tr}_{\tilde{L}}\left[|\mathrm{TFD}\rangle_{LR}\langle \mathrm{TFD}| \right]. \tag{8.31}$$

We give the derivation of the correlators in appendix F.

We also note that the numerators in the above correlators can be written as

$$\langle \mathrm{TFD}|\psi_{i,L}(t-i\delta) \left(I_{\tilde{L}} \otimes \rho_{KR} \right) \psi_{i,L}(t+i\delta)|\mathrm{TFD}\rangle$$
$$= \mathrm{tr}_{KR}\left[\mathrm{tr}_{\tilde{L}}\left[\psi_{i,L}(t+i\delta) |\mathrm{TFD}\rangle_{L,R}\langle \mathrm{TFD}| \psi_{i,L}(t-i\delta)^\dagger \right] \rho_{KR} \right]$$
(8.32)

and

$$\langle \mathrm{TFD}|\psi_{i,L}(t-i\delta) \left(\rho_{\tilde{L}} \otimes I_{KR} \right) \psi_{i,L}(t+i\delta)|\mathrm{TFD}\rangle$$
$$= \mathrm{tr}_{\tilde{L}}\left[\mathrm{tr}_{KR}\left[\psi_{i,L}(t+i\delta) |\mathrm{TFD}\rangle_{L,R}\langle \mathrm{TFD}| \psi_{i,L}(t-i\delta)^\dagger \right] \rho_{\tilde{L}} \right].$$
(8.33)

These expressions are also useful to see that these quantities are related to "Renyi-2" quantities, as explained below.

Below, we would like to evaluate these correlators analytically, but the expressions (8.29) and (8.30) are not suitable for analytic treatment. This is because they are "specific site" correlators; thus, we can not apply the large-N techniques to evaluate them. However, since we are basically interested in typical behaviors under highly chaotic dynamics in our setup, the specific choice of the embedding would *not* be essential. Therefore, below, we consider the "typical" embedding of the code information into the whole $\tilde{L}$ system uniformly. Therefore, we replace these correlators with their averages on $\tilde{L}$,

$$\frac{1}{Z_\delta} \cdot \frac{\langle \mathrm{TFD}|\psi_{i,L}(t-i\delta) \left(I_{\tilde{L}} \otimes \rho_{KR} \right) \psi_{i,L}(t+i\delta)|\mathrm{TFD}\rangle}{\mathrm{tr}_{KR}\left[(\rho_{KR})^2 \right]}$$
$$\to \frac{1}{N-K} \sum_{i=1}^{N-K} \frac{1}{Z_\delta} \cdot \frac{\langle \mathrm{TFD}|\psi_{i,L}(t-i\delta) \left(I_{\tilde{L}} \otimes \rho_{KR} \right) \psi_{i,L}(t+i\delta)|\mathrm{TFD}\rangle}{\mathrm{tr}_{KR}\left[(\rho_{KR})^2 \right]}$$
(8.34)

and

$$\frac{1}{Z_\delta} \cdot \frac{\langle \text{TFD}|\psi_{i,L}(t-i\delta)\left(\rho_{\tilde{L}} \otimes I_{KR}\right)\psi_{i,L}(t+i\delta)|\text{TFD}\rangle}{\text{tr}_{KR}\left[(\rho_{KR})^2\right]}$$

$$\rightarrow \frac{1}{N-K}\sum_{i=1}^{N-K}\frac{1}{Z_\delta} \cdot \frac{\langle \text{TFD}|\psi_{i,L}(t-i\delta)\left(\rho_{\tilde{L}} \otimes I_{KR}\right)\psi_{i,L}(t+i\delta)|\text{TFD}\rangle}{\text{tr}_{KR}\left[(\rho_{KR})^2\right]}. \tag{8.35}$$

These replacements would change the correlators in sub-leading orders of N, but the essential physics would not be changed, because of typicality.

These averaged two-point functions are special cases of the (right-left) modular-flowed correlators of the form

$$\frac{1}{N-K}\sum_{i=1}^{N-K}\frac{\langle \text{TFD}|\psi_{i,R}(\tau)\left(\rho_{\tilde{L}}^{n-1-k} \otimes \rho_{KR}^{k}\right)\psi_{i,L}(\tau')|\text{TFD}\rangle}{\text{tr}\left[\rho_{KR}^{n}\right]}, \tag{8.36}$$

where one of the fermions is put on the left system, and the other one is on the right system. In the Euclidean regime, they are computed by using the replica trick in [14] when $K \ll N$.

We use the result to compute "Rényi-2" (left-left) modular-flowed correlators (8.34) and (8.35) from the Euclidean (right-left) correlator (8.36), by taking the limits $k \rightarrow n-1$ (and $k \rightarrow 0$), and $n \rightarrow 2$, then analytically continuing to the Lorentzian regime. We note that there is a difference between the above correlator (8.36) computed in [14] and our correlators (8.34) and (8.35), namely that in (8.36) two fermions are living on opposite sides but in our correlators they live on the same side. In our setup, one can relate the correlator to the following diagrams (figure 28).

We study the correlators in the large-βJ limit because their analytic expressions are available in the limit. One can instead work in the large-q limit while keeping the value of βJ finite. We will not do this here because it is the former limit where the generalization to two-dimensional CFTs is straightforward [16]. The right hand side of (8.34) and (8.35) in the Euclidean regime are evaluated in the large βJ and $K \ll N$ limit as

$$\frac{1}{N-K}\sum_{i=1}^{N-K}\frac{\langle \text{TFD}|\psi_{i,L}(\tau)\left(I_{\tilde{L}} \otimes \rho_{KR}\right)\psi_{i,L}(\tau')|\text{TFD}\rangle}{\text{tr}_{KR}\left[(\rho_{KR})^2\right]}$$

$$= G_{2\beta}(\tau+2\beta-\tau') + 2\frac{K}{N}\left(\mathcal{F}(\tau+2\beta,\tau';\beta,0) - \mathcal{F}_0(\tau+2\beta,\tau';\beta,0)\right) + \mathcal{O}\left(\left(\frac{K}{N}\right)^2\right), \tag{8.37}$$

$$\frac{1}{N-K}\sum_{i=1}^{N-K}\frac{\langle \text{TFD}|\psi_{i,L}(\tau)\left(\rho_{\tilde{L}} \otimes I_{KR}\right)\psi_{i,L}(\tau')|\text{TFD}\rangle}{\text{tr}_{KR}\left[(\rho_{KR})^2\right]}$$

$$= G_{2\beta}(\tau+\beta-\tau') + 2\frac{K}{N}\left(\mathcal{F}(\tau+\beta,\tau';\beta,0) - \mathcal{F}_0(\tau+\beta,\tau';\beta,0)\right) + \mathcal{O}\left(\left(\frac{K}{N}\right)^2\right). \tag{8.38}$$
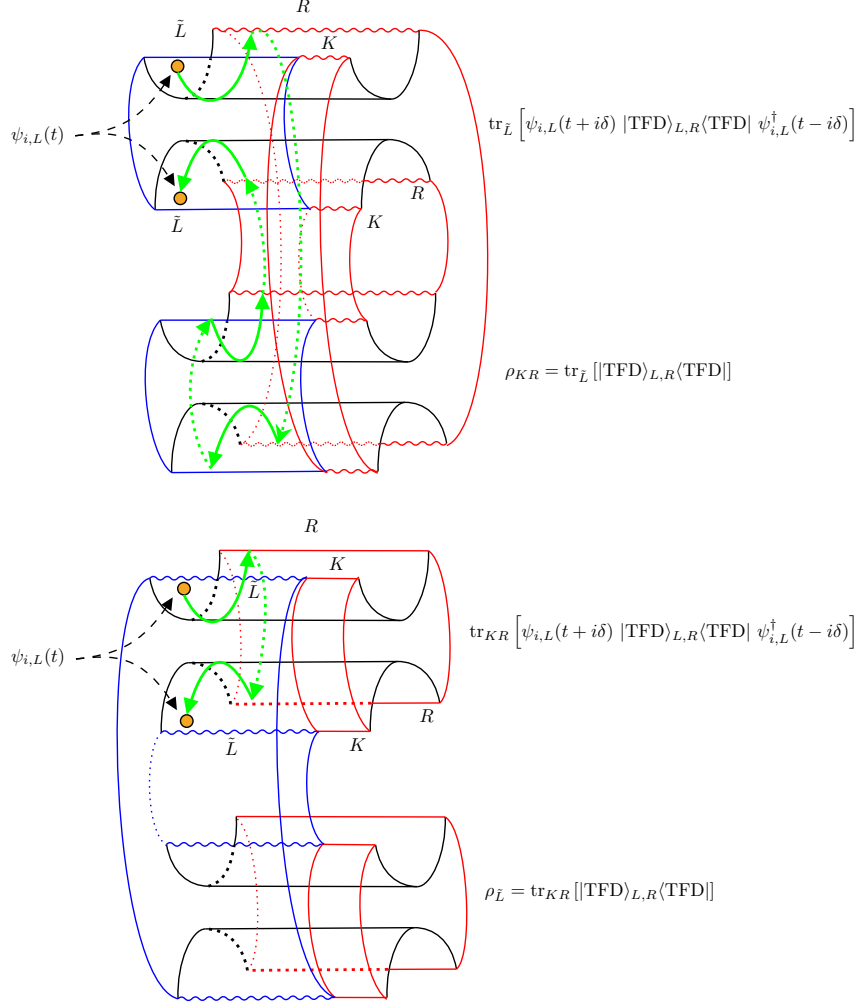
Figure 28: Diagrams for the path integral calculation of the correlator (8.29) with using the relation (8.32) (Top), and the other correlator (8.30) with (8.33) (Bottom). The red regions in the figure correspond to subsystem RK, and the blue regions correspond to subsystem $\tilde{L}$. The semicircles correspond to the Euclidean segments that prepare the TFD states. Orange dots represent the insertions of the SYK Majorana fermion with the regularization, $\psi_{i,L}(t + i\delta)$. The combination of the upper two semicircles with the operator insertions corresponds to the density matrix $\mathrm{tr}_{\tilde{L}}[\psi_{i,L} | \mathrm{TFD}\rangle_{L,R} \langle \mathrm{TFD}| \psi_{i,L}^\dagger]$ (and $\mathrm{tr}_{KR}[\psi_{i,L} | \mathrm{TFD}\rangle_{L,R} \langle \mathrm{TFD}| \psi_{i,L}^\dagger]$), and the remaining combination represents the other one ρ_{KR} (and $\rho_{\tilde{L}}$). Solid green arrows in the figure correspond to $\beta/2$ Euclidean evolutions. The two insertions are separated by Euclidean time 2β (Top) and β (Bottom). These separations are directly related to $\tau + 2\beta$ and $\tau + \beta$ appearing in (8.37) and (8.38) respectively.

Here, $G_{2\beta}(\tau)$ is a Euclidean thermal SYK two-point function for subsystem $\tilde{L}$ with periodicity 2β, and $\mathcal{F}(\tau_1, \tau_2; \tau_3, \tau_4)$ is the connected SYK four-point function, which is related to the bare one $\mathcal{F}_0(\tau_1, \tau_2; \tau_3, \tau_4)$ by the so-called ladder kernel $K_c(\tau_1, \tau_2; \tau_3, \tau_4)$,

$$
\begin{aligned}
\mathcal{F}(\tau_1, \tau_2; \tau_3, \tau_4) &= \int d\tau \int d\tau' \frac{1}{1 - K_c(\tau_1, \tau_2; \tau, \tau')} \mathcal{F}_0(\tau, \tau'; \tau_3, \tau_4), \\
\mathcal{F}_0(\tau_1, \tau_2; \tau_3, \tau_4) &= G_{2\beta}(\tau_{13})G_{2\beta}(\tau_{42}) - G_{2\beta}(\tau_{14})G_{2\beta}(\tau_{32}), \qquad \tau_{ij} = \tau_i - \tau_j, \\
K_c(\tau_1, \tau_2; \tau_3, \tau_4) &= -J^2(q-1)G_{2\beta}(\tau_{13})G_{2\beta}(\tau_{24}) \left(G_{2\beta}(\tau_{34})\right)^{q-2}.
\end{aligned}
\tag{8.39}
$$

In the SYK model, these two-point and four-point functions are well-studied in many papers, e.g., [35, 36, 40–43]. See also [33, 34] for the review and references therein.

The Euclidean times τ, τ' in (8.37) and (8.38) are continued to the Lorentzian time with a regularization parameter $0 < \delta \ll 1$; $\tau \rightarrow -it - \delta, \tau' \rightarrow -it + \delta$. In this way, the correlator (8.37) is continued to Lorentzian time as an out-of-time ordering correlator (OTOC), $\tau_1 > \tau_3 > \tau_2 > \tau_4$, under the condition $1 \ll \beta J \ll N/K$. This correlator with the ordering is given by [34, 35],

$$
\mathcal{F}(\tau_1, \tau_2; \tau_3, \tau_4) = G_{2\beta}(\tau_{12})G_{2\beta}(\tau_{34})\frac{2\beta J}{q^2 \pi C}\left[1 - \frac{\pi}{2}\frac{\sin\left(\frac{\pi}{\beta}\tau_{12;34}\right)}{\sin\left(\frac{\pi}{\beta}\cdot\frac{\tau_{12}}{2}\right)\sin\left(\frac{\pi}{\beta}\cdot\frac{\tau_{34}}{2}\right)}\right], \tag{8.40}
$$

where $\tau_{12;34} = (\tau_1 + \tau_2)/2 - (\tau_3 + \tau_4)/2$, and C is a constant related to an overall constant of the Schwarzian action derived from the Schwinger-Dyson equation of the SYK model [34, 35]. Thus, we have the following continuation

$$
\begin{aligned}
\mathcal{F}(\tau + 2\beta, \tau'; \beta, 0) \rightarrow &\mathcal{F}(-it - \delta + 2\beta, -it + \delta; \beta, 0) \\
&= 2G_{2\beta}(2\beta - 2\delta)G_{2\beta}(\beta) \cdot \frac{2\beta J}{q^2 \pi C}\left[1 - \frac{\pi}{2}\frac{\cosh\left(\frac{\pi}{\beta}t\right)}{\sin\left(\frac{\pi\delta}{\beta}\right)}\right] \\
&\approx -2G_{2\beta}(2\beta - 2\delta)G_{2\beta}(\beta) \cdot \frac{\beta J}{2q^2 C} \cdot \frac{\exp\left(\frac{\pi}{\beta}t\right)}{\sin\left(\frac{\pi\delta}{\beta}\right)}.
\end{aligned}
\tag{8.41}
$$

In particular, the correlator is exponentially growing in time. On the other hand, the other correlator (8.38) is continued to Lorentzian time with the ordering $\tau_3 > \tau_1 > \tau_2 > \tau_4$ under the condition $1 \ll \beta J \ll N/K$, therefore it is not OTOC. The correlator with the ordering

$\tau_3 > \tau_1 > \tau_2 > \tau_4$ is given by

$$\mathcal{F}(\tau_1, \tau_2; \tau_3, \tau_4)$$

$$= -G_{2\beta}(\tau_{12})G_{2\beta}(\tau_{34})\frac{2\beta J}{q^2\pi C}\left[\left(\frac{\pi\tau_{12}}{2\beta\tan\left(\frac{\pi}{\beta}\cdot\frac{\tau_{12}}{2}\right)} + \frac{\pi}{\tan\left(\frac{\pi}{\beta}\cdot\frac{\tau_{12}}{2}\right)} - 1\right)\left(\frac{\pi\tau_{34}}{2\beta\tan\left(\frac{\pi}{\beta}\cdot\frac{\tau_{34}}{2}\right)} - 1\right)\right],$$
$$(8.42)$$

and its analytic continuation is

$$\mathcal{F}(\tau + \beta, \tau'; \beta, 0)$$

$$\rightarrow \mathcal{F}(-it - \delta + \beta, -it + \delta; \beta, 0) = -2G_{2\beta}(\beta - 2\delta)G_{2\beta}(\beta)\cdot\frac{2\beta J}{q^2\pi C}\left[1 - \left(\frac{\pi}{2} - \frac{\pi\delta}{\beta}\right)\tan\left(\frac{\pi\delta}{\beta}\right)\right].$$
$$(8.43)$$

Clearly, this is time-independent, unlike the previous case.

We do not evaluate bare four-point functions $\mathcal{F}_0(\tau_1, \tau_2; \tau_3, \tau_4)$ for (8.37) and (8.38), because they are particular combinations of the thermal SYK two-point functions with the power low behavior with respect to time, therefore they do not give dominant contributions to the correlators (8.37) and (8.38).

Combining the above results, we can obtain the analytic expressions of the quantities (8.37) and (8.38),

$$\left\langle \hat{d}_{\tilde{L}} \right\rangle_\beta \cdot \langle 1|\mathcal{N}_{K,R\rightarrow T}^{\text{SYK}\dagger}\left[\mathcal{N}_{T\rightarrow K,R}^{\text{SYK}}[|0\rangle_T\langle 0|]\right]|1\rangle$$

$$\approx \frac{1}{Z_\delta}\left[G_{2\beta}(2\beta - 2\delta) - G_{2\beta}(2\beta - 2\delta)G_{2\beta}(\beta)\cdot\frac{2\beta J}{q^2 C}\cdot\frac{K}{N}\frac{\exp\left(\frac{\pi}{\beta}t\right)}{\sin\left(\frac{\pi\delta}{\beta}\right)} + \cdots\right]$$
$$(8.44)$$

$$\approx \frac{G_{2\beta}(2\beta - 2\delta)}{G_\beta(2\delta)}\left[1 - \frac{G_{2\beta}(\beta)}{\sin\left(\frac{\pi\delta}{\beta}\right)}\cdot\frac{2\beta J}{q^2 C}\cdot\frac{K}{N}\exp\left(\frac{\pi}{\beta}t\right)\right],$$

and

$$\left\langle \hat{d}_{\tilde{L}} \right\rangle_\beta \cdot \langle 0|\mathcal{N}_{K,R\rightarrow T}^{\text{SYK}\dagger}\left[\mathcal{N}_{T\rightarrow K,R}^{\text{SYK}}[|0\rangle_T\langle 1|]\right]|1\rangle$$

$$\approx \frac{1}{Z_\delta}\left[G_{2\beta}(\beta - 2\delta) - G_{2\beta}(\beta - 2\delta)G_{2\beta}(\beta)\cdot\frac{8\beta J}{q^2\pi C}\cdot\frac{K}{N}\left[1 - \left(\frac{\pi}{2} - \frac{\pi\delta}{\beta}\right)\tan\left(\frac{\pi\delta}{\beta}\right)\right] + \cdots\right]$$

$$\approx \frac{G_{2\beta}(\beta - 2\delta)}{G_\beta(2\delta)}\left[1 - G_{2\beta}(\beta)\cdot\frac{8\beta J}{q^2\pi C}\cdot\frac{K}{N}\left[1 - \left(\frac{\pi}{2} - \frac{\pi\delta}{\beta}\right)\tan\left(\frac{\pi\delta}{\beta}\right)\right]\right],$$
$$(8.45)$$

where $\cdots$ includes bare four-point functions $\mathcal{F}_0(\tau_1, \tau_2; \tau_3, \tau_4)$, would-be sub-leading terms, coming from the replacements (8.34) and (8.35) in (8.29) and (8.30), and the sub-sub-leading

terms of the averaged correlators. In the final lines, we ignored them. These ignored terms do not change the essential physics of the discussions below. Thus, for simplicity of the discussions below, we do not consider their contributions explicitly, but we need to keep in mind that these ignored terms include order-(K/N) contributions.

Let us consider the consequences of the above results. First, we focus on the ratios $G_{2\beta}(2\beta-2\delta)/G_\beta(2\delta)$ and $G_{2\beta}(\beta-2\delta)/G_\beta(2\delta)$ appearing in the above results. Since the SYK two-point function under the conformal limit $\beta J \gg 1$ is given by [35],

$$G_\beta(\tau) = b \left[\frac{\pi}{\beta \sin \frac{\pi\tau}{\beta}} \right]^{2\Delta}, \qquad \Delta = \frac{1}{q}, \quad J^2 b^q \pi = \left(\frac{1}{2} - \Delta \right) \tan \pi\Delta, \tag{8.46}$$

we can evaluate the ratios as follows

$$\frac{G_{2\beta}(2\beta - 2\delta)}{G_\beta(2\delta)} = \cos^{2\Delta} \left(\frac{\pi\delta}{\beta} \right), \tag{8.47}$$

and

$$\frac{G_{2\beta}(\beta - 2\delta)}{G_\beta(2\delta)} = \sin^{2\Delta} \left(\frac{\pi\delta}{\beta} \right). \tag{8.48}$$

Thus, these ratios can not be 1 simultaneously for general δ and β. However, since $\Delta = 1/q$ when q is large, these ratios are close to 1. We give plots of the above two functions for several q in figure 29. As we can see from plots 29 or directly from (8.47) and (8.48), we need to consider a (relatively) large-q regime, which implies that the SYK Majorana fermion has a small conformal dimension, $\Delta = 1/q \ll 1$, in order to achieve recovery.

One may wonder why here we take the large-q limit, because the $(\text{SYK})_q$ is chaotic for all $q \geq 4$ thus the identities (8.27), (8.28) are expected to hold for any value of q in this range. Nevertheless, here we have to take the large-q limit because we define the code subspace using the SYK Majorana fermion operator $\psi_{i,L}$ and the calculations of the relevant correlation functions can be possible only in the large-βJ limit where the entanglement between L and R is weak. Because of the weakness of the entanglement, the recovery is only possible when the dimension of the operator that defines the code subspace is small, implying the necessity of taking the large-q limit.

Next, we consider the two-point function $G_{2\beta}(\beta)$ appearing in the sub-leading terms. The two-point function $G_{2\beta}(\beta)$ can be written as

$$G_{2\beta}(\beta) = b \left[\frac{\pi}{2\beta \sin \frac{\pi}{2}} \right]^{2\Delta} = \left[\left(\frac{1}{2} - \Delta \right) \frac{\pi \tan \pi\Delta}{(2\beta J)^2} \right]^\Delta. \tag{8.49}$$

The above expression includes $(1/\beta J)^\Delta$, thus in $\beta J \to \infty$ limit, the SYK two-point function $G_{2\beta}(\beta)$ vanishes. We also note the q-dependence of the SYK two-point function. Plots of the above function and $\beta J G_{2\beta}(\beta)$ for several $q = \Delta^{-1}$ are given in figure 30 and 31 respectively.
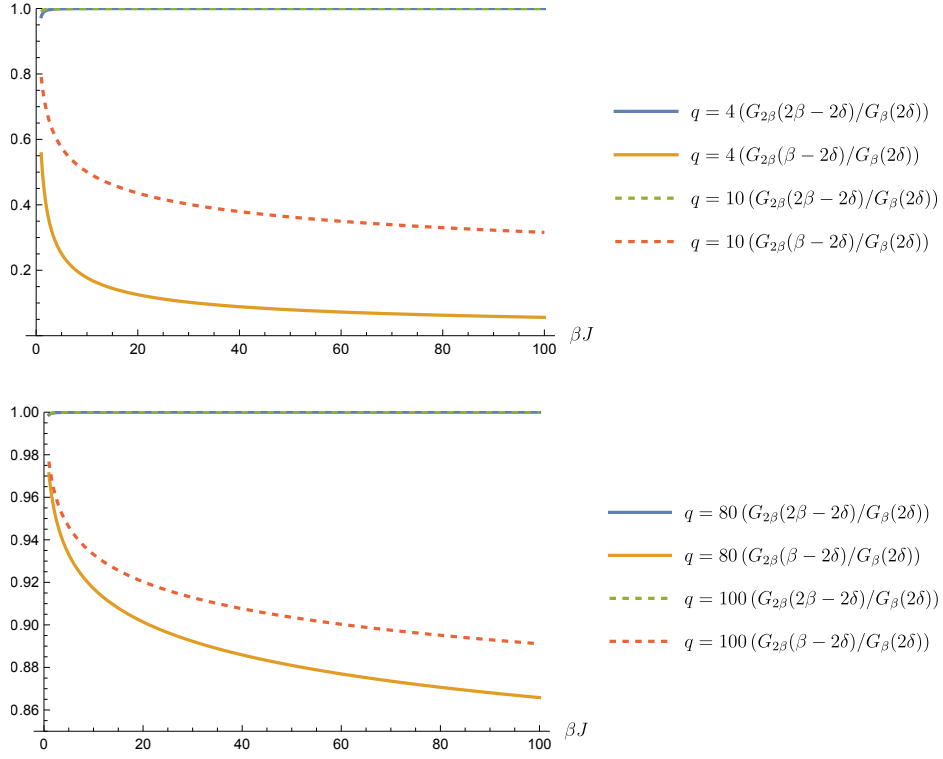
Figure 29: Plots of ratios (8.47) and (8.48) as a function of βJ for smaller q (Top), and for larger q (Bottom). Here, we set $\delta J = 0.1$. For large q regions, all the ratios become close to 1.
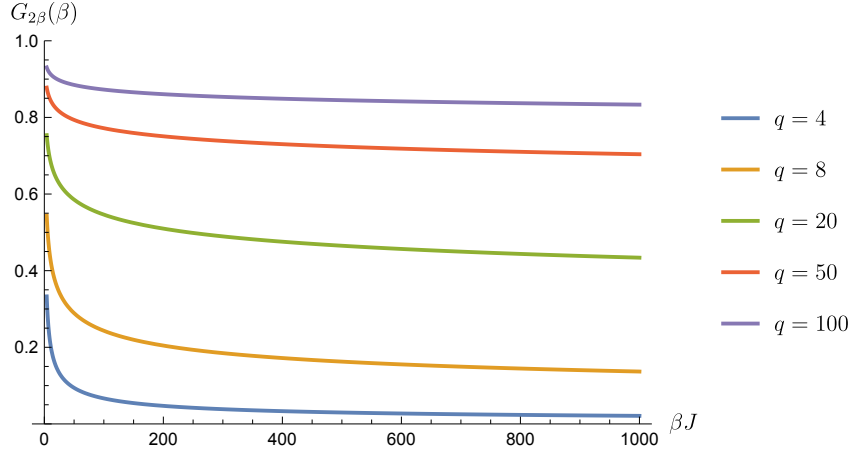

Figure 30: Plots of the SYK two-point function $G_{2\beta}(\beta)$, (8.49) as a function of βJ for several $q = \Delta^{-1}$.
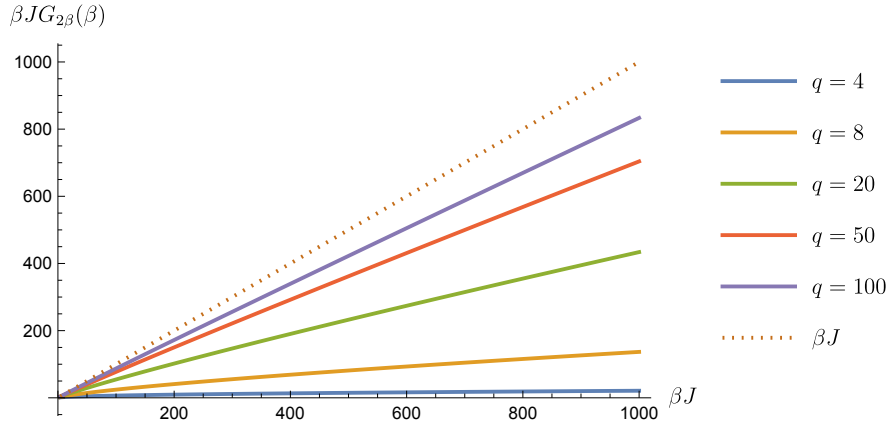
Figure 31: Plots of $\beta J G_{2\beta}(\beta)$ as a function of βJ for several $q = \Delta^{-1}$. The dotted line is just βJ, which is equivalent to $\beta J G_{2\beta}(\beta)$ under the $q \to \infty$ limit.

The plots show that as q increases, the two-point function $G_{2\beta}(\beta)$ and $\beta J G_{2\beta}(\beta)$ take larger values.

Thus, from the above discussion, in the strict $\beta J \to \infty$ limit[19], we have $G_{2\beta}(\beta) \to 0$, hence the second terms including $G_{2\beta}(\beta)$ in (8.44) and (8.45) vanish if we keep the exponential factor $\exp(\pi t/\beta)$ in (8.44) fixed. Therefore, in this strict $\beta J \to \infty$ limit, we can not have contributions from the second terms including $G_{2\beta}(\beta)$ in (8.44) and (8.45). These terms are of order K/N and crucial for the following discussion.

Finally, let us focus on the time dependence of the results (8.44) and (8.45). First, we focus on the second case (8.45). This result is time-independent at least up to the K/N-order, and the second term is always suppressed by the time-independent factor at the K/N-order, thus the second term is very small compared with the first term. This implies that the quantity (8.45) is almost given by the ratio $G_{2\beta}(\beta - 2\delta)/G_\beta(2\delta)$, which becomes close to 1 when q is large.

Next, we focus on (8.44). Because of the exponential time-dependent factor, this correlator has crucially different behavior as a function of time from (8.45). For early times $t \ll 1$, the exponential in the second term can be approximated by 1, they are similar. However, because of the exponentially growing factor, the perturbative expansion with respect to K/N breaks down, similar to the fact that the perturbative calculations of OTOCs in $1/N$ become

---

[19]We note that to consider the perturbative expansion, we have assumed $\beta J \ll N/K$, and also implicitly assumed $q \ll N/K$ for large q. Thus, we can not take the $\beta J \to \infty$ or $q \to \infty$ limits, unless we take the $N/K \to \infty$ limit. However, the limit $N/K \to \infty$ implies that there is almost no Hawking radiation compared to the entire Hawking radiation $K/N \to 0$. Intuitively, in such a situation, we would not be able to recover the diary information from the Hawking radiation.

invalid. The time scale of this breakdown can be estimated by equating the second term with the first term in (8.44). From the condition, we can find a critical time t_*[20],

$$\frac{K}{N} \exp\left(\frac{\pi}{\beta} t_*\right) \sim 1 \qquad \implies \qquad t_* = \frac{\beta}{\pi} \log\left(\frac{N}{K}\right) = 2 t_{\text{Scram}}, \tag{8.50}$$

where we introduce the usual scrambling time t_{Scram} [44] given by

$$t_{\text{Scram}} = \frac{\beta}{2\pi} \log\left(\frac{N}{K}\right). \tag{8.51}$$

Using this time scale, we can rewrite the correlator (8.44) as

$$\left\langle \hat{d}_{\tilde{L}} \right\rangle_{\beta} \cdot \langle 1 | \mathcal{N}_{K,R\to T}^{\text{SYK}\dagger} \left[\mathcal{N}_{T\to K,R}^{\text{SYK}} [|0\rangle_T \langle 0|] \right] |1\rangle$$

$$\approx \frac{G_{2\beta}(2\beta - 2\delta)}{G_{\beta}(2\delta)} \left[1 - \frac{G_{2\beta}(\beta)}{\sin\left(\frac{\pi\delta}{\beta}\right)} \cdot \frac{2\beta J}{q^2 C} \cdot \exp\left(\frac{\lambda_L}{2} \left(t - 2t_{\text{Scram}}\right)\right) \right], \tag{8.52}$$

where we introduce the Lyapunov exponent λ_L for a black hole with temperature β,

$$\lambda_L = \frac{2\pi}{\beta}. \tag{8.53}$$

Thus, around the critical time, which is twice the scrambling time, we can see that the overall coefficient of $G_{2\beta}(2\beta - 2\delta)/G_{2\beta}(2\delta)$ becomes very small as usual OTOC correlators. This reproduces the expected result (8.27) under the condition $\beta J \gg 1$.

From the discussion so far, we have confirmed that the matrix elements (8.24), (8.25) and (8.26) do behave as we expect them to under the condition $1 \ll \beta J \ll N/K$.

8.3   Expected properties of the Petz-lite under the SYK dynamics

So far, we have confirmed that the matrix elements we computed (8.27) and (8.28) reproduce our expected results under the conditions of relatively large-q interaction, after the critical time $t_* = 2t_{\text{Scram}}$. Additionally, of course, the following trivial matrix element is equal to 1 by the definition,

$$\left\langle \hat{d}_{\tilde{L}} \right\rangle_{\beta} \cdot \langle 0 | \mathcal{N}_{K,R\to T}^{\text{SYK}\dagger} \left[\mathcal{N}_{T\to K,R}^{\text{SYK}} [|0\rangle_T \langle 0|] \right] |0\rangle = 1. \tag{8.54}$$

---

[20]In defining the critical time, we might have the ambiguity of which factors should be included in the critical time (or correspondingly the scrambling time), e.g., βJ and also $G_{2\beta}(\beta)$. However, as we saw before, the two-point function is typically order one $G_{2\beta}(\beta) = \mathcal{O}(1)$, thus we might not need to include the factor to the scrambling time. Another factor $1/\sin\left(\frac{\pi\delta}{\beta}\right)$ can be set to be $\mathcal{O}(1)$ by setting the cutoff δ suitably. For the other factor βJ, since we have the condition $\beta J \ll N/K$, the factor can not give a significant contribution compared to the leading factor N/K; thus, including the factor would be redundant. Therefore, the critical time here would be the simplest choice.

Also, we can obtain the same consequences for two related matrix elements. Let us explain them. First, the matrix element (8.27), which becomes close to 0, is directly related to

$$\left\langle \hat{d}_{\tilde{L}} \right\rangle_{\beta} \cdot \langle 1|\mathcal{N}_{K,R\to T}^{\text{SYK}\dagger} \left[\mathcal{N}_{T\to K,R}^{\text{SYK}}[|0\rangle_T\langle 0|]\right]|1\rangle = \left\langle \hat{d}_{\tilde{L}} \right\rangle_{\beta} \cdot \langle 0|\mathcal{N}_{K,R\to T}^{\text{SYK}\dagger} \left[\mathcal{N}_{T\to K,R}^{\text{SYK}}[|1\rangle_T\langle 1|]\right]|0\rangle \quad (8.55)$$

via the definition of the adjoint channel (5.7). Thus, this matrix element also becomes close to 0 after the critical time, and the behavior is consistent with our expectation.

Next, for the matrix element (8.28), being almost equal to 1, we have the following relation through the definition of the adjoint channel (5.7) again,

$$\left\langle \hat{d}_{\tilde{L}} \right\rangle_{\beta} \cdot \langle 0|\mathcal{N}_{K,R\to T}^{\text{SYK}\dagger} \left[\mathcal{N}_{T\to K,R}^{\text{SYK}}[|0\rangle_T\langle 1|]\right]|1\rangle = \left\langle \hat{d}_{\tilde{L}} \right\rangle_{\beta} \cdot \langle 1|\mathcal{N}_{K,R\to T}^{\text{SYK}\dagger} \left[\mathcal{N}_{T\to K,R}^{\text{SYK}}[|1\rangle_T\langle 0|]\right]|0\rangle . \quad (8.56)$$

Thus, although we have eight non-trivial matrix elements (8.23) that should be checked, we already know the behavior of the above five matrix elements, and there are still three matrix elements. However, since two of them are related by complex conjugation, essentially we need to investigate the following two matrix elements

$$\left\langle \hat{d}_{\tilde{L}} \right\rangle_{\beta} \cdot \langle 0|\mathcal{N}_{K,R\to T}^{\text{SYK}\dagger} \left[\mathcal{N}_{T\to K,R}^{\text{SYK}}[|1\rangle_T\langle 0|]\right]|1\rangle , \quad (8.57)$$

and

$$\left\langle \hat{d}_{\tilde{L}} \right\rangle_{\beta} \cdot \langle 1|\mathcal{N}_{K,R\to T}^{\text{SYK}\dagger} \left[\mathcal{N}_{T\to K,R}^{\text{SYK}}[|1\rangle_T\langle 1|]\right]|1\rangle . \quad (8.58)$$

Here, the first matrix element is related to the following one

$$\left(\left\langle \hat{d}_{\tilde{L}} \right\rangle_{\beta} \cdot \langle 0|\mathcal{N}_{K,R\to T}^{\text{SYK}\dagger} \left[\mathcal{N}_{T\to K,R}^{\text{SYK}}[|1\rangle_T\langle 0|]\right]|1\rangle\right)^* = \left\langle \hat{d}_{\tilde{L}} \right\rangle_{\beta} \cdot \langle 1|\mathcal{N}_{K,R\to T}^{\text{SYK}\dagger} \left[\mathcal{N}_{T\to K,R}^{\text{SYK}}[|0\rangle_T\langle 1|]\right]|0\rangle .$$
$$(8.59)$$

In evaluating these matrix elements, we can not directly use the technique of [14], unlike the cases for the matrix elements (8.29) and (8.30)[21]. In the upcoming paper [16], we will report their results, but here we explain their expected behaviors from our obtained results. To this end, it would be useful to introduce the Kraus representation of the quantum channel (8.10),

$$\mathcal{N}_{T\to K,R}^{\text{SYK}}[\rho_T] = \sum_{m=1}^{d_{\tilde{L}}} E_m^{\text{SYK}} \rho_T E_m^{\text{SYK}\dagger} \quad (8.60)$$

---

[21]We briefly explain the reason why the evaluations of the matrix elements (8.58) and (8.59) are difficult. The reason is that they do not have simple expressions like (8.32) and (8.33) naively. Of course, for matrix element (8.58), we can consider a similar expression like (8.32) with replacing the TFD state with the excited state $\psi_{i,L}|\text{TFD}\rangle_{L,R}$, but in that case, we can no longer use the techniques in [14], and we need to consider the modular operator for the excited state. For the other matrix element (8.59), we naively need to introduce transition matrices, not density matrices, to write it in terms of a correlator.

where E_m^{SYK} is the Kraus operator given by

$$E_m^{\text{SYK}} = \,_{\tilde{L}}\langle m| U_L V_{T,L\to L} |\text{TFD}\rangle_{L,R}. \tag{8.61}$$

We can obtain this Kraus representation by introducing an orthonormal basis of the subsystem $\tilde{L}$ as $\{|m\rangle_{\tilde{L}}\}_{m=1}^{d_{\tilde{L}}}$. We also note that the adjoint channel (8.11) can be written as

$$\mathcal{N}^{\text{SYK}\dagger}_{K,R\to T}[\mathcal{O}_{KR}] = \sum_{m=1}^{d_{\tilde{L}}} E_m^{\text{SYK}\dagger} \mathcal{O}_{KR} E_m^{\text{SYK}}. \tag{8.62}$$

Using this Kraus representation, it is possible to extract the very important "typical" relation from our results. Here, the "typical" means that the relation almost does not depend on the detail of a specific state $|m\rangle_{\tilde{L}}$ in the subsystem $\tilde{L}$, corresponding to a black hole microstate. First, the matrix elements (8.54) is equal to 1 and can be expressed as

$$\left\langle \hat{d}_{\tilde{L}}\right\rangle_\beta \cdot \langle 0|\mathcal{N}^{\text{SYK}\dagger}_{K,R\to T}\left[\mathcal{N}^{\text{SYK}}_{T\to K,R}[|0\rangle_T\langle 0|]\right]|0\rangle = \left\langle \hat{d}_{\tilde{L}}\right\rangle_\beta \sum_{m,n=1}^{d_{\tilde{L}}} \,_T\langle 0|E_m^{\text{SYK}\dagger} E_n^{\text{SYK}}|0\rangle_T \,_T\langle 0| E_n^{\text{SYK}} E_m^{\text{SYK}\dagger}|0\rangle_T$$

$$= \left\langle \hat{d}_{\tilde{L}}\right\rangle_\beta \sum_{m,n=1}^{d_{\tilde{L}}} \left| \,_T\langle 0|E_m^{\text{SYK}\dagger} E_n^{\text{SYK}}|0\rangle_T\right|^2, \tag{8.63}$$

and we expect the typical relation

$$_T\langle 0|E_m^{\text{SYK}\dagger} E_n^{\text{SYK}}|0\rangle_T \sim \frac{1}{\sqrt{d_{\tilde{L}} \cdot \left\langle \hat{d}_{\tilde{L}}\right\rangle_\beta}}\delta_{mn}. \tag{8.64}$$

Next, we focus on the matrix element (8.28). This matrix element is also equal to 1, and we can express the matrix element in terms of the Kraus operators,

$$\left\langle \hat{d}_{\tilde{L}}\right\rangle_\beta \cdot \langle 0|\mathcal{N}^{\text{SYK}\dagger}_{K,R\to T}\left[\mathcal{N}^{\text{SYK}}_{T\to K,R}[|0\rangle_T\langle 1|]\right]|1\rangle = \left\langle \hat{d}_{\tilde{L}}\right\rangle_\beta \sum_{m,n=1}^{d_{\tilde{L}}} \,_T\langle 0|E_m^{\text{SYK}\dagger} E_n^{\text{SYK}}|0\rangle_T \,_T\langle 1| E_n^{\text{SYK}} E_m^{\text{SYK}\dagger}|1\rangle_T. \tag{8.65}$$

By using the relation (8.64), we extract a similar relation,

$$_T\langle 1|E_m^{\text{SYK}\dagger} E_n^{\text{SYK}}|1\rangle_T \sim \frac{1}{\sqrt{d_{\tilde{L}} \cdot \left\langle \hat{d}_{\tilde{L}}\right\rangle_\beta}}\delta_{mn}. \tag{8.66}$$

Finally, the time-dependent matrix element (8.27), which almost vanishes around the

critical time t_*, can be written as

$$\left\langle \hat{d}_{\tilde{L}} \right\rangle_\beta \cdot \langle 1|\mathcal{N}_{K,R\to T}^{\text{SYK}\dagger} \left[\mathcal{N}_{T\to K,R}^{\text{SYK}}[|0\rangle_T\langle 0|]\right]|1\rangle = \left\langle \hat{d}_{\tilde{L}} \right\rangle_\beta \sum_{m,n=1}^{d_{\tilde{L}}} {}_T\langle 1|E_m^{\text{SYK}\dagger}E_n^{\text{SYK}}|0\rangle_T\langle 0|E_n^{\text{SYK}}E_m^{\text{SYK}\dagger}|1\rangle_T$$

$$= \left\langle \hat{d}_{\tilde{L}} \right\rangle_\beta \sum_{m,n=1}^{d_{\tilde{L}}} \left| {}_T\langle 1|E_m^{\text{SYK}\dagger}E_n^{\text{SYK}}|0\rangle_T \right|^2 .$$

$$(8.67)$$

From this expression, we expect the following relation and its complex conjugation,

$$_T\langle 1|E_m^{\text{SYK}\dagger}E_n^{\text{SYK}}|0\rangle_T \sim 0, \tag{8.68}$$

around and after the critical time.

Combining the above expectations, we obtain the typically expected relation[22]

$$_T\langle T|E_m^{\text{SYK}\dagger}E_n^{\text{SYK}}|T'\rangle_T \sim \frac{1}{\sqrt{d_{\tilde{L}} \cdot \left\langle \hat{d}_{\tilde{L}} \right\rangle_\beta}} \delta_{mn}\delta_{TT'} \qquad \text{for } t \gtrsim t_*, \tag{8.69}$$

which corresponds to the Knill-Laflamme condition [20].

Using this relation, the remaining matrix elements (8.57) and (8.58) are expected to behave as follows

$$\left\langle \hat{d}_{\tilde{L}} \right\rangle_\beta \cdot \langle 0|\mathcal{N}_{K,R\to T}^{\text{SYK}\dagger} \left[\mathcal{N}_{T\to K,R}^{\text{SYK}}[|1\rangle_T\langle 0|]\right]|1\rangle = \left\langle \hat{d}_{\tilde{L}} \right\rangle_\beta \sum_{m,n=1}^{d_{\tilde{L}}} {}_T\langle 0|E_m^{\text{SYK}\dagger}E_n^{\text{SYK}}|1\rangle_T\langle 0|E_n^{\text{SYK}}E_m^{\text{SYK}\dagger}|1\rangle_T$$

$$\sim 0 \qquad \text{for } t \gtrsim t_*, \tag{8.70}$$

and

$$\left\langle \hat{d}_{\tilde{L}} \right\rangle_\beta \cdot \langle 1|\mathcal{N}_{K,R\to T}^{\text{SYK}\dagger} \left[\mathcal{N}_{T\to K,R}^{\text{SYK}}[|1\rangle_T\langle 1|]\right]|1\rangle = \left\langle \hat{d}_{\tilde{L}} \right\rangle_\beta \sum_{m,n=1}^{d_{\tilde{L}}} {}_T\langle 1|E_m^{\text{SYK}\dagger}E_n^{\text{SYK}}|1\rangle_T\langle 1|E_n^{\text{SYK}}E_m^{\text{SYK}\dagger}|1\rangle_T$$

$$\sim 1. \tag{8.71}$$

These results are, of course, consistent with our original expectation (8.23), but the discussion so far using the typical relation is indirect (8.69). Nevertheless, since this typicality is strong enough for a highly chaotic theory, we expect that nearly identical results can be obtained by direct calculations of the matrix elements (8.57) and (8.58).

---

[22]Here, we check the Knill-Laflamme condition from our obtained results. However, in principle, it would be possible to investigate the Knill-Laflamme condition directly by introducing a basis [39]. It would be interesting to investigate this topic.

9 Conclusion and discussion

9.1 Conclusion

In this paper, we studied a recovery map for the Hayden-Preskill type scrambling channel $\mathcal{N}$. We showed that one can use a simplified recovery map, called Petz-lite, consisting of the adjoint channel $\mathcal{N}^\dagger$ with a suitable normalization factor. We considered two examples, the Hayden-Preskill setup and the SYK model, and showed that in both cases, the Petz-lite indeed works as a recovery map. Also, we found that if the Petz-lite for the SYK case is used to recover information of a given code subspace, it takes twice the scrambling time for the recovery. However, in the SYK model case, we did not evaluate all of the matrix elements necessary to show the recovery because of technical difficulties. Instead, we indirectly evaluated them in section 8.3. In the upcoming paper [16], we will explain their results, and also some generalizations of our results.

Let us discuss our results. First, we focus on the physical interpretation of the critical time given by twice the scrambling time, $t_* = 2t_{\text{Scram}}$, when the matrix elements give the input information, $\mathcal{R}[\mathcal{N}[\rho]] \sim \rho$. It was argued in [44] that information of a diary thrown into a black hole appears after the scrambling time. This means that, after the scrambling time, the HP scrambling channel $\mathcal{N}$ maps the diary information to Hawking radiation completely. However, even if the diary information appears in the Hawking radiation, it is difficult to get it directly since the information is uniformly embedded into the Hawking radiation. To extract the information, we need a recovery operation given by the Petz-lite $\mathcal{R} \sim \mathcal{N}^\dagger$. Since it is the adjoint of the HP channel $\mathcal{N}$, it again takes the scrambling time to apply the recovery map. Thus, in total, we need to wait for twice the scrambling time for the identity (8.23) to be satisfied.

Next, let us explain the bulk interpretation of our results[23]. The bulk interpretation comes from the island prescription [1, 2]. First, the Hayden-Preskill setup concerns post-Page time regimes. In these regimes, there is an island, which is a non-trivial entanglement wedge of Hawking radiation in the black hole interior. Thus, if one throws a diary into a black hole and waits for the scrambling time, then the diary enters the island region, implying that the diary is encoded into the Hawking radiation in a very complicated way. The mechanism that the thrown diary is encoded into the Hawking radiation corresponds to our quantum channel $\mathcal{N}$. To recover the diary information from the Hawking radiation, we need to consider the recovery operation corresponding to the map $\mathcal{R} \sim \mathcal{N}^\dagger$. The recovery map is given by the

---

[23]We note that since currently there is no clear understanding of a dual gravitational theory for a subset of the SYK Majorana fermions (or Majorana spin chain), we can not check the interpretation using the gravity side explicitly at least in the context of $\text{NAdS}_2/\text{NCFT}_1$ context. However, there are several proposals for such a gravitational treatment, e.g., in [14]. One would be able to use them to check the bulk interpretation.

adjoint channel of the quantum channel $\mathcal{N}$. In the bulk side, the action of the adjoint channel $\mathcal{N}^\dagger$ means that the "reverse" process of the original quantum channel $\mathcal{N}$[24]. More precisely, the "reverse" process is given as follows: first, we start from the output state provided by the action of the quantum channel $\mathcal{N}$, implying the diary is located on the island at some time slice Σ. The application of the adjoint channel $\mathcal{N}^\dagger$ is then interpreted as replacing the future of this time slice Σ by a white hole. Because of the replacement, the diary on the island region of the original black hole is coming out from the horizon of the white hole. Here, the reason why the white hole appears is that the adjoint channel includes the Hermitian conjugation of unitaries U (and $U^\dagger$) compared to the quantum channel $\mathcal{N}$. Thus, the diary thrown into the black hole reappears from the white hole induced by $\mathcal{N}^\dagger$. This bulk interpretation is consistent with the critical time. This is because, after throwing the diary, it takes the scrambling time for the diary to enter the island region, and in the "reverse" process, it would also take the scrambling time for the diary to go outside the island region and the horizon.

9.2 Discussion

Finally, we end with discussing some of our in-progress works and future directions:

Analysis in high temperature regime, $\beta J \ll 1$ In this paper, we have focused on the large-βJ limit (low-temperature limit) in the SYK model to make the calculation analytic and for the purpose of the generalization to a two-dimensional CFT case. In the limit, we can use emergent conformal symmetry of the SYK model, and also we would be able to use semi-classical intuition of the dual Jackiw-Teitelboim gravity, but we have a relatively weak initial entangled state $|\text{TFD}\rangle_{L,R}$ between the left and right SYK systems. Due to this weak entangled state, we would require some conditions to consider a successful recovery protocol, e.g., large-q regime. Thus, analysis without taking the large-βJ limit would be interesting. In that case, we would need to consider numerical approaches.

Direct bulk analysis and relation to other protocols In this paper, we studied the recovery protocol from the boundary CFT perspective. One would be able to consider corresponding bulk computations. Also, it would be interesting to figure out the relation between other proposed protocols, e.g., [45–48] and ours[25].

Generalization to (Holographic) CFT$_2$ and other systems While this paper focuses on the SYK model, which is a $0+1$-dimensional quantum system, it can also be interpreted as

---

[24]Here, we note that in these two processes, we need to use two different (remaining) black holes since, in defining the quantum channel, (remaining) black holes are treated as internal degrees of freedom of the quantum channel.

[25]For such protocols, one can characterize protocol by computing "price", "distance", etc. as in [14, 49, 50]. One would be able to find the relation between our results and such quantities.

a spin chain with q-body SYK interactions. Thus, we can interpret that the SYK model has a spatial direction effectively. As a result, we expect that a similar analysis can be applied to a two-dimensional CFT exhibiting chaos, e.g., two-dimensional holographic CFT. Indeed, one of the Hayden-Preskill setups in a two-dimensional holographic CFT is introduced in [37].

Also, there are other possibilities for generalizations to other systems exhibiting chaos. For example, studying the Petz-lite in a chaotic spin chain would be interesting.

Chaotic-Integrable transition In this paper, the chaotic nature is important for the simplification of the Petz map to the Petz-lite. Thus, if a system does not exhibit a chaotic nature, in other words, the system is integrable, then the Petz-lite (also the original Petz map) is not expected to work correctly. This is because, in an integrable system, the decoupling condition is not expected to hold. In the framework of the SYK model, we can prepare integrable and non-integrable (chaotic) situations by adding two-body interaction [51]. Using the setup, we would be able to study the Petz-lite.

Higher dimensional code sub-space? The SYK version of the HP setup studied in this paper treats the two-dimensional code sub-space spanned by the vacuum and the excited state. However, in a more realistic situation, one needs to deal with code sub-spaces with dimensions greater than two. For example, the interior of a black hole, when it is viewed as a code subspace embedded into the Hawking radiation, the dimension of its Hilbert space has to be large enough to accommodate a part of the semi-classical QFT degrees of freedom to have a geometric interpretation of the black hole interior[26]. To this end, one would need to consider a more complicated embedding involving, for example, states like $\psi_{i,L}\psi_{j\neq i,L}\left|\text{TFD}\right\rangle_{L,R}$. In that case, we can evaluate corresponding matrix elements in principle, but it would be difficult to evaluate them analytically since we encounter higher-point functions.

Another possibility for higher dimensional code sub-space is to consider a random embedding and the double-scaling limit. For example, we might be able to use the state $\kappa_{ij}\psi_{i,L}\psi_{j,L}\left|\text{TFD}\right\rangle_{L,R}$, where κ_{ij} is random like observables in the double-scaled SYK model [53]. In this case, by taking the double-scaling limit and using chord diagram techniques, we might be able to evaluate the resulting matrix element analytically. Also, this might open up an interesting connection between QEC in the SYK model and recent discussions of the von Neumann algebra of quantum gravity, in particular, [54].

---

[26]Of course, the interior degrees of freedom may appear to be infinite, but almost all of them can not contribute due to post-selection [52]. Even in that case, there can be degrees of freedom with Bekenstein-Hawking entropy.

Acknowledgements

A Uhlmann's monotonicity theorem

In this appendix, we review the derivation of the Uhlmann's monotonicity theorem by following the paper of Petz [21]. In subsection 4.2.2, we explained that if there exists a recovery map $\mathcal{R} : B(\mathcal{K}) \to B(\mathcal{H})$ such that $\mathcal{R}[\mathcal{N}[\rho]] = \rho$ for a quantum state $\rho \in B(\mathcal{H})$ and a given noise channel $\mathcal{N} : B(\mathcal{H}) \to B(\mathcal{K})$, the sufficiency $S(\rho||\sigma) = S(\mathcal{N}[\rho]||\mathcal{N}[\sigma])$ is satisfied for any $\rho, \sigma \in B(\mathcal{H})$. Here, the relative entropy between two density matrices $\rho, \sigma \in B(\mathcal{H})$ is defined as

$$S(\rho||\sigma) = \text{tr}[\rho(\log\rho - \log\sigma)]. \tag{A.1}$$

In section 4, we defined quantum noise channel $\mathcal{N}$ as a linear map which satisfies complete positive (CP) and trace preserving (TP). However, in order to prove Uhlmann's monotonicity theorem, we can loosen the CP condition to 2-positive for $\mathcal{N}$.

Definition 6 (course graining)**.** Let $\rho, \sigma, \tau, \upsilon$ any density matrices contained in $B(\mathcal{H})$. A linear map $\mathcal{N} : B(\mathcal{H}) \to B(\mathcal{K})$ is called course graining if $\mathcal{N}$ satisfies the following two conditions:

1. $\text{tr}[\mathcal{N}[\rho]] = \text{tr}[\rho]$ (TP).

2. If $\begin{pmatrix} \rho & \sigma \\ \tau & \upsilon \end{pmatrix}$ is positive, $\begin{pmatrix} \mathcal{N}[\rho] & \mathcal{N}[\sigma] \\ \mathcal{N}[\tau] & \mathcal{N}[\upsilon] \end{pmatrix}$ is also positive (2-positive).

Course graining $\mathcal{N}$ satisfies Schwarz inequality:

$$\mathcal{N}[\rho^\dagger\rho] \geq \mathcal{N}[\rho]\mathcal{N}[\rho]^\dagger \quad, \forall\rho \in B(\mathcal{H}). \tag{A.2}$$

Since course graining contains CPTP noise channel and essentially use Schwarz inequality for the proof of Uhlmann's monotonicity theorem, we can discuss $\mathcal{N}$ is noise channel which we explained in section 4. Adjoint of course graining is also defined as explained in section 4: adjoint $\mathcal{N}^\dagger : B(\mathcal{K}) \to B(\mathcal{H})$ is defined for $\rho \in B(\mathcal{H})$ and $\mathcal{O} \in B(\mathcal{K})$ as $\text{tr}[\mathcal{O}\mathcal{N}[\rho]] = \text{tr}[\mathcal{N}^\dagger[\mathcal{O}]\rho]$. $\mathcal{N}^\dagger$ is also a course graining and satisfies Schwarz inequality. We show the statement of Uhlmann's monotonicity theorem.

Theorem 5 (Uhlmann's monotonicity theorem)**.** *For dencity matrices $\rho, \sigma \in B(\mathcal{H})$ and course graining $\mathcal{N} : B(\mathcal{H}) \to B(\mathcal{K})$,*

$$S(\rho||\sigma) \geq S(\mathcal{N}[\rho]||\mathcal{N}[\sigma]). \tag{A.3}$$

Proof. We prove by relative modular operator method, which was developed by Araki for modular theory of operator algebra. We assume $\rho, \sigma \in B(\mathcal{H})$ invertible and define relative modular operator Δ as

$$\Delta\tau \equiv \sigma\tau\rho^{-1} \quad \tau \in B(\mathcal{H}). \tag{A.4}$$

Δ can be written as the product of positive operators L, K:

$$L\tau \equiv \sigma\tau$$
$$R\tau \equiv \tau\rho^{-1} \tag{A.5}$$
$$\Delta = LR = RL\,.$$

Since $\log\Delta$ can be evaluated as

$$\log\Delta = \log L + \log R$$
$$= \log\sigma - \log\rho\,, \tag{A.6}$$

relative entropy between ρ and σ can be evaluated as

$$S(\rho||\sigma) = \mathrm{tr}[\rho(\log\rho - \log\sigma)]$$
$$= \langle\rho^{1/2}, (\log\rho - \log\sigma)\rho^{1/2}\rangle \tag{A.7}$$
$$= -\langle\rho^{1/2}, (\log\Delta)\rho^{1/2}\rangle\,.$$

We assume $\mathcal{N}[\rho]$ is also invertible and define $\Delta_0 \in B(\mathcal{K})$ as

$$\Delta_0\mathcal{O} \equiv \mathcal{N}[\sigma]\mathcal{O}\mathcal{N}[\rho]^{-1}\,, \quad \mathcal{O} \in B(\mathcal{K})\,. \tag{A.8}$$

If we use $\log x = \int_0^\infty dt\left((1+t)^{-1} - (x+t)^{-1}\right)$ and $\mathrm{tr}[\rho] = \langle\rho^{1/2}, \rho^{1/2}\rangle = 1$, the relative entropy can be written as

$$S(\rho||\sigma) = -\langle\rho^{1/2}, (\log\Delta)\rho^{1/2}\rangle$$
$$= \int_0^\infty dt\left(\langle\rho^{1/2}, (\Delta+t)^{-1}\rho^{1/2}\rangle - (1+t)^{-1}\right) \tag{A.9}$$

Similarly $S(\mathcal{N}[\rho]||\mathcal{N}[\sigma])$ becomes

$$S(\mathcal{N}[\rho]||\mathcal{N}[\sigma]) = -\langle\mathcal{N}[\rho]^{1/2}, (\log\Delta)\mathcal{N}[\rho]^{1/2}\rangle$$
$$= \int_0^\infty dt\left(\langle\mathcal{N}[\rho]^{1/2}, (\Delta+t)^{-1}\mathcal{N}[\rho]^{1/2}\rangle - (1+t)^{-1}\right) \tag{A.10}$$

Thus if we succeed to prove

$$\langle\rho^{1/2}, (\Delta+t)^{-1}\rho^{1/2}\rangle \geq \langle\mathcal{N}[\rho]^{1/2}, (\Delta+t)^{-1}\mathcal{N}[\rho]^{1/2}\rangle \quad \forall t \in \mathbb{R}\,, \tag{A.11}$$

we can tell the theorem is true.

We define $V : B(\mathcal{K}) \to B(\mathcal{H})$ as follows:

$$V\mathcal{O}\mathcal{N}[\rho]^{1/2} \equiv \mathcal{N}^\dagger[\mathcal{O}]\rho^{1/2} \tag{A.12}$$

Then we evaluate $\|\mathcal{N}^\dagger[\mathcal{O}]\rho^{1/2}\|^2$ using Schwarz inequality as follows.

$$\begin{aligned}
\|\mathcal{N}^\dagger[\mathcal{O}]\rho^{1/2}\|^2 &= \mathrm{tr}\Big[\rho\mathcal{N}^\dagger[\mathcal{O}]^\dagger\mathcal{N}^\dagger[\mathcal{O}]\Big] \\
&\leq \mathrm{tr}\Big[\rho\mathcal{N}^\dagger[\mathcal{O}^\dagger\mathcal{O}]\Big] \\
&= \mathrm{tr}\Big[\mathcal{N}[\rho]\mathcal{O}^\dagger\mathcal{O}\Big] \\
&= \|\mathcal{O}\mathcal{N}[\rho]^{1/2}\|^2
\end{aligned} \tag{A.13}$$

In the second line, we used Schwarz inequality and in the third line, we used the definition of adjoint map. Since $\|\mathcal{N}^\dagger[\mathcal{O}]\rho^{1/2}\|^2 \leq \|\mathcal{O}\mathcal{N}[\rho]^{1/2}\|^2$, we find that V in (A.12) is a contraction. By similar evaluation, we can said that $V^\dagger\Delta V \leq \Delta_0$. Using this and the fact that $f(y) = (y+t)^{-1}$ decreases monotonically, we can show the inequality:

$$(\Delta_0 + t)^{-1} \leq (V^\dagger\Delta V + t)^{-1} \leq V^\dagger(\Delta + t)^{-1}V. \tag{A.14}$$

If we apply $\mathcal{O} = I$ to (A.12), we get $V\mathcal{N}[\rho]^{1/2} = \rho^{1/2}$. Using these relations, we can calculate as

$$\begin{aligned}
\langle\rho, (\Delta + t)^{-1}\rho\rangle &= \langle V\mathcal{N}[\rho]^{1/2}, (\Delta + t)^{-1}V\mathcal{N}[\rho]^{1/2}\rangle \\
&= \langle\mathcal{N}[\rho]^{1/2}.V^\dagger(\Delta + t)^{-1}V\mathcal{N}[\rho]^{1/2}\rangle \\
&\geq \langle\mathcal{N}[\rho]^{1/2}, (\Delta_0 + t)^{-1}\mathcal{N}[\rho]^{1/2}\rangle
\end{aligned} \tag{A.15}$$

We succeeded to prove the inequality (A.11) and thus we proved Uhlmann's monotonicity theorem. $\qquad\square$

Next, we focus on the condition for equality. The necessary and sufficient condition of the equality of the theorem $S(\rho||\sigma) = S(\mathcal{N}[\rho]||\mathcal{N}[\sigma])$ is

$$\langle\mathcal{N}[\rho]^{1/2}, V^\dagger(\Delta + t)^{-1}V\mathcal{N}[\rho]^{1/2}\rangle = \langle\mathcal{N}[\rho]^{1/2}, (\Delta_0 + t)^{-1}\mathcal{N}[\rho]^{1/2}\rangle \quad \forall t \in \mathbb{R}. \tag{A.16}$$

This comes from the equality of the second inequality of (A.14):

$$V^\dagger(\Delta + t)^{-1}V = (\Delta_0 + t)^{-1} \tag{A.17}$$

By acting $\mathcal{N}[\rho]^{1/2}$ to the right and using $V\mathcal{N}[\rho]^{1/2} = \rho^{1/2}$ which we showed above,

$$V^\dagger(\Delta + t)^{-1}\rho^{1/2} = (\Delta_0 + t)^{-1}\mathcal{N}[\rho]^{1/2}, \quad \forall t \in \mathbb{R}. \tag{A.18}$$

By differentiating this in terms of t,

$$V^\dagger(\Delta + t)^{-2}\rho^{1/2} = (\Delta_0 + t)^{-2}\mathcal{N}[\rho]^{1/2}, \quad \forall t \in \mathbb{R}. \tag{A.19}$$

By using these, we can evaluate as

$$
\begin{aligned}
\|V^\dagger(\Delta+t)^{-1}\rho^{1/2}\|^2 &= \langle(\Delta_0+t)^{-1}\mathcal{N}[\rho]^{1/2},(\Delta_0+t)^{-1}\mathcal{N}[\rho]^{1/2}\rangle \\
&= \langle(\Delta_0+t)^{-2}\mathcal{N}[\rho]^{1/2},\mathcal{N}[\rho]^{1/2}\rangle \\
&= \langle V^\dagger(\Delta+t)^{-2}\rho^{1/2},\mathcal{N}[\rho]^{1/2}\rangle \\
&= \langle(\Delta+t)^{-1}\rho^{1/2},(\Delta+t)^{-1}V\mathcal{N}[\rho]^{1/2}\rangle \\
&= \|(\Delta+t)^{-1}\rho^{1/2}\|^2 .
\end{aligned}
\tag{A.20}
$$

If we write $\xi=(\Delta+t)^{-1}\rho^{1/2}$, $\xi^\dagger V V^\dagger\xi = \|V^\dagger\xi\|^2 = \|\xi\|^2 = \xi^\dagger\xi$ is satisfied, so $VV^\dagger\xi = \xi$. Therefore, we get

$$
VV\dagger(\Delta+t)^{-1}\rho^{1/2} = (\Delta+t)^{-1}\rho^{1/2} .
\tag{A.21}
$$

Applying this to (A.18), we obtain

$$
\begin{aligned}
V(\Delta_0+t)^{-1}\mathcal{N}[\rho]^{1/2} &= VV^\dagger(\Delta+t)^{-1}\rho^{1/2} \\
&= (\Delta+t)^{-1}\rho^{1/2} .
\end{aligned}
\tag{A.22}
$$

By Stone-Weierstrass approximation, we can use $Vf(\Delta_0)\mathcal{N}[\rho]^{1/2} = f(\Delta)\rho^{1/2}$ for some function f. We use this for the function $f(x)=x^{it}$ and get

$$
V\Delta_0^{it}\mathcal{N}[\rho]^{1/2} = \Delta^{it}\rho^{1/2} .
\tag{A.23}
$$

By using (A.12), the left side becomes

$$
V\Delta_0^{it}\mathcal{N}[\rho]^{1/2} = \mathcal{N}^\dagger[\Delta_0^{it}]\rho^{1/2} .
\tag{A.24}
$$

Thus we get the relation

$$
\mathcal{N}^\dagger[\Delta_0^{it}] = \Delta^{it} .
\tag{A.25}
$$

Since $\Delta = \sigma\rho^{-1}$ and $\Delta_0 = \mathcal{N}[\sigma]\mathcal{N}[\rho]^{-1}$, we have derived the relation (4.64) explained in section 4.2.2:

$$
\mathcal{N}^\dagger\left[\mathcal{N}[\sigma]^{it}\mathcal{N}[\rho]^{-it}\right] = \sigma^{it}\rho^{-it} .
\tag{A.26}
$$

We can summarize the result as the following theorem.

Theorem 6 (The condition for equality of Uhlmann's monotonicity theorem)**.** *Let $\mathcal{N}:$ $B(\mathcal{H})\to B(\mathcal{K})$ some course graining and let $\rho,\sigma\in B(\mathcal{H})$ and $\mathcal{N}[\rho],\mathcal{N}[\sigma]\in B(\mathcal{K})$ be invertible density matrices. The necessary and sufficient condition to satisfy $S(\rho||\sigma) = S(\mathcal{N}[\rho]||\mathcal{N}[\sigma])$ is the following equivalent conditions:*

1. *$\mathcal{N}^\dagger\left[\mathcal{N}[\sigma]^{it}\mathcal{N}[\rho]^{-it}\right] = \sigma^{it}\rho^{-it}, \quad \forall t\in\mathbb{R}$*

2. *$\mathcal{N}^\dagger\left(\log\mathcal{N}[\rho]-\log\mathcal{N}[\sigma]\right) = \log\rho-\log\sigma$*

We can derive the second condition by differentiating in terms of t and setting $t = 0$. In subsection 4.3.2, we constructed the Petz map by using this relation (A.26). Thus we can tell that if sufficiency is satisfied, the recovery is possible by constructing the Petz map. We showed that if recovery is possible sufficiency is satisfied in 4.2.2. We have succeeded to prove the both directions, so here we end this appendix.

B JT gravity and Schwarzian action

In this appendix, we explain Jackiw-Teitelboim (JT) gravity model briefly from introducing the action to deriving thermal entropy with Schwarzian action, following the paper of Sárosi [33]. It is two-dimensional dilaton gravity, which exhibits AdS_2 geometry. Magnetically charged Reisner-Nordström solution in four dimension:

$$
\begin{aligned}
ds^2 &= -\frac{(r-r^+)(r-r^-)}{r^2}dt^2 + \frac{r^2}{(r-r^+)(r-r^-)}dr^2 + r^2 d\Omega_2^2\,, \\
F &= Q\sin\theta d\phi \wedge d\theta\,, \\
r^\pm &= Ql_P + El_P^2 \pm \sqrt{2QEl_P + E^2 l_P^4}
\end{aligned}
\tag{B.1}
$$

is the classical solution of Einstein-Maxwell action

$$
S_{Einstein-Maxwell} \sim \frac{1}{l_P^2}\int d^4x\sqrt{-g}\left(R_g - \frac{l_P^2}{4}F_{\mu\nu}F^{\mu\nu}\right)\,.
\tag{B.2}
$$

R_g is Ricci scalar of the metric $g_{\mu\nu}$ and $F_{\mu\nu}$ is the field strength of Maxwell field. $d\Omega_2^2$ is the line element of the two-sphere. Q is the magnetic charge and $l_P = \sqrt{G_N}$ is the Planck length and E is the excitation energy:

$$
E = M - \frac{Q}{l_P}\,.
\tag{B.3}
$$

When this black hole is extremal, i.e. $E = 0$, if we consider near horizon limit, the metric ds^2 becomes $AdS_2 \times S^2$. To see this, we define the new coodinate

$$
z = \frac{Q^2 l_P^2}{r - r^+}
\tag{B.4}
$$

and take the limit $l_P \to 0$ with z fixed in order to consider the near horizon limit $r \to r^+$. In this limit, the metric becomes

$$
ds^2 \approx l_P^2 Q^2\left(\frac{-dt^2 + dz^2}{z^2} + d\Omega_2^2\right)\,.
\tag{B.5}
$$

AdS_2 metric is written as

$$
\begin{aligned}
ds^2 &= l_{AdS}^2 \frac{-dt^2 + dz^2}{z^2} \quad \text{(Poincaré)} \\
&= \frac{-4l_{AdS}du^+du^-}{\sin^2(u^+ - u^-)} \quad u^\pm = \arctan(t \pm z) \quad \text{(Global light cone)} \\
&= l_{AdS}^2 \frac{-d\nu^2 + d\sigma^2}{\sin^2\sigma} \quad u^\pm = \frac{\nu \pm \sigma}{2} \quad \text{(Global)}\,.
\end{aligned}
\tag{B.6}
$$

l_{AdS} is the curvature radius and it corresponds to l_P as $l_{AdS} = l_P Q$. In Rindler coordinate (ρ, τ), which corresponds to Poincaré coordinate (t, z) as

$$
z \pm t = \frac{(1 \pm \cosh\rho)e^{\tau/2} - \sinh\rho\, e^{-\tau/2}}{(1 \pm \cosh\rho)e^{\tau/2} + \sinh\rho\, e^{-\tau/2}}\,,
\tag{B.7}
$$

we can write the metric as $ds^2 = l_{\text{AdS}}^2 (d\rho^2 - \sinh^2 \rho \, d\tau^2)$.

Static and spherically symmetric solution of $S_{Einstein-Maxwell}$ is obtained by imposing the ansatz

$$ds^2 = h_{ij} dx^i dx^j + e^{2\psi(r,t)} d\Omega^2 \quad i,j = 1,2$$

$$F = Q \sin \theta d\phi \wedge d\theta$$

(B.8)

and restricting to two-dimensional $(x^1, x^2) = (t, r)$ plane, $S_{Einstein-Maxwell}$ reduces to

$$
\begin{aligned}
S_{Einstein-Maxwell} &\to \frac{4\pi}{l_P^2} \int dt dr \sqrt{-h} \left[e^{2\psi} \left(R_h + 2(\partial\psi)^2 \right) + 2 - \frac{1}{2} e^{-2\psi} Q^2 l_P^2 \right] \\
&= \frac{4\pi}{l_P^2} \int dt dr \sqrt{-h} \left[\Phi^2 R_h + 2(\partial\Phi)^2 + 2 - \frac{1}{2} \Phi^{-2} Q^2 l_P^2 \right],
\end{aligned}
$$

(B.9)

where we set $\Phi = e^\psi$. This is the special instance of general dilaton gravity model:

$$I = \frac{1}{16\pi G_N} \int d^2 x \sqrt{-h} \left[\Phi^2 R_h + \lambda(\partial\Phi)^2 - U\left(\frac{\Phi^2}{d^2}\right) \right]$$

(B.10)

where U is an arbitrary scalar potential and λ is dimensionless coefficient for kinetic term. Φ^2 is called a dilaton field. When the dilaton is constant, this action exhibits the solution of AdS_2. Setting the dilaton to constant $\Phi^2 = \phi_0$ and extremizing the action, we obtain the relation between $l_{\text{AdS}}, d, \phi_0$:

$$\frac{2}{l_{\text{AdS}}^2} + \frac{1}{d^2} U'\left(\frac{\phi_0}{d^2}\right) = 0.$$

(B.11)

d is the extremal length scale, which is $d = l_P Q$ for Reisner-Nordström example. It relates to UV length scale of AdS_2. We consider a small deformation for the dilaton to consider some dynamics:

$$\Phi^2 = \phi_0 + \phi \quad (|\phi| \ll 1)$$

(B.12)

and set cutoff on $z = \epsilon$

$$\frac{\phi(\epsilon)}{d^2} \equiv \eta \ll 1$$

(B.13)

since in Poincaré coodinate the dilaton expected to diverge as $\phi \sim \frac{1}{z}$ $(z \to 0)$. We can expand the potential $U\left(\frac{\Phi^2}{d^2}\right)$ around $\Phi^2 = \phi_0$:

$$
\begin{aligned}
I = \frac{1}{16\pi G_N} \Bigg[&\int d^2 x \sqrt{-h} \left(\phi_0 R_h - U\left(\frac{\phi_0}{d^2}\right) \right) \\
&+ \int d^2 x \sqrt{-h} \, \phi \left(R_h + \frac{2}{l_{\text{AdS}}^2} \right) \\
&+ \int d^2 x \sqrt{-h} \frac{\lambda}{4} \frac{(\partial\phi)^2}{\phi_0 + \phi} \Bigg] + \mathcal{O}(\eta^2).
\end{aligned}
$$

(B.14)

We used (B.11) in the second line. The first line is Einstein gravity in two dimensions. IR divergent volume term $\int d^2 x \sqrt{-h} U(\phi_0/d^2)$ can be removed by local counter term. Adding

boundary term, this gives Euler character because of Gauss-Bonnet theorem and it becomes topologically invariant. The second term is the action of JT gravity and gives dynamics. The third term can be ignored since it is $\mathcal{O}(\eta^2)$. $\phi \sim (length)^2$ should be proportional to $G_N = l_P^2$ and E, so ϕ is expected to be $\phi \sim \frac{l_P^2 l_{AdS}^2 E}{z}$. $\frac{(\partial \phi)^2}{\phi_0 + \phi}$ is evaluated as

$$\frac{(\partial \phi)^2}{\phi_0 + \phi} \sim \frac{g^{zz}\left(\frac{l_P^2 l_{AdS}^2 E}{z^2}\right)}{\phi_0 + \phi} = \frac{\phi^2}{l_{AdS}} \frac{1}{\phi_0 + \phi} \tag{B.15}$$

where we used $g^{zz} = z^2/l_{AdS}^2$. If we set $\phi_0 = d^2$ and use (B.11),

$$\frac{(\partial \phi)^2}{\phi_0 + \phi} \sim \frac{|U'(1)|}{1 + \frac{\phi}{d^2}} \left(\frac{\phi}{d^2}\right)^2 = |U'(1)|\eta^2(1 + \mathcal{O}(\eta)) = \mathcal{O}(\eta^2). \tag{B.16}$$

After removing the volume term and setting $l_{AdS}^{-2} = 1$, the action governing the dynamics inside the cutoff surface is written as follows.

$$I = \frac{\phi_0}{16\pi G_N} \int d^2x \sqrt{-h}\, R_h + \frac{1}{16\pi G_N} \int d^2x \sqrt{-h}\, \phi\, (R_h + 2) \tag{B.17}$$

Next, we discuss Euclidean JT gravity to consider boundary theory. In Euclidean signature $t_{Lorentz} = -it_{Euclidean}$, $\tau_{Lorentz} = -i\tau_{Euclidean}$, AdS_2 is the hyperbolic disk:

$$\begin{aligned} ds^2 &= \frac{dt^2 + dz^2}{z^2} \quad \text{(Poincaré)} \\ &= d\rho^2 + \sinh^2 \rho d\tau^2 \quad \text{(Rindler)} \end{aligned} \tag{B.18}$$

Euclidean action is

$$\begin{aligned} I = &-\frac{\phi_0}{16\pi G_N} \left[\int_{\mathcal{M}} d^2x \sqrt{h} R_h + 2 \int_{\partial \mathcal{M}} K\right] \\ &- \frac{1}{16\pi G_N} \left[\int_{\mathcal{M}} d^2x \sqrt{h}\, \phi(R_h + 2) + 2 \int_{\partial \mathcal{M}} \phi_b K\right]. \end{aligned} \tag{B.19}$$

We added the Gibbons-Hawking-York term, which is necessary to impose Dirichlet boundary condition on the boundary of the manifold $\mathcal{M}$. K is the extrinsic curvature $K = -\frac{h(T, \nabla_T n)}{h(T, T)}$. The boundary condition of ϕ is given by ϕ_b. The first line is topological Einstein-Hilbert term. The second line is the dynamical part. We consider boundary time u and the boundary curve $u \mapsto (t(u), z(u))$. Unlike ordinary AdS/CFT, we impose dynamical UV cutoff to the induced metric of the boundary curve:

$$g|_{bdy} = \frac{1}{\epsilon^2} \quad (\epsilon \ll 1). \tag{B.20}$$

This condition implies the relation between parameters as

$$z = \epsilon \sqrt{(t')^2 + (z')^2} = \epsilon t' + \mathcal{O}(\epsilon^3). \tag{B.21}$$

Variation in ϕ leads to $R = -2$, which tells that the metric is AdS$_2$. Then we study the boundary term since it breaks $SL(2, \mathbb{R})$ symmetry of the reparametrization of the boundary time. The boundary term is

$$
\begin{aligned}
I_{\text{bdy}} &= -\frac{1}{8\pi G_N} \int_{\partial \mathcal{M}} \phi_b K \\
&= -\frac{1}{8\pi G_N} \int \frac{du}{\epsilon^2} \phi_r(u) K \,.
\end{aligned}
\tag{B.22}
$$

In the second line, we used (B.20) and set the boundary condition for the dilaton as

$$
\phi_b = \frac{\phi_r(u)}{\epsilon}
\tag{B.23}
$$

where $\phi_r(u)$ behaves like the source for the operator in ordinary AdS/CFT. Calculating the extrinsic curvature K by using $T^a = (t', z')$, $n^a = \frac{z}{\sqrt{t'^2 + z'^2}}(-z', t')$,

$$
\begin{aligned}
K &= \frac{t'(t'^2 + z'^2 + z'z'') - zz't''}{(t'^2 + z'^2)^{3/2}} \\
&= 1 + \text{Sch}[t(u), u]\epsilon^2 + \mathcal{O}(\epsilon^4)
\end{aligned}
\tag{B.24}
$$

where we again met the Schwarzian derivative:

$$
\text{Sch}[t(u), u] = \frac{2t't''' - 3t''^2}{2t'^2} \,.
\tag{B.25}
$$

We obtain the Schwarzian action

$$
I_{\text{Sch}} = -\frac{1}{8\pi G_N} \int du \, \phi_r(u) \, \text{Sch}[t(u), u] \,.
\tag{B.26}
$$

We assume that the boundary value of the dilaton is constant: $\phi_r(u) = \bar{\phi}_r$. We want the solution of this action. The equation of motion is

$$
\frac{\text{Sch}[t, u]'}{t'} = 0 \,.
\tag{B.27}
$$

We should look for the non-constant function which makes the Schwarzian constant. Using the relation $\text{Sch}[f \circ g, t] = g'^2 \text{Sch}[f, g] + \text{Sch}[g, t]$ and setting the boundary limit of the relation between Poincaré to Rindler (B.7) $t(u) = \tan\frac{\tau(u)}{2}$, we obtain

$$
\text{Sch}[t, u] = \text{Sch}[\tau, u] + \frac{1}{2}\tau'^2 \,.
\tag{B.28}
$$

If $\tau(u)$ is linear, the Schwarzian is constant and that is the solution. Since Euclidean Rindler τ has 2π periodicity, so we get the solution:

$$
\tau(u) = \frac{2\pi}{\beta} u \,.
\tag{B.29}
$$

Plugging this solution back into the Schwarzian action, we obtain

$$I_{\text{Sch}} = -2\pi^2 C \frac{1}{\beta}, \quad C = \frac{\bar{\phi}_r}{8\pi G_N}. \tag{B.30}$$

When $G_N \to 0$, boundary partition function is $Z(\beta) = e^{-I_{\text{grav}}}$. Since topological Einstein-Hilbelt term gives ground entropy $-S_0$, total on-shell action becomes

$$I_{\text{grav}} = -S_0 - 2\pi^2 C \frac{1}{\beta}. \tag{B.31}$$

Thus we get the thermal entropy of near extremal black hole as

$$S_{\text{th}} = (1 - \beta \partial_\beta) \log Z(\beta) = S_0 + 4\pi^2 \frac{C}{\beta}. \tag{B.32}$$

We find that this is proportional to black hole temperature.

C Derivation of the Petz lite using the Kraus representation

In this appendix, we derive the Petz-lite with a different normalization factor based on paper [22]. See, e.g., §10.3 of [19] for related reviews.

We start with the Kraus representation of the HP channel (5.3). The Kraus representation can be introduced by expressing the trace as

$$
\begin{aligned}
\mathcal{N}_{T \to D,B}\left[\rho_T\right] &= \mathrm{tr}_C\left[(U_{T,A \to C,D} \otimes I_B)(\rho_T \otimes |\mathrm{EPR}\rangle_{A,B}\langle\mathrm{EPR}|)(U_{T,A \to C,D}^\dagger \otimes I_B)\right] \\
&= \sum_{m=1}^{d_C} {}_C\langle m|(U_{T,A \to C,D} \otimes I_B)\,|\mathrm{EPR}\rangle_{A,B}\,\rho_{T\,A,B}\,\langle\mathrm{EPR}|\,(U_{T,A \to C,D}^\dagger \otimes I_B)|m\rangle_C \\
&= \sum_{m=1}^{d_C} E_m \rho_T E_m^\dagger,
\end{aligned}
\tag{C.1}
$$

where $|m\rangle_C$ is an orthonormal basis of subsystem C, and E_m is the Kraus operator defined by

$$
E_m = {}_C\langle m|\,(U_{T,A \to C,D} \otimes I_B)\,|\mathrm{EPR}\rangle_{A,B}.
\tag{C.2}
$$

Here, we note that since the state $|m\rangle_C$ is a basis state of the remaining black hole C. We also note that the adjoint HP channel is expressed in terms of the Kraus operators,

$$
\mathcal{N}\left[\mathcal{O}\right] = \sum_{m=1}^{d_C} E_m^\dagger \mathcal{O} E_m.
\tag{C.3}
$$

Using this Kraus operator, let us investigate the Knill-Laflamme condition [20],

$$
P_{code} E_m^\dagger E_n P_{code} = \alpha_{mn} P_{code} \quad \left(\alpha_{mn} = \alpha_{nm}^* \in \mathbb{C}\,\text{with}\,\sum_{m=1}^{d_C} \alpha_{mm} = 1\right), \text{for } \forall m,n = 1,\cdots,d_C.
\tag{C.4}
$$

where P_{code} is a projection operator onto a code subspace in general, but in our setup, P_{code} is assumed to be just given by the identity operator $P_{code} = I_T$, since all input states should be recoverable under the Hayden-Preskill setup. If this condition holds, we can construct a recovery map[27].

Under Haar random averaging, we can easily evaluate the Knill-Laflamme condition from the expression (C.2) and Haar average (5.17),

$$
\overline{E_m^\dagger E_n} = \frac{1}{d_C}\delta_{mn} I_T.
\tag{C.5}
$$

This result appears to imply that the Knill-Laflamme condition holds *always* under the averaging, but this is not correct. This is because, even if the Knill-Laflamme condition is satisfied,

---

[27]See, e.g., §10.3, in particular, theorem 10.1, of [19] for the review.

higher moments of the Knill-Laflamme condition, e.g., $\overline{\left|P_{code}E_m^\dagger E_n P_{code}\right|^2}$, might not hold due to contributions coming from Weingarten calculus. We can see their contributions by directly evaluating the second moment[28],

$$\overline{\left|P_{code}E_m^\dagger E_n P_{code}\right|^2} \approx \frac{1}{(d_C)^2} \cdot I_T \left[\delta_{mn} + \frac{d_T}{d_D d_B}\right] \tag{C.6}$$

where we used the known result (5.20) with large-d approximation. Thus, when we do not have enough Hawking radiation D, B compared to the diary T, that is, $d_D d_B \lesssim d_T$, we can not ignore the second term, implying the breakdown of the Knill-Laflamme condition. On the other hand, in the opposite limit $d_D d_B \gg d_T$, where we have enough Hawking radiation, we can ignore the second term, and we get the Knill-Laflamme condition. We note that this is consistent with the decoupling condition (5.2), since the unitarity means the relation

$$\frac{d_T}{d_D d_B} = \frac{1}{d_C} \cdot \left(\frac{d_T}{d_D}\right)^2, \tag{C.7}$$

and the factor $(d_T/d_D)^2$ gives an upper bound of the decoupling condition (5.2).

Next, we construct a recovery map for the HP quantum channel. With the Knill-Laflamme condition in mind, we consider the following map, which is equal to the adjoint HP channel up to the overall factor d_C,

$$\mathcal{R}[\mathcal{O}] := d_C \sum_{m=1}^{d_C} E_m^\dagger \mathcal{O} E_m = d_C \mathcal{N}^\dagger [\mathcal{O}]. \tag{C.8}$$

Under the Haar random average, this map gives

$$
\begin{aligned}
\overline{\mathcal{R}[\mathcal{N}[\rho_T]]} &= d_C \sum_{m,n=1}^{d_C} \overline{E_m^\dagger E_n \rho_T E_n^\dagger E_m} \\
&\approx d_C \sum_{m,n=1}^{d_C} \left[\overline{E_m^\dagger E_n} \rho_T \overline{E_n^\dagger E_m} + \overline{E_m^\dagger E_n \rho_T E_n^\dagger E_m}\right] \\
&= d_C \sum_{m,n=1}^{d_C} \frac{1}{(d_C)^2} \left[\delta_{mn} \rho_T + \frac{\operatorname{tr}[\rho_T]}{d_D d_B} I_T\right] \\
&= \rho_T + \left(\frac{d_T}{d_D}\right)^2 \cdot \frac{1}{d_T} I_T,
\end{aligned} \tag{C.9}
$$

where in the second line, we used the fact that in the large-Hilbert space dimension limit, Weingarten calculus reduces to Wick calculus, and in the final line, we used $\operatorname{tr}\rho_T = 1$ and the relation $d_T d_B = d_C d_D$. In the third line, we encountered the Knill-Laflamme condition

---

[28]See also [55] for related discussions.

for the first term (C.5), and the second term disturbs the Knill-Laflamme condition. These two terms in the third line correspond to the first and second terms in (C.6). Thus, under the situation $d_B d_D \gg d_T$ where the Knill-Laflamme condition holds (approximately), we can ignore the second term of the above result, implying that the map (C.8) works as a recovery map. This is a quantum information theoretic derivation of the Petz-lite. However, we note that the recovery map here is a little bit different from the one (5.11) up to the overall factor, but the difference almost vanishes when the condition $d_B d_D \gg d_T$ is satisfied.

Finally, we end this appendix by giving the connection between the Petz map and the Petz-lite in terms of the Kraus operator and the Knill-Laflamme condition. Generally, since the coefficients (α_{mn}) is Hermitian, we can diagonalize the Knill-Laflamme condition by some unitary (U_{mn}) as follows [19],

$$P_{code} F_m^\dagger F_n P_{code} = \lambda_m \delta_{mn} P_{code} \quad \left(\lambda_m \in \mathbb{R}, \text{with} \sum_{m=1}^{d_C} \lambda_m = 1, \lambda_m > 0 \right), \text{ for } \forall m, n = 1, \cdots, d_C,$$
(C.10)

where $F_m = \sum_n U_{mn} E_n$ is the newly defined Kraus operator. Using this Kraus operator, one can define the following map

$$\mathcal{R}[\mathcal{O}] := \sum_{m=1}^{d_C} \frac{1}{\lambda_m} P_{code} F_m^\dagger \mathcal{O} F_m P_{code}.$$
(C.11)

This map can also be expressed in terms of the original quantum channel by introducing some full rank reference state σ as follows [22]

$$\mathcal{R}[\mathcal{O}] = \sigma^{1/2} \mathcal{N}^\dagger \left[(\mathcal{N}[\sigma])^{-1/2} \mathcal{O} (\mathcal{N}[\sigma])^{-1/2} \right] \sigma^{1/2},$$
(C.12)

and this is exactly the Petz map. In the recovery map (C.11), the factor λ_m prevents us from directly giving the adjoint channel $\mathcal{N}^\dagger$, and we need to introduce the curious factors $(\mathcal{N}[\sigma])^{-1/2}$ and $\sigma^{1/2}$. However, for the case where $\lambda_m = 1/d_C$ $(m = 1, \cdots, d_C)$, one can consider the map (C.8) instead of the above map. As we have seen, the Haar random case with the Knill-Laflamme condition (C.5) is certainly this case.
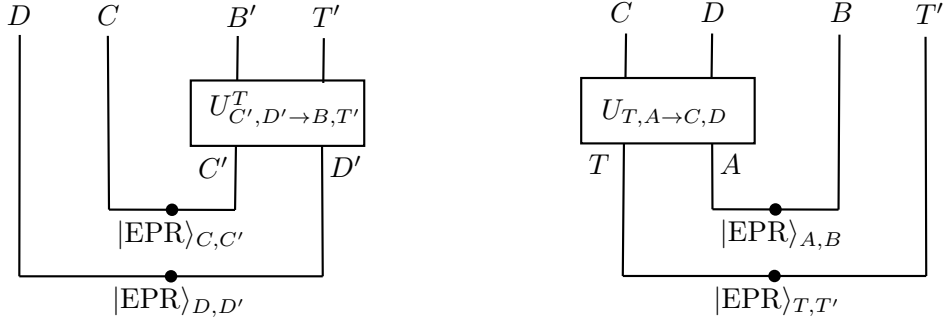
Figure 32: Diagrams representing left and right hand sides of the relation (5.54). **Left**: The left hand side of the relation. **Right**: The right hand side of the relation. The left and right diagrams are equivalent.

D Operator Transpose for the EPR state

In this appendix, we derive the relation (5.54) algebraically. We can show the relation directly as follows;

$$
\begin{aligned}
&U_{C',D'\to B,T'}^{T}\left|\mathrm{EPR}\right\rangle_{C,C'}\otimes\left|\mathrm{EPR}\right\rangle_{D,D'}\\
&=\left(I_{C}\otimes I_{D}\otimes U_{C',D'\to B,T'}^{T}\right)\left|\mathrm{EPR}\right\rangle_{C,C'}\otimes\left|\mathrm{EPR}\right\rangle_{D,D'}\\
&=\frac{1}{\sqrt{d_{C}d_{D}}}\sum_{\tilde{C}=1}^{d_{C}}\sum_{\tilde{D}=1}^{d_{D}}\left|\tilde{C},\tilde{D}\right\rangle_{C,D}\otimes\left(U_{C',D'\to B,T'}^{T}\left|\tilde{C},\tilde{D}\right\rangle_{C',D'}\right)\\
&=\frac{1}{\sqrt{d_{C}d_{D}}}\sum_{\tilde{C}=1}^{d_{C}}\sum_{\tilde{D}=1}^{d_{D}}\sum_{\tilde{B}=1}^{d_{B}}\sum_{\tilde{T}=1}^{d_{T}}\left|\tilde{C},\tilde{D}\right\rangle_{C,D}\otimes\left|\tilde{B},\tilde{T}\right\rangle_{B,T'}\cdot{}_{B,T'}\!\left\langle\tilde{B},\tilde{T}\right|U_{C',D'\to B,T'}^{T}\left|\tilde{C},\tilde{D}\right\rangle_{C',D'}\\
&=\frac{1}{\sqrt{d_{C}d_{D}}}\sum_{\tilde{C}=1}^{d_{C}}\sum_{\tilde{D}=1}^{d_{D}}\sum_{\tilde{B}=1}^{d_{B}}\sum_{\tilde{T}=1}^{d_{T}}\left|\tilde{C},\tilde{D}\right\rangle_{C,D}\otimes\left|\tilde{B},\tilde{T}\right\rangle_{B,T'}\cdot{}_{C,D}\!\left\langle\tilde{C},\tilde{D}\right|U_{A,T\to C,D}\left|\tilde{B},\tilde{T}\right\rangle_{A,T}\\
&=\frac{1}{\sqrt{d_{B}d_{T}}}\sum_{\tilde{B}=1}^{d_{B}}\sum_{\tilde{T}=1}^{d_{T}}\left(U_{A,T\to C,D}\left|\tilde{B},\tilde{T}\right\rangle_{A,T}\right)\otimes\left|\tilde{B},\tilde{T}\right\rangle_{B,T'}\\
&=\left(U_{A,T\to C,D}\otimes I_{B}\otimes I_{T'}\right)\left|\mathrm{EPR}\right\rangle_{A,B}\otimes\left|\mathrm{EPR}\right\rangle_{T,T'}\\
&=U_{A,T\to C,D}\left|\mathrm{EPR}\right\rangle_{A,B}\otimes\left|\mathrm{EPR}\right\rangle_{T,T'}\,,
\end{aligned}
$$
(D.1)

where in the fifth equality, we used the unitarity condition of the Hilbert space dimensions $d_{T}\,d_{B}=d_{C}\,d_{D}$. $\qquad\square$

The above relation implies that the left and right diagrams in figure 32 are equivalent.

E   Convention in the SYK Hayden-Preskill protocol

In this appendix, we gather some important definitions and conventions that we use in section 8.

Majorana SYK fermions

- Anti-commutation relation

$$\{\psi_i, \psi_j\} = 2\delta_{ij}$$

- The unitary time evolution operator

$$U_\alpha = U_\alpha(t) = \exp(itH_\alpha) \quad (\alpha = L, R)$$

- Positive direction of time evolutions in left and right SYK systems (in Lorentzian signature)

$$\psi_{i,L}(t) \equiv U_L \psi_{i,L}(0) U_L^\dagger = e^{itH_L} \psi_{i,L}(0) e^{-itH_L},$$

$$\psi_{i,R}(t) \equiv U_R^\dagger \psi_{i,R}(0) U_R = e^{-itH_R} \psi_{i,R}(0) e^{itH_R},$$

which can be written as

$$\psi_{i,\alpha}(t) = \Delta_L^{-i\frac{t}{\beta}} \psi_{i,\alpha}(0) \Delta_L^{i\frac{t}{\beta}} = \Delta_R^{i\frac{t}{\beta}} \psi_{i,\alpha}(0) \Delta_R^{-i\frac{t}{\beta}} \quad (\alpha = L, R), \tag{E.1}$$

where $\Delta_L = \Delta_R^{-1}$ is the modular operator defined by

$$\Delta_L = \rho_L \otimes \rho_R^{-1} = e^{-K_L} \otimes e^{K_R} = e^{-(K_L - K_R)}, \qquad K_\alpha \equiv \beta H_\alpha \quad (\alpha = L, R). \tag{E.2}$$

Here ρ_α $(\alpha = L, R)$ is defined by

$$\rho_L = \mathrm{tr}_R \left[|\mathrm{TFD}\rangle_{L,R} \langle \mathrm{TFD}| \right], \quad \rho_R = \mathrm{tr}_L \left[|\mathrm{TFD}\rangle_{L,R} \langle \mathrm{TFD}| \right] \tag{E.3}$$

In the Euclidean signature, one can rewrite the above formal formula as

$$\psi_{i,\alpha}(\tau) = \Delta_L^{\frac{\tau}{\beta}} \psi_{i,\alpha}(0) \Delta_L^{-\frac{\tau}{\beta}} \quad (\alpha = L, R), \tag{E.4}$$

and recover the Lorentzian operator by the analytic continuation $\tau \to -it$.

- Euclidean regularization parametrized by the cutoff δ

$$\psi_{i,L}(t + i\delta) \equiv e^{i(t+i\delta)H_L} \psi_{i,L}(0) e^{-i(t+i\delta)H_L} = e^{(-\delta+it)H_L} \psi_{i,L}(0) e^{(\delta-it)H_L} \tag{E.5}$$

This regularized operator is related to the Euclidean evolved operator (E.4) by continuation $\tau \to -it + \delta$.

SYK Hayden-Preskill channel

- SYK Hayden-Preskill channel (8.10)

$$\mathcal{N}_{T \to K,R}^{\mathrm{SYK}}[\rho_T] := \mathrm{tr}_{\tilde{L}} \left[U_L V_{T,L \to L} \left(\rho_T \otimes |\mathrm{TFD}\rangle_{L,R} \langle \mathrm{TFD}| \right) V_{T,L \to L}^\dagger U_L^\dagger \right]$$

- Adjoint SYK Hayden-Preskill channel (8.11)

$$\mathcal{N}_{K,R \to T}^{\mathrm{SYK}\dagger}[\mathcal{O}_{KR}] := \mathrm{tr}_{L,R} \left[|\mathrm{TFD}\rangle_{L,R} \langle \mathrm{TFD}| \left(V_{L \to T,L}^\dagger U_L^\dagger \mathcal{O}_{KR} U_L V_{L \to T,L} \right) \right]$$
$$= {}_{L,R} \langle \mathrm{TFD}| \left(V_{L \to T,L}^\dagger U_L^\dagger \mathcal{O}_{KR} U_L V_{L \to T,L} \right) |\mathrm{TFD}\rangle_{L,R}$$

F   Derivation of correlator from quantum channels

In this appendix, we give the derivation of the relations (8.29) and (8.30). We can derive the relation graphically, but below, we give an algebraic derivation of the relation.

We start with the derivation of the relation (8.29), which can be obtained straightforwardly from the definition of the quantum channels (8.10) and (8.11). We first note that, from the definition of the quantum channel (8.10), the state $|0\rangle_T\langle 0|$ is mapped to

$$\mathcal{N}^{\text{SYK}}_{T\to K,R}[|0\rangle_T\langle 0|] = \text{tr}_{\tilde{L}}\left[U_L |\text{TFD}\rangle_{L,R}\langle\text{TFD}| U_L^\dagger\right]$$
$$= U_R \,\rho_{KR}\, U_R^\dagger, \tag{F.1}$$

where we used the fact that $(H_L - H_R)|\text{TFD}\rangle_{L,R}$ leading to $U_L|\text{TFD}\rangle_{L,R} = U_R|\text{TFD}\rangle_{L,R}$, and ρ_{KR} is defined by (8.31). For this density matrix, we consider the action of the adjoint channel (8.11), and take the following matrix element;

$$\left\langle \hat{d}_{\tilde{L}}\right\rangle_\beta \cdot \langle 1|\mathcal{N}^{\text{SYK}\dagger}_{K,R\to T}\left[\mathcal{N}^{\text{SYK}}_{T\to K,R}[|0\rangle_T\langle 0|]\right]|1\rangle = \frac{\langle 1|\mathcal{N}^{\text{SYK}\dagger}_{K,R\to T}\left[U_R\,\rho_{KR}\,U_R^\dagger\right]|1\rangle}{\text{tr}\left[(\rho_{KR})^2\right]}, \tag{F.2}$$

where we used the definition (8.16). Using the definition (8.11), we can evaluate the denominator as

$$\langle 1|\mathcal{N}^{\text{SYK}\dagger}_{K,R\to T}\left[U_R\,\rho_{KR}\,U_R^\dagger\right]|1\rangle$$
$$= \left(\,_{L,R}\langle\text{TFD}| \otimes\,_T\langle 1|\right)\left(V^\dagger_{L\to T,L}U_L^\dagger U_R\,\rho_{KR}\,U_R^\dagger U_L V_{L\to T,L}\right)\left(|\text{TFD}\rangle_{L,R} \otimes |1\rangle_T\right)$$
$$= \frac{1}{Z_\delta} \cdot\,_{L,R}\langle\text{TFD}|\left(\psi^\dagger_{i,L}(-i\delta)\,U_L^\dagger U_R\,\rho_{KR}\,U_R^\dagger U_L\,\psi_{i,L}(i\delta)\right)|\text{TFD}\rangle_{L,R}$$
$$= \frac{1}{Z_\delta} \cdot\,_{L,R}\langle\text{TFD}|\left(U_R\psi^\dagger_{i,L}(-i\delta)\,U_L^\dagger\,\rho_{KR}\,U_L\,\psi_{i,L}(i\delta)\,U_R^\dagger\right)|\text{TFD}\rangle_{L,R} \tag{F.3}$$
$$= \frac{1}{Z_\delta} \cdot\,_{L,R}\langle\text{TFD}|\left(U_L\psi^\dagger_{i,L}(-i\delta)\,U_L^\dagger\,\rho_{KR}\,U_L\,\psi_{i,L}(i\delta)\,U_R^\dagger\right)|\text{TFD}\rangle_{L,R}$$
$$= \frac{1}{Z_\delta} \cdot\,_{L,R}\langle\text{TFD}|\left(\psi^\dagger_{i,L}(t-i\delta)\,\rho_{KR}\,\psi_{i,L}(t+i\delta)\right)|\text{TFD}\rangle_{L,R},$$

where in the 4-th equality, we used the relation $U_L|\text{TFD}\rangle_{L,R} = U_R|\text{TFD}\rangle_{L,R}$. Thus, by combining the above expressions, we obtain the relation (8.29),

$$\left\langle \hat{d}_{\tilde{L}}\right\rangle_\beta \cdot \langle 1|\mathcal{N}^{\text{SYK}\dagger}_{K,R\to T}\left[\mathcal{N}^{\text{SYK}}_{T\to K,R}[|0\rangle_T\langle 0|]\right]|1\rangle = \frac{1}{Z_\delta} \cdot \frac{\langle\text{TFD}|\psi_{i,L}(t-i\delta)\left(I_{\tilde{L}}\otimes\rho_{KR}\right)\psi_{i,L}(t+i\delta)|\text{TFD}\rangle}{\text{tr}_{KR}\left[(\rho_{KR})^2\right]}.$$

Next, we derive the relation (8.30). Since $\left\langle\hat{d}_{\tilde{L}}\right\rangle_\beta^{-1} = \text{tr}_{KR}\left[(\rho_{KR})^2\right]$ by the definition (8.16), we focus on the remaining factor $\langle 0|\mathcal{N}^{\text{SYK}\dagger}_{K,R\to T}\left[\mathcal{N}^{\text{SYK}}_{T\to K,R}[|0\rangle_T\langle 1|]\right]|1\rangle$. To evaluate the

factor, we use the definition of the adjoint channel (5.7),

$$
\begin{aligned}
&\langle 0| \mathcal{N}^{\mathrm{SYK}\dagger}_{K,R\to T} \left[\mathcal{N}^{\mathrm{SYK}}_{T\to K,R}[|0\rangle_T\langle 1|] \right] |1\rangle \\
&= \mathrm{tr}_{K,R} \left[\mathcal{N}^{\mathrm{SYK}}_{T\to K,R}[|0\rangle_T\langle 1|] \, \mathcal{N}^{\mathrm{SYK}}_{T\to K,R}[|1\rangle_T\langle 0|] \right] \\
&= \mathrm{tr}_{K,R} \left[\mathrm{tr}_{\tilde{L}} \left[U_L \, |\mathrm{TFD}\rangle_{L,R}\langle\mathrm{TFD}| \, \psi^\dagger_{i,L}(-i\delta)U_L^\dagger \right] \mathrm{tr}_{\tilde{L}} \left[U_L \psi_{i,L}(i\delta) \, |\mathrm{TFD}\rangle_{L,R}\langle\mathrm{TFD}| \, U_L^\dagger \right] \right] \\
&= \mathrm{tr}_{K,R} \left[\mathrm{tr}_{\tilde{L}} \left[U_R \, |\mathrm{TFD}\rangle_{L,R}\langle\mathrm{TFD}| \, \psi^\dagger_{i,L}(-i\delta)U_L^\dagger \right] U_R U_R^\dagger \, \mathrm{tr}_{\tilde{L}} \left[U_L \psi_{i,L}(i\delta) \, |\mathrm{TFD}\rangle_{L,R}\langle\mathrm{TFD}| \, U_R^\dagger \right] \right] \\
&= \mathrm{tr}_{K,R} \left[U_R \, \mathrm{tr}_{\tilde{L}} \left[|\mathrm{TFD}\rangle_{L,R}\langle\mathrm{TFD}| \, U_R \, \psi^\dagger_{i,L}(-i\delta)U_L^\dagger \right] \mathrm{tr}_{\tilde{L}} \left[U_L \psi_{i,L}(i\delta)U_R^\dagger \, |\mathrm{TFD}\rangle_{L,R}\langle\mathrm{TFD}| \right] U_R^\dagger \right] \\
&= \mathrm{tr}_{K,R} \left[\mathrm{tr}_{\tilde{L}} \left[|\mathrm{TFD}\rangle_{L,R}\langle\mathrm{TFD}| \, U_L \, \psi^\dagger_{i,L}(-i\delta)U_L^\dagger \right] \mathrm{tr}_{\tilde{L}} \left[U_L \psi_{i,L}(i\delta)U_L^\dagger \, |\mathrm{TFD}\rangle_{L,R}\langle\mathrm{TFD}| \right] \right] \\
&= \mathrm{tr}_{K,R} \left[\mathrm{tr}_{\tilde{L}} \left[|\mathrm{TFD}\rangle_{L,R}\langle\mathrm{TFD}| \, \psi^\dagger_{i,L}(t-i\delta) \right] \mathrm{tr}_{\tilde{L}} \left[\psi_{i,L}(t+i\delta) \, |\mathrm{TFD}\rangle_{L,R}\langle\mathrm{TFD}| \right] \right].
\end{aligned}
$$
(F.4)

By explicitly introducing bases for the traces, we can rewrite the last expression as follows,

$$
\begin{aligned}
&\mathrm{tr}_{K,R} \left[\mathrm{tr}_{\tilde{L}} \left[|\mathrm{TFD}\rangle_{L,R}\langle\mathrm{TFD}| \, \psi^\dagger_{i,L}(t-i\delta) \right] \mathrm{tr}_{\tilde{L}} \left[\psi_{i,L}(t+i\delta) \, |\mathrm{TFD}\rangle_{L,R}\langle\mathrm{TFD}| \right] \right] \\
&= \sum_{\alpha,\alpha'=1}^{d_K d_R} \sum_{a,a'=1}^{d_{\tilde{L}}} \left({}_{KR}\langle\alpha| \otimes {}_{\tilde{L}}\langle a| \right) \left(|\mathrm{TFD}\rangle_{L,R}\langle\mathrm{TFD}| \, \psi^\dagger_{i,L}(t-i\delta) \right) \left(|\alpha'\rangle_{KR} \otimes |a\rangle_{\tilde{L}} \right) \\
&\qquad\qquad\qquad \times \left({}_{KR}\langle\alpha'| \otimes {}_{\tilde{L}}\langle a'| \right) \left(\psi_{i,L}(t+i\delta) \, |\mathrm{TFD}\rangle_{L,R}\langle\mathrm{TFD}| \right) \left(|\alpha\rangle_{KR} \otimes |a'\rangle_{\tilde{L}} \right) \\
&= \sum_{\alpha,\alpha'=1}^{d_K d_R} \sum_{a,a'=1}^{d_{\tilde{L}}} {}_{L,R}\langle\mathrm{TFD}| \, \psi^\dagger_{i,L}(t-i\delta) \left(|\alpha'\rangle_{KR} \otimes |a\rangle_{\tilde{L}} \right) \\
&\qquad\qquad\qquad \times \left({}_{KR}\langle\alpha| \otimes {}_{\tilde{L}}\langle a| \right) |\mathrm{TFD}\rangle_{L,R}\langle\mathrm{TFD}| \left(|\alpha\rangle_{KR} \otimes |a'\rangle_{\tilde{L}} \right) \\
&\qquad\qquad\qquad\qquad\qquad \times \left({}_{KR}\langle\alpha'| \otimes {}_{\tilde{L}}\langle a'| \right) \psi_{i,L}(t+i\delta) \, |\mathrm{TFD}\rangle_{L,R} \\
&= {}_{L,R}\langle\mathrm{TFD}| \, \psi^\dagger_{i,L}(t-i\delta) \left(\mathrm{tr}_{KR} \left[|\mathrm{TFD}\rangle_{L,R}\langle\mathrm{TFD}| \right] \otimes I_{KR} \right) \psi_{i,L}(t+i\delta) \, |\mathrm{TFD}\rangle_{L,R} \\
&= {}_{L,R}\langle\mathrm{TFD}| \, \psi^\dagger_{i,L}(t-i\delta) \left(\rho_{\tilde{L}} \otimes I_{KR} \right) \psi_{i,L}(t+i\delta) \, |\mathrm{TFD}\rangle_{L,R},
\end{aligned}
$$
(F.5)

where $d_K, d_R, d_{\tilde{L}}$ are the Hilbert space dimensions of subsystems K, R, $\tilde{L}$ respectively.

Therefore, we get the relation (8.30),

$$
\left\langle \hat{d}_{\tilde{L}} \right\rangle_\beta \cdot \langle 0| \mathcal{N}^{\mathrm{SYK}\dagger}_{K,R\to T} \left[\mathcal{N}^{\mathrm{SYK}}_{T\to K,R}[|0\rangle_T\langle 1|] \right] |1\rangle = \frac{1}{Z_\delta} \cdot \frac{\langle\mathrm{TFD}|\psi_{i,L}(t-i\delta) \left(\rho_{\tilde{L}} \otimes I_{KR} \right) \psi_{i,L}(t+i\delta)|\mathrm{TFD}\rangle}{\mathrm{tr}_{KR}\left[(\rho_{KR})^2 \right]}.
$$

References

[1] G. Penington, *Entanglement Wedge Reconstruction and the Information Paradox*, *JHEP* **09** (2020) 002 [1905.08255].

[2] A. Almheiri, N. Engelhardt, D. Marolf and H. Maxfield, *The entropy of bulk quantum fields and the entanglement wedge of an evaporating black hole*, *JHEP* **12** (2019) 063 [1905.08762].

[3] A. Almheiri, R. Mahajan, J. Maldacena and Y. Zhao, *The Page curve of Hawking radiation from semiclassical geometry*, *JHEP* **03** (2020) 149 [1908.10996].

[4] G. Penington, S. H. Shenker, D. Stanford and Z. Yang, *Replica wormholes and the black hole interior*, *JHEP* **03** (2022) 205 [1911.11977].

[5] A. Almheiri, T. Hartman, J. Maldacena, E. Shaghoulian and A. Tajdini, *Replica Wormholes and the Entropy of Hawking Radiation*, *JHEP* **05** (2020) 013 [1911.12333].

[6] P. Hayden and J. Preskill, *Black holes as mirrors: Quantum information in random subsystems*, *JHEP* **09** (2007) 120 [0708.4025].

[7] E. Verlinde and H. Verlinde, *Black Hole Entanglement and Quantum Error Correction*, *JHEP* **10** (2013) 107 [1211.6913].

[8] K. Papadodimas and S. Raju, *An Infalling Observer in AdS/CFT*, *JHEP* **10** (2013) 212 [1211.6767].

[9] H. Barnum and E. Knill, *Reversing quantum dynamics with near-optimal quantum and classical fidelity*, *Journal of Mathematical Physics* **43** (2000) 2097.

[10] D. Petz, *Sufficient subalgebras and the relative entropy of states of a von Neumann algebra*, *Commun. Math. Phys.* **105** (1986) 123.

[11] M. Ohya and D. Petz, *Quantum Entropy and Its Use*, Theoretical and Mathematical Physics. Springer Berlin Heidelberg, 2004.

[12] B. Yoshida, *Recovery algorithms for Clifford Hayden-Preskill problem*, 2106.15628.

[13] B. Yoshida, *Decoding the Entanglement Structure of Monitored Quantum Circuits*, 2109.08691.

[14] V. Chandrasekaran and A. Levine, *Quantum error correction in SYK and bulk emergence*, *JHEP* **06** (2022) 039 [2203.05058].

[15] Y. Nakata and M. Tezuka, *Hayden-Preskill Recovery in Hamiltonian Systems*, 2303.02010.

[16] Y. Nakayama, A. Miyata and T. Ugajin, *Work in progress*, .

[17] G. Ping, J. Daniel, Louis and C. W. Aron, *Traversable Wormholes via a Double Trace Deformation*, 1608.05687.

[18] B. Yoshida and A. Kitaev, *Efficient decoding for the Hayden-Preskill protocol*, 1710.03363.

[19] M. A. Nielsen and I. L. Chuang, *Quantum Computation and Quantum Information: 10th Anniversary Edition*. Cambridge University Press, 2010, 10.1017/CBO9780511976667.

[20] E. Knill and R. Laflamme, *A Theory of quantum error correcting codes*, *Phys. Rev. Lett.* **84** (2000) 2525 [`quant-ph/9604034`].

[21] D. Petz, *MONOTONICITY OF QUANTUM RELATIVE ENTROPY REVISITED*, *Rev. Math. Phys.* **15** (2003) 79 [`quant-ph/0209053`].

[22] H. Barnum and E. Knill, *Reversing quantum dynamics with near-optimal quantum and classical fidelity*, 2000.

[23] D. Petz, *SUFFICIENCY OF CHANNELS OVER VON NEUMANN ALGEBRAS*, *Quart. J. Math. Oxford Ser.* **39** (1988) 97.

[24] B. Schumacher and M. A. Nielsen, *Quantum data processing and error correction*, *Phys. Rev. A* **54** (1996) 2629 [`quant-ph/9604022`].

[25] M. A. Nielsen and D. Poulin, *Algebraic and information-theoretic conditions for operator quantum error correction*, *Physical Review A* **75** (2007) .

[26] S. Vardhan, J. Kudler-Flam, H. Shapourian and H. Liu, *Mixed-state entanglement and information recovery in thermalized states and evaporating black holes*, *JHEP* **01** (2023) 064 [`2112.00020`].

[27] J. Kudler-Flam and P. Rath, *Large and small corrections to the JLMS Formula from replica wormholes*, *JHEP* **08** (2022) 189 [`2203.11954`].

[28] N. Lashkari, *Modular Hamiltonian for Excited States in Conformal Field Theory*, *Phys. Rev. Lett.* **117** (2016) 041601 [`1508.03506`].

[29] J. Kudler-Flam, *Relative Entropy of Random States and Black Holes*, *Phys. Rev. Lett.* **126** (2021) 171603 [`2102.05053`].

[30] J. Kudler-Flam, V. Narovlansky and S. Ryu, *Distinguishing Random and Black Hole Microstates*, *PRX Quantum* **2** (2021) 040340 [`2108.00011`].

[31] S. Sachdev and J. Ye, *Gapless spin fluid ground state in a random, quantum Heisenberg magnet*, *Phys. Rev. Lett.* **70** (1993) 3339 [`cond-mat/9212030`].

[32] A. Kitaev, "A simple model of quantum holography.." `http://online.kitp.ucsb.edu/online/entangled15/kitaev/`,`http://online.kitp.ucsb.edu/online/entangled15/kitaev2/`.

[33] G. Sárosi, *AdS$_2$ holography and the SYK model*, *PoS* **Modave2017** (2018) 001 [`1711.08482`].

[34] D. A. Trunin, *Pedagogical introduction to the Sachdev–Ye–Kitaev model and two-dimensional dilaton gravity*, *Usp. Fiz. Nauk* **191** (2021) 225 [`2002.12187`].

[35] J. Maldacena and D. Stanford, *Remarks on the Sachdev-Ye-Kitaev model*, *Phys. Rev. D* **94** (2016) 106002 [`1604.07818`].

[36] J. Polchinski and V. Rosenhaus, *The Spectrum in the Sachdev-Ye-Kitaev Model*, *JHEP* **04** (2016) 001 [`1601.06768`].

[37] V. Chandrasekaran, T. Faulkner and A. Levine, *Scattering strings off quantum extremal surfaces*, *JHEP* **08** (2022) 143 [2108.01093].

[38] S. Sachdev, *Bekenstein-Hawking Entropy and Strange Metals*, *Phys. Rev. X* **5** (2015) 041025 [1506.05111].

[39] X.-L. Qi and A. Streicher, *Quantum Epidemiology: Operator Growth, Thermal Effects, and SYK*, *JHEP* **08** (2019) 012 [1810.11958].

[40] D. Bagrets, A. Altland and A. Kamenev, *Power-law out of time order correlation functions in the SYK model*, *Nucl. Phys. B* **921** (2017) 727 [1702.08902].

[41] D. J. Gross and V. Rosenhaus, *All point correlation functions in SYK*, *JHEP* **12** (2017) 148 [1710.08113].

[42] A. Kitaev and S. J. Suh, *The soft mode in the Sachdev-Ye-Kitaev model and its gravity dual*, *JHEP* **05** (2018) 183 [1711.08467].

[43] A. Romero-Bermúdez, K. Schalm and V. Scopelliti, *Regularization dependence of the OTOC. Which Lyapunov spectrum is the physical one?*, *JHEP* **07** (2019) 107 [1903.09595].

[44] Y. Sekino and L. Susskind, *Fast Scramblers*, *JHEP* **10** (2008) 065 [0808.2096].

[45] P. Gao and D. L. Jafferis, *A traversable wormhole teleportation protocol in the SYK model*, *JHEP* **07** (2021) 097 [1911.07416].

[46] A. R. Brown, H. Gharibyan, S. Leichenauer, H. W. Lin, S. Nezami, G. Salton et al., *Quantum Gravity in the Lab. I. Teleportation by Size and Traversable Wormholes*, *PRX Quantum* **4** (2023) 010320 [1911.06314].

[47] T. Schuster, B. Kobrin, P. Gao, I. Cong, E. T. Khabiboulline, N. M. Linke et al., *Many-Body Quantum Teleportation via Operator Spreading in the Traversable Wormhole Protocol*, *Phys. Rev. X* **12** (2022) 031013 [2102.00010].

[48] S. Nezami, H. W. Lin, A. R. Brown, H. Gharibyan, S. Leichenauer, G. Salton et al., *Quantum Gravity in the Lab. II. Teleportation by Size and Traversable Wormholes*, *PRX Quantum* **4** (2023) 010321 [2102.01064].

[49] F. Pastawski and J. Preskill, *Code properties from holographic geometries*, *Phys. Rev. X* **7** (2017) 021022 [1612.00017].

[50] G. Bentsen, P. Nguyen and B. Swingle, *Approximate Quantum Codes From Long Wormholes*, 2310.07770.

[51] A. M. García-García, B. Loureiro, A. Romero-Bermúdez and M. Tezuka, *Chaotic-Integrable Transition in the Sachdev-Ye-Kitaev Model*, *Phys. Rev. Lett.* **120** (2018) 241603 [1707.02197].

[52] C. Akers, N. Engelhardt, D. Harlow, G. Penington and S. Vardhan, *The black hole interior from non-isometric codes and complexity*, 2207.06536.

[53] M. Berkooz, M. Isachenkov, V. Narovlansky and G. Torrents, *Towards a full solution of the large N double-scaled SYK model*, *JHEP* **03** (2019) 079 [1811.02584].

[54] H. W. Lin and D. Stanford, *A symmetry algebra in double-scaled SYK*, 2307.15725.

[55] J. Liu, *Scrambling and decoding the charged quantum information*, *Phys. Rev. Res.* **2** (2020) 043164 [2003.11425].